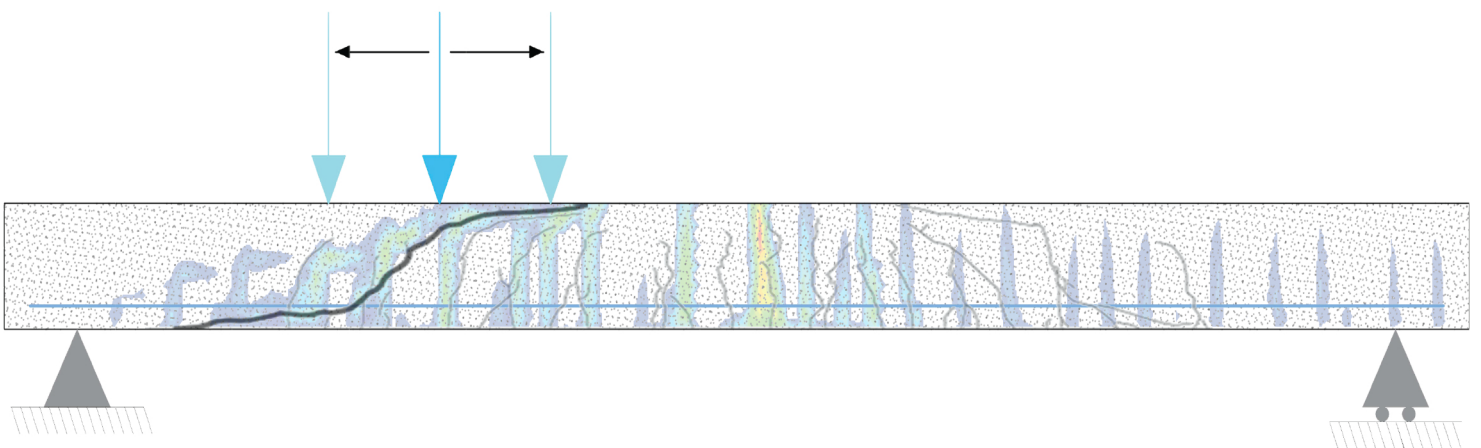# Validation of a Newly Proposed Global Factor Method Applied in the Assesment of Reinforced Concrete Structures Modelled by NLFEA

Daniela Patricia Tavera Diaz

October 2021

TU Delft

Validation of a Newly Proposed Global Factor Method Applied in the Assessment of Reinforced Concrete Structures Modelled by Nonlinear Finite Element Analysis

Verifying the new Global Factor Method as a safety format in assessing the structural capacity of reinforced concrete structures with non-linear finite element analysis in the case of clustered failure modes.

by

Daniela Patricia Tavera Diaz

Master of Science Thesis

Master Of Science in Civil Engineering
Delft University of Technology
Master Track: Structural Engineering

Student number: 5047498
Thesis committee: Prof. dr. ir. M.A.N Hendriks,   TU Delft, chair
                    Prof. dr. ir. O. Morales-Nápoles,   TU Delft
                    Dr. ir. Y. Yang,   TU Delft

October, 2021

TUDelft   Delft
University of
Technology

Summary

Nowadays, one of the main requirements from civil engineering structures is the level of reliability and safety that they must provide to the users. In structural analysis, the exponential application of numerical methods, as the nonlinear finite element analysis (NLFEA), is due to the increasing growth of computational power. These powerful tools provide the opportunity to study the global behavior of complex systems: with a more accurate and elaborate approach. The latter is especially relevant for cases where nonlinearities highly impact the performance of the structure. However, to ensure a certain level of safety, the stochastic nature of all the influencing parameters must be accounted for during the analysis and design stages. The latter is precisely the role of Safety Formats: a mathematical procedure to ensure an imposed level of reliability while computing the design resistance of structures.

Several existing safety formats have been implemented along with the NLFEA in the structural reliability assessment of reinforced concrete structures. Some of the most relevant ones are the Partial Safety Factor, worldwide present in many codes and standards, or the Estimation of Coefficient of Variation (ECOV) methods, which seem the most efficient and suitable option when using NLFEA up to date. Nonetheless, these formats face some criticism in their usability due to some of the assumptions implied in their derivation. For instance, the resistance variable modeled with a log-normal distribution is not an accurate assumption for complex systems: the mechanism leading to global failure might not be unique but a combination of at least two or more concurrent mechanisms, which directly transform the probability distribution of the resistance.

Therefore, Monti et al. (2021) recently proposed a safety format: a new Global Factor Method that aims to be applicable in the nonlinear finite element analysis of reinforced concrete structures with concurrent failure mechanisms influencing the global performance at a predefined limit state. In a general description, the method requires the output obtained from two nonlinear finite element analyses and the calculation of a Global Safety Factor related to the resistance of the whole structural system. The first analysis is performed by modeling the structure with the mean values of the main variables and material parameters. The result of this analysis is assumed to be the mean value of the resistance, which divided by the Global Safety Factor will provide the final design resistance of the system with the defined reliability. The second analysis requires running the model with the parameters influencing the Local Critical Failure Mechanisms identified from the first analysis, but decreased by the perturbation parameter c. The resistance obtained takes part in the calculation of the Global Safety Factor.

This thesis aims to provide scenarios to validate the new safety format for its future implementation in codes and the industry since, currently, they are extremely limited. Especially referring to structures modelled with continuum elements given that the method has been developed for frame-type ones. Therefore, the GFM is implemented in three overall case studies with increasing levels of complexity.

Case 1a and 1b consist of two reinforced concrete cross-sections subjected only to bending moment and shear force respectively. Instead of NLFEA, explicit analytical expressions are utilized in calculating the resistance. The GFM was implemented by assuming different Engineer Decision-based Scenarios when choosing the Critical Local Failure Mechanisms and the related basic variables to be perturbed. The decisions were based on the results and observations from the application of other existing formats. Even though, for balanced cross-sections, the division of bending failure into two concurrent mechanisms working in series resulted in highly fictitious outcomes and did not improve the reliability of the design resistance. The validation of the results was performed by a Crude Monte Carlo simulation and by comparing the results with the ones computed with other existing safety formats.

While searching for less fictitious scenarios where two different concurrent failure mechanisms were present at failure, case study 1c is defined as a simply supported beam with longitudinal reinforcement. The position of the point load varying between the support and the mid-span caused the beam to fail in Bending, Shear, or Mixed Failure Mechanisms. The GFM had problems in reaching the target reliability when shear was identified as the CLFM. It is concluded that the method does not perform with the desired reliability in the analytical cases, this is mainly due to the philosophy of the method of only perturbing the basic variables

of the CLFM, which is not suitable for the use of analytical expressions.

Finally, moving to the use of NLFEA in the framework of the GFM, case study 2 presents the same simple support beam analyzed at three fixed positions of the point load. They produced three different Local Failure Mechanisms: Bending, Shear, and Mixed mechanisms. The three models and design resistances appear to be extremely sensitive to the selected solution strategy and the value of the modeling uncertainty. Once again, the method gave space for different scenarios in terms of the identified CLFM, its location, and the basic variables involved. Validation was partially done by the results from a full probabilistic analysis (DARS method) found in the literature for the same structures.

During the case studies, special attention is given to the size of the perturbation (described by the so-called c parameter) that proportionally decreases the basic variables for the second nonlinear analysis. Since clear guidelines about its value are not available, a parametric study was performed on each one of the three cases. From the analytical cases, it seems that the value of the design resistance decreases for increasing values of the c parameter. However, the design resistance of the three beams in case study 2 is not as sensitive to the various values of c and does not show inverse proportional behavior: the value of the design resistance does not decrease the value of c is increased.

As the main outcome of this study, it was concluded that the GFM implemented to reinforced concrete structures can provide reliable and accurate design value of the resistance part, however, this is subjected to some conditions. For structures with a single LFM, the method works similarly to already existing safety formats. For continuum structures where two concurrent failure mechanisms lead to global failure, the GFM still needs to be revised to provide more accurate guidelines and reduce the space for decisions made by the analyst that highly impact the performance of the method. These decisions are related to identifying and locating the LFM and their basic variables, selecting the solution strategy implemented in the NLFEA, and choosing a suitable modeling uncertainty. At this point, the application of the method demands an experienced analyst and several parametric studies regarding all those decisions, which reduces its efficiency in terms of engineering and computational time.

Acknowledgements

Contents

List of Figures

List of Tables

1

Introduction

1.1. Introduction

The world is an impressive stage where nature and human creations incorporate. For instance, civil engineering works are an extensive part of today's landscape. Therefore, they must be aesthetic, practical, economical, sustainable, and last but not least: safe. Even though a structure can never be completely 'safe' [38], especially due to human errors during the design, modeling, manufacturing, and usage stages; the public and users increasingly demand, through codes and standards, a certain level of reliability.

In the past century, the use of numerical methods to approximately solve engineering problems has been limited by computational power, with the exponential growth in this area, the usage and fields of application of these methods (e.i. finite element method) have rapidly extended. Moreover, the use of nonlinear finite element analysis (NLFEA) in assessing the structural capacity of structures is widely spread nowadays [5][35]. For instance, many reinforced concrete structures in which non-linear effects highly impact the global and local behavior, the application of simplified linear analyses or analytical solutions is not suitable anymore. The latter is due to the inability of these methods to accurately or efficiently model the real response of the structures. Thus, NLFEA play an important role.

An application of NLFEA in the Netherlands is the assessment of a large number of old structures as bridges and retaining walls that need to be studied to find their remaining life span subjected under higher traffic loads than in the original designs. There, the use of NLFEA is highly recommended, as it is the use of safety procedures to ensure the reliability of the results. If the prediction of the capacity still available in these structures is accurate, maintenance and retrofit measures may be avoided leading to a great reduction in monetary and environmental costs.

Following all the previous ideas, in structural analysis and design of structures, reliability methods aim to ensure the safety requirements of today's standards. Better known as Safety Formats, they are defined as a mathematical approach to calculate the design resistance of a structural system while assuring an imposed target reliability. These methods keep being developed and updated since the past century, seeking procedures able to include the stochastic nature of the influencing parameters in the reliability calculation of the design capacity. Thus, along with the increase in the use of NLFEA appropriate safety formats must be at hand. Subsequently, proper guidance should be available to become their practical application in a standard exercise; currently, some governments and institutions, as the Dutch Ministry of Infrastructure, do not allow the implementation of NLFEA for new projects.

The core of this thesis is to provide scenarios to validate a new safety format recently proposed by Monti et al. in [29]. The new format aims to be applicable in the nonlinear finite element analysis of reinforced concrete structures. In a general description, the method requires the output obtained from two nonlinear finite element analyses and the calculation of a Global Safety Factor related to the resistance of the whole structural system. The first analysis is performed by modeling the structure with the mean values of the main variables and material parameters. The result of this analysis is assumed to be the mean value of the resistance, which divided by the Global Safety Factor will provide the final design resistance of the

system. The second analysis requires the model to run with the value of the same parameters being slightly perturbed. The resistance obtained takes part in the calculation of the Global Safety Factor. Especial attention will be given to the size of the perturbation (described by the so-called 'c' parameter) that proportionally decreases the basic variables. Its value is not yet clearly defined in [29] and its value might highly impact the performance of the new Global Factor Method.

1.2. Research Project

This project aims to investigate the application of the new Global Factor Method (GFM) proposed by Monti et al. (2021) in assessing the structural reliability and capacity of statically loaded reinforced concrete structures failing under concurrent or clustered failure modes, to provide validation of the new safety format and guidance on its practical application and usability. Existing methods in literature are suitable for the usage of NLFEA in structures with an identified dominant failure mechanism influencing their global capacity; however, in many cases, the behavior of the RC structures is not easy to predict or identify beforehand. In addition, reinforced concrete (RC) is a composite material with non-homogeneous, non-isotropic, and non-linear characteristics. Therefore, the existence of a verified method that allows the correct and conservative assessment of the capacity of a structure with the aforementioned characteristics becomes of critical importance. There is an enormous amount of literature and studies for structures with one predominant failure mode, however, the focus of the project is to provide inside in cases where at least two relevant modes play a role. [19] [33]

The most representative contribution of the new GFM is implementing a methodology that allows for the inclusion of several failure modes in the calculation for the design resistance with NLFEA. The challenge now is to verify the GFM's success, especially for continuous systems. With its application in simple scenarios, comparison with full probabilistic methods is possible in the validation process. This step allows a better understanding of the GFM method since it will provide the basis of critical thinking when moving for more complex cases. Additionally, simple scenarios allow parametric studies of the influencing parameters i.e. the identification of failure mechanism, the choice of basic variables and relationships between them, and the perturbation parameter (c).

The application of complex cases faces the same drawbacks as in practical application of NLFEA in relation with the verification of the results: a full probabilistic method is not time efficient at this stage. Then, once again the use of simple models is highlighted. In this way, guidance and benchmark cases will be provided along with conclusion and recommendations about the practical application and scope of the GFM.

1.3. Research Question

1.3.1. Main Research Question

How does the new Global Factor Method proposed by Monti et al. (2021) assess the structural reliability and capacity of a statically loaded reinforced concrete structure failing under concurrent modes?

1.3.2. Sub-Questions

- What are the existing safety formats applied to the nonlinear finite element analysis of RC structures, and how do they relate to the new Global Factor Method by Monti et al. (2021)?

- While implementing the Global Factor Method, the identification of local failure mechanisms influencing global failure is essential. Sometimes in NLFEA, this is not a straightforward procedure. How does the GFM perform in cases where identification and definition of failure mechanisms and their variables give space for different decision scenarios?

- Global Factor Method by Monti et al. (2021) does not provide a specific value for the perturbation parameter c. How sensible is the resulting design resistance, in the analytical and NLFEA cases, for different values of the perturbation parameter c?

- Does the GFM result in a reliable estimation of the global capacity by complying with the set target reliability index in the analytical cases and comparing it with already existing safety formats in the

NLFEA cases??

1.4. Aims, Objectives and Scope

The aim of this project is to investigate the application of the new Global Factor Method in assessing the structural reliability and capacity of a statically loaded reinforced concrete structure failing under concurrent modes in order to provide validation of the method and guidance on its practical application and usability.

1.4.1. Objectives

1. To study the application of existing safety formats aiming for the correct implementation of the new Global Factor Method.

2. To define and model three appropriate case studies based on reinforced concrete structures with progressive complexity that fit into the requirement of failing under concurrent modes:

   - Reinforced concrete cross-sections with one known failure mechanism, analyze and modelled by analytical expressions.
   - Simply reinforced concrete beam with 2 concurrent failure modes leading to global failure, analyze and modelled by analytical expressions.
   - Reinforced concrete beams with concurrent failure modes, analyzed and modelled by NLFEA.

3. To provide guidance and benchmark values through parametric studies of the the influencing parameters: the identification of failure mechanism, the choice of basic variables and relationships between them, and the perturbation parameter (c).

4. To provide a future benchmark guidance in the practical application of the Global Factor Method based on the chosen case studies.

1.4.2. Scope

It is highly important to establish the boundaries and limitations of the investigation. For the present project, several points must be account for since the beginning of the process. They provide a better understating of the scope of the investigation and give future guidance for the direction to take.

1. Only structures subjected to quasi-static, monotonic loading effects are considered as suitable case studies. As a consequence, the final outcome of the research must not be directly used as benchmark or guidance for structures under dynamic and cyclic loads, transient effects (creep or shrinkage) or pre-stressed concrete structures.

2. The chosen solution strategy applied in all the case studies related to the use of NLFEA is based on the Dutch guidelines (2021). [23]

3. The modelling uncertainty for the previously mentioned solution strategy is not the main focus of this thesis. Therefore, it is not calculated specifically for each NLFE models. It requires a long and detailed process itself and thus, it is taken from the recently developed master thesis from De Putter, where similar cases are studied. [12]

4. The validation of the second case study is done by comparing the results from the GFM with the already existing full probabilistic analysis included in the work of A. Roy. In this research, the DARS method is applied for the same case analysed in the second phase of the project and the results will contribute to the verification of the new method.[32]

1.5. Outline and Methodology

First, a more profound literature study is carried out in **chapter 2**. It provides a first look into the framework of the application of nonlinear finite element analysis in structural reliability. The focus is the study of existing safety formats applicable to the nonlinear analysis of reinforced concrete structures. Especial emphasis is done on the ECOV methods since they are the most closely related to the new Global Factor Method by Monti et al. (2021). Subsequently, **chapter 3** presents a revision of the derivation of the new Global Factor Method and the guidelines in its application.

Chapter 4 shows the definition of the first case study: divided into case studies 1a and 1b. The RC concrete sections are selected from the work presented by Pimentel et al. in [31]. The idea is to apply the existing safety formats by using an analytical expression in finding the capacity for varying longitudinal and shear reinforcement ratios. This step allows a better understanding of the application of the new GFM in **chapter 5**: it provides scenarios to implement the method according to different decisions taken in terms of the identification and definition of the local failure mechanisms since sometimes this is not a straightforward process. At the same time, it allows a sensitivity study of the perturbation parameter 'c' influencing the basic variables in the second NLFEA, since insufficient guidance about its range of suitable values is given by Monti et al. in [29]. The use of analytical expressions facilitates the validation of the results by a Monte Carlo analysis since these simple cases have an available limit state function in an explicit form.

Chapter 6 presents case study 1c. This case study is included to study the performance of the GFM with analytical expressions in structures with at least two concurrent failure mechanisms:according to the position of the load in the simply supported beam, bending and shear might be present in an almost concurrent manner.

Moving to case study 2, **chapter 7** presents a simple case, this time with the use of NLFEA. The methodology proposed is to use the three RC beams used by Roy in [32] and shown in figure 1.1. The first beam fails in bending, the second one in shear, and the third is a structure switching between both failure modes called a mixed beam. In **chapter 8**, the application of the new GFM, in cases 2a, 2b, and 2c, as a safety format provides the opportunity to have a point of comparison and verification in reaching the final goal of this project. The obtained are compared, to some extent, with the results from the DARS method in [32].
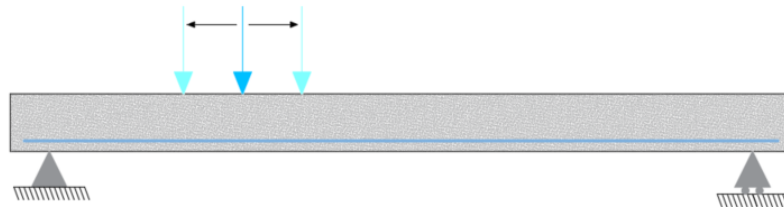
Figure 1.1: Summarize representation Case Study 2

The models for the second case study run with the use of the finite element software DIANA FEA. Finally, **chapter 9** presents the general observations, conclusions in relation to the research questions, and further recommendations.

Case Study	Description	Definition	GFM application	Modelled by…	Varying parameter…	Validation
Case 1a	RC cross-section failing in bending	Chapter 4	Chapter 5	Analytical expression	Reinforcement Ratio ρ	Monte Carlo Simulation
Case 1b	RC cross-section in failing shear	Chapter 4	Chapter 5	Analytical expression	Shear Reinforcement Ratio ρ	Monte Carlo simulation
Case 1c	RC Simply supported beam: failing in bending, shear or mixed mechanism	Chapter 6	Chapter 6	Analytical expression	Load position + Reinforcement Ratio ρ	Monte Carlo simulation
Case 2	RC Simply supported beam: • 2a – Bending mechanism • 2b - Shear mechanism • 2c – Mixed mechanisms	Chapter 7	Chapter 8	NLFEA	Load position	In literature: DARS method

Figure 1.2: Summary of the case studies: Outline and methodology

2

Existing literature and background

There is an increasing amount of literature and research related to reliability-based analysis and existing safety formats. The following chapter presents some of the basic concepts closely related to the topic of interest: the implementation and validation of the newly proposed Global Factor Method. It intends to give a concise general framework and expose the state of the art of the existing safety formats available for the use of NLFEA.

2.1. Levels of Approximation

As stated in the *fib* MC2010 [20], it is possible to perform the design and assessments of new and existing RC structures with different methods according to the desired level of detail and sophistication included in the model. Every model intends to approximate reality to some extent, and according to their accuracy, the applied methods may be classified in the so-called Levels of Approximation (LoA). This approach is highly efficient, particularly when applied to different phases and stages during the development of structural projects. For instance, at a pre-design stage, a Level I method is more suitable since detailed modeling of the structure is not yet required. On the contrary, a first idea on the general behaviour of the structure proves to be safe and convenient enough. As the complexity of a project increases, refinement in the models of the physical parameters might be required to obtain better accuracy in the behavior and capacity.

Thus, in situations where high accuracy is required, higher levels of approximation play their role. Another example is the assessment of existing structures. By including the nonlinear behavior of the structure during the analysis, the possibility of an 'extra' capacity might lead to representative monetary savings in reparation costs which compensates for the increase in computational and engineering time needed for higher-level methods.

The use of Non-linear Finite Element Analysis is closely related to the highest levels of approximation. They demand high computational time and give space for refined models of the physical parameters. Therefore, it is essential to understand the needs related to every case to determine the most suitable method within the LoA approach.

2.2. From the Classical Approach to NLFEA

In the design and assessment of concrete structures, the classical approach, included in several codes nowadays i.e Eurocode, consists of two main phases. The first one is to determine the general response of the structural system under the imposed loads, usually by a linear elastic analysis with mean values of the material parameters. Once the stresses and design effects values E_d are known, the design and assessment of the structure are performed at a member level in a specific number of cross-sections, the most critical ones according to the distribution of internal forces. The local design resistance R_d is obtained with a semi-probabilistic approach i.e. the Partial Factors Method. Only there, non-linear effects are accounted in the classical assessment procedure employing established constitutive laws for the design values of the material

parameters. [2] [35][24]

Therefore, the classical approach aims to provide a sufficient safety margin between the existing actions or effects and the resistance at a cross-section level. [24] The following inequality must be fulfilled:

$$E_d \leq R_d \tag{2.1}$$

This methodology has proven to be safe and conservative for many situations where the non-linear behavior of the structures does not have a great impact on the global resistance, and the section level assessment is enough. However, the concern arises in cases where non-linearity affects not only the local performance of the structure but its capacity as a whole. In those situations, the classical approach can not accurately describe the global failure mechanism of the system. Therefore, the use of Non-linear Finite Element Analysis (NLFEA), based on the attainment of a predefined Limit State to obtain the complete picture, is essential.

NLFEA should be implemented in a practical situation when facing at least one of the two following issues:

- The problem involves large structures where the test of their future performance is out of the possibilities. Structures as long-span bridges, high-rise buildings, or offshore platforms might get some of their parts tested in a lab or even on-site, but their whole behavior is impossible to evaluate on a real scale. Then, the possibility of a numerical simulation becomes the desired solution. [21]

- Classical methods, Linear finite element analysis, or analytical expressions are incapable of model a realistic behaviour of the structures. The capacity is either underestimated due to the lack of redistribution of stresses during the analysis or overestimated by assuming a higher performance. In both cases, it leads to economic, human, and environmental losses.

Moreover, NLFEA becomes relevant in situations where the material or geometrical non-linear strongly affects the capacity of the structures. In other cases, the need for NLFEA derives from the dynamic character of the load or when there is a difficulty in assessing the load effects only at a member level due to the constant interaction and transmission of forces between structural members. In all these situations, the structural reliability is affected and simplifies analytical models stop being suitable. The new version of the *fib* Model Code 2020 lists the following typical fields of application of NLFEA:

- Quantifying the inelastic deformation capacity of a concrete structure for quasi-static push-over loading

- Determination of the distribution of action effects in a structural system for further capacity control of cross-sections, when significant concrete cracking and/or reinforcement yielding influences the load paths

- Assessing the seismic capacity of an existing structure under earthquake action, including, if needed, also non-structural elements

- Assessing the shear capacity of an existing structure with outdated reinforcement detailing

- Assessing the activation of a second bearing path in a design of a bridge

- Assessing the risk of thermal cracks in massive concrete structures such as dams, foundations, and tunnels, during the early hardening process in concrete, due to restraints and uneven temperatures

- Simulating the failure mode and loading capacity of post-tensioned fiber reinforced concrete slab without conventional longitudinal reinforcement for distributed loading,

- Assessing the bearing capacity of a tunnel section subject to fire and temperature-dependent material deterioration

- Simulating the behavior of a building subject to impact or explosion

- Verifying serviceability limit state requirements of a concrete outer wall of a liquefied natural gas storage tank, at low temperatures under a liquid spill condition

- Assessing the failure mode and capacity of disturbed regions with complex detailing and boundary conditions, such as anchorage zones, subjected to concentrated loads

- Assessing the residual capacity of corroded structures with deteriorated steel and concrete properties due to carbonation and/or chloride penetration

- Simulating the capacity of a building, including soil-structure interaction effects, for seismic actions

As mentioned in section 1.1, the use of NLFEA must come with appropriate safety formats. In the following sections, various existing formats applicable to NLFEA are briefly described; especially those proposed in the EUROCODE and in the fib Model Code 2010 are presented to illustrate the state of the art of Safety Formats in the NLFEA field.

2.3. The Resistance as a Stochastic Variable

The base assumption made along the derivation of the majority existing safety formats, proposes a simple stochastic model for the resistance R, expressed as the product of the nominal resistance R_m by the random variables F, G and θ: [31][35][14]:

$$R = R_\mathrm{m} \cdot F \cdot G \cdot \theta \tag{2.2}$$

Where F, G, and θ represent the material, geometrical, and modeling uncertainties. As the model is a product of random variables, it is possible to assume that R follows a log-normal distribution. The latter agrees with avoiding negative values for a physical quantity, for instance, the resistance. Under the previous assumption, the coefficient of variation of the resistance, that includes all the earlier mentioned uncertainties, can be expressed as:

$$V_R = \sqrt{V_{R_x}^2 + V_G^2 + V_\theta^2} \tag{2.3}$$

Where V_{R_x}, V_G, and V_θ represent the coefficient of variation of the material, geometrical and modelling uncertainties respectively.

2.4. Current Safety Formats for NLFEA

A NLFEA provides insight into the integral performance of the structure. Therefore, a global design condition in terms of local effects is not suitable anymore. However, inequality 2.1 might be adjusted for the NLFEA framework as [9]:

$$F_\mathrm{d} < R_\mathrm{d} \tag{2.4}$$

In equation 2.4, the global design quantity referring to the actions F_d is decoupled from the global design quantity related to the capacity of the system. From now on, the methods presented are focusing only on the safety margins related to the resistance part of 2.4.

2.4.1. Eurocode 2

Partial Factor Method

The Partial Factor method proposed in EN 1992-1-1, in essence, results in the design capacity of the members by analyzing the structure at hand with the design values of the material properties and the nominal values of the geometrical parameters a_{nom}. Those design values are calculated by the ratio between the characteristic values (with a 5% probability of not being exceeded) and the corresponding partial safety factors, γ_m. [35] For example, equation (2.5) shows the design resistance of a RC beam obtained with the format:

$$R_{\mathrm{d}} = R\{f_{cd}, f_{yd}, a_{nom}\} = R\left\{\frac{f_{ck}}{\gamma_c}, \frac{f_{yk}}{\gamma_s}, a_{nom}\right\} \tag{2.5}$$

$$\gamma_c \rightarrow \text{Partial factor for concrete}$$

$$\gamma_s \rightarrow \text{Partial factor for reinforcement steel}$$

However, when facing a RC structure, where NLFEA is a more suitable procedure to describe the global capacity, the Partial Factor method might not be suitable anymore. Due to running models with extremely low design values, the obtained stress distribution might not represent the real performance of the structure, which results in scenarios with significantly little probability of occurrence. The method is advisable for the reliability assessment at a member level. [1]

Global Resistance Factor Method

Therefore, in EN1992-2 a modification of the Partial Factor method results in another Safety Format for NLFEA. In summary, a NLFEA is performed with material properties with values closer to their most likely value. These new values are higher than the previously used design values, which represents an improvement in how realistic the response is modeled. Then, the value of the resistance is reduced by an additional resistance safety factor γ_R to finally obtain the design value of the capacity.[15]

$$R_{\mathrm{d}} = \frac{R_{\mathrm{NLFEA}}\{\tilde{f}_c, \tilde{f}_y, a_{nom}\}}{\gamma_R} \tag{2.6}$$

$$\tilde{f}_y = 1.1 f_{yk} = 1.27 f_{yd} \tag{2.7}$$

$$\tilde{f}_c = 1.1 \frac{\gamma_s}{\gamma_c} \alpha_{cc} f_{ck} = 1.27 f_{cd} \tag{2.8}$$

According to EN 1992-2:

$$\gamma_R = \gamma_\theta \times \gamma_{R_x} \tag{2.9}$$

$$\gamma_\theta = 1.06 \text{ and } \gamma_{R_x} = 1.20 \text{ then } \gamma_R = 1.27 \tag{2.10}$$

$$\gamma_{R_x} \rightarrow \text{Overall safety factor for the resistance related to the material uncertainty}$$

From this point onwards, the factor γ_θ always refers to the partial factor for the modeling uncertainty of the resistance. The concept of modeling uncertainty represents the accuracy of the numerical model in predicting the structural capacity. It is the relation between the results obtained by the NLFEA and benchmark tests. It provides an estimation of how accurate is the model, and how the assumptions made by the analyst influence the final results.

In the Eurocode, γ_θ is known as γ_{Rd}. Nevertheless, this document aims to unify the different notations among safety formats. Table 2.1 shows the unified symbols used along with the document and their equivalent in the original version of each Safety Format.

Even though the method deals with the concern of using extremely low material properties and establishes an "overall" resistance safety factor, there are still a few drawbacks. First, the modeling uncertainty factor that Eurocode suggests and uses for the derivation of the safety factors is derived from the analysis of beams and columns failing under bending or compression. More complex structures had more complex failure modes, which in most cases increases the modeling uncertainty. [35] Second, the procedure still focuses more on local checks and less on the general performance of the structure.

2.4.2. *fib* Model Code 2010

In the *fib* Model Code 2010 [21], section 7.11 refers to the "Verification assisted by numerical simulations" of reinforced concrete structures. The purpose of the section is to provide procedures to reach a target reliability level in applying numerical simulations, i.e. numerical methods as the NLFEA, for structural analysis problems. Thus, it provides an alternative to real-life testing procedures when they are not feasible. Besides establishing the need for clearly defined a solution strategy (all the decisions related to the kinematic, constitutive, and equilibrium conditions of the FE model) and guiding the calculation of the modeling uncertainty, it proposes three different safety formats fitting into different reliability levels for the calculation of the design resistance.

The design condition for checking the implicit limit state function follows a similar philosophy as equation (2.1), the main difference is that here it refers to the global bearing capacity of the structure and not only to local checks. It is relevant to highlight that when performing a NLFEA the limit state function is not explicitly formulated.

Sampling-based Method or 'Probabilistic' Method

The first method is based on a level I reliability method. The *fib* MC2010 calls it the Probabilistic Method. The design resistance, equation (2.11), is obtained directly from a required probability of failure or reliability index. The latter can be calculated by a Monte Carlo sampling or by Latin Hypercube sampling (LHS). Equal as in reliability theory, this method is the most accurate. However, it has a high cost regarding computational and engineering time. It requires running a great amount of deterministic NLFEA, which highlights the drawbacks of the approach. Once again, the more complex the structure, the more time the analysis takes, which leads to the searching for more practical and applicable methods for the industry.

$$P\left(\theta R_{\mathrm{NLFEA}}(\boldsymbol{x}) \le R_{\mathrm{d}}\right) = \Phi\left(-\alpha_R \beta_{\mathrm{LS}}\right) \tag{2.11}$$

$$R_{\mathrm{NLFEA}}(\boldsymbol{x}) \to \text{Estimated capacity by the NLFEA in function of the basic random variables } \boldsymbol{x}$$

$$\theta \to \text{Modelling uncertainty}$$

$$\beta_{\mathrm{LS}} \to \text{Target Reliability index for the limit state of interest}$$

$$\alpha_R \to \text{Reduction factor for the resistance}$$

Partial Factor Method

A Partial Factor method is presented as another alternative. It is mainly the same Partial Factor method proposed by the Eurocode in EN 1992-1-1 but with the use of NLFEA and explained in section 2.4. The previous means that the NLFEA is performed with the design values of the material properties.

$$R_{\mathrm{d}} = R_{NLFEA}\{f_{cd}, f_{yd}, a_{nom}\} = R_{NLFEA}\left\{\frac{f_{ck}}{\gamma_c}, \frac{f_{yk}}{\gamma_s}, a_{nom}\right\} \tag{2.12}$$

Global Resistance Methods

The last safety format proposed has two variants that fall into the category of Global Resistance Methods. They are based on a "simplified probabilistic approach" as defined in the *fib* MC2010. The first variant is the **Global Resistance Factor Method** (GRF). This method is mainly the modified Partial Safety method proposed in EN 1992-2 for NLFEA. It appears in the Dutch Guidelines [23] as the proposed safety format for NLFEA assessing ultimate limit state. Therefore, equations from (2.6) to (2.10) applied.

Estimation of a Coefficient of Variation: ECOV by Cervenka

The second approach relates with the so-called **Methods of Estimation of a Coefficient of Variation** or **ECOV** methods. This method calculates the design resistance, assuming it can be described as a random variable with a two-parameter log-normal distribution, as in Second Moment Reliability Methods. The two

parameters are the mean R_m and the coefficient of variation V_R or standard deviation σ_R of the resistance. The final design value is obtained as follows:

$$R_\mathrm{d} = \frac{R_\mathrm{m}}{\gamma_\theta \gamma_R} \tag{2.13}$$

$$R_\mathrm{m} = R_\mathrm{NLFEA}(f_{ym}, f_{cm}, a_{nom}) \tag{2.14}$$

$$\gamma_\theta \rightarrow \text{Model uncertainty factor}$$

$$\gamma_R \rightarrow \text{Global Factor of the resistance}$$

The main difference between the Global Resistance Methods resides in the formulation of the Global Factor of the resistance. In the ECOV method, γ_R is obtained using the Coefficient of Variation of the resistance random distribution. Equations (2.17) and (2.15) show the formulation for γ_R and the Coefficient of Variation of the resistance V_R. The formulas come from assuming a log-normal distribution with $V_R < 0.2$. Another aspect of the ECOV method is the need for a second NLFEA performed with the characteristic values of the material properties. It approximates the characteristic value of the resistance, R_k. The method includes this value in the derivation of the coefficient of variation.

$$V_{R_x} = \frac{1}{1.65} \ln\left(\frac{R_\mathrm{m}}{R_\mathrm{k}}\right) \tag{2.15}$$

$$R_\mathrm{k} = R_\mathrm{NLFEA}(f_{yk}, f_{ck}, a_{nom}) \tag{2.16}$$

$$\gamma_R = \exp(\alpha_R \beta_\mathrm{LS} V_R) \tag{2.17}$$

$$\gamma_\theta = \frac{1}{\mu_\theta} \exp(\alpha_R \beta_\mathrm{LS} V_\theta) \tag{2.18}$$

Ideally, the mean value of the modeling uncertainty, μ_θ, should be close to the unit since the NLFEA should lead to unbiased results.

2.4.3. Variations of the ECOV Method

Even though in the *fib* Model Code 2010, only one format of the ECOV method is presented, there are at least two other variations. Each of them mainly differs in the derivation of the coefficient of variation and in the number of NLFEA to be run during the application of the safety format. The ECOV method exposed in section 2.4.2 is derived by **Cervenka** in [8][7]

ECOV by Schlune

Another variation of the method is presented by **Schlune** et al. in [35]. This method seeks a wider application than the existing safety formats, which are most suitable for beams and columns. The previous is done by directly including the modeling uncertainty inside the calculation of the Global Factor of the resistance instead of using a separate modeling uncertainty factor, γ_θ. The design capacity as defined by Schlune is as follows:

$$R_\mathrm{d} = \frac{R_\mathrm{NLFEA}\left\{f_\mathrm{ym}, f_\mathrm{cm,is}, a_\mathrm{nom}\right\}}{\gamma_R} \tag{2.19}$$

$$\gamma_R = \frac{\exp(\alpha_R \beta_\mathrm{LS} V_R)}{\mu_\theta} \tag{2.20}$$

The assumption of the log-normal distribution for the resistance comes from the formulation of a simple stochastic model (section 2.3). It assumes that the resistance R is related to the nominal resistance R_n

by its product with the random variables F, G, and θ, representing the uncertainty in the material, in the geometrical parameters and the model (modeling uncertainty). The variables F, G, and M, in equation (2.21), are the ratios between the actual value of these quantities to their modeled or nominal value. If the resistance is taken as the product of random variables, according to the Central limit theorem the distribution of R tends to be log-normal.

Then, Schlune et al. in [35] proposed a calculation of the coefficient of variation of the resistance based on applying a first-order Taylor approximation for the limit state function (similar to what is done in the FORM calculation or level II reliability methods). In the final expression, the coefficient of variation of every random variable influencing the final resistance is accounted for separately. Equation (2.22) shows the formulation of V_R. Guidance for the calculation of the coefficients of variation of the modeling, geometrical and material uncertainties is provided in this alternative approach. For the modeling uncertainty, further research must be done depending on the case at hand. The geometrical coefficient of variation is proposed in [35] as $V_G = 5\%$. Focus is mainly given to the V_{R_x} value related to material uncertainty in the model.

$$R = R_{\mathrm{m}} \cdot F \cdot G \cdot \theta \tag{2.21}$$

$$V_R = \sqrt{V_{R_x}^2 + V_G^2 + V_\theta^2} \tag{2.22}$$

$$V_{R_x} \approx \frac{1}{R_{\mathrm{m}}} \sqrt{\sum_i^N \left(\frac{R_{\mathrm{m}} - R_{\Delta f_i}}{\Delta f_i} \sigma_{f_i} \right)^2} \tag{2.23}$$

$$V_G \approx 5\% \tag{2.24}$$

The design capacity equation (2.13) and equation (2.19) differ in the manner to include the coefficient of variation of the model uncertainty the safety format. For Schlune is through equation (2.22) and in the MC2010 (ECOV by Cervenka) is included through equation (2.18). The geometrical coefficient of variation is not included in the MC2010.

ECOV by Rosenblueth

The third ECOV approach is given by **Rosenblueth**. This method was proposed back in 1975. The method requires 2^N NLFEA with N being the number of random parameters included in the resistance calculation. Equations (2.25) and (2.26) present the general framework of the method. One drawback of this approach quickly pops up as the number of NLFEA to perform could be represented, and then the method might not be as effective as desired in practical applications. However, the method is widely applied in geotechnical analysis, also for NLFEA. [31]

$$R_{\mathrm{m}} \approx \frac{1}{2^N} \sum_i^{2^N} R_i \tag{2.25}$$

$$V_F \approx \frac{1}{R_m} \sqrt{\frac{1}{2^N} \sum_i^{2^N} (R_i - R_m)^2} \tag{2.26}$$

Pimentel et al. in [31] applied the three ECOV methods previously presented to simple structures with a unique failure mode: a RC beam under bending, a short column under axial force, and the same RC beam subjected to shear. His goal was to compare the effectiveness of the methods and draw conclusions on this. Figure 2.1 compares the number of NLFEA necessaries for each method, including a Monte Carlo simulation and the Partial Factor method from EN 1992-2. It also illustrates the value of the material parameters that must be utilized in each nonlinear analysis.
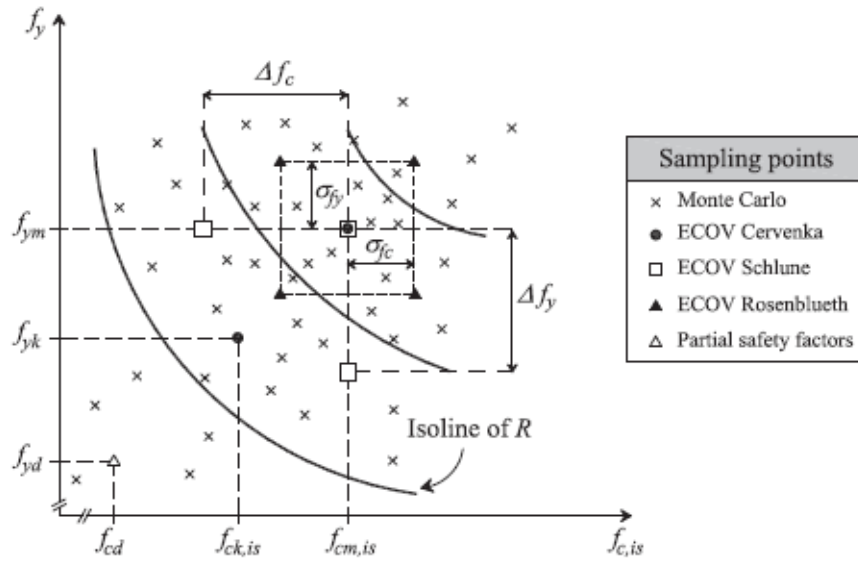
Figure 2.1: Sampling points used for the estimation of the material uncertainty coefficient of variation for the three presented ECOV methods. Source: [31]

Now, some questions arise from all the safety formats previously exposed. They have two main problems. First, the more accurate the safety formats are, as the probabilistic method, the more they require an enormous amount of NLFEA. The latter demands time, and in the industry, the time has a monetary cost. Second, according to the literature, methods in the category of the Global Resistance Methods are excellent in predicting the design capacity of simple structures with one 'easy to predict' failure mode, however: are they suitable for more complex systems where the failure mechanism is not evident at first and several failure modes are influencing the final performance of the structure and the stochastic description of the capacity?. At the same time, what happens when the resistance can not be approximated anymore as a log-normal distribution? How is the correlation between the input random variables included in the existing semi-probabilistic approaches?

Parameter	Notation in this document	GFM	GRF	ECOV Cervenka	ECOV Schlune
Safety Factor accounting for Modelling Uncertainty	γ_θ	-	γ_{Rd}	γ_{Rd}	-
Coefficient of Variation related to the Materials Uncertainty	V_{R_x}	V_{R_x}	-	V_R	V_F

Table 2.1: Unified symbols among Safety Formats

2.5. Background of the research

The focus of the *fib* Model Codes is to serve as worldwide guidance in all the stages related to the planning, design, execution, and posterior operational life of new concrete structures, as well as maintenance, rehabilitation, and dismantlement of existing ones. Additionally, safety is one of the major aspects that the Model Codes are willing to fulfill while including the latest technologies and requirements. [11] The Model Code is intended to be a source of updated information and background for those who are constantly involved in the development of new codes or versions of existing ones. [20]

As stated in previous sections, Non-linear Finite Element Analyses (NLFEA) are applied for determining the global structural capacity of concrete structures and their elements during the design of new structures and the assessment or strengthening of existing ones. The forthcoming *fib* Model Code 2020 (MC2020) includes the publication of chapter 27.10: Evaluation assisted by non-linear finite element analyses, which

gives guidance on the use of NLFEA in practice while achieving the desired target reliability.

First, the chapter introduces the concept of a solution strategy. Accounting to the problem at hand, the analyst should define a solution strategy applicable for the NLFEA. This solution must include the choices related to:[19]

1. Kinematic compatibility, e.g. finite element types and sizes

2. Equilibrium, e.g. iterative solution method

3. Material models, e.g. constitutive relations for concrete and reinforcement steel

Once the solution strategy is clearly defined, its accuracy in predicting the structural capacity is described by the modeling uncertainty. Here, the random nature of the parameters and decisions, directly and indirectly, influencing the model (like the ones made during the definition of the solution strategy) needs to be accounted for. The MC2020 established that the modeling uncertainty should be assessed by comparing NLFEA predictions to benchmark experimental outcomes. Moreover, it provides different methods in which the modeling uncertainty must be included depending on the choice of safety format: a mean value and a standard deviation or coefficient of variation is, in this case, relevant for the coming step. [19]

At this point, the structural capacity by NLFEA can be assessed. Three alternative methods (safety formats) will be available for this task. One of them is the new Global Factor Method (GFM). The GFM output is the design value of the resistance of a structure by performing two NLFEAs. The latter aligns with the necessity of reducing the amount of NLFEAs due to their high computational time. A smaller number of NLFEA means that the method is most likely to be included in practical applications. The GFM is closely related to the ECOV methods presented in Chapter 2, specifically the one proposed by Cervenka in [8]. It also includes some features of the ECOV by Schlune, especially in relation to the inclusion of the geometrical and modeling uncertainty. The GFM of the MC2020 is based on unpublished work by Monti, G. et al. (2021). The most relevant contribution of the GFM is the ability to account for so-called multiple concurrent failure mechanisms. To date, the verification and validation of the performance of the new GFM are very limited and the purpose of this project is to contribute to this direction.

3

New Global Factor Method

This section gives special attention to the theory behind the newly developed GFM. The main assumptions, logical arrangements, and probabilistic-based background utilized in the derivation of the analytical expressions of the design resistance, Global Safety Factor, and coefficient of variation are presented. It summarises the procedure of including and directly accounting for several Local Failure Mechanisms. These LFMs impact the overall capacity of the structure. Moreover, the general expressions for the practical application of the method are introduced. Finally, the section shows a simplified version of the Safety Format. Equations 3.3 and 3.4 respectively provide an upper and lower bound in terms of the survival probability. In the end, equivalent upper and lowers bounds for the design value of the capacity R_d are found.

3.1. Global Factor Method

Following the same format of previous Global Resistance Methods, the New GFM expresses the global design value of the capacity as the ratio of its mean value over a single Global Safety Factor γ_R related to the structure as a whole. The mean value is assumed to be the outcome of a NLA performed with the mean values of the influencing parameters or basic random variables. The Global Safety Factor must account for all the uncertainties influencing the analysis and the overall behavior of the structure. The previous implies that such a factor (γ_R) is case-specific. In consequence, providing predefined or standard values is not possible. The final goal is to obtain a design value of the global capacity that can reach the imposed target reliability.

Proposed by Monti et. al, the new approach aims to simplify the use of NLFEA, especially in complex systems. It provides an analytical expression for the Global Safety Factor γ_R that is derived based on the following facts and assumptions:

- The capacity of the system might be express in terms of any global quantity. That includes a global displacement, a global force, or any other outcome describing the overall non-linear behavior of the structure.

- Resisting mechanisms in a structural system might work as parallel or series systems. According to a predefined Limit State (LS) establishing failure, parallel arranged mechanisms must all fail in order to consider failure in the structure. On the contrary, in the case of mechanisms arrange in series the survival of the structure depends on the survival of each one of the mechanisms in the system.

- Monti et al. define failure as the exceeding of a predefined LS. The latter includes Serviceability LS (SLS) and Ultimate LS (ULS) for quasi-static loads. An example of the definition of a ULS is the yielding of the reinforcement caused by bending stresses. Additionally, Monti et. al define three more LS for seismic situations: Damage, Life Safety, and Collapse prevention LS. According to the chosen LS, a target reliability index β must be defined.

- During a NLFEA, the structure is taken into the inelastic range. At this stage, several resisting mechanisms at different elements or locations within the structure might reach the point of failure (LS-exceedance) in a concurrent or almost concurrent manner. Here, the importance of first identify all

17

possible Local Failure Mechanisms (LFM) influencing the attainment of global failure is highlighted. Subsequently, each LFM must be arranged in a hierarchical manner; series and parallel subsystems. The arrangement is based on how the role of each LFM influences the global probability of failure.

Monti et. al limits the organization of the LFM to three logical levels:

- LFMs ($k = 1...n_{\mathrm{m},ij}$) arranged into series subsystems (SS)

- SSs ($j = 1...n_{\mathrm{p},i}$) arranged into parallel subsystems (PS)

- PSs ($i = 1...n_{\mathrm{s}}$) arranged into series subsystems (SP)

Then, it defines the failure probability of each LFM and level as:

- $P_{f,ijk}$ is the failure probability of each LFM.

- $P_{f,ij}$ is the failure probability of each SS.

- $P_{f,i}$ is the failure probability of each PS.

- P_f is the failure probability of the structure, SP.

Therefore, the failure probability of each LFM as a function of the global quantity variable (R) can be define in terms of its capacity cumulative density function:

$$P_{f,ijk}(R) = F_{f,ijk}(R) \tag{3.1}$$

The failure probability of the structural system is presented as a function $\mathscr{F}[...]$ of the individual failure probability of each LFM playing a role in the global attainment of failure.

$$\mathscr{F}\left[P_{f,ijk}(R_{\mathrm{d}})\right] = \mathscr{F}\left[F_{ijk}(R_{\mathrm{d}})\right] = \hat{P}_f = \Phi\left(-\alpha_R \hat{\beta}\right) \tag{3.2}$$

Where:

- $\mathscr{F}[...] \rightarrow$ overall failure probability of the structural system as a function of the different failure probabilities $P_{f,ijk}(R)$

- $\hat{P}_f \rightarrow$ target probability of the predefined LS

- $\hat{\beta} \rightarrow$ target reliability index related to the LF

- $\alpha_R \rightarrow$ sensitivity factor related to the resistance part

- $R_{\mathrm{d}} \rightarrow$ the design value of the global response fulfilling the imposed reliability requirements

When defining $\mathscr{F}[...]$, the degree of correlation between the basic variables influencing the LFMs is decisive. However, its exact value is difficult to determine in real practice. Therefore, the GFM method produces two expressions for the survival probability of the systems: equations 3.3 and 3.4 respectively provide an upper and lower bound. The former equation (upper bound) is the product of assuming independent basic variables among the LFMs and the latter (lower bound) is the outcome of assuming fully correlated variables, which in the framework of the method coincides with the case of structures with a unique Failure Mechanism. In the end, equivalent upper and lowers bounds for the design value of the capacity R_{d} are found.

Upper bound: independent basic variables

$$\min_{n_{\mathrm{s}}} \max_{n_{\mathrm{p},i}} \min_{n_{\mathrm{m},ij}} \bar{F}_{ijk}(R_{\mathrm{d}}) = \left[1 - \left(1 - \Phi\left(\alpha_R\hat{\beta}\right)^{\frac{1}{n_{\mathrm{s}}}}\right)^{\frac{1}{n_{\mathrm{p}}}}\right]^{\frac{1}{n_{\mathrm{m}}}} \tag{3.3}$$

Lower bound: fully dependent basic variables

$$\min_{n_{\mathrm{s}}} \max_{n_{\mathrm{p},i}} \min_{n_{\mathrm{m},ij}} \bar{F}_{ijk}\left(R_{\mathrm{d}}\right) = \Phi\left(\alpha_R \hat{\beta}\right) \tag{3.4}$$

The next step in finding an analytical solution for the design resistance R_{d} is to assume a probability distribution for the capacity of each LFM, meaning the definition of $F_{f,ijk}(R)$. The final formulation of the method chooses the Log-normal distribution to that end. Thus:

$$R_{\mathrm{d}} = R_{\mathrm{m}} \exp\left[V_R \cdot z_{n_{\mathrm{s}},n_{\mathrm{p}},n_{\mathrm{m}}}\left(\alpha_R, \hat{\beta}\right)\right] \tag{3.5}$$

with:

$$z_{n_{\mathrm{s}},n_{\mathrm{p}},n_{\mathrm{m}}}\left(\alpha_R, \hat{\beta}\right) = \begin{cases} -\dfrac{1}{2}\left(\ln n_{\mathrm{m}} + \dfrac{\ln n_{\mathrm{s}} + 2\alpha_R \hat{\beta}}{n_{\mathrm{p}}}\right) & \text{upper bound (independent)} \\ -\alpha_R \hat{\beta} & \text{lower bound (fully dependent)} \end{cases} \tag{3.6}$$

Where:

- $n_{\mathrm{p}} = \max_{n_{\mathrm{s}}} n_{\mathrm{p},i}$

- $n_{\mathrm{m}} = \min_{n_{\mathrm{s}}}\left(\max_{n_{\mathrm{p},i}} n_{\mathrm{m},ij}\right)$

Finally, the Global Factor is defined from equation 3.5 as:

$$\gamma_R = \begin{cases} \exp\left[\dfrac{1}{2}V_R\left(\ln n_{\mathrm{m}} + \dfrac{\ln n_{\mathrm{s}} + 2\alpha_R \hat{\beta}}{n_{\mathrm{p}}}\right)\right] & \text{upper bound (independent)} \\ \exp\left(V_R \alpha_R \hat{\beta}\right) & \text{lower bound (fully dependent)} \end{cases} \tag{3.7}$$

Several Global Resistance Methods, as the ECOV methods or the one proposed in Eurocode 2, applied in the NLFEA environment were discussed in the previous chapter 2. The section 2.3 highlighted the principal assumption about the global resistance of the structures: the resistance as a log-normally distributed random variable. On the contrary, the new GFM does not require any specific knowledge about the type of distribution followed by the global quantity, which is an advantage of the format. In theory, this allows the Safety Format to be suitable to any structure independently of the amount of LFM influencing the stochastic structural behavior. However, the new GFM does assume a Log-normal distribution for the local resistance of each Failure Mechanisms. The derivation of the Global Safety Factor includes this assumption.

Hereafter, the complete set-up of equations of the GFM is summarized. The result is the design value of the overall capacity of the structure calculated with the application of NLFEA. The modelling (μ_{theta} and V_θ) and geometrical (V_G) uncertainties are finally included.

$$R_{\mathrm{d}} = \frac{R_{\mathrm{m}}}{\gamma_R} \approx \frac{R_{\mathrm{NLFEA}}\left(\boldsymbol{x}_{\mathrm{m}}\right)}{\gamma_R} \tag{3.8}$$

$$\gamma_R = \frac{1}{\mu_\theta} \exp\left[\frac{1}{2}V_R\left(\ln n_{\mathrm{m}} + \frac{\ln n_{\mathrm{s}} + 2\alpha_R \beta_{LS}}{n_{\mathrm{p}}}\right)\right] \tag{3.9}$$

$$R_{\mathrm{m}} = \min_{n_{\mathrm{s}}} \max_{n_{\mathrm{p},i}} \min_{n_{\mathrm{m},ij}} \mu_{\mathrm{R},ijk} \tag{3.10}$$

Where $\mu_{R,ijk}$ is the value of the global quantity that corresponds to the attainment of the local mean capacity $\mu_{L,ijk}$ in the $ijk-th$ LFM while performing a NLFEA with the mean values of the basic variables, therefore it is defined as the global mean capacity of the system. The LFM fulfilling this criterion will be called the 'Critical Local Failure Mechanism' (CLFM).

$$V_{R_x} \approx \frac{1}{c} \ln \frac{R_{\mathrm{m}}}{R_{\mathrm{var}}\left(x_{\mathrm{m}} - c\sigma_x\right)} \tag{3.11}$$

$$V_R = \sqrt{V_{R_x}^2 + V_G^2 + V_\theta^2} \tag{3.12}$$

Equation 3.11 refers to the Coefficient of Variation only related to the uncertainty of the basic variables or material parameters, V_{R_x}. The expression highlights the need for a second NLFEA, with perturbed values of the material parameters and relevant basic variables. The forthcoming section 3.1.1 includes a throughout revision of this formula. Finally, there is a final remark regarding the choice of the basic variables to be perturbed in the second NLFEA R_{var}. Given the case of assuming fully independent random variables between LFM, only the variables directly influencing the CLFM are perturbed. Nonetheless, whether full correlation among all the basic variables in the system is assumed, the perturbation $c\sigma_x$ will be applied to all the basic variables included in the NLFE model.

3.1.1. Revision of the formulation of the Coefficient of Variation with the sensitivity approach

Monti et. al propose an expression to calculate the coefficient of variation of the resistance related to the basic variables (equation 3.13). This section revises the derivation of the formula to obtain a better understanding of the background of the 'c' parameter and its inclusion in the new safety format. Some of the assumptions made in the derivation of the formula are clarified.

$$V_{R_x} \approx \frac{1}{c} \ln \left(\frac{R_{\mathrm{NLFEA}}(x_{\mathrm{m}})}{R_{\mathrm{NLFEA}}(x_{\mathrm{m}} - c\sigma_x)} \right) \tag{3.13}$$

As mentioned at the end of the previous section, the first assumption is related to the local resistance of each Failure Mechanism being modeled as a product of variables as in equation 3.14. Therefore, a log-normal distribution is used to describe the variability of each local quantity. Equation 3.15 shows the respective cumulative density function.

$$R_{ijk} = R_{\mathrm{m},ijk} \cdot F \cdot G \cdot \theta \tag{3.14}$$

$$F_{\mathrm{R}}(r) = \Phi \left(\frac{\ln(r) - \mu_y}{\sigma_y} \right) \tag{3.15}$$

From this point on, R refers to the local resistance of the CLFM, R_{ijk}. If R is log-normal distributed and $\ln R = Y$, then Y is normally distributed with mean μ_Y and standard deviation σ_Y. Then, the probability of the resistance to be in the interval lower or equal than a certain value R_{var} can be described by equation 3.16. Figure 3.1a shows the probability density function of the resistance where the blue shaded area in the graph represents the aforementioned probability $F_R(R_{var}) = P(r \leq R_{\mathrm{var}})$.

$$F_{\mathrm{R}}(R_{\mathrm{var}}) = P(r \leq R_{\mathrm{var}}) = \Phi \left(\frac{\ln(R_{\mathrm{var}}) - \mu_Y}{\sigma_Y} \right) \tag{3.16}$$

Figure 3.1b shows the probability density function of a standard normal distribution ($\mu = 0$ and $\sigma = 1$). The shaded area in green represents the probability of obtaining a value in the interval lower or equal than a certain value $-c$.

$$F_{\mathrm{X}}(c) = P(x \leq -c) = \Phi(-c) \tag{3.17}$$

By stating that the two shaded areas must have the same value for the probability, then:

$$F_{\mathrm{R}}(R_{\mathrm{var}}) = P(r \leq R_{\mathrm{var}}) = P(x \leq -c) = \Phi(-c) \tag{3.18}$$
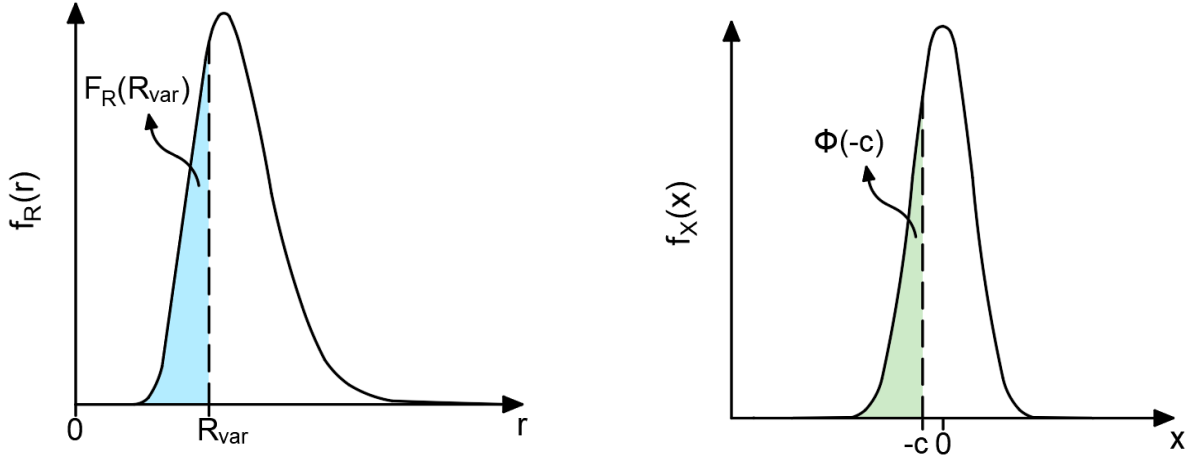
(a) Probability density function of the log-normal distributed resistance for the Critical Local Failure Mechanism

(b) Probability density function of a standard normal distribution

Figure 3.1: Probability density function of the log-normal distributed resistance for the Critical Local Failure Mechanism vs. a standard normal distribution

$$\Phi\left(\frac{\ln\left(R_{\text{var}}\right)-\mu_Y}{\sigma_Y}\right) = \Phi(-c) \tag{3.19}$$

$$\frac{\ln\left(R_{\text{var}}\right)-\mu_Y}{\sigma_Y} = -c \tag{3.20}$$

$$R_{\text{var}} = \exp(\mu_Y - c\sigma_Y) \tag{3.21}$$

With:

$$\sigma_Y = \sqrt{\ln\left(1+V_{R_x}^2\right)} \tag{3.22}$$

$$\mu_Y = \ln\left(R_{\text{m}}\right) - \frac{1}{2}\ln\left(1+V_{R_x}^2\right) \tag{3.23}$$

Where:

- $R_{\text{m}} = R_{NLFEA}(x_{\text{m}}) \rightarrow$ is the mean value of the resistance

- $V_{R_x} \rightarrow$ is the coefficient of variation of the resistance related to the material uncertainty

Replacing equations 3.22 and 3.23 in equation 3.21, a simplified expression for R_{var} is found:

$$R_{\text{var}} = \frac{R_{\text{m}}}{\sqrt{1+V_{R_x}^2}}\exp\left(-c\sqrt{\ln(1+V_{R_x}^2)}\right) \tag{3.24}$$

The previous expression can be further simplified if the value of the coefficient of variation of the resistance V_R is assumed to be always lower than 0.2. Therefore:

$$R_{\text{var}} \approx R_{\text{m}}\exp(-cV_{R_x}) \tag{3.25}$$

Finally, from equation 3.25, an expression for the coefficient of variation V_R can be found and it is comparable to equation 3.26 proposed by Monti et. al:

$$V_{R_x} \approx \frac{1}{c}\ln\left(\frac{R_{\text{m}}}{R_{\text{var}}}\right) \tag{3.26}$$

The remained issue is the definition of the R_{var} value of the resistance. According to Monti et. al (2021), this value can be determined by performing a NLFEA with the mean value of the basic variables reduced by the product of the 'c' parameter and the corresponding standard normal deviation of each variable. This definition of R_{var} implies that all the basic variables are normally distributed, which might not be the case for some of the material parameters usually assumed as log-normally distributed.

$$R_{\text{var}} = R_{\text{NLFEA}}(x_{\text{m}} - c\sigma_x) \tag{3.27}$$

3.2. Simplified Proposal: *fib* MC2020

A simplified approach of the method is finally included in the forthcoming version of the *fib* MC2020. The method is limited to the occurrence of two concurrent failure mechanisms in series or in parallel. The relation for the design value of the capacity is maintain.

$$R_{\text{d}} = \frac{R_{\text{m}}}{\gamma_R} \approx \frac{R_{\text{NLFEA}}(\boldsymbol{x}_{\text{m}})}{\gamma_R} \tag{3.28}$$

Single failure mechanisms or two (nearly) correlated concurrent failure mechanisms

$$\gamma_R = \frac{1}{\mu_\theta} \exp\left(\alpha_R \beta_{Ls} V_R\right) \tag{3.29}$$

Two (nearly) uncorrelated concurrent failure mechanisms

$$\gamma_R = \begin{cases} \dfrac{1}{\mu_\theta} \exp\left(\ln \sqrt{2} V_R + \alpha_R \beta_{LS} V_R\right), & \text{for series systems} \\[2mm] \dfrac{1}{\mu_\theta} \exp\left(\tfrac{1}{2}\alpha_R \beta_{LS} V_R\right), & \text{for parallel systems} \end{cases} \tag{3.30}$$

Equation 3.30 for series mechanisms is derived from equation 3.9 with: $n_{\text{m}} = 1$, $n_{\text{s}} = 2$ and $n_{\text{p}} = 1$. For parallel mechanisms: $n_{\text{m}} = 1$, $n_{\text{s}} = 1$ and $n_{\text{p}} = 2$.

The used of the characteristic value of the resistance is brought back in the calculation of the Coefficient of Variation, with x_{k} being the characteristic 5%-fractiles of the basic variables.

$$V_{R_x} = \frac{1}{1.645} \ln \frac{R_{\text{m}}}{R_{\text{k}}} \approx \frac{1}{1.645} \ln \frac{R_{\text{NLFEA}}(\boldsymbol{x}_{\text{m}})}{R_{\text{NLFEA}}(x_{\text{k}})} \tag{3.31}$$

3.3. Discussions

The new GFM appears as an alternative to the existing ECOV methods. The safety format aims to produce a final design value of the global capacity of complex systems by directly accounting for the influence of several Local Failure Mechanisms in the derivation of an analytical expression for the Global Safety Factor. Up to this point, all the assumptions about the probability distributions of the global capacity have been avoided. Therefore, the method seems to adjust by itself to possible bi-modal or even higher modes distributions.

While revising the proposed formulation for the Coefficient of Variation, the resistance modeled as a Log-normally distributed random variable comes to the picture once again. However, it is related to the stochastic behavior of the Local Resistance of each LFM and not to the Global Resistance of the system. This assumption seems to be supported by the fact that for relatively simple structures with a unique or dominant failure mechanism the resistance is accurately described by this type of distribution. It is relevant to highlight that the final expression of the Coefficient of Variation has a limitation of V_{R_x} being smaller or equal to 0.20.

At the same time, the assumption about the probability distribution of the input basic variables is discussed. The method implies that all the parameters to be perturbed follow a normal distribution. Often,

this is not the case for physical quantities since they present a better fit to a log-normal distribution. It is possible that in most cases this assumption will not highly impact the outcome of the analysis: the shape of the log-normal distribution might be similar enough to an equivalent normal distribution.

Finally, it is noticeable that the method provides instructions about handling correlated or uncorrelated parameters among LFM. Nonetheless, it seems to ignore the correlation between parameters of the same LFM, or at least it lacks clarity in the perturbation of such variables. From a more general point of view, the new GFM seems to leave to the engineering judgment the choice of the material parameters included as random variables in the analysis and the ones taken as deterministic variables. The deterministic characteristic might be directly derivated from the chosen random parameters.

Along with the following chapters, these points of attention will be analyzed and studied with the help of different case studies.

4

Analytical Expressions and Existing Safety Formats: Case 1

4.1. General considerations

In line with the proposed methodology in section 1.5, to validate and verify the usability of the new GFM method, especially on its applicability for continuous systems, a simplified representation of statically determined structures is studied in this chapter. Usually, a single dominant failure mode is assumed in these cases. The structures are analyzed by means of analytical expressions instead of NLFEA. The assumption of describing the failure mode only as one mechanism; named bending or shear is studied and discussed along with the derivation of the analytical expressions.

These simplified cases are included mainly to get experience and understanding in the application of existing safety formats. Moreover, it provides solid bases and better criteria for the implementation of the new Global Factor Method presented in chapter 5. The step-wise approach (starting from simplified cases up to more complex ones) provide tools and scenarios for the comparison and verification of the new GFM method. At the same time, it allows the possibility of study the consequences of engineer judging errors, since this is one of the main causes of structural failure. [37]

Pimentel et al. already demonstrated in [31] that for statically determinate structures analyzed at a member level, applying different safety formats leads to comparable results as long as the same target reliability is considered. Consequently, the results obtained by Pimentel et al. with the partial safety factor (PSF) and the global safety factor with the estimation of the coefficient of variation according to Cervenka (ECOV Cervenka) are reproduced aiming to obtain a valid starting point. For statically determined structures "any differences in the calculated capacity should depend mainly on the accuracy of the method of analysis and not of the safety format itself".[31]. At the same time, the correct derivation of the analytical expressions for the cross-section capacity, named bending resistance or shear resistance, becomes of importance in drawing valid conclusions from the results obtained with the Global Factor Method.

The geometrical and material properties, along with the derivation of the analytical expression, are presented in the following sections. Subsequently, the two mentioned safety formats are applied and verified with results in [31]. Finally, employing a Monte Carlo simulation procedure (a full probabilistic reliability method), the resistance value obtained by the two partial safety formats (semi-probabilistic methods) is analyzed. The aim is to determine its reliability and identify the regions where the results are not conservative enough. [32]

4.2. Basic variables

A basic variable can be described as the relevant part of a set of variables representing a physical quantity, related to actions and environmental influences, geometrical quantities, and material properties. [20] The uni-axial concrete compressive strength f_c is the most often tested and analyzed parameter related to this

Case study 1a

RC cross-section in bending
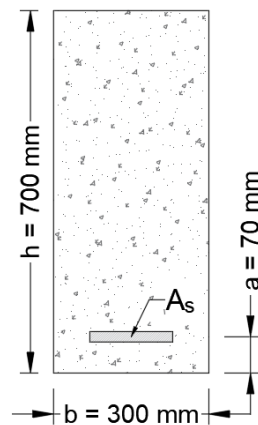
Figure 4.1: Rectangular RC cross-section with longitudinal reinforcement in bending. Source: [31]

material. Other representative parameters as Young's modulus of elasticity E_c or ultimate strain ε_{cu} are strongly correlated with the concrete compressive strength. Therefore, they are usually derived from this quantity. [42] Moreover, together with the yielding strength of the reinforcement f_y, their dispersion have the most influence on the variability of the resistance of beams. Dispersion for other variables may be neglected, and their value is normally taken as their most likely values i.e mean value. [20]

Likewise, in the coming sections, the parameters considered to induce the majority of the material uncertainty, and used as input basic variables in future calculations are:

- Concrete compressive strength $\rightarrow f_c$
- Reinforcement yield strength $\rightarrow f_y$

The values of the mean and standard deviations besides the models and assumed distributions applied in Pimentel are based on proposed statistical information available in [42] and accordingly implemented in this thesis.

For basic variables, design values include reliability margins. For other variables, whose dispersion may be neglected or is covered by a set of partial factors, they are normally taken equal to their most likely values.

4.3. Case 1a: Rectangular RC cross-section in Bending

The first case, introduced in the previous section 4.1, is a representation of a simply supported beam with longitudinal reinforcement in the tensile side. The member is assumed to be subjected to bending: the moment resistance defines the capacity for the given limit state. The chosen analytical expression results in the moment capacity of a rectangular cross-section for variable reinforcement ratios. This provides the opportunity to verify and compare, at a member level, the results obtained by the GFM with the existing safety formats: the Partial safety factor (PSF) proposed in Eurocode 2 and the global safety factor with the estimation of the coefficient of variation according to Cervenka (ECOV Cervenka) proposed in the *fib* Model Code 2010.

4.3.1. Geometrical and material properties

Figure 4.1 shows the cross-section configuration and the mean values of the geometrical parameters. The analysis has been carried out with non-linear material models according to Eurocode 2; parabola-rectangle constitutive law for the concrete and an elastic-perfectly plastic law for the reinforcement steel.

The same mean values and probability distributions from the setup proposed by Pimentel et al. [31]

are applied, which provides a point of reference to verify the accuracy of the results. The concrete is class C30. The characteristic yield strength is 500 MPa. The yielding strain of the reinforcement is assumed to be obtained by the ratio between the corresponding yielding strength f_y^* and Young's modulus ($E_s = 200\,GPa$). Table 4.1 shows the mean and characteristic values of the relevant parameters for each material. Figure 4.2 illustrates a graphic representation of the selected constitutive relations. The Young's modulus of the reinforcement steel (E_s), as well as the limit strains in the concrete (ε_{c2} and ε_{cu2}) are assumed to be deterministic. The material parameters used in this section are closely related to real values present in several structures in daily practice.

Parameters	
Concrete	
Characteristic compressive strength	$f_{ck} = 30\,\text{MPa}$
Mean compressive strength	$f_{cm} = f_{ck} + 8 = 38\,\text{MPa}$
In-situ mean compressive strength	$f_{cm,is} = \frac{f_{cm}}{1.15} = 33\,\text{MPa}$
Strain at reaching maximum strength	$\varepsilon_{c2} = 2\%_o$
Ultimate strain	$\varepsilon_{cu2} = 3.5\%_o$
Reinforcement steel	
Characteristic yielding strength	$f_{yk} = 500\,\text{MPa}$
Mean yielding strength	$f_{ym} = 534\,\text{MPa}$
Young's modulus	$E_s = 200\,\text{GPa}$

Table 4.1: Relevant material parameters

In Eurocode 2, the equation of the parabola for the stress in the concrete when the strain in the material ε_c is smaller or equal than ε_{c2} is:

$$\sigma_c = f_c^* \left[1 - \left(1 - \frac{\varepsilon_c}{\varepsilon_{c_2}} \right)^n \right] \quad for \quad \varepsilon_c \leq \varepsilon_{c2} \tag{4.1}$$

Where:

- $f_c^* \rightarrow$ is the relevant value of the concrete strength (mean, characteristic, design...)

- $\varepsilon_c \rightarrow$ is the strain in the concrete

- $\varepsilon_{c2} \rightarrow$ is the strain at reaching the maximum strength depending on the strength concrete class

- $\varepsilon_{cu2} \rightarrow$ is the ultimate strain depending on the strength concrete class

- $n \rightarrow$ exponential depending on the strength concrete class

(a) Concrete   (b) Steel
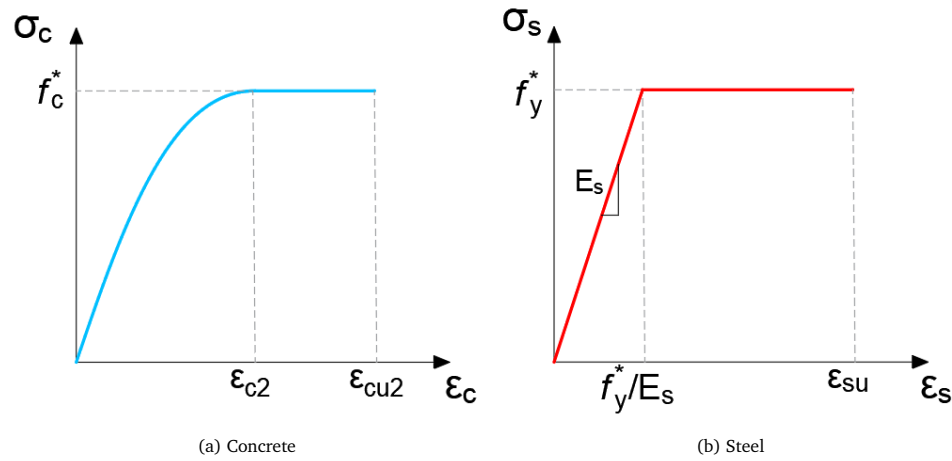
Figure 4.2: Eurocode constitutive material relations

4.3.2. Analytical expression for the limit state

The analytical model is based on assuming that the equilibrium of forces is fulfilled at any stage. Figure 4.3 shows the stress-strain diagram for the rectangular cross-section. It is assumed that the most upper fiber of the concrete in compression always reaches the ultimate strain. The resultant force in the concrete along with its application point is obtained by integration over the height of the compression zone. The complete derivation can be found in Appendix A.

The equilibrium of internal horizontal forces and moments around the neutral axis is given by equations 4.2 and 4.3, as follows:

$$F_c = F_s \tag{4.2}$$

$$M_R = F_c \cdot z \tag{4.3}$$

where:

$$F_c = \frac{17}{21} b x f_c^* \tag{4.4}$$

$$F_s = A_s \sigma_s^* \tag{4.5}$$

Finally, an expression for the bending resistance of the cross-section is obtained in equation 4.6 as function of different reinforcement ratios $0.005 \leq \rho \leq 0.05$:

$$\frac{M_R}{bd^2} = \rho \sigma_s^* - \frac{297}{578} \frac{\rho^2 \sigma_s^{*2}}{f_c^*} \tag{4.6}$$

with:

$$\rho = \frac{A_s}{bd} \tag{4.7}$$

As a unique expression referring to the bending capacity can define the resistance of the cross-section, two different descriptions of the actual failure mechanism are possible. This division can be relevant for the future application of the GFM: it is one of the key points in the applicability of the new method for continuous structures. The amount of reinforcement defines two possible failure scenarios: assuming a linear distribution and the compatibility of strains between the concrete and the reinforcement. For low reinforcement ratios ($\rho < 0.02$), a ductile failure is governed by the yielding of the reinforcement. On the other side, for over-reinforced sections ($\rho > 0.03$), brittle failure is governed by the crushing of concrete. The analytical expression includes this division by using the relevant value of the reinforcement steel stress σ_s^*. Then:

$$\sigma_s^* = E_s \varepsilon_s \qquad \text{if } \varepsilon_s < \varepsilon_{sy} \tag{4.8}$$

$$\sigma_s^* = f_y^* \qquad \text{if } \varepsilon_s \geq \varepsilon_{sy} \tag{4.9}$$

A theoretical calculation of the strain in the reinforcement steel ε_s when the most outer fiber of the concrete reaches its ultimate strain ε_{cu2} is found in Appendix A.
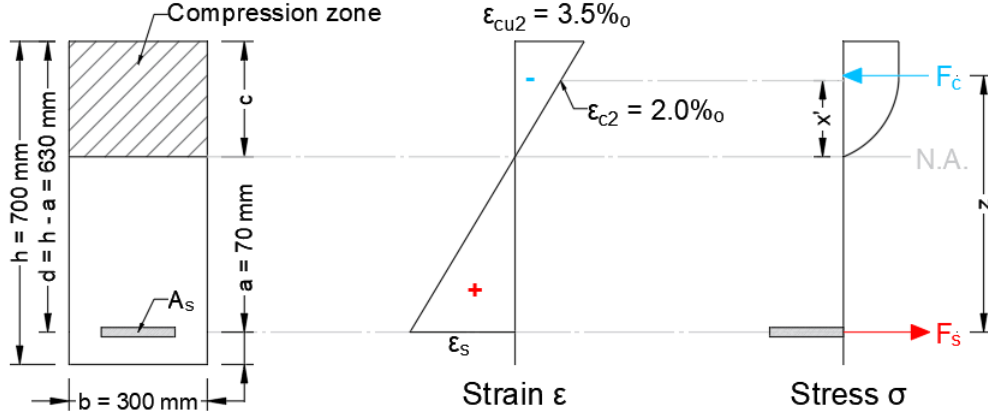
Figure 4.3: Stresses, strains and force equilibrium assumed along the cross-section.

4.3.3. Design resistance: PSF and ECOV Cervenka

One of the main objectives in this section is getting insight into the application of existing safety formats. The design value of the resistance is obtained using the Partial Safety Factor (PSF) method [15] and the Global Factor method with the calculation of the coefficient of variation of the resistance according to Cervenka (ECOV Cervenka)[8].

The PSF accounts for all types of uncertainties through a material partial safety factor. The design resistance at a cross-section level $M_{Rd,PSF}$ is obtained by performing only one analysis with reduced material parameters; the design values. These are obtained by the ratio between the characteristic values of the relevant material properties and their corresponding partial safety factor. Therefore, the values of the material parameters used in calculating the design bending moment resistance with equation 4.6 according to the PSF are:

$$f_c^* = f_{cd} = \frac{f_{ck,is}}{\gamma_c} = 20\,MPa \tag{4.10a}$$

$$f_y^* = f_{yd} = \frac{f_{yk}}{\gamma_s} = 434.78\,MPa \tag{4.10b}$$

With the well-known values for the partial factor for concrete and reinforcement steel:

$$\gamma_c = 1.5$$
$$\gamma_s = 1.15$$

Then, the resistance is calculates by the design values of the two basic variables:

$$M_{Rd,PSF} = M_R(f_{cd}, f_{yd}, \rho) \tag{4.11}$$

In the ECOV method, two analyzes must be performed; the formulation of the global coefficient of variation V_R requires the mean M_{Rm} and characteristic values M_{Rk} of the resistance. The former is obtained by evaluating the analytical expression for the cross-section capacity (equation 4.6) with mean in-situ values of the basic material parameters. The latter uses the 5% percentile values of the in situ material strength parameters known as characteristic values. These are determined by their mean values and the coefficient of variation of each material. Table 4.2 summarize the characteristic values for the concrete compressive strength, reinforcement yielding strength, and corresponding lumped coefficient of variations.

$$f_{ck,is} = f_{cm,is} \cdot e^{-1.645 V'_{fc}} \tag{4.12a}$$

$$f_{yk} = f_{ym} \cdot e^{-1.645 V'_{fy}} \tag{4.12b}$$

Pimentel et al. implemented the use of a lumped coefficient of variation V_f' specific to each material. It includes the material and model uncertainties. It allows a direct comparison between the results of both safety formats; a global modeling uncertainty is not defined for the analytical case, therefore it is included in the safety format in an alternative way. The calculation of the lumped coefficient V_f' is as follows:

$$V_f' = \sqrt{V_f^2 + V_{\theta_i}^2} \tag{4.13}$$

Material	V_f	V_{θ_i}	V_f'	$f_{k_i}\,[MPa]$
Concrete	0.15	0.05	0.158	25.46
Reinf. steel	0.04	0.025	0.047	494.01

Table 4.2: Lumped coefficient of variation for each material and characteristic value

Since the variability caused by the modeling uncertainty is implied in the lumped V_f' of each material and therefore directly included in the coefficient of variation of the system related to the material uncertainty V_F calculated as in equation 4.14; only the variation due to geometrical uncertainty V_G remains to be included in the global coefficient of variation of the resistance V_R. Then, the global coefficient of variation of the resistance is finally obtained with expression 4.16. Equation 4.17 calculated the global safety factor for the resistance γ_R with a target reliability index $\hat{\beta} = 3.8$ and a sensitivity factor for the resistance part $\alpha_R = 0.8$.

$$V_F = \frac{1}{1.645} \ln\left[\frac{M_{Rm}(f_{cm,is}, f_{ym}, \rho)}{M_{Rk}(f_{ck,is}, f_{yk}, \rho)} \right] \tag{4.14}$$

$$V_G = 0.05 \tag{4.15}$$

$$V_R = \sqrt{V_F^2 + V_G^2} \tag{4.16}$$

$$\gamma_R = \exp(0.8 \cdot 3.8 \cdot V_R) \tag{4.17}$$

Finally, it is possible to calculate the design value of the resistance according to ECOV Cervenka for different reinforcement ratios as follows:

$$M_{Rd,Cervenka} = \frac{M_{Rm}(f_{cm,is}, f_{ym}, \rho)}{\gamma_R} \tag{4.18}$$

In figure 4.4a four different lines representing the bending moment resistance for longitudinal reinforcement ratios between $0.005 \leq \rho \leq 0.05$ are plotted; the first three are the result of evaluating the same analytical expression (equation 4.6) with the mean M_{Rm}, characteristic M_{Rk} and design $M_{Rd,PSF}$ basic material parameters for different reinforcement ratios. The last line is the design resistance $M_{Rd,Cervenka}$ obtained by the ECOV Cervenka approach.

(a) Bending moment resistance

(b) Resistance safety factor
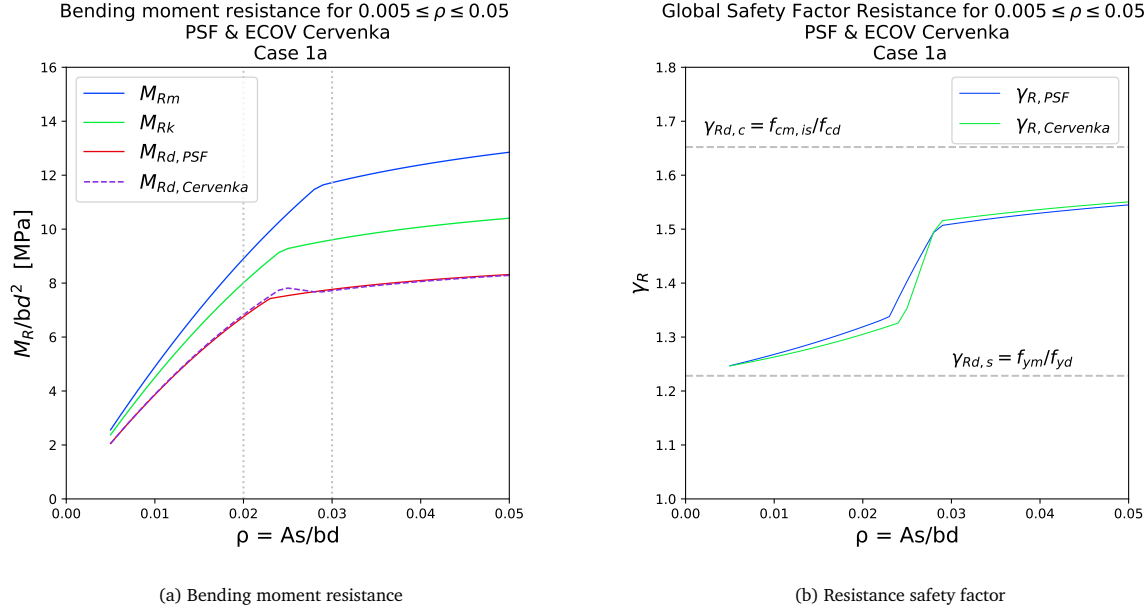
Figure 4.4: Results Existing Safety Formats: case 1a

Even though there is only one general analytical expression in calculating the bending resistance of the cross-section, the value of the strain reached by the reinforcement causes the change in slope around the middle range of reinforcement ratios (around $\rho \approx 0.025$) in figure 4.4a. The previous has a well-known explanation: for low reinforcement ratios, the yielding strain value is reached, then it is assumed that stresses in the reinforcement can be taken as the yielding strength f_y and a ductile failure mechanism develops mainly influenced by this property. On the other side, for high reinforcement ratios, the compression zone above the neutral axis crushes since the concrete ultimate strain ε_{cu2} in the most outer upper fiber appears before the yielding strain in the reinforcement has developed. In that case, the concrete strength f_c is the property leading to a brittle failure mechanism.

The region around the point where the analytical expression goes from one failure mechanism description to another is of high interest in the upcoming application of the new GFM. It opens a discussion about bending failure as a single mechanism. The different descriptions of local damage, in the properties and regions of the section involved in the global failure, lead to the idea that the term "bending failure" might not be enough. Therefore, a detailed division might be implemented to obtain more conservative results in regions where the capacity is closely related to both mechanisms. It is interesting to observe that, around this region, two different failure mechanisms develop for the mean and characteristic values of the material parameters. At the same time, the design resistance obtained by the ECOV method by Cervenka seems to overestimate the design resistance in comparison to the resistance calculated with PSF for the same intermediate zone.

In figure 4.4b an estimate for a global resistance factor is obtained for the PSF method approach by dividing the mean value of the resistance with the design resistance calculated with this format. At the same time, the figure shows the global factor for the resistance calculated by the ECOV Cervenka method with equation 4.17. It is observed that for the middle region of the reinforcement ratios the global factor obtain by the ECOV Cervenka is smaller than the estimated for the PSF, which is in agreement with the overestimation of the resistance previously observed in figure 4.4a. Upper and lower limits for the γ_R are also plotted: the upper limit is the partial safety factor of the concrete strength and the lower limit marks the partial safety factor of the yielding strength. Once again, a transition from obtaining γ_R closer to the partial safety factor of the reinforcement steel for low reinforcement ratios and γ_R tending to the partial safety factor of the concrete for high reinforcement ratios is noticed. Thus, opening once again the idea of having two concurrent failure mechanisms in sections with intermediate reinforcement ratio.

$$\gamma_{R,PSF} = \frac{M_{Rm}}{M_{Rd,PSF}} \tag{4.19}$$

Cross-sections with intermediate reinforcement ratios are a more suitable representation of structures in real practice. That is because the balanced section will not lead to a brittle failure or to under reinforced structures. Therefore, it is important to verify if the reliability of the resistance obtained by the PSF method and the ECOV Cervenka method complies with the impose target reliability index for the resistance part ($\alpha_R = 0.8 \cdot \hat{\beta} = 3.8$), especially in the intermediate region. Hereafter, a Monte Carlo simulation is applied as a full probabilistic reliability method, allowing for comparing the level of reliability of each safety format with the obtain probability distribution for the resistance.

4.3.4. Monte Carlo simulation: comparison and verification

A Monte Carlo Simulation is a Level III reliability method: in its crude form, the probability of failure related to a defined Limit State Function (LSF) is calculated exactly by generating a representative amount of random samples or simulations of the input random variables distributions to finally perform deterministic evaluations of the LSF for each of these set of samples. [27] The failure probability is obtained from the number of failures over the total number of simulations. [32] Usually in reliability-based procedures the performance of the structure must be expressed by a clear relationship among resistance and load variables. This relation is presented in the form of a LSF, Z, which in its simplest form can be expressed as:

$$g(X) = Z = R - S = 0 \tag{4.20}$$

R is the resistance variable and S refers to the load effects. Thus, the probability of failure of the system is $P_f = P[R < S]$, given that failure occurs when Z is smaller than zero. Even though MCS is based on simple concepts, the accuracy of the obtained failure probability highly depends on the number of simulations performed. [32] In more practical or complex cases, for instance, when non-linear finite element analyses are applied to study structural reliability of systems, these LSF might be available only in an implicit form. Therefore the cost of highly time-consuming numerical methods would transform MCS into an unpractical tool. [6]

In Case 1a, and further in Cases 1b and 1c, since an analytical expression is derived for the resistance part, the problem does not lay in the definition of an explicit formulation. The issue arises in defining a Limit State Function that focuses only on the resistance part since the load effects are not being included. Therefore, the aim is to evaluate the performance of the two applied safety formats by defining the LSF as:

$$g(X) = Z = M(X) - M_{Rd,SF} = 0 \tag{4.21}$$

Where:

- $M(X) \rightarrow$ is simulated by evaluating the analytical expression with random samples of each variable in the vector X.

- $X \rightarrow$ is the vector of random variables

- $M_{Rd,SF} \rightarrow$ is the design capacity obtained with the relevant Safety Format for each reinforcement ratio ρ. Thus, SF being PSF in the case of the capacity obtained with the Partial Factor method and SF being Cerv for the capacity obtained by ECOV by Cervenka method.

For 45 reinforcement ratios between $0.005 \leq \rho \leq 0.05$, one million simulations of $M(X)$ are performed. Figure 4.3 presents the distribution of the random variables in vector X used in the Monte Carlo simulation. The probability of failure related to the estimation of the design resistance by each Safety Format is defined as $P_f = P[M_{Rd,SF} < M(X)]$. A reliability index β_{SF} associated with the reliability of the estimation of the design resistance by each Safety Format might be express as:

$$\beta_{SF} = -\frac{\Phi^{-1}(P_f)}{\alpha_R} \tag{4.22}$$

The coefficient of variation $V_{R,M(X)}$ of the simulated resistance $M(X)$ for each reinforcement ratio is obtain by calculating the mean and the standard deviation of the $n = 1000000$ simulations. Figures 4.5a and 4.5b illustrate the reliability index for the Safety Formats in comparison with the defined target reliability (β_{SF}

and $\hat{\beta} = 3.8$), and the coefficient of variation $V_{R,M(X)}$ along the range of reinforcement ratios in comparison with the estimation of the coefficient of variation by the ECOV method.

$$\bar{x}_{M(X)} = \frac{\sum_{i=1}^{n} M(X_i)}{n} \tag{4.23}$$

$$\sigma_{M(X)} = \sqrt{\frac{\sum_{i=1}^{n} (M(X_i) - \bar{x}_{M(X)})^2}{n-1}} \tag{4.24}$$

$$V_{R,M(X)} = \frac{\sigma_{M(X)}}{\bar{x}_{M(X)}} \tag{4.25}$$

Variable	Distribution	Mean	Standard Dev.	Units
$f_{c,is}$	Lognormal	33	5.22	MPa
f_y	Lognormal	534	25.2	MPa
h	Normal	700	10	mm
b	Normal	300	5	mm
a	Normal	70	10	mm
A_s	Normal	Variable	0.02∗Mean	mm^2

Table 4.3: Random basic variables used in the Monte Carlo simulation: case 1a. Source:[31]
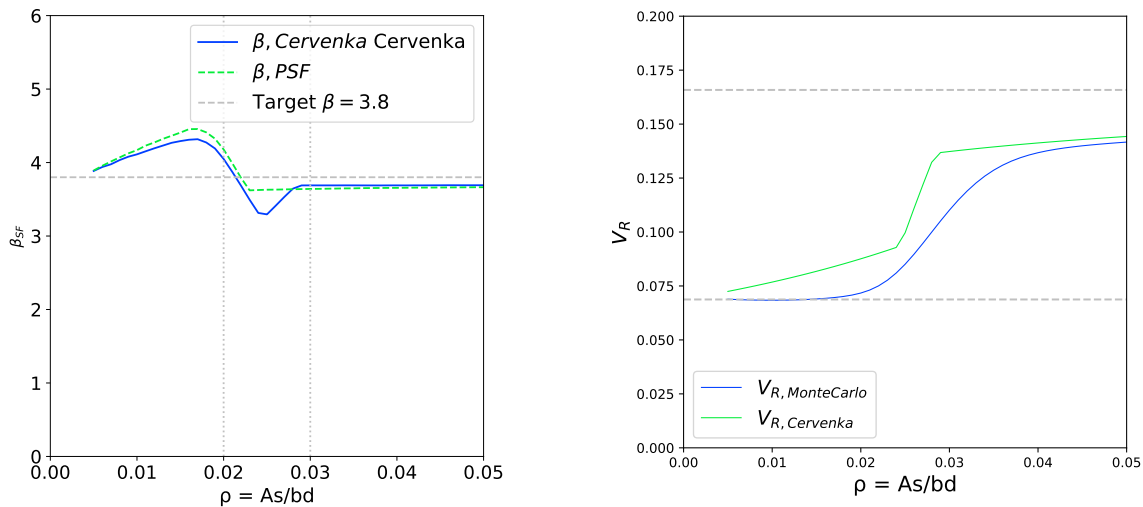
(a) Reliability index related to each estimation of the design resistance by PSF and ECOV by Cervenka

(b) Coefficient of Variation Resistance

Figure 4.5: Monte Carlo Simulation Results: Case 1a

Pimentel followed a similar procedure in [31]. The assumption of the resistance being log-normally distributed is evaluated by plotting the normalized histograms of the 1 million simulations of the moment resistance for some relevant reinforcement ratios as visualizing in figures 4.6. A log-normal distribution is fitted per graph. In addition, the percentage of samples falling in a ductile bending mode and brittle bending mode are presented. The left upper corner shows the mean and standard deviation of the sample used to fit the log-normal distributions.
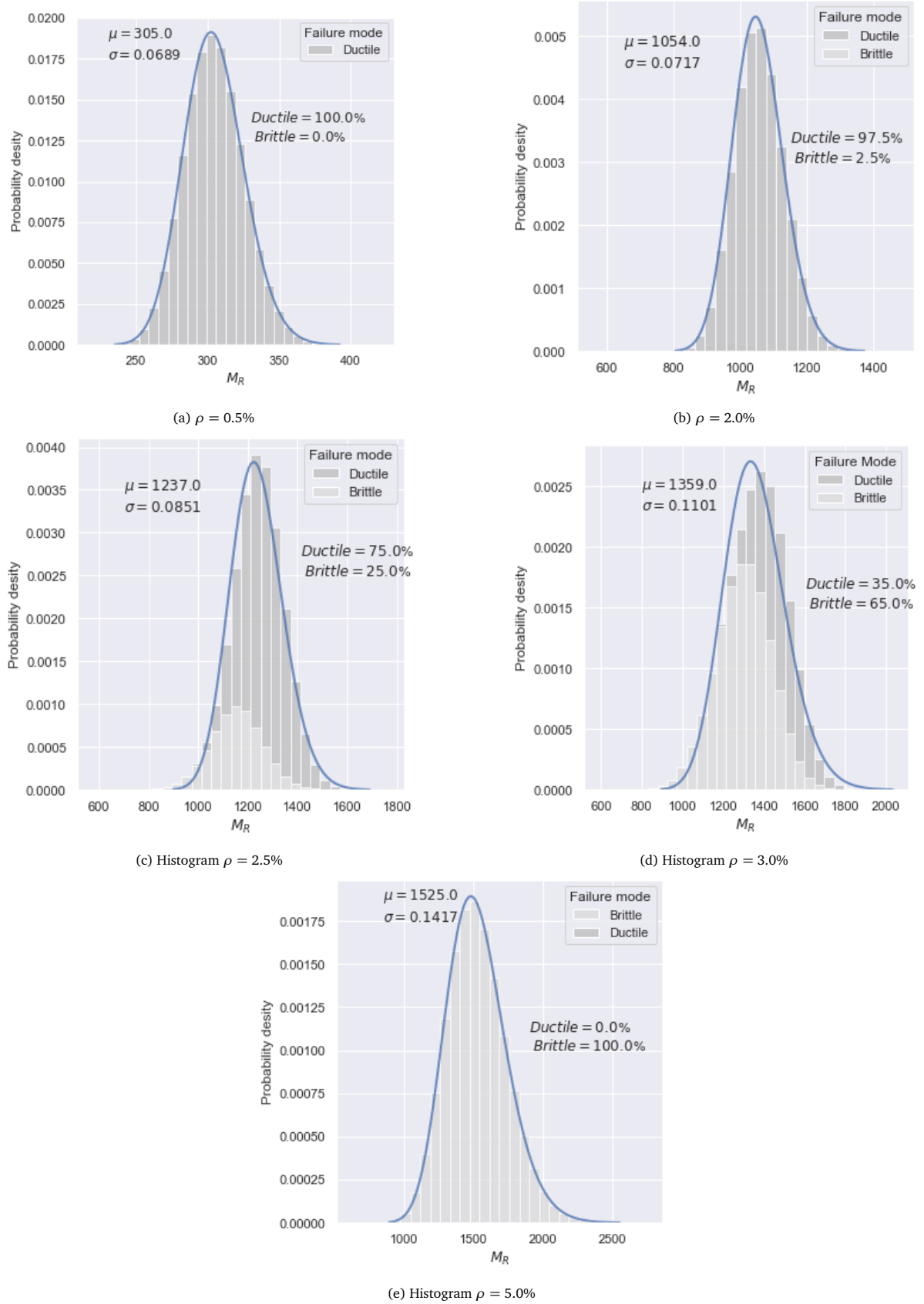
Figure 4.6: Histograms obtained from the Monte Carlo simulations for the Bending moment resistance and fitted log-normal distribution for longitudinal reinforcement ratios $\rho = [0.5\%, 2.0\%, 2.5\%, 3\%, 5\%]$

Discussion

In figure 4.6, it is noticed that for very low reinforcement ratios $\rho \approx 0.5\%$, all the simulated samples fail in the same ductile manner. On the contrary, highly over-reinforced cross-sections $\rho \approx 5\%$ fail in the described brittle bending failure with the sudden crushing of concrete. However, when looking into the regions for intermediate reinforcement ratios, the percentage of having one bending failure or the other highly varies. There is a clear transition between the two extreme cases as the reinforcement ratio in the cross-section increases, supporting the further arbitrary definition of the boundaries limiting the transition zone between brittle and ductile failure in the next chapter.

An interesting observation, done by Pimentel et. al in [31], is discussed hereafter. For intermediate reinforcement ratios, the fitted log-normal distribution does not agree with the simulated samples as accurately as for higher or lower ratios. It is highlighted that, with more refined statistical inference methods, new values for the mean and standard deviation could be found. They could provide a better fit to the calculated distribution, especially for the lower tail region: the most critical one when studying the resistance part. However, the global factor method does not make use of the probability distribution of the Global Resistance. Thus, this path is out of the scope of this work. A study in this direction would provide better accuracy to the already existing ECOV by Cervenka safety format, but it will not impact the formulation of the GFM. Besides, in practice, the mean and standard deviation of the simulated sample is not known: the idea is to avoid a high number of computationally expensive numerical methods that in the end is the only way to provide such knowledge.

In the GFM the challenges related to concurrent failure mechanisms are directly accounted for in the derivation and calculation of the Global Safety Factor, γ_R.

4.4. Case 1b: Rectangular RC cross-section in Shear

In this section, Case 1b is once again a representation of a simply supported beam. The design shear resistance for a cross-section with stirrups is studied in this case. For a range of shear reinforcement ratios, the capacity is calculated using an analytical expression derived from the framework of the Variable-strut-angle method found in EN1992-1-1. The longitudinal reinforcement of the cross-section remains in the same location as in case 1a: it is necessary for the transmission of forces in the truss analogy model. The obtained design capacity of the section is compared between applied safety formats: the PSF and the ECOV by Cervenka method. The results from the Monte Carlo Simulation are analyzed to determine the effectiveness of existing methods for case 1b.

4.4.1. Geometrical and material properties

Figure 4.7 shows the same cross-section configuration and the nominal values of the geometrical parameters than in case 1a with the addition of the shear reinforcement, A_{sw}. Since the set up of the RC cross-section is taken from Pimentel et al. [31] as in case 1a, identical values of the material parameters, probability distributions ans constitutive laws are applied in this case. Reference is made to table 4.1 for mean and characteristic values of the in-situ concrete compressive strength and the reinforcement yielding strength.
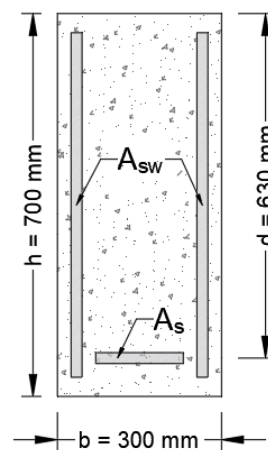
Figure 4.7: Rectangular RC cross-section with shear and longitudinal reinforcement subjected to shear. Set up taken from [31]

4.4.2. Analytical expression

Achieve an accurate description of shear behaviour is one of the most challenging aspects of the study of reinforced concrete structures. [30] A simplified analytical expression for the shear resistance of the RC cross-section is derived from the equations given in section 6.2.3 (Members requiring shear reinforcement) in Eurocode 2 (EC2). Those design expressions are obtained by applying the Variable-Strut-Tie model: the concept is based on the lower bound theorem of plasticity. The transmission of internal forces within the beam is represented by a truss model with reinforcement elements working in tension (ties) and concrete zones in compression (struts). It is acknowledged that the present model is a highly simplified procedure and some of the shear transfer mechanisms listed hereafter are not included

- Interface shear transfer

- Dowel action of longitudinal reinforcement

- Shear stress in the un-cracked compression zone

Nonetheless, the method has proven to provide conservative values of the resistance, especially for beams with low shear reinforcement ratios when they are comparing to tests results. This is mainly due to neglecting the concrete contribution to shear resistance. [30][4][22]
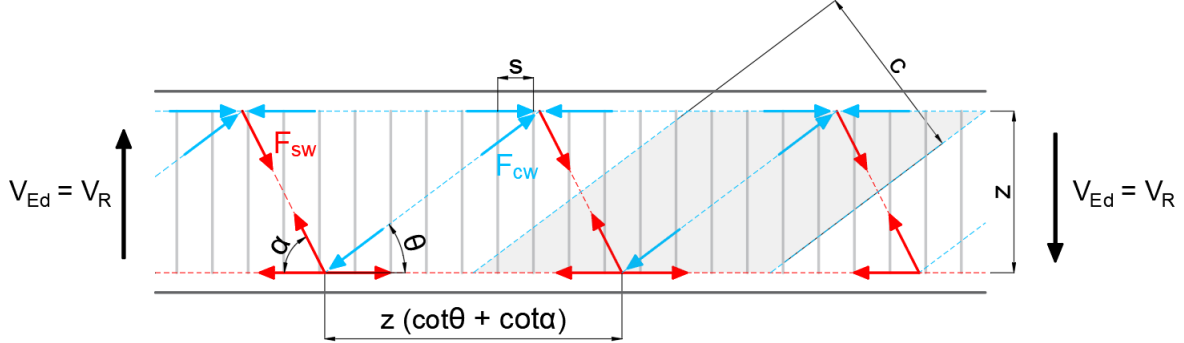
Figure 4.8: Forces of the truss model

According to EC2 [15], the design shear resistance of members with vertical shear reinforcement is governed by the minimum value between the shear force which can be sustained by the yielding shear reinforcement (equation 4.26a) and the maximum allowed shear force in the concrete compressive strut (equation 4.26b). The design equations for the shear resistance, as found in EC2, for members with vertical shear reinforcement are:

$$
V_{Rd} = \min \begin{cases} V_{Rd,s} = \dfrac{A_{sw}}{s} z f_{ywd} cot(\theta) & \text{(4.26a)} \\[3mm] V_{Rd,max} = \dfrac{\alpha_{cw} b_w z \nu_1 f_{cd}}{cot(\theta) + tan(\theta)} & \text{(4.26b)} \end{cases}
$$

Where:

- $A_{sw} \rightarrow$ is the cross-sectional area of the shear reinforcement

- $s \rightarrow$ is the spacing between stirrups

- $f_{ywd} \rightarrow$ design yielding strength of the shear reinforcement in the web of the beam

- $\nu_1 \rightarrow$ is a strength reduction factor for concrete cracked in shear

- $\alpha_{cw} = 1 \rightarrow$ is a coefficient taking into account the state of the stress in the compression chord, taken as 1 for non-prestressed structures

A more detailed derivation of equations 4.26a and 4.26b is shown in appendix B. The equations are modified in order to include the shear reinforcement ratio ρ_w and normalized in order to obtain results in the same units as case 1a. The same analytical expression is used to find any value of the resistance i.e. design, characteristic or mean value, even though it is acknowledged that in EC2 it is only applicable for design purposes. The previous is achieved by replacing the corresponding values of f_{yw}^* and f_c^* depending on the desired quantity. Finally, the analytical expression applied henceforth is defined as:

$$
\frac{V_R}{bd} = \min \begin{cases} \dfrac{V_{R,s}}{bd} = \rho_w f_{yw}^* cot(\theta) & \text{(4.27a)} \\[3mm] \dfrac{V_{R,max}}{bd} = \nu_1 f_c^* \dfrac{1}{cot(\theta) + tan(\theta)} & \text{(4.27b)} \end{cases}
$$

It remains the definition of two parameters: ν_1 and θ. As previously explained, ν is a reduction factor applied under the assumption the concrete struts being already crack in the ultimate limit state. Following EC2, the parameter depends on the concrete strength class and the reinforcement yielding strength. Thus:

If $f_{yd} > 0.8 \cdot f_{yk}$:

$$\nu_1 = 0.6 * (1 - \frac{f_{ck}}{250}) \tag{4.28}$$

However, when $f_{yd} < 0.8 \cdot f_{yk}$:

$$\nu_1 = \begin{cases} 0.6 & if \ \ f_{ck} \leq 60 \ MPa & \text{(4.29a)} \\[2mm] \max(0.9 - \dfrac{f_{ck}}{200}, 0.5) & if \ \ f_{ck} \geq 60 \ MPa & \text{(4.29b)} \end{cases}$$

In the procedure to define the angle of the compressive strut θ, the designer is free to choose an angle between 21.8° and 45°. The smaller the value of the angle, the more reinforcement is crossed by the shear crack, however by doing so the compressive stress in the inclined concrete struts increases therefore limiting the maximum allowable shear capacity. Usually, the lower bound of the angle is used as the initial value and only increased in the case the shear resistance given by yielding of the reinforcement is not governing anymore. [41]

4.4.3. Design resistance: PSF and ECOV Cervenka

The following section presents the design value of the shear resistance obtained by means of the PSF method [15] and the Global Factor method with ECOV by Cervenka [8]. Once again the design values of the input material parameters are calculated by the ratio of their characteristic value over the corresponding partial safety factor used in the framework of the PSF method.

$$f_c^* = f_{cd} = \frac{f_{ck,is}}{\gamma_c} = 20 \, MPa \tag{4.30a}$$

$$f_{yw}^* = f_{ywd} = \frac{f_{ywk}}{\gamma_s} = 434.78 \, MPa \tag{4.30b}$$

With:

$$\gamma_c = 1.5$$
$$\gamma_s = 1.15$$

The design value of the shear resistance according to the PSF is obtain by evaluating equations 4.27a and 4.27b with the design values:

$$V_{Rd,PSF} = V_R(f_{cd}, f_{ywd}, \rho_w, ...) \tag{4.31}$$

Following the same procedure as in section 4.3.3 while calculating the design shear resistance according to the ECOV by Cervenka method, two analysis with different values of the basic variables are performed. One analysis is the results of evaluating the analytical expression with the mean values as inputs, implicitly assuming that it results in the mean value of the capacity, V_{Rm}. Instead, the second analysis results in the characteristic value of the resistance V_{Rk} by evaluating the analytical expression with the values of the material parameters representing the 5% quantile in their probability distribution. The lumped coefficient of variation is used as stated in section 4.3.3:

$$f_{ck,is} = f_{cm,is} \cdot e^{-1.645 V_{fc}'} \tag{4.32a}$$

$$f_{yk} = f_{ym} \cdot e^{-1.645 V_{fy}'} \tag{4.32b}$$

Table 4.2 summarizes the values for the material and geometrical uncertainty for each basic variable, along with the resultant lumped coefficient of variation and characteristics values. More relevant is to introduce the specific formulation leading to the desired design shear resistance according to the current method. Therefor, the expressions of the coefficient of variation for the resistance related to the material uncertainty V_F, to the geometrical uncertainty V_G and the final coefficient of variation including both types of uncertainties $V_{R,CoV}$ are:

$$V_F = \frac{1}{1.645} \ln\left[\frac{V_{Rm}(f_{cm,is}, f_{ym}, \rho)}{V_{Rk}(f_{ck,is}, f_{yk}, \rho)}\right] \tag{4.33}$$

$$V_G = 0.05 \tag{4.34}$$

$$V_{R,CoV} = \sqrt{V_F^2 + V_G^2} \tag{4.35}$$

The global factor of the resistance is:

$$\gamma_R = \exp\left(0.8 \cdot 3.8 \cdot V_{R,CoV}\right) \tag{4.36}$$

It is important to mention that $V_{R,CoV}$ differs from V_R which represents the shear resistance of the cross-section in the current section 4.4). Figure 4.9a displays the mean, characteristic and design values of the shear resistance according to the PSF and ECOV by Cervenka.

(a) Shear resistance

(b) Resistance safety factor
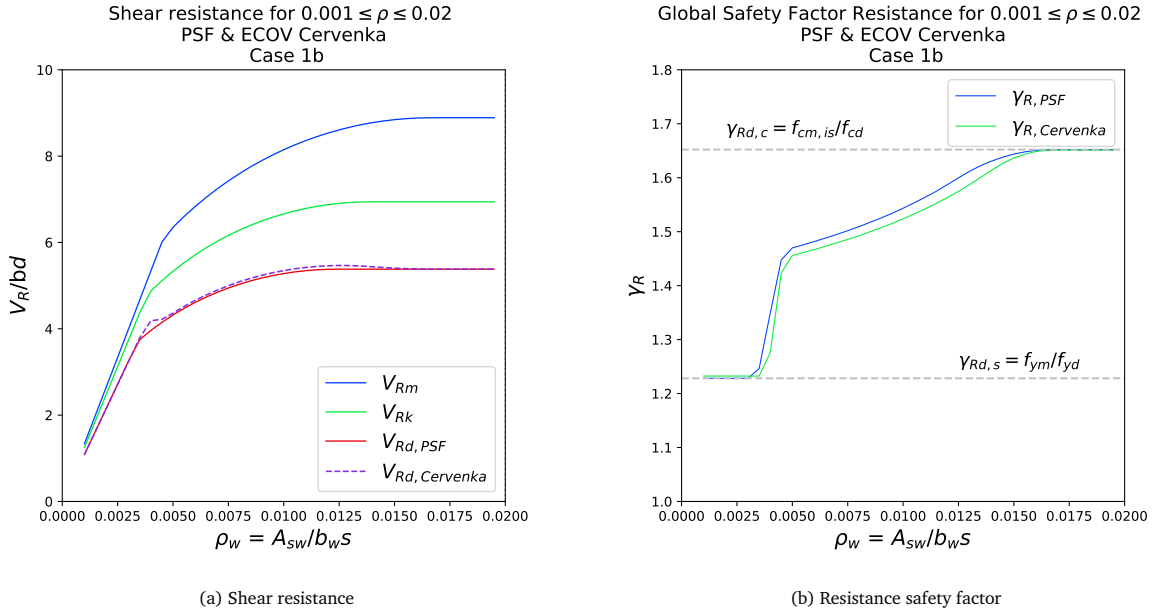
Figure 4.9: Results: case 1b

4.4.4. Monte Carlo simulation: comparison and verification

Previous section 4.3.4 already address the challenge in the definition of the LSF for the MCS implementation. The performance of the ECOV by Cervenka Safety Format for the present case 1b is then study by the evaluation of the following LSF.

$$g(X) = Z = V(X) - V_{Rd,SF} = 0 \tag{4.37}$$

Where:

- $V(X) \rightarrow$ is simulated by evaluating the analytical expression with random samples of each variable in the vector X.

- $X \rightarrow$ is the vector of random variables

- $V_{Rd,Cervenka} \rightarrow$ is the design capacity obtained with the ECOV by Cervenka method.

One million simulations of $V(X)$ are performed for a given set of reinforcement ratios between $0.001 \leq \rho \leq 0.02$. The stochastic properties of the input random variables in vector X are shown in table 4.4. The probability of failure related to the estimation of the design resistance by each Safety Format is defined as $P_f = P[V_{Rd,SF} < V(X)]$. A reliability index β_{SF} associated to the reliability of the estimation of the design resistance by each Safety Format might be express as:

$$\beta_{SF} = -\frac{\Phi^{-1}(P_f)}{\alpha_R} \tag{4.38}$$

Variable	Distribution	Mean	Standard Dev.	Units
$f_{c,is}$	Lognormal	33	5.22	MPa
f_{ywd}	Lognormal	534	25.2	MPa
h	Normal	700	10	mm
b	Normal	300	5	mm
a	Normal	70	10	mm
$\frac{A_{sw}}{s}$	Normal	Variable	$0.045*\text{Mean}$	mm^2

Table 4.4: Random basic variables used in the Monte Carlo simulation: Case 1b. Source: [31]

The reliability index related to the probability of failure of the ECOV by Cervenka method is plotted in figure 4.10a. In this case, even though there is a transitions in the used analytical expression which could be interpreted as a change of failure mechanism, the reliability index reached by the design resistance according to the ECOV by Cervenka shows the ability of existing Safety Formats to reproduce conservative results in the cases of single LFM. This observations is fundamental for future decisions made in the application of the GFM in the forthcoming chapter.
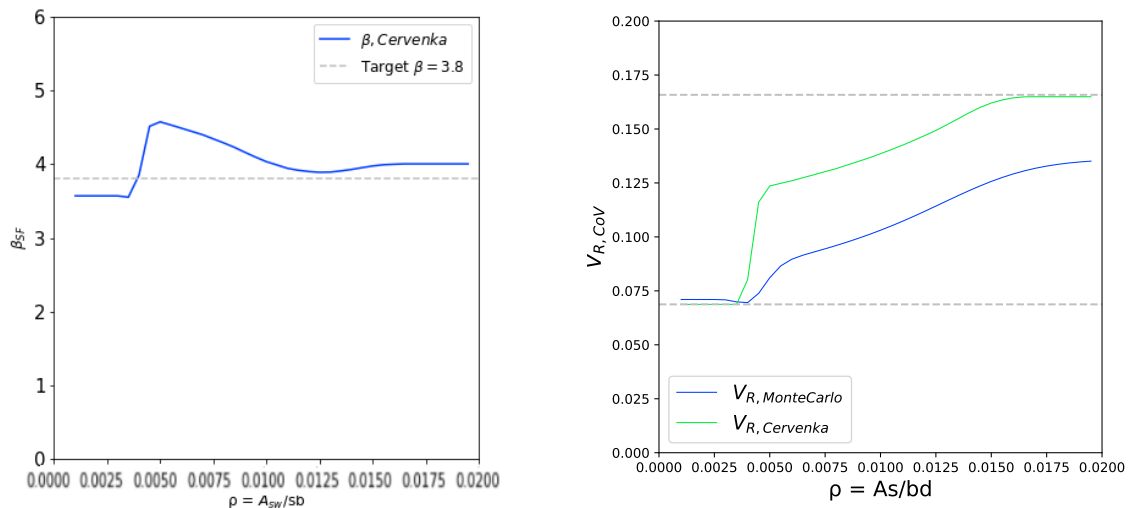
(a) Reliability index related to each estimation of the design resistance by PSF and ECOV by Cervenka

(b) Coefficient of Variation Resistance

Figure 4.10: Monte Carlo Simulation Results: Case 1a

4.5. Discussion and conclusions

It is relevant to highlight that the philosophy in the design of new RC structures, avoids extreme scenarios as over-reinforced beams or structures with too little reinforcement since they lead to dangerous situations. The cases presented in this study are mostly focused on research. Even though, they might adjust to represent practical situations of several existing structures.

From case 1a, the most remarkable observation is the critical performance of existing safety formats in regions where possibly two different mechanisms develop in an almost concurrent manner. It highlights the need for a broader format able to explicitly account for more complex systems, which is one of the main starting points of the GFM. It provides the basis of different scenarios in which the GFM will be tested. Finally, it brings attention to the classical definition of bending failure and how the selected description will affect the critical random variables to be perturbed in the future application of the GFM.

In the framework of Case 1b, it is decided that shear failure will be treated as a single mechanism based on two main reasons. The first one is related to the way the analytical model for the resistance is derived. The second one is related to the results obtained from the Monte Carlo Simulation: the reliability index related to the ECOV by Cervenka already shows a good agreement with the imposed target reliability. Therefore, even though it is a less interesting scenario in terms of testing the GFM in the situations of concurrent or clustered failure mechanisms, Case 1b provides an opportunity to validate the method in situations where the existing safety formats already provide a good level of reliability. For instance, the case of a single failure mechanism.

In the following chapter, the implementation of the GFM for cases 1a and 1b is presented following the conclusions drawn in the present section.

5

Application of the New GFM in Engineer Decision-based Scenarios: Case 1

Some local failure mechanisms are not easy to identify in continuum systems. Consequently, choosing the basic random variables to be perturbed in the GFM formulation is not a straightforward process, even using analytical expressions. Based on the observations in the previous chapter 4, this chapter presents the application of the Global Factor method for different fictitious engineer decision-based scenarios within the framework of case study 1a: a RC section in bending. Here, two definitions of the local mechanisms allow recreating the practical challenges of the application of the GFM in NLFEA. The obtained results are analyzed and compared with those obtained from the application of the PSF and ECOV by Cervenka safety formats applied in chapter 4. Different values of the perturbation parameter 'c' are analyzed, seeking its most suitable range of values for the further application of the GFM method in NLFEA.

Additionally, the GFM method is applied for case study 1b: a RC section in shear. This case studies shear failure as a single mechanism. The main objective is to verify the applicability of the method where other safety formats already produce reliable results. Moreover, it provides another opportunity to study the influence of 'c' by implementing different values of the perturbation parameter. Finally, conclusions related to each case are drawn.

5.1. GFM formulation and required parameters

The expressions and parameters required for the implementation of the GFM are summarized hereafter. Starting with the expression for the design resistance $R_{\mathrm{d,GFM}}$:

$$R_{\mathrm{d,GFM}} = \frac{R_{\mathrm{m}}}{\gamma_R} \tag{5.1}$$

$$\gamma_R = \exp\left[\frac{1}{2}V_R\left(\ln(n_{\mathrm{m}}) + \frac{\ln(n_{\mathrm{s}}) + 2\alpha_R\beta_{LS}}{n_{\mathrm{p}}}\right)\right] \tag{5.2}$$

$$V_R \approx \sqrt{V_{R_{\mathrm{x}}}^2 + V_G^2 + V_\theta^2} \tag{5.3}$$

$$V_{R_{\mathrm{x}}} \approx \frac{1}{c}\ln\left(\frac{R_m}{R_{\mathrm{var}}}\right) \tag{5.4}$$

Where:

- $R_{\mathrm{m}} \rightarrow$ is the mean value of the moment/shear resistance obtained by evaluating the analytical expression with the in-situ mean value of the basic variables influencing the Critical Local Failure Mechanism (CLFM).

- $R_{\text{var}} \rightarrow$ is the value of the moment/shear resistance obtained by evaluating the analytical expression with the in-situ mean value of basic variables $\mathbf{x}_m$ influencing the Critical Local Failure Mechanism (CLFM) reduced by the product of the 'c' parameter and the corresponding standard deviation $\sigma_{\mathbf{x}}$.

- $\alpha_R = 0.8 \rightarrow$ is the total sensitivity factor only for the resistance part

- $\beta_{LS} = 3.8 \rightarrow$ is the target reliability index for Limit State

- $n_m \rightarrow$ the maximum number of LFM in series subsystems inside each parallel subsystems, and then the minimum of those maximum.

- $n_p \rightarrow$ is the maximum number of parallel systems inside a series system.

- $n_s \rightarrow$ is the total number of series subsystems conformed by parallel subsystems contributing to failure.

- $V_G \rightarrow$ is the coefficient of variation related to the geometrical uncertainty

- $V_\theta \rightarrow$ is the coefficient of variation related to the modelling uncertainty

- $V_{R_x} \rightarrow$ is the coefficient of variation related to the material uncertainty

The coefficients of variation of the geometrical and modeling uncertainties are zero throughout the chapter ($V_G = 0$ and $V_\theta = 0$). The aim is to investigate the effects of the uncertainty related only to the material parameters. The decision seeks a procedure where the only source of uncertainty and variability is related to the materials involved in the local failure mechanisms. The decision impacts the variables included in the Monte Carlo Simulation. Now the only variables to be sample are the basic variable: f_y and f_c. The results in chapter 4, obtained with the existing formats, are modified by including $V_G = 0$ and $V_\theta = 0$ to keep them as reference.

The same analytical expressions described in section 4.3.2 and 4.4.2 for the moment and shear capacity are used within the framework of the GFM. The mean values and standard deviation of the basic variables (f_y and f_c) are taken from the work of Pimentel et al. [31] to obtain comparable results. In table 5.1 the relevant values are summarized.

Material properties		In-situ Mean [MPa]	Standard Deviation [MPa]
Concrete Compressive Strength	$f_{cm,is}$	33	5.22
Reinf. Yielding Strength	f_{ym}	534	25.2

Table 5.1: Mean and Standard Deviation of the Basic Variables

5.2. Case 1a: Engineer Decision-based Scenarios and GFM

5.2.1. Definition of the Engineer Decision-based Scenarios

One of the greatest challenges when performing NLFEA is the correct identification of the failure mechanisms. This obstacle becomes more relevant in the application of the new GFM. As presented in chapter 3, to correctly apply the new safety format, all the possible Local Failure Mechanisms (LFM) must be identified, localized, and organized hierarchically. The method was initially derived for NLFEA of RC frames. Therefore, the aforementioned process is more transparent for frame-type structures than for continuum systems: slabs, walls, bridges, tunnels, etc.

With this in mind, the simplest representation of a continuous system is taken as a slender simply supported beam. In chapter 4, case 1a shows a RC cross-section, subjected to bending, analyzed by two existing safety formats. An observation from the obtained results is the inability of the applied formats to reach the target reliability for cross-sections with intermediate values of reinforcement ratios. This middle region coincides with a change in the description of the bending failure mechanism: from a ductile failure caused by yielding of the reinforcement to brittle failure due to crushing of the compression zone in the concrete when the reinforcement ratio increases enough. Therefore, the intermediate region of reinforcement ratios

is here defined as a 'transition zone' from one mechanism to another; in terms of the new GFM, a zone with concurrent LFM.

The question arising now is related to define "bending" as a unique failure mechanism. It might be advisable to divide it into a local ductile bending failure and a local brittle bending failure to improve the agreement with the target reliability in the transition zone. A new challenge may arise in defining the boundaries of this zone where the two so-called concurrent mechanisms are assumed to work as a series system. Simultaneously, the rule of perturbing only the basic variables (f_y or f_c) related to the Critical Local Failure Mechanism (CLFM) is studied along with the definition of the fictitious scenarios.

As a first attempt in defining the boundaries for the transition zone, the reinforcement ratios for which the mean and characteristic value of the resistance presented a different failure mechanism were selected. However, the use of the characteristic value is not efficient. The application of the new proposed safety format does not require the calculation of this value. Therefore, it is a criterion that would ask for an extra NLFEA, decreasing the efficiency of the method.

In a second attempt, the criteria were adjusted to the possibilities of the GFM. Instead of using the characteristic value, a comparison would be performed between the mean value and the perturbed value of the resistance. The disadvantage of this approach is that the transition zone would become strongly dependant on the value of the parameter 'c', which up to this point is not yet defined. Moreover, in the core of the GFM, there is the idea of the parameter c being 'sufficiently' small to catch the same failure mechanism with R_m and R_{var}. Accordingly, taking a small value of the parameter i.e. $c = 0.1$, non of the reinforcement ratios would fall in the established criteria.

Therefore, a more practical approach is taken. From the observations in the application of the PSF, the ECOV by Cervenka, and the Monte Carlo simulation results in chapter 4, a rough estimation sets the boundaries for the transition zone between reinforcement ratios with a value of $0.02 \leq \rho \leq 0.03$. When performing several trials with different values of the parameter 'c', the majority of the cases agreed with these boundaries. Therefore, two fictitious scenarios based on the possible decisions of the engineer while performing a reliability-based NLFEA are defined following the established boundaries. These scenarios provide insight into the consequence of the decisions taken by the engineer and how the GFM performs in case these decisions are not on the conservative side.

5.2.2. Design resistance with GFM: Scenario 1
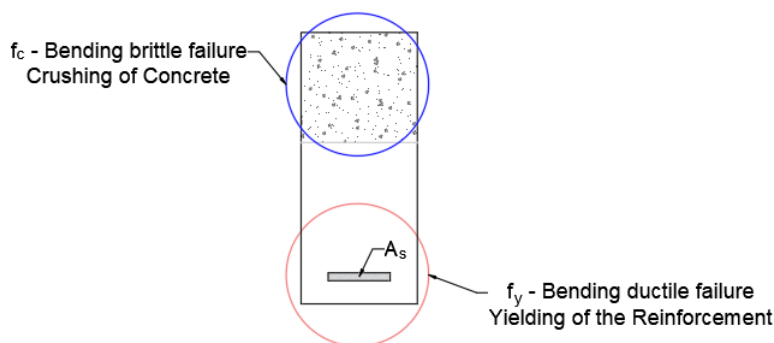
Figure 5.1: Engineer Decision-based Scenario 1: Bending as two LFM

The first Engineer Decision-based Scenario divides "bending" failure into two different mechanisms. In the transition zone, the cross-section is close to failing in one way or the other. Aiming to improve the inability of existing safety formats (e.i. the ECOV by Cervenka) to provide a conservative and reliable value for the capacity within this region, the engineer defines two almost concurrent failure modes in the region for intermediate reinforcement ratios $0.02 \leq \rho \leq 0.03$.

Even though when using an analytical expression is clearer whether the failure occurs due to one mode or the other, in a NLFEA the stress and strain state of the structure as a whole is available. The previous

allows defining for each material or region how close they are to their limit state. Therefore, making possible the identification of concurrent failure mechanisms.

Consequently, equal boundaries are implemented in the calculation of the global safety factor of the resistance γ_R. In this case, the expression of the safety factor for the transition zone ($0.02 \leq \rho \leq 0.03$) is obtain by replacing $n_s = 2$, $n_p = 1$ and $n_m = 1$ into equation 5.2. For the regions with a unique failure mechanism, equation 5.2 was evaluated with n_s, $n_p = 1$ and $n_m = 1$:

$$\gamma_R = \begin{cases} \exp(0.8 \cdot 3.8 \cdot V_R) \quad \rightarrow \quad if \ : \ \rho < 0.02 \ or \ \rho > 0.03 \\ \exp\left(\ln(\sqrt{2})V_R + 0.8 \cdot 3.8 \cdot V_R\right) \quad \rightarrow \quad if \ : \ 0.02 \leq \rho \leq 0.03 \end{cases}$$

The second decision made by the engineer is about the failure modes being independent. The previous translates into uncorrelated basic variables. Meaning:

- For ρ's with a local ductile bending failure ($\varepsilon_s \geq \varepsilon_{sy}$), the basic variable is the yielding strength of the reinforcement, f_y.

- ρ's with a local brittle bending failure ($\varepsilon_s < \varepsilon_{sy}$), the basic variable is the concrete compressive strength, f_c.

In summary:

$$M_{R_{var}} = \begin{cases} M_R(f_{cm,is}, f_{ym} - c\sigma_{f_{ym}}) \quad \rightarrow \quad if \ : \ \varepsilon_s \geq \varepsilon_{sy} \\ M_R(f_{cm,is} - c\sigma_{f_{cm,is}}, f_{ym}) \quad \rightarrow \quad if \ : \ \varepsilon_s < \varepsilon_{sy} \end{cases}$$

The results obtained are shown in figures 5.2, 5.4 and 5.5 with the 'c' parameter taking values of $c = [0.1, 1.645, 2.5]$. The plotted graphs present the values of the bending moment resistance, the global safety factor, and the coefficient of variation of the resistance for different reinforcement ratios. The design values of the moment resistance obtained in chapter 4 with the PSF and the ECOV by Cervenka are plotted as a comparison tool of the results. The coefficient of variation of the resistance obtain by the Monte Carlo simulation is also available in figures 5.2d, 5.4d and 5.5d.

Observations

Following the idea behind the perturbation parameter being "sufficiently" small, 'c' takes a value equal to 0.1. The results obtained in this case are first discussed. In figure 5.2a, for the transition zone as well as for the low reinforcement regions zone, the design moment resistance obtained by the GFM is higher than the values previously obtained for the PSF and ECOV Cervenka.

For the low reinforcement region, the overestimation of the capacity is a drawback for the approach. The GFM can not reach the target reliability, even in the classical case of a single failure mechanism. A deeper look into the possible explanations suggested that for the particular case of the used analytical expression (equation 4.6), the ratio between the mean value of the resistance M_{Rm} and M_{Rvar} is smaller than the ration between M_{Rm} and $M_{Rk,Cervenka}$. The previous occurs when only the basic variable related to local ductile bending failure, i.e. the yielding strength, is reduced, and the mean in-situ value of the concrete compressive strain is maintained. Moreover, the ratio keeps decreasing with increasing values of ρ. Therefore, in figures 5.2c and 5.2d the coefficient of variation and global safety factor are less conservative in the low reinforcement region.

It is noticed that to obtain reliable results, in terms of reaching the imposed target reliability in the transition zone, the value of the coefficient of variation must be higher than the Monte Carlo reference. Otherwise, the calculation of the global safety factor should provide enough a value sufficiently higher, which is not the case in figure 5.2c.

For the transition zone, the value of the design moment resistance is higher than expected. The results are further from reach the target reliability. A better fit is observed for the region of high ρ's. In this case, the use of a small parameter 'c' seems to reproduce a higher reliability index than the existing safety formats, which means the GFM might be accurate enough for this type of failure mechanism. However, brittle failures are never advisable in the design of reinforced concrete structures due to their brittle nature.
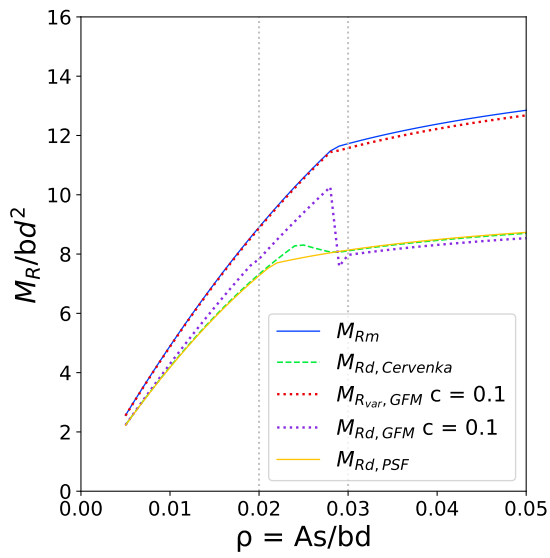
(a) Bending moment resistance
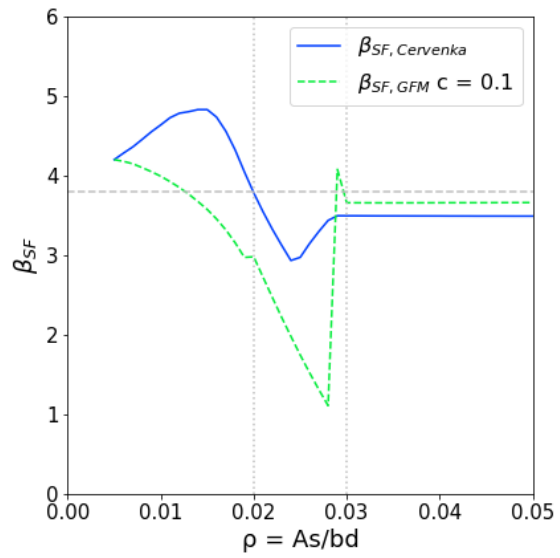
(b) Reliability index related to Safety format
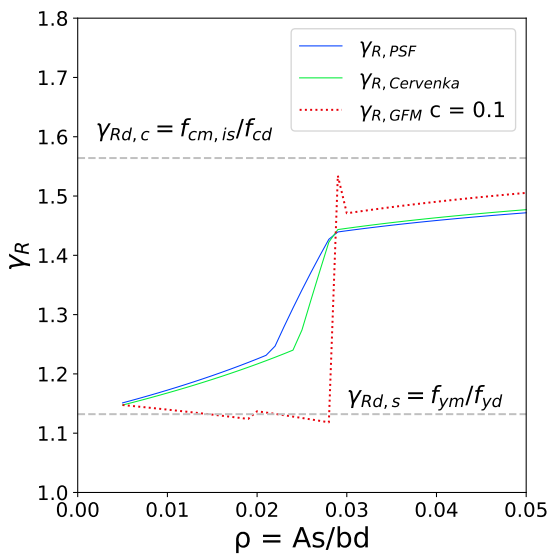
(c) Global Safety Factor

(d) Coefficient of Variation

Figure 5.2: Case 1a: Scenario 1 - GFM by Monti et al. with c = 0.1, PSF and ECOV Cervenka

(a) Bending moment resistance

(b) Reliability index related to Safety format

(c) Global Safety Factor

(d) Coefficient of Variation

Figure 5.3: Case 1a: Scenario 1 - GFM by Monti et al. with c = 1.0, PSF and ECOV Cervenka

(a) Bending moment resistance

(b) Reliability index related to Safety format

(c) Global Safety Factor
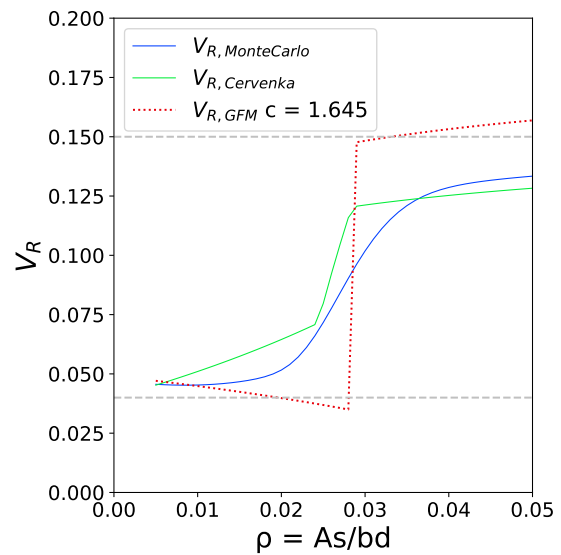
(d) Coefficient of Variation

Figure 5.4: Case 1a: Scenario 1 - GFM by Monti et al. with c = 1.645, PSF and ECOV Cervenka

(a) Bending moment resistance

(b) Reliability index related to Safety format

(c) Global Safety Factor

(d) Coefficient of Variation

Figure 5.5: Case 1a: Scenario 1 - GFM by Monti et al. with c = 2.5, PSF and ECOV Cervenka

A value of c equal to 1 presents a similar behavior as with the value being 0.1. For the other two values implemented $c = [1.645, 2.5]$, the problem of overestimating the design value of the resistance in the low reinforcement region is even more noticeable. The reliability target in the transition zone is far to be reached. The design values for the high reinforcement rations seem to be underestimating the capacity of the section, which once again might be a positive outcome given the previously discussed brittle nature of this type of structure.

5.2.3. Design resistance with GFM: Scenario 2

The second engineer scenario goes back to the classical approach of calling bending a single local failure mechanism. Therefore, along the whole spectrum of reinforcement ratios, both basic variables (f_y and f_c) are perturbed by the product of 'c' and the corresponding standard deviation. This approach is much

more similar to the ECOV by Cervenka method. The difference mainly lies in the value taken by 'c' and the assumption of the probability distribution of the basic random variables. The expression of the GFM for the global safety factor γ_R is simplified to a unique failure mechanism with $n_m = 1$, $n_p = 1$ and $n_s = 1$. Therefore, the following equations apply for the complete range of reinforcement ratios:

$$M_{R_{var}} = M_R(f_{cm,is} - c\sigma_{f_{cm,is}}, f_{ym} - c\sigma_{f_{ym}}) \tag{5.5}$$

$$V_{R_x} = \frac{1}{c}\ln\left(\frac{M_{R_m}}{M_{R_{var}}}\right) \tag{5.6}$$

$$V_R = V_{R_x} \tag{5.7}$$

$$\gamma_R = \exp(0.8 \cdot 3.8 \cdot V_R) \tag{5.8}$$
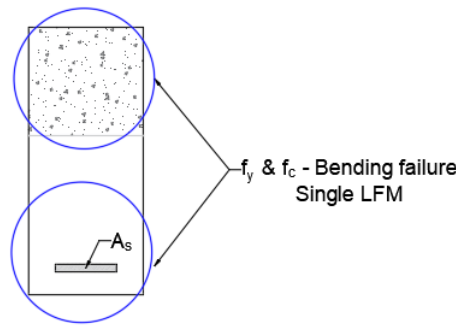
Figure 5.6: Engineer Decision-based Scenario 2: Bending as two LFM

Figures 5.7, 5.9 and 5.10 show the resultant Bending moment capacity $M_{Rd,GFM}$, the global factor for the resistance part γ_R and the coefficient of variation of the resistance V_R with the 'c' parameter being $c = [0.1, 1.645, 2.5]$. Once more, the design value of the moment resistance obtained in chapter 4 with the PSF and the ECOV Cervenka are shown for comparison.

Observations

Analyzing first the results obtained with a value of $c = 0.1$ in figure 5.7, the coefficient of variation and the safety factor for the regions of low and high reinforcement ratios, as well as the value of the moment resistance, present a better agreement with the ECOV by Cervenka and the PSF. The improvement in the fit for the lower reinforcement ratios is because, in this case, the perturbation applies for both basic variables or material parameters. The transition zone is still problematic, even more than with the ECOV by Cervenka method. With the assumption of a single LFM, any improvement regarding the change in failure description is implemented. The equation of the γ_R does not account for any concurrent LFM in the intermediate region.

Continuing with the remaining values of 'c' used. Figures 5.8, 5.9 and 5.5 illustrate the results. For a value of $c = 1.645$, which should produce a R_{var} similar to the characteristic value of the resistance (with the only difference being the assumed distribution of the basic variables), improved performance of the method is observed. Equally in the case of $c = 1.0$. For low reinforcement ratios, the value of the resistances maintains a similar level of reliability as in the ECOV by Cervenka. A value for c as higher as 2.5 is not advisable: first, due to the philosophy of the method to maintain the same failure mechanism between the two analyses needed, and second because it produces highly conservative design resistance, which might lead to over-design and uneconomical structures or expensive retrofitting procedures.

For intermediate and high reinforcement ratios, the results are more conservative. For the latter, the resistance is noticeably underestimated. Figures 5.8d, 5.9d and 5.10d show a value of $V_{R,GFM}$ much higher than the Monte Carlo simulation one, which serves as a reference. Thus, it is crucial to highlight that when the engineer assumes bending failure as a single Local Failure Mechanisms working in series, a small value of 'c' is not advisable, at least from the analytical expression point of view. A much higher value is needed to avoid overestimation of the capacity.
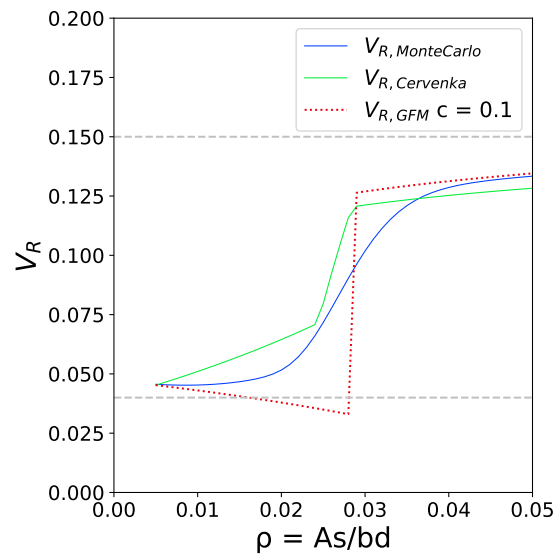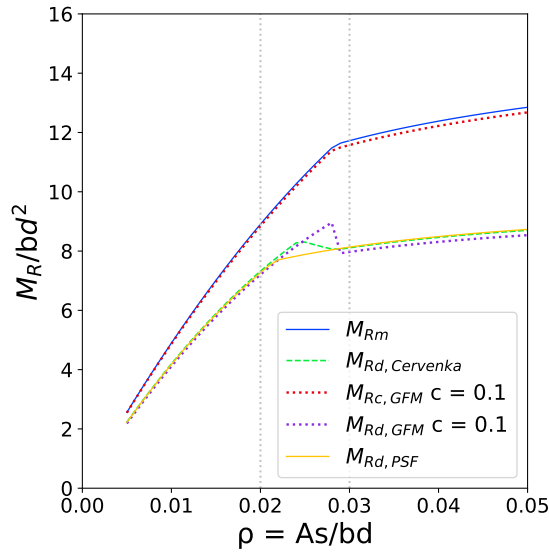
(a) Bending moment resistance
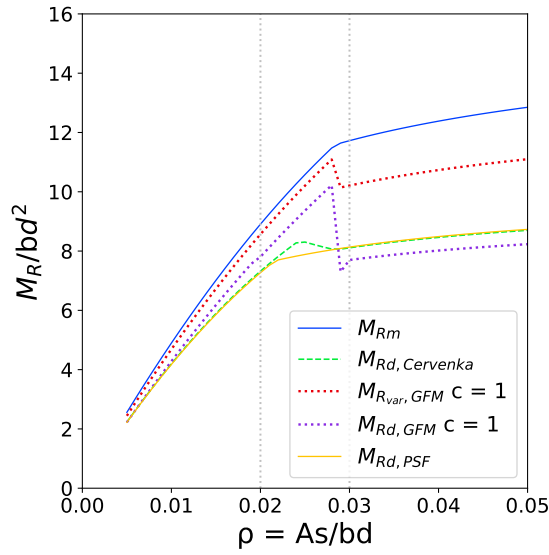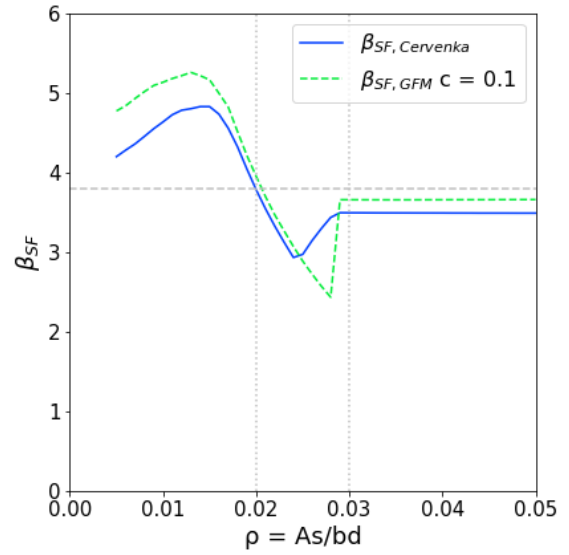

(b) Reliability index related to Safety format
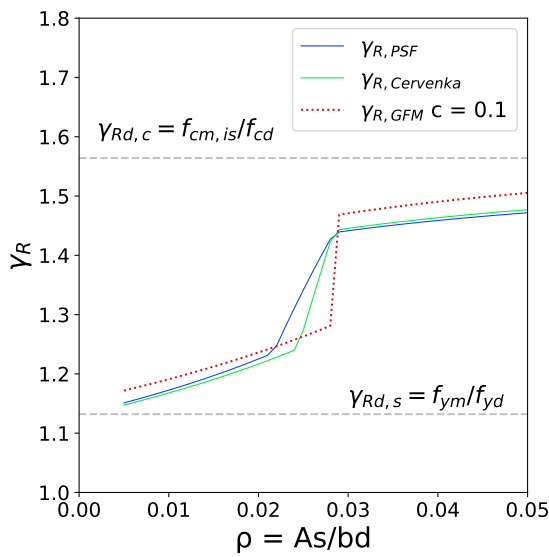
(c) Global Safety Factor
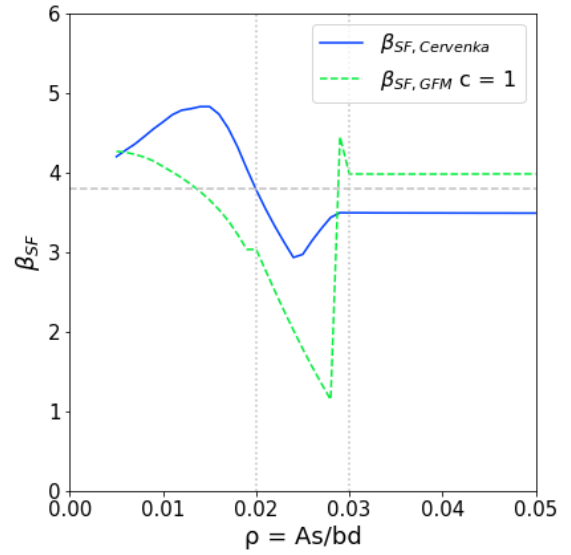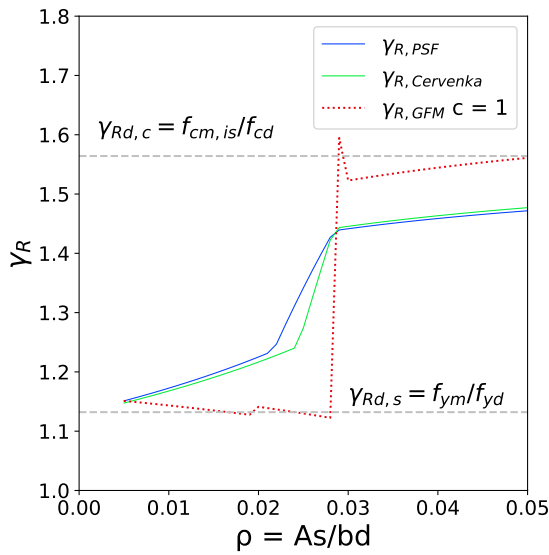

(d) Coefficient of Variation

Figure 5.7: Case 1a: Scenario 2 - GFM by Monti et al. with c = 0.1, PSF and ECOV Cervenka
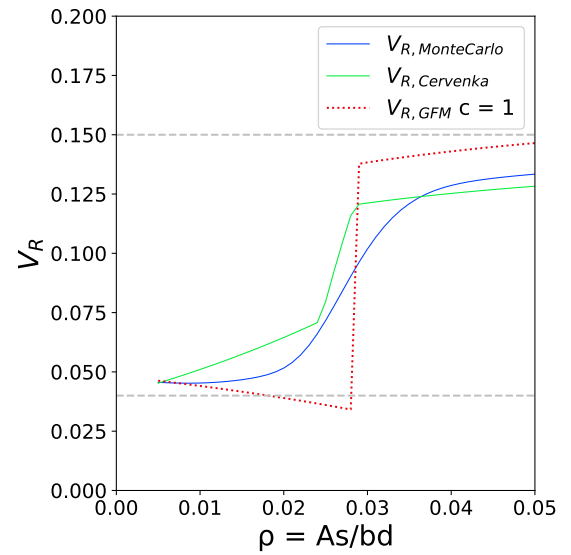
(a) Bending moment resistance
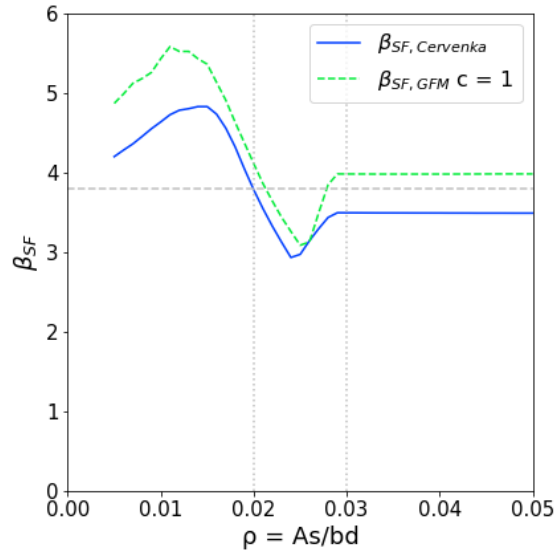
(b) Reliability index related to Safety format

(c) Global Safety Factor

(d) Coefficient of Variation

Figure 5.8: Case 1a: Scenario 2 - GFM by Monti et al. with c = 1.0, PSF and ECOV Cervenka
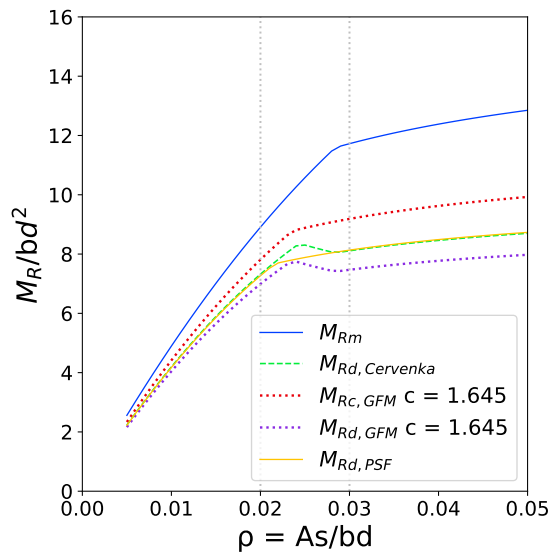
(a) Bending moment resistance
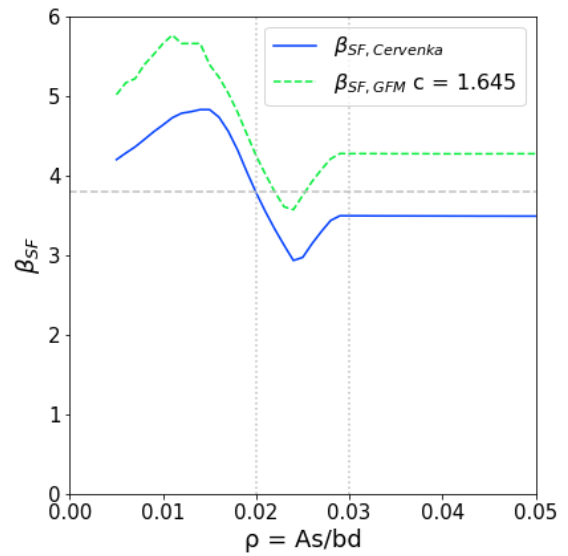
(b) Reliability index related to Safety format

(c) Global Safety Factor

(d) Coefficient of Variation

Figure 5.9: Case 1a: Scenario 2 - GFM by Monti et al. with c = 1.645, PSF and ECOV Cervenka
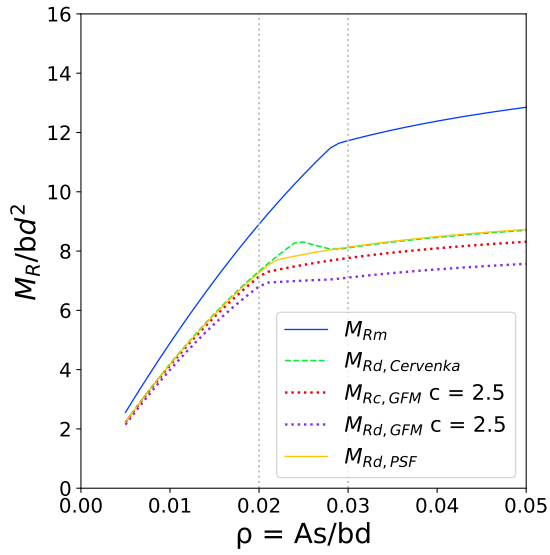
(a) Bending moment resistance
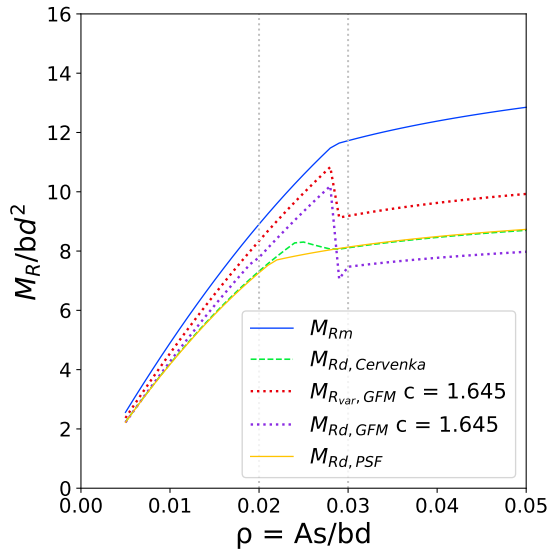
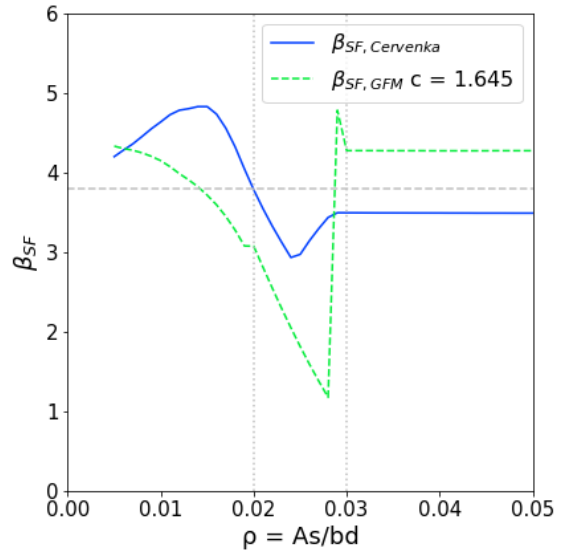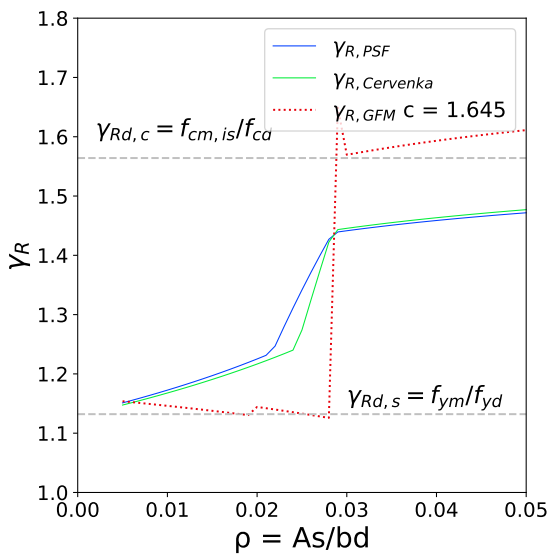(b) Reliability index related to Safety format

(c) Global Safety Factor

(d) Coefficient of Variation

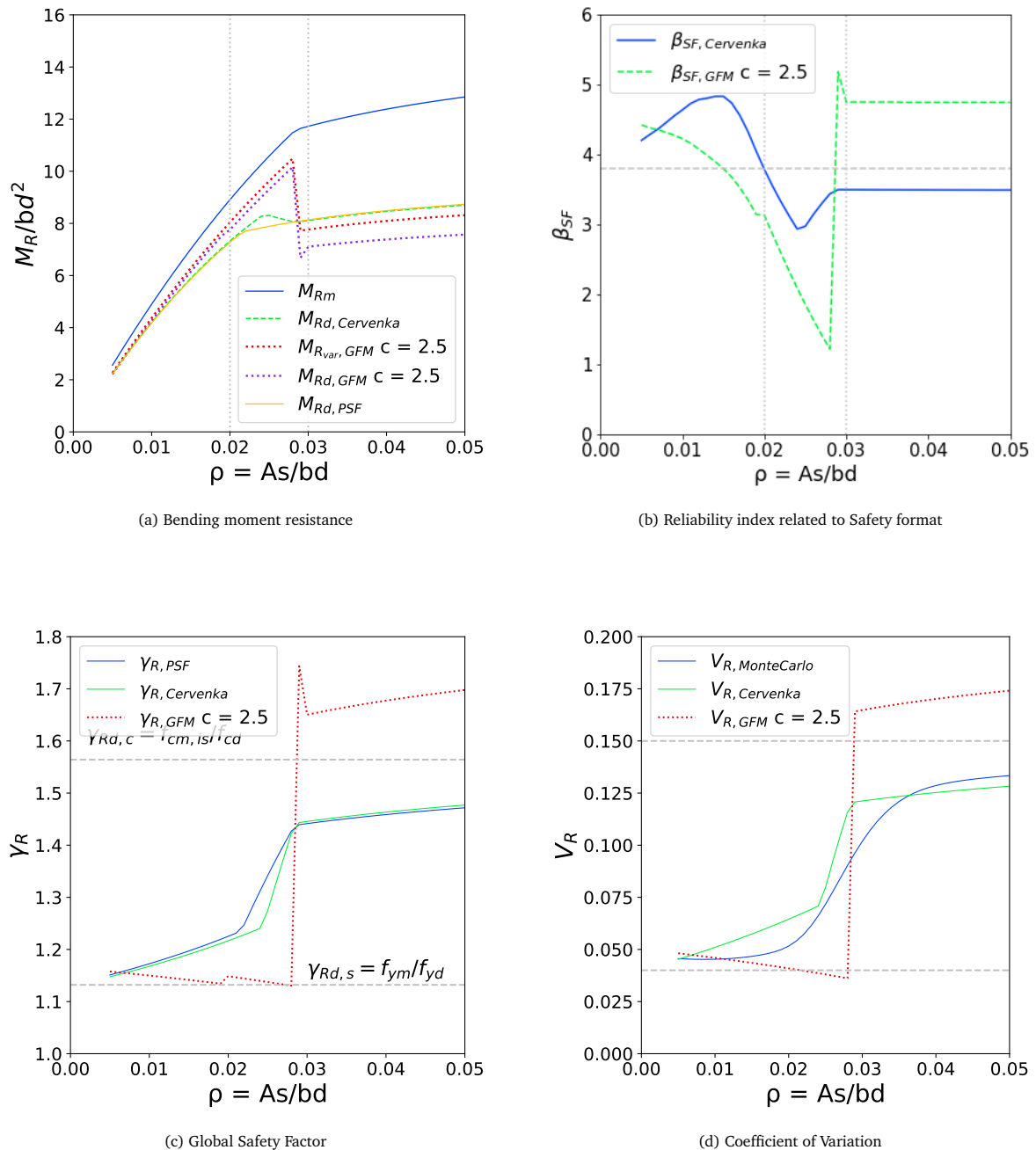Figure 5.10: Case 1a: Scenario 2 - GFM by Monti et al. with c = 2.5, PSF and ECOV Cervenka

5.2.4. Design resistance with GFM: Simplified Scenario

A simplified version of the GFM is analyzed as an alternative proposed in a more recent draft version of chapter 27.10 of the upcoming *fib* MC2020. In this case, the characteristic value is used to calculate the coefficient of variation, as in equation 5.12, which implies a 'c' parameter equal to 1.645 and a log-normal distribution of the material parameters or basic variables. Assuming that two concurrent and independent LFM in series develop in the transition zone and only one LFM for the reinforcement ratios out of those boundaries, the expression for the global safety factor of the resistance is presented in equation 5.10:

$$M_{Rd,GFM} = \frac{M_{R_\mathrm{m}}}{\gamma_R} \tag{5.9}$$

$$\gamma_R = \begin{cases} \exp(\alpha_R \beta_{LS} V_R) & \rightarrow \quad if : \ \rho < 0.02 \text{ or } \rho > 0.03 \\ \exp\left(\ln(\sqrt{2}) V_R + \alpha_R \beta_L S V_R\right) & \rightarrow \quad if : \ 0.02 \leq \rho \leq 0.03 \end{cases} \tag{5.10}$$

$$V_R \approx V_{R_\mathrm{x}} \tag{5.11}$$

$$V_{R_\mathrm{x}} \approx \frac{1}{1.645} \ln\left(\frac{M_{R_\mathrm{m}}}{M_{R_\mathrm{k}}}\right) \tag{5.12}$$

Observations

At first sight, the obtained results present a better agreement with the design resistance produced by the existing safety formats: this behavior was expected for the cross-sections outside the transition zone since the simplified expressions for low and high reinforcement ratios are the same as in the ECOV method. It might be possible to predict an improvement in the reliability for the critical sections within the transition zone in figure 5.11a. The design value obtained with the new simplified approach is considerably lower, which directly impacts the reliability index in the Monte Carlo simulation. Consequently, figure 5.11b already shows an improvement in the reliability level reached.

From this analysis, the simplified version can be seen as an improvement when comparing only to the previous ECOV by Cervenka method included in previous *fib* MC2010.

5.2.5. Monte Carlo simulation: involved random variables

A relevant remark is highlighted in this section. In chapter 4, the simulation of the resistance included the parameters related to the geometrical uncertainty of the capacity. That was essential to reproduce the same results obtained by Pimentel et al. in [31] and verify the analytical expressions and the correct application of the existing safety formats.

In the present chapter, the main concern is the application and performance of the new GFM; special emphasis is given to the effect of the coefficient of variation of the resistance part related to the material parameters. Therefore, besides setting $V_G = 0$, only two independent basic random variables are included this time for the simulation of $R(x)$ and posterior calculation of the reliability index related to the GFM $\beta_{SF,GFM}$. The same stochastic properties for f_y and f_c given in table 4.3 are implemented.

(a) Bending moment resistance

(b) Reliability index related to Safety format

(c) Global Safety Factor

(d) Coefficient of Variation
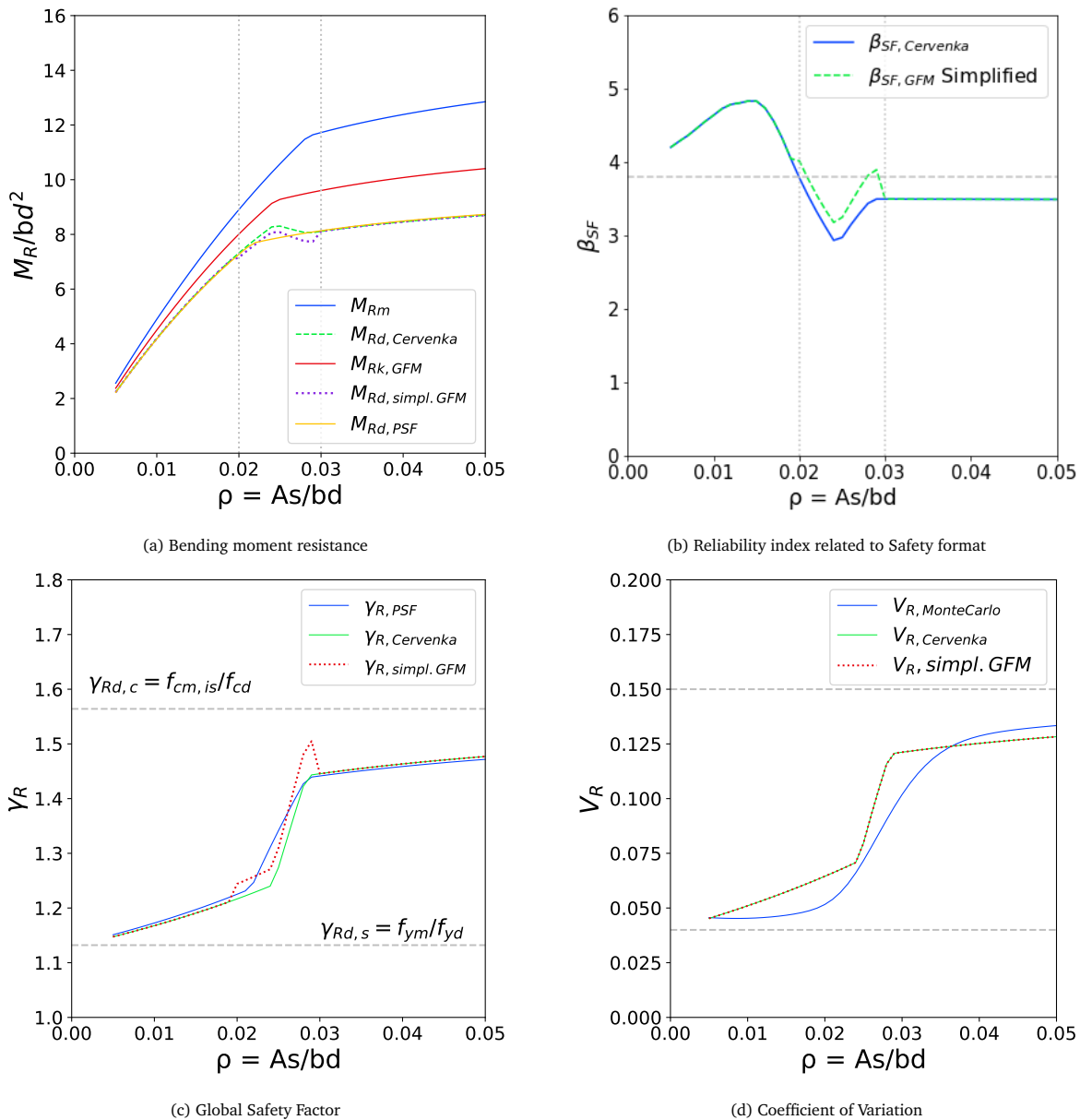
Figure 5.11: Case 1a: Simplified GFM in *fib* MC2020, PSF and ECOV Cervenka

5.3. Case 1b: Shear Resistance according GFM

Even though the possibility of categorizing shear failure in two or even three mechanisms is considered, the final decision assumes shear as a single local failure mechanism. In the derivation of the analytical shear resistance, there are two expressions. The first one is related to the yielding of the stirrups, and the second one is related to the maximum allowable force in the concrete strut. However, the variable-strut-tie model is based on a constant interaction between the tensile ties and the concrete struts. That translates into a continuous interaction between the two formulas. The yielding of the shear reinforcement, when using the lowest allowable value for the strut angle ($\theta = 21.8°$), leads directly to failure. However, the increase in the reinforcement ratio means that the rotation of the compressive struts is determinant for the yielding of the stirrups. Consequently, the chapter presents hereafter a unique scenario for the application of the GFM.

The specific formulation for the shear resistance according to the GFM is introduced. Both basic variables ($f_y w$ and f_c) are perturbed along with the whole range of reinforcement ratios for the second analysis. A parameter study for different values of 'c' is performed. The final expression for the global safety factor ,γ_R,

is simplified to a unique failure mechanism, meaning $n_m = 1$, $n_p = 1$ and $n_s = 1$.

$$V_{R_{var}} = V_R(f_{cm,is} - c\sigma_{f_{cm,is}}, f_{ywm} - c\sigma_{f_{ywm}}) \tag{5.13}$$

$$V_{R_x} = \frac{1}{c}\ln\left(\frac{V_{Rm}}{V_{Rvar}}\right) \tag{5.14}$$

$$\gamma_R = \exp(0.8 \cdot 3.8 \cdot V_{R_x}) \tag{5.15}$$

Figures 5.12 until 5.15 illustrate the resultant shear capacity $V_{Rd,GFM}$, the global safety factor for the resistance part γ_R and the coefficient of variation of the resistance V_R with the 'c' parameter taking four different values $c = [0.1, 1.0, 1.645, 2.5]$. The outcomes are contrasted with the obtain design shear capacities according to the PSF and ECOV by Cervenka methods.

5.4. Discussion and Conclusions

A detailed discussion is made for each one of the application scenarios for the GFM. The conclusions presented in this section followed straight from those detailed observations. Indeed, the Decision-based Scenarios represent possible decisions and challenges faced by the engineer when performing a NLFEA. Even though the scenarios presented in the chapter are rather specific and fictitious, their implementation draws attention to some of the key discussion points of the GFM.

From scenario 1, the assumption of bending failure divided into two failure mechanisms is tested within the application of the new GFM: the results are not showing any representative improvement for the low and transition zone of reinforcement ratios with any of the values of the perturbation parameter 'c'. However, since the method seems to predict reliable design resistance for the region with high ratios, it is concluded that the inability to reproducing conservative and accurate results is closely related to the formulation of the analytical expression. Exclusively reducing the yielding strength of the reinforcement does not represent the real interaction implicit in the analytical model between the concrete and reinforcing steel properties. As in the case of shear failure, the used analytical model includes constant interaction between the yielding of the reinforcement and the compressive strength of the concrete. Furthermore, when calculating whether the steel reached the yielding stress or not, the compressive strength of the concrete is involved. Therefore, overall conclusions about the poor performance of the GFM itself seem premature at this point.

Assuming bending as a single failure mechanism presents a better agreement between the existing and new safety formats. In conclusion, it is better to define LFMs according to their location within the element or structure and take into the perturbation process all the relevant random basic variables involved in the selected CLFM. The previous contradicts to some extent the comments by Pimentel. In [31], he refers to two and three different mechanisms for bending and shear failure respectively. However, up to now in the framework of the GFM, they are better defined as a single failure occurring at a certain location of a member. This conclusion is in agreement with the examples given by Monti et. al in the unpublished paper [29].
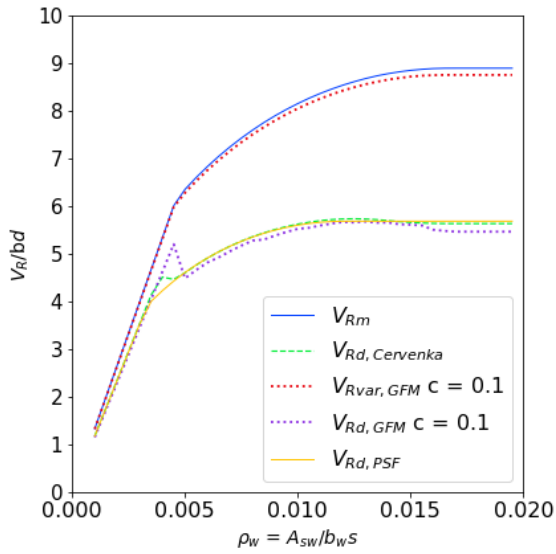
(a) Shear resistance
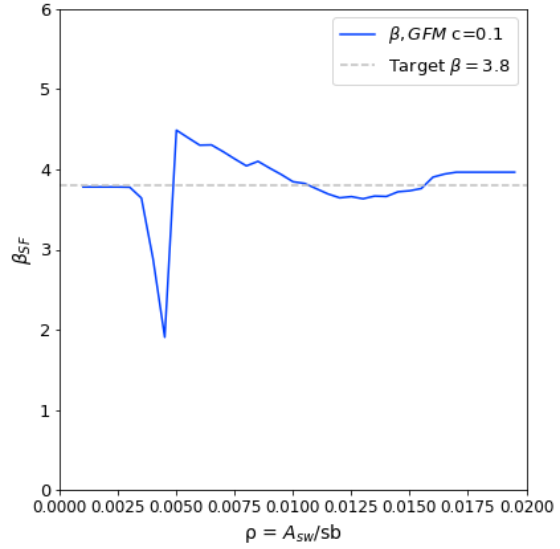
(b) Reliability index related to Safety format
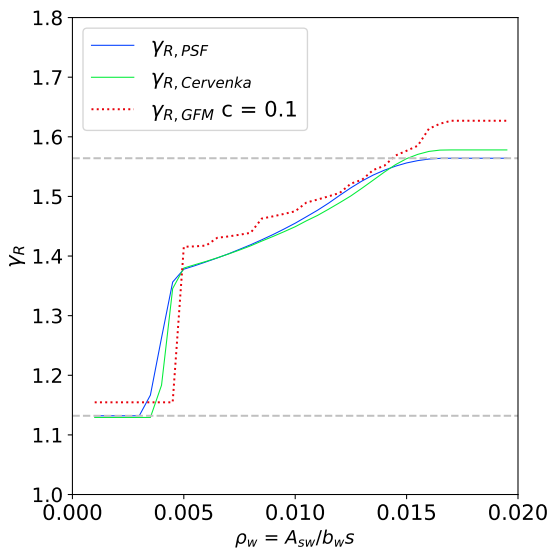
(c) Global Safety Factor
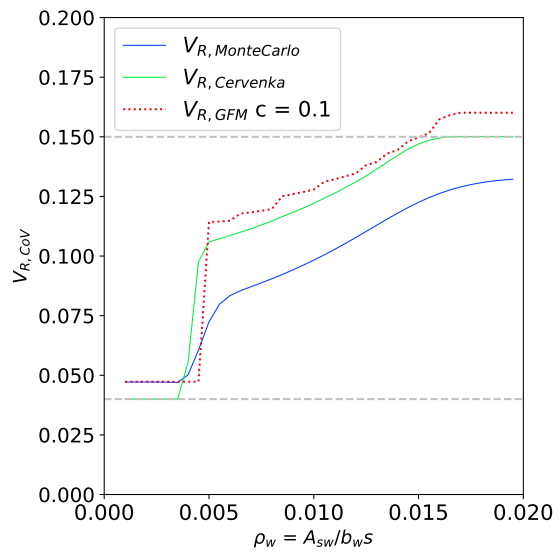
(d) Coefficient of Variation

Figure 5.12: Case 1b: GFM with c = 0.1, PSF and ECOV Cervenka
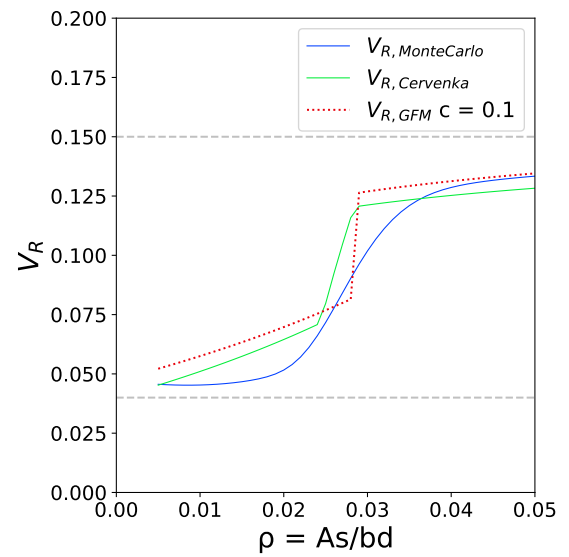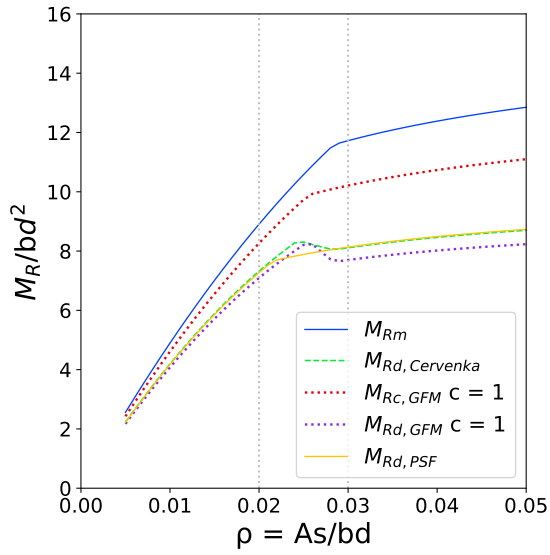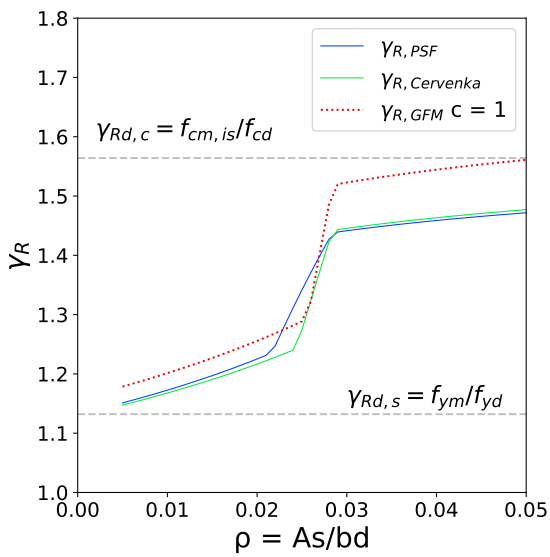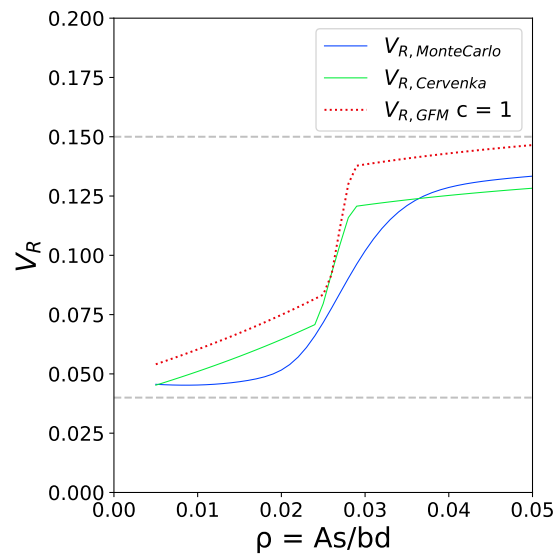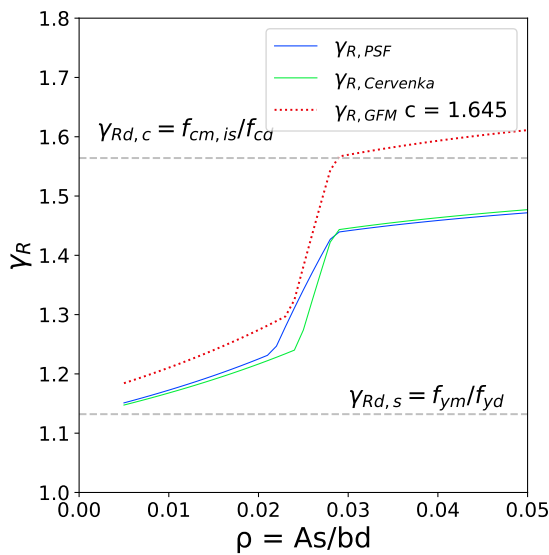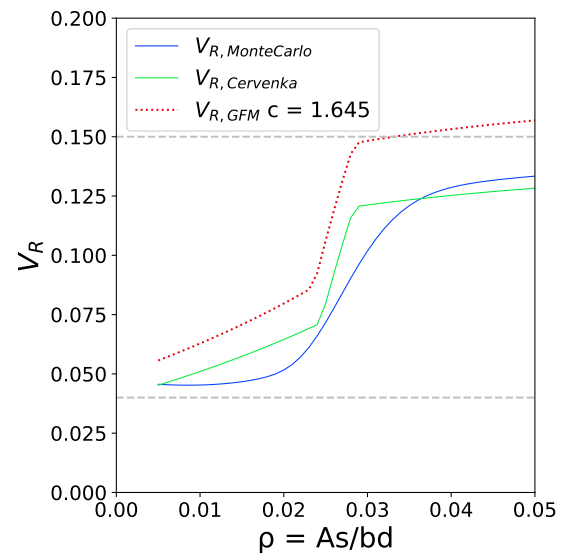
(a) Shear resistance

(b) Reliability index related to Safety format

(c) Global Safety Factor

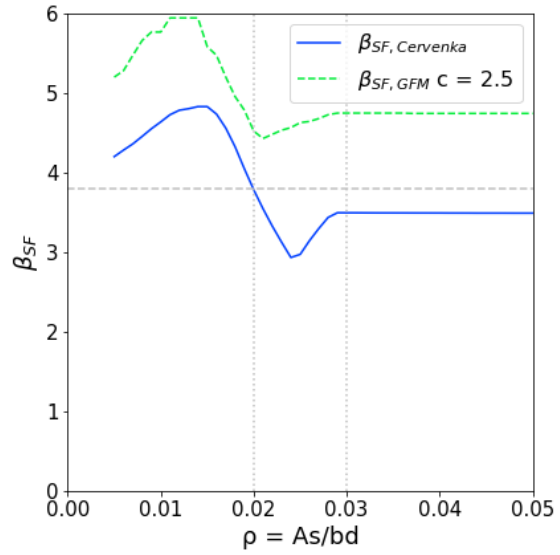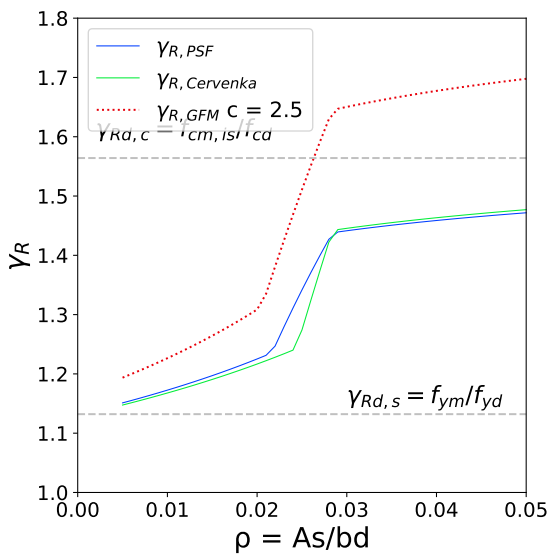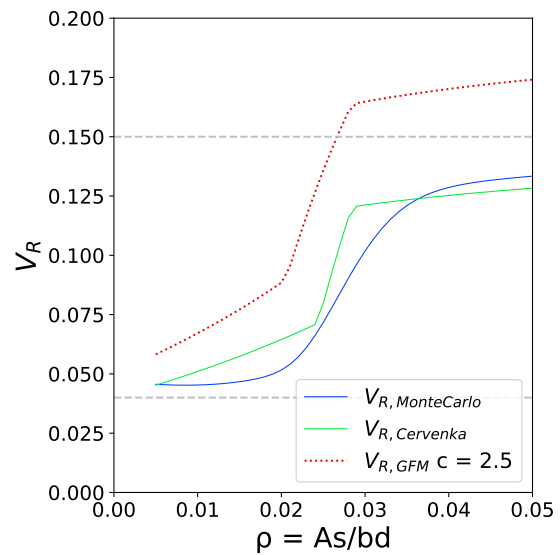(d) Coefficient of Variation
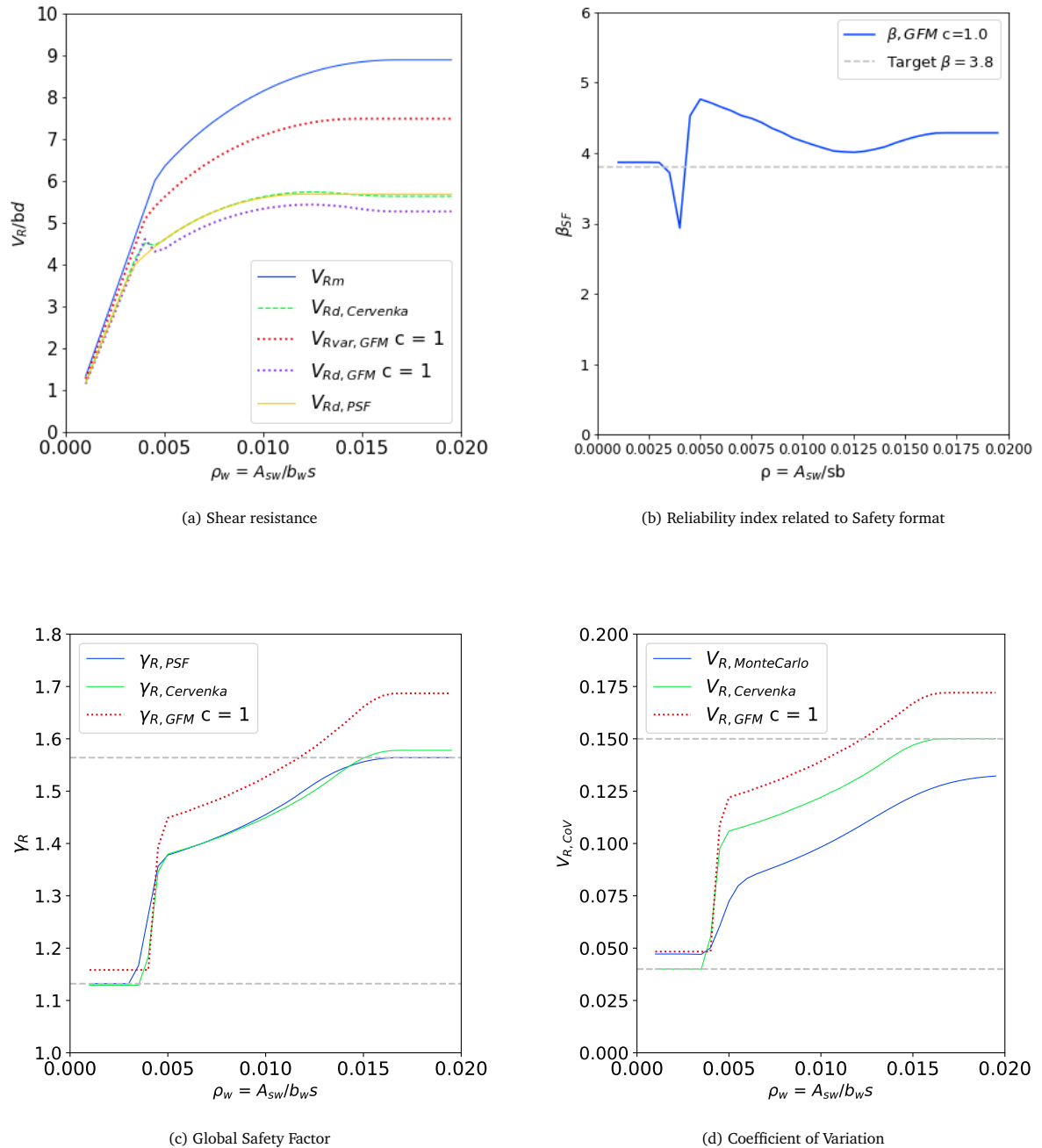
Figure 5.13: Case 1b: GFM with c = 1.0, PSF and ECOV Cervenka
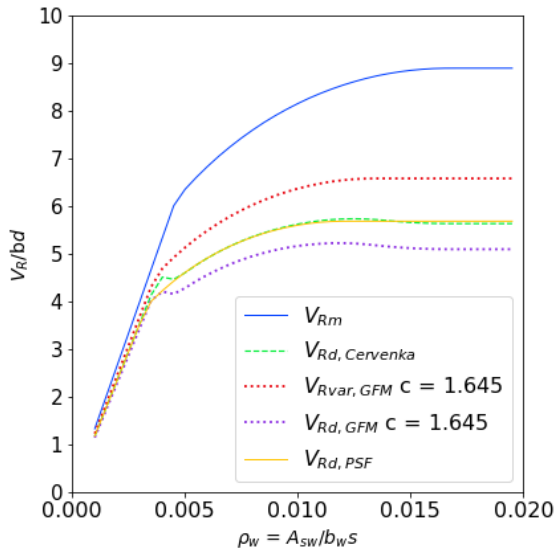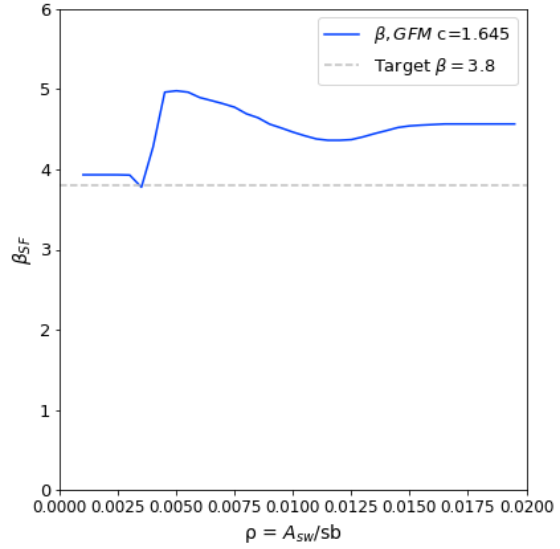
(a) Shear resistance

(b) Reliability index related to Safety format
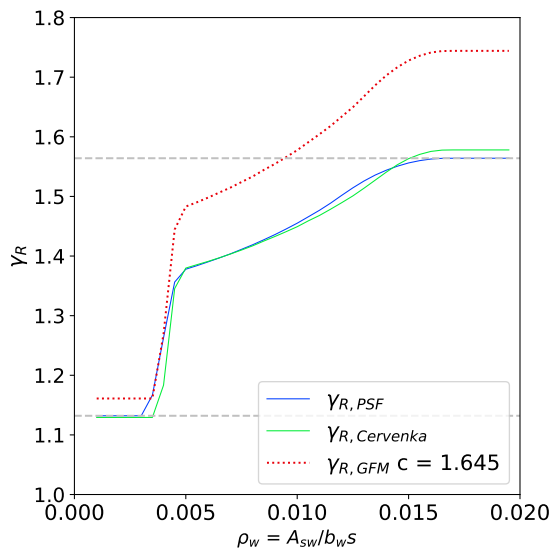
(c) Global Safety Factor
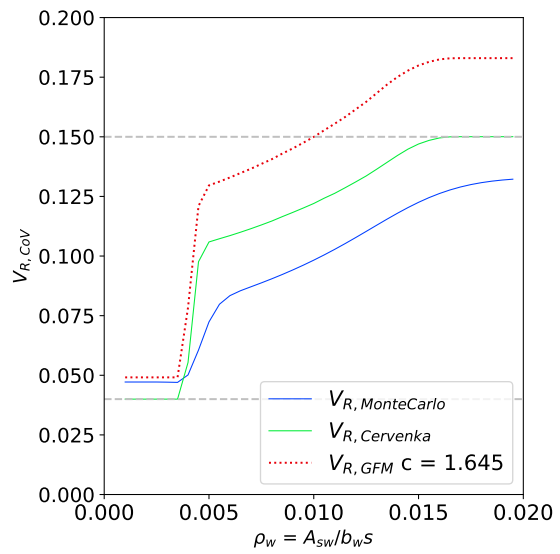
(d) Coefficient of Variation

Figure 5.14: Case 1b: GFM with c = 1.645, PSF and ECOV Cervenka
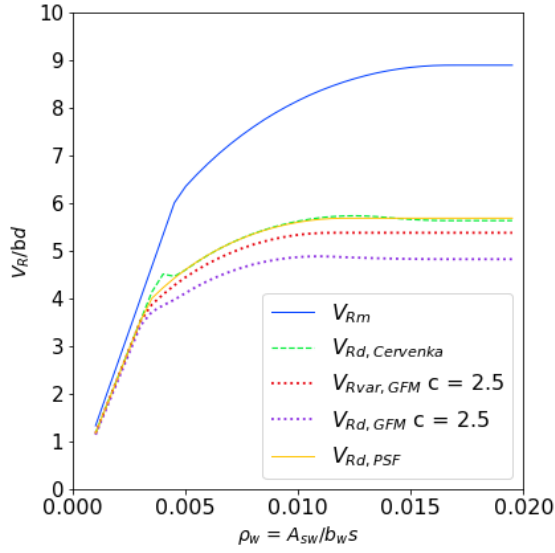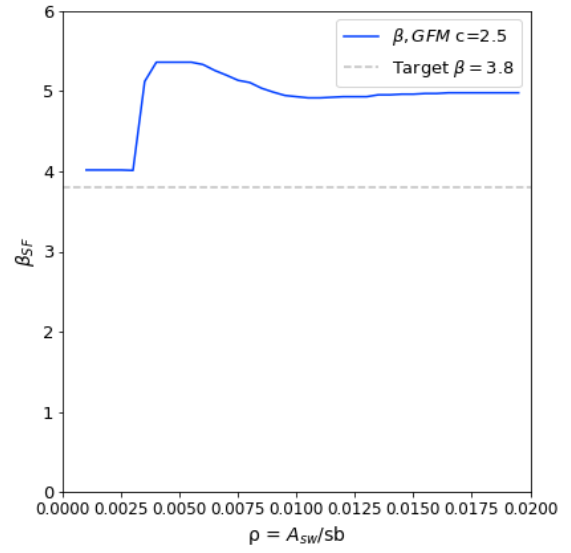
(a) Shear resistance

(b) Reliability index related to Safety format
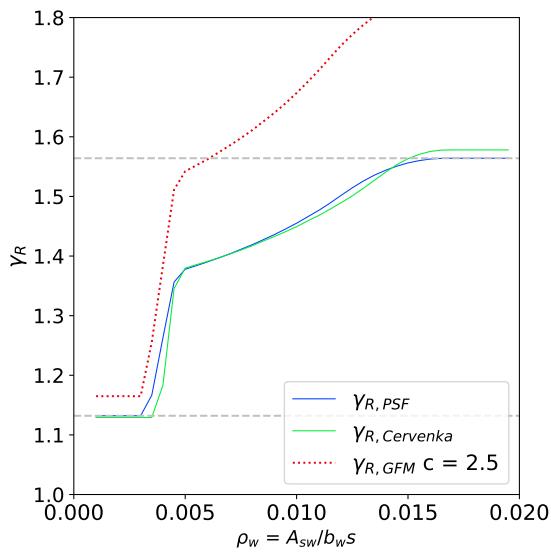
(c) Global Safety Factor
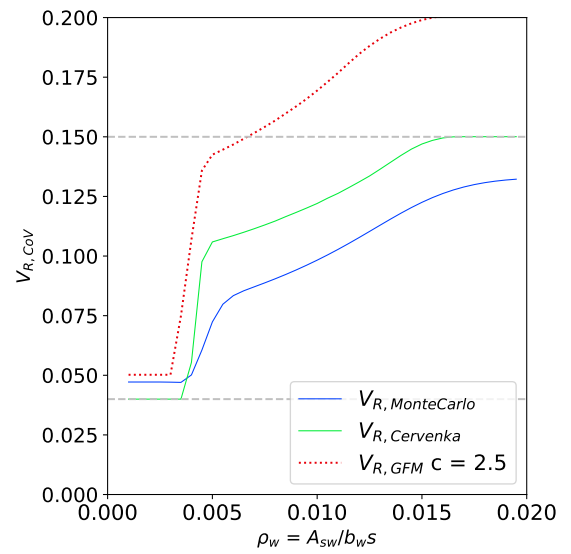
(d) Coefficient of Variation

Figure 5.15: Case 1b: GFM with c = 2.5, PSF and ECOV Cervenka

6

Simply Supported beam with concurrent failure mechanism: Case 1c

Previous cases study 1a and 1b provided an opportunity to gain insight into the application of the GFM at a cross-section level. This chapter presents a third analytical model where the implementation of the new safety format is performed at a higher scale: a simple continuum structural member. In this case, the same configuration of the simply supported beam subjected to a quasi-static point load, and investigated in the following chapters 7 and 8, is analyzed through analytical expressions. The setup is inspired by the beams without shear reinforced studied in the experimental research on reinforced concrete carried out at the Delft University of Technology. [28] Now, bending and shear failure mechanisms can affect the structure in a single or concurrent manner, depending on the point of application of the point load. The use of analytical expressions provides insight into the future performance of the RC beam during the nonlinear finite element analyses. It allows the investigation of the transition zone where shear and bending mechanisms perform as concurrent ones by analyzing a larger range of load configurations due to a less time-consuming computational model.

First, the geometrical and material parameters are introduced along with the statistical properties of the basic variables. Then, section 6.2 presented the analytical expressions used for the analysis at a member level. The analytical models are based on the Eurocode. Later on, section 6.3 refers to the application of the GFM in computing the design resistance of the simply supported beam for varying positions of the load. Finally, comparison with existing formats and discussion of the results are presented in section 6.4
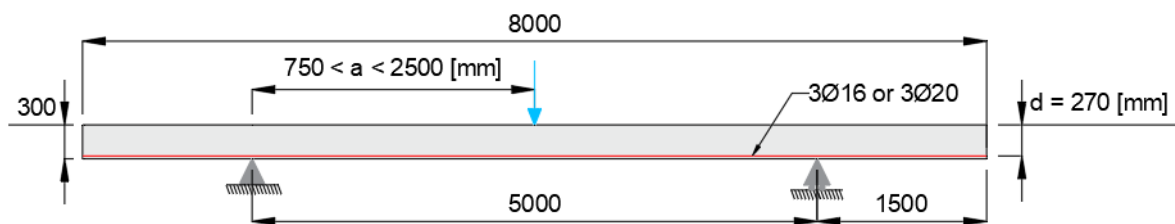
Figure 6.1: Case study 1c: a simply supported beam subjected to a quasi-static point load.

6.1. Material, Geometrical and statistical properties
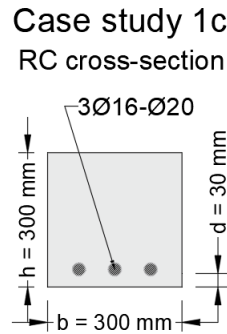
Figure 6.2: Case study 1c: Reinforced concrete cross section with longitudinal reinforcement

Figure 6.2 illustrates the cross-section along the complete length of the beam. The mean values of concrete compressive strength and yielding strength of the reinforcement are taken from the experimental results obtained in [28]. As described in section 4.2, these two parameters are selected as the basic random variables since they are the most influencing ones in the analytical calculation of the design resistance, and they are assumed to carry the stochastic and uncertain nature of the two materials in the model. The values of the standard deviations for the two chosen random variables are taken from [32]. Table 2.5 summarize the material and statistical properties. The coefficient of variation is calculated as the ratio between the corresponding standard deviation and the mean value of the property.

Material Property		Mean Value	Standard deviation	Coefficient of Variation
Concrete Compressive Strength	f_{cm}	78.5 [MPa]	9.645 [MPa]	0.1236
Reinforcement Yielding Strength	f_{ym}	550 [MPa]	65 [MPa]	0.1182

Table 6.1: Mean values of the material parameters

6.2. Analytical expressions

In this section, the analytical expressions presented are based on the models proposed in the Eurocode for the design and analysis of reinforced concrete structures under bending and shear solicitations. It is acknowledged that the models are used to provide an estimation, usually a conservative one, of the real performance of the structure. However:

- It is not possible to study the structural performance as a whole only at a member level. Stress redistribution or redundancy are not accounted for by the analytical model.

- The model cannot explicitly account for cracking of the concrete, especially for the modeling of shear failure leading to a conservative value of the resistance.

- The analytical expression is calibrated for inputting design or characteristic values of the material parameters. Therefore, the use of the same expressions with the perturbed or mean values might not be accurate.

The global quantity expressing the capacity of the structure, P_u, is defined as the ultimate load-bearing capacity given by computing the maximum value of the point load resisted by the beam before failure.

6.2.1. Analytical Expression for Bending Resistance

Assuming the parabola-rectangle constitutive law for the concrete, an elastic perfectly plastic behavior of the reinforcement, strain compatibility, and linear strain stress distribution along the cross-section, the maximum bending moment resistance of a cross-section subjected to bending is given by:

$$M_R = \left[\rho f_y^* - \frac{297}{578} \frac{\rho^2 f_y^{*2}}{f_c^*} \right] bd \tag{6.1}$$

with:

- $\rho = \dfrac{A_s}{bd}$ → Longitudinal Reinforcement Ratio

- f_y^* → Yielding Strength of the Reinforcement

- f_c^* → Concrete compressive strength

- b → Width of the rectangular cross-section

- d → Effective height of the rectangular cross-section

The stress in the reinforcement is assumed to be the yielding strength given the two low longitudinal reinforcement ratios analyzed: $\rho_1 \approx 0.0074$ and $\rho_2 \approx 0.0116$. Knowing that M_R is the maximum bending moment resisted by the member, the value of the maximum load-bearing capacity causing this effect can be computed by the equilibrium of forces in the structure. Therefore:

$$P_{u,M,max} = \frac{M_R}{a \cdot \dfrac{L_2 - a}{L_2}} \tag{6.2}$$

- a → Length from the closest support until the point of application of load

- L_2 → Length of the span between the supports

6.2.2. Analytical Expression for Shear Resistance

In literature, several models with varying complexity and level of refinement attempt to provide an accurate estimation of the shear resistance of reinforced concrete structures. [3] [34] [15] [40] [43] In this case, the implemented expression follows the guidelines from the Eurocode in EN 1992-1-1, section 6.2.2, referring to the design resistance of structural members that do not require shear reinforcement. In [3], a comparison between existing analytical models for computing the shear strength of reinforced concrete slender beams was carried out. There, equation 6.3 proved to perform on the conservative side for beams without stirrups.

$$V_R = C_{R,c} \, k \, (100\rho f_c^*)^{\frac{1}{3}} \, b_w d \tag{6.3}$$

with:

- $C_{R,c} = 0.18$

- $k = 1 + \sqrt{\dfrac{200}{d}}$

- f_c^* → Concrete compressive strength

- b_w → Width of the rectangular cross-section

- d → Effective height of the rectangular cross-section

Knowing that V_R is the maximum shear force resisted by the member, the value of the maximum load-bearing capacity causing this effect can be computed as:

$$P_{u,V,max} = \frac{V_R}{\dfrac{L_2 - a}{L_2}} \tag{6.4}$$

- a → Length from the closest support until the point of application of load

- L_2 → Length of the span between the supports

Finally, by comparing the outputs of equations 6.2 and 6.4 the resistance of the simply supported is given by the minimum P_u. The previous fulfills the requirement of the GFM in choosing the CLFM and the mean value of the resistance: when two LFM are working as a series system, the minimum value of the resistance between the failure mechanism should be taken as the critical one.

6.3. Design resistance by the GFM

First, the mean ultimate load-bearing capacity of the beam must be obtained by evaluating the analytical expressions of the material parameters. Figures 6.4 and 6.5 illustrate the followed procedure in a flowchart. Since the RC beam has a constant concrete cross-section, the same computed mean value of the bending, $M_{R,m}$, and shear resistance, $V_{R,m}$ apply independently of the position of the load. The given location starts playing a relevant role when identifying the CLFM. Two values of the maximum load that the beam can resist are calculated. By applying static equilibrium, the bending moment and shear force distribution, acting along the beam, provided equations 6.5 and 6.6 to calculate the maximum effects and their location. By assuming that the most critical effects can reach the value of the mean bending and shear resistance, $P_{u,M_{R,m},max}$ and $P_{u,V_{R,m},max}$ are found with equations 6.7 and 6.8.

$$M_{max} = P \cdot a \cdot \frac{L_2 - a}{L_2} \tag{6.5}$$

$$V_{max} = P \cdot \frac{L_2 - a}{L_2} \tag{6.6}$$

$$P_{u,M_{R,m},max} = \frac{M_{R,m}}{a \cdot \dfrac{L_2 - a}{L_2}} \tag{6.7}$$

$$P_{u,V_{R,m},max} = \frac{V_{R,m}}{\dfrac{L_2 - a}{L_2}} \tag{6.8}$$

Therefore, the Critical Local Failure Mechanisms and the mean value of the resistance is given by:

$$P_{u,m} = \min\{P_{u,M_{R,m},max}, P_{u,V_{R,m},max}\} \tag{6.9}$$
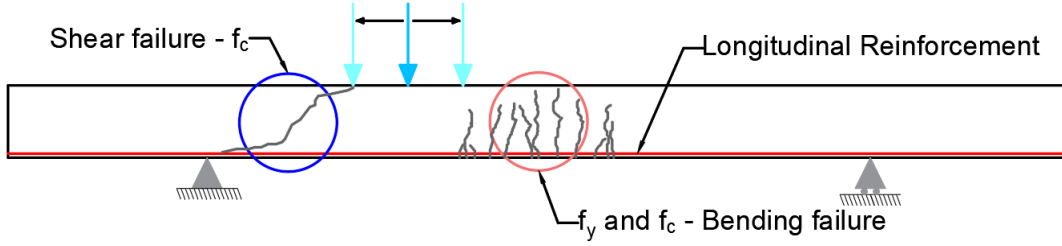
Figure 6.3: RC simply supported beam with possible concurrent failure mechanisms - Case 1c

A key point in the application of the GFM is the explicit inclusion of concurrent failure mechanisms in the expression to calculate the Global Safety Factor, γ_R. One of the advantages of the analytical model is that the location of the load where the change in failure mechanisms occurs can be identified. Additionally, a quantitative criterion for the boundaries of the position of the load that might cause the two LFM (shown in figure 6.3) to work as a series system of concurrent failure mechanisms is presented. The Percentage Difference is calculated for the non-critical Local Failure Mechanisms. For instance:

$$P.D. = \begin{cases} \dfrac{V_{R,m} - V}{\dfrac{V_{R,m} + V}{2}} * 100 \;\; \rightarrow \;\; \text{with}: \;\; V = P_{u,m} \cdot \dfrac{L_2 - a}{L_2} \;\; \text{and} \;\; P_{u,m} = P_{u,M_{R,m},max} \;\; \text{if}: \text{CLFM} = \text{Bending} \\[6mm] \dfrac{M_{R,m} - M}{\dfrac{M_{R,m} + M}{2}} * 100 \;\; \rightarrow \;\; \text{with}: \;\; M = P_{u,m} \cdot a \cdot \dfrac{L_2 - a}{L_2} \;\; \text{and} \;\; P_{u,m} = P_{u,V_{R,m},max} \;\; \text{if}: \text{CLFM} = \text{Shear} \end{cases}$$

(6.10)

Now, when computing the Coefficient of Variation of the related to the material uncertainty, V_{R_x}, a second value of the resistance, $P_{u,var}$, must be obtained with the reduced basic variables, $x_{var} = x_m - c \cdot \sigma_x$, belonging to the CLFM.

$$P_{u,var} = \begin{cases} \min\{P_{u,M_{R,var},max}, P_{u,V_{R,m},max}\} \;\; \rightarrow \;\; \text{with}: \;\; P_{u,M_{R,var},max} = \dfrac{M_{R,var}}{a \cdot \dfrac{L_2 - a}{L_2}} \;\; \text{if}: \text{CLFM} = \text{Bending} \\[8mm] \min\{P_{u,M_{R,var},max}, P_{u,V_{R,m},max}\} \;\; \rightarrow \;\; \text{with}: \;\; P_{u,V_{R,var},max} = \dfrac{V_{R,var}}{\dfrac{L_2 - a}{L_2}} \;\; \text{if}: \text{CLFM} = \text{Shear} \end{cases}$$

(6.11)

In this case, the perturbation parameter was evaluated with $c = [0.1, 0.5, 1.0, 1.645, 2.5]$. The Coefficients of Variation of the geometrical and modeling uncertainty are not taken into account. Therefore:

$$V_R = V_{R_x} = \frac{1}{c} \ln\left(\frac{P_{u,m}}{P_{u,var}} \right)$$

(6.12)

Finally, the Global Safety Factor for the resistance and the design ultimate load-bearing capacity of the beam is obtained for the position of the load varying from $750[mm] \leq a \leq 2500[mm]$:

$$\gamma_R = \begin{cases} \exp(0.8 \cdot 3.8 \cdot V_R) \;\; \rightarrow \;\; if : \; P.D \geq 10\% \\ \exp\left(\ln(\sqrt{2}) V_R + 0.8 \cdot 3.8 \cdot V_R \right) \;\; \rightarrow \;\; if : \; P.D \leq 10\% \end{cases}$$

(6.13)

$$P_{u,d} = \frac{P_{u,m}}{\gamma_R}$$

(6.14)
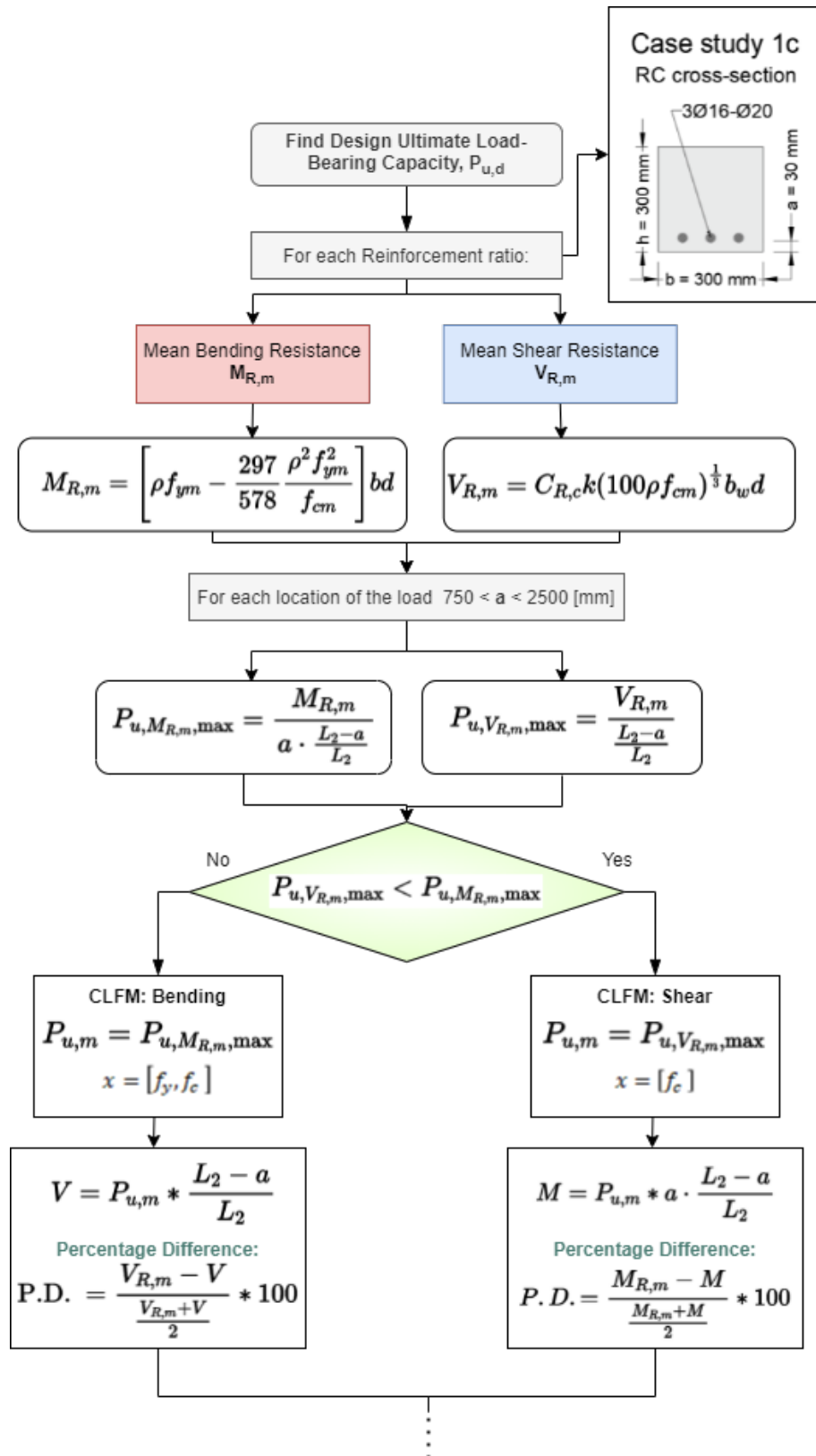
Figure 6.4: Flowchart GFM: Mean Ultimate Load-Bearing Capacity simply supported beam - Case 1c

$$x_{var} = x_m - c \cdot \sigma_x$$

CLFM = Shear

No → **CLFM: Bending**

$$x = [f_y, f_c]$$

$$M_{R,var} = \left[\rho f_{y,var} - \frac{297}{578} \frac{\rho^2 f_{y,var}^2}{f_{c,var}}\right] bd$$

$$P_{u,M_{R,var},max} = \frac{M_{R,var}}{a \cdot \frac{L_2-a}{L_2}}$$

$$P_{u,var} = \min\{P_{u,M_{R,var},max}, P_{u,V_{R,m},max}\}$$

Yes → **CLFM: Shear**

$$x = [f_c]$$

$$V_{R,var} = C_{R,c} k (100\rho f_{c,var})^{\frac{1}{3}} b_w d$$

$$P_{u,V_{R,var},max} = \frac{V_{R,var}}{\frac{L_2-a}{L_2}}$$

$$P_{u,var} = \min\{P_{u,M_{R,m},max}, P_{u,V_{R,var},max}\}$$

$$V_R = V_{R_x} = \frac{1}{c} \ln\left(\frac{P_{u,m}}{P_{u,var}}\right)$$

P.D. <= 10%

No → **Single FM**

$$\gamma_R = \exp(\alpha_R \beta_{LS} V_R)$$

Yes → **Concurrent FM**

$$\gamma_R = \exp\left(\ln(\sqrt{2})V_R + \alpha_R \beta_{LS} V_R\right)$$

$$P_{u,d} = \frac{P_{u,m}}{\gamma_R}$$
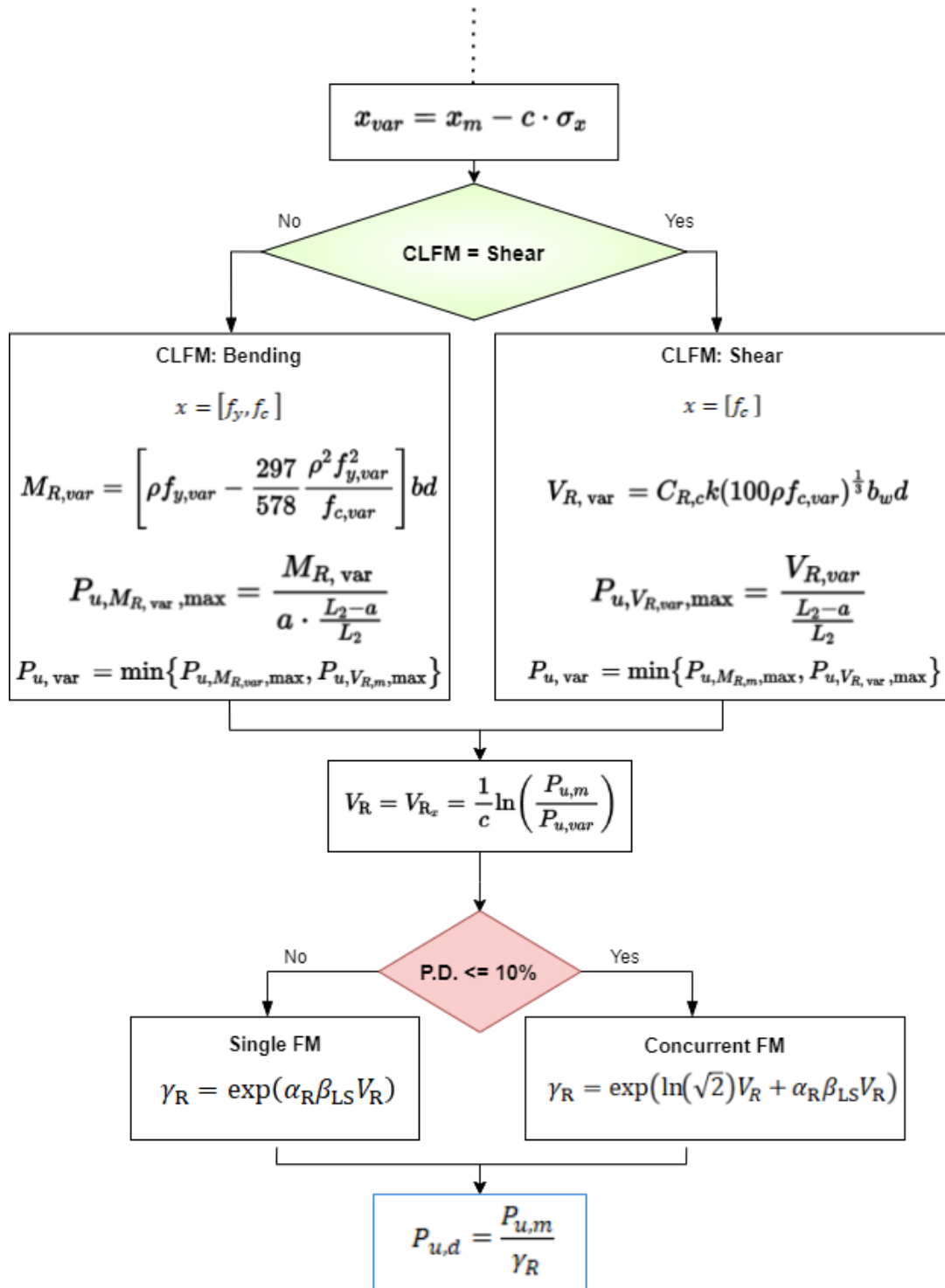
Figure 6.5: Flowchart GFM: Design Ultimate Load-Bearing Capacity simply supported beam - Case 1c

6.3.1. Results GFM

(a) Resistance with c = 0.1

(b) c = [0.1, 0.5, 1.0, 1.645, 2.5]
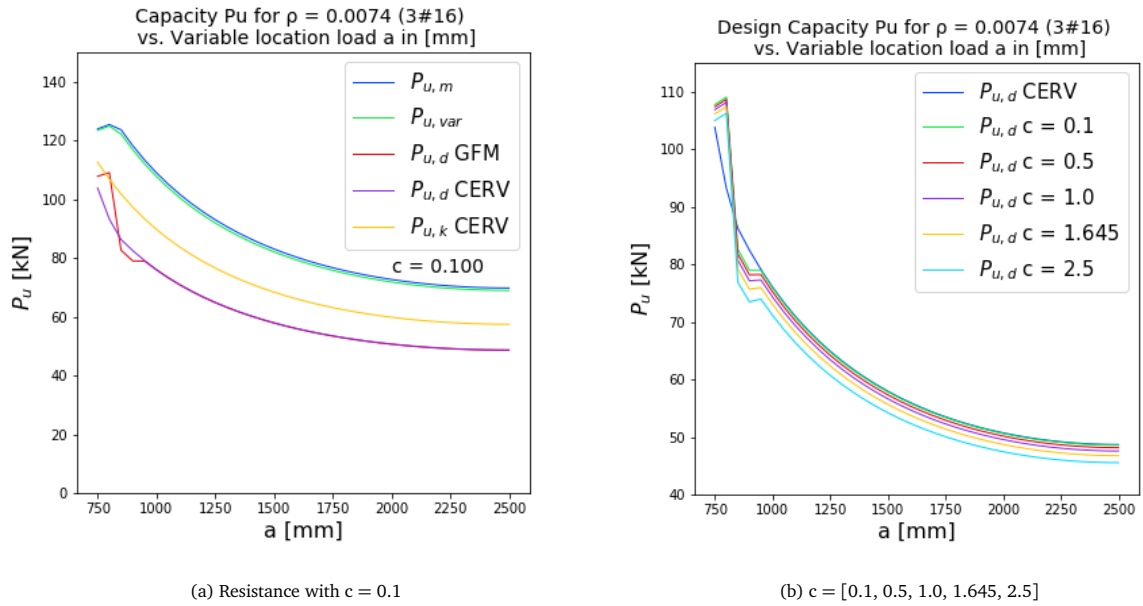
Figure 6.6: Resistance ECOV and GFM: case 1c - $\rho = 0.0074$

(a) Resistance with c = 0.1

(b) c = [0.1, 0.5, 1.0, 1.645, 2.5]
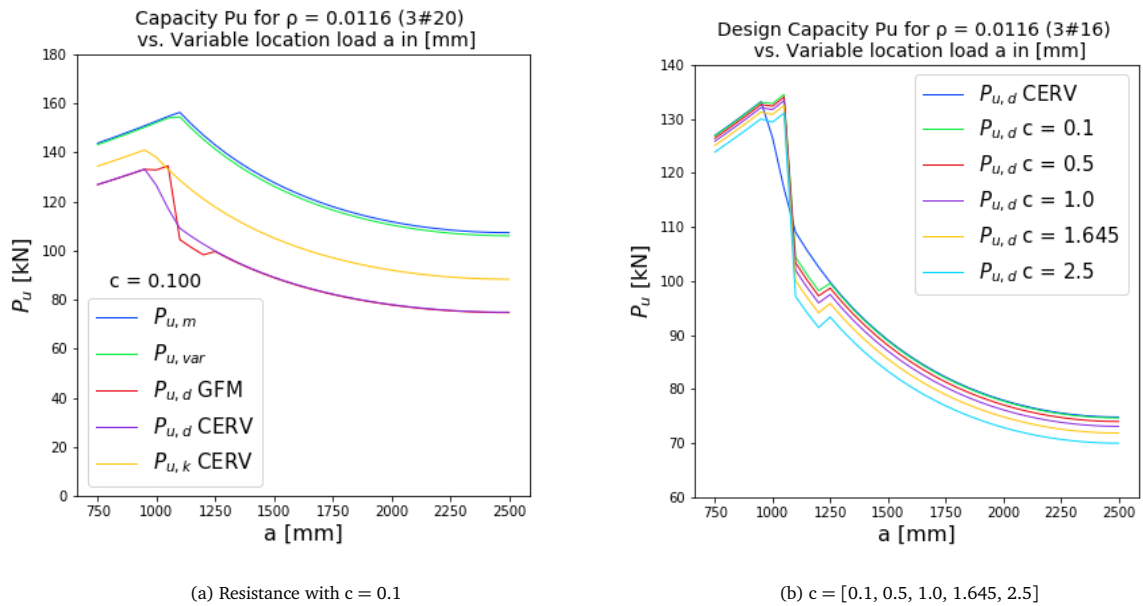
Figure 6.7: Resistance ECOV and GFM: case 1c - $\rho = 0.0116$

Results: Monte Carlo Simulation

(a) $\rho = 0.0074$ (b) $\rho = 0.0116$
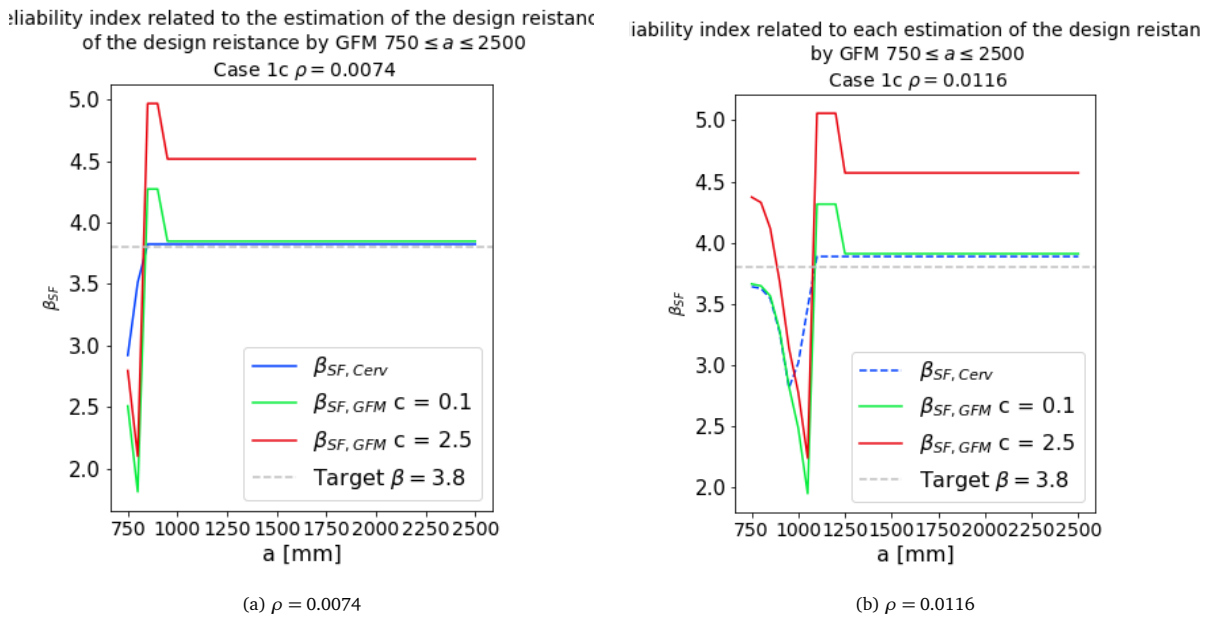
Figure 6.8: Reliability index related to the estimation of the design resistance computed with ECOV method and GFM with c = 0.1 and 2.5

6.4. Discussion and Conclusions

- The point of transition from bending failure mechanisms to shear failure mechanism moves away from the support for structures with higher reinforcement ratio. As expected, lower reinforcements ratios provide a more ductile behaviour of the structure, but a lower load-bearing capacity.

- The beam with $\rho = 0.0116$ shows the transition of failure mechanisms when the load is around 1200 [mm] away from the nearest support, which coincides with distances determined in experimental tests performed in [28]. This gives an estimation of the expected nature, ductile or brittle, of the mechanism of the mixed beam analyzed in the following chapter with NLFEA.

- In comparison to the design capacity obtained with the Cervenka method, the GFM with a value of c = 0.1 provides the same level of reliability and accuracy for positions of the loads that cause bending failure. Higher values of the perturbation parameters c proportionally scaled the design value of the resistance, increasing the reliability and providing more conservative results when the load is closer to the mid-span.

- For $\rho = 0.0074$, the ECOV method do not produce any failure in shear, no matter how close the load is applied to the support. Even though the resistance is being conservative estimated, the nature of the actual mechanisms might be overlooked, which would lead to a dangerous and unexpected brittle failure. The GFM represents an improvement in identifying the CLFM, but the value of the resistance for the position of the load causing shear failure is, still, not able to reach the target reliability in figures 6.8a and 6.8b.

- The coefficient of variation when the CLFM is identified as shear ($V_{R_x} = 0.0412$) is relatively lower than the one in bending ($V_{R_x} = 0.0412$), this contradicts the usual stochastic nature observed in those type of failure. Shear failure usually has a greater variability than flexural failure: this is due to the higher variability of the concrete basic random variables impacting shear behaviour. The reason is found in the use of analytical expressions, the basic variables chosen and the way they are being decreased.

7

Existing safety formats in NLFEA: Case 2

7.1. General Considerations

Simplified analytical expressions provide a wide range of alternatives and scenarios to be studied due to their short computational time. However, implementation in the framework of NLFEA is the aim of the GFM. Therefore, it is relevant to provide classic but representative application cases to evaluate its performance. This section narrows the study to the ultimate limit state load-bearing capacity of three high stress concrete simply supported beams. The analyzed beams are extracted from [32], the structures are based on the experimental set-up from the test series on reinforced concrete beams without shear reinforced carried out in Delft University of Technology between 2015 and 2016. [28] Reproducing existing models provides the opportunity to focus on the application and validation of the new Safety Format in cases where choices as the solution strategy and modeling uncertainty are already verified, reducing some of the sources of uncertainty.

First, section 7.2 presents the configuration of the three reinforced concrete beams along with their geometrical parameters and material properties. Section 7.3 shows the solution strategy for all the NLFE analyses performed within chapter 7 and 8. Furthermore, the chapter introduces the implemented modeling uncertainty taken from the work of De Putter in [12]. As a reference Safety Format, the design resistance is obtained by the ECOV by Cervenka.

7.2. Three RC simply supported beams

The experimental research on reinforced concrete beams without shear reinforcement, carried out at the Delft University of Technology, presents an adequate opportunity to study how the new GFM performs in structures where several Local Failure Mechanisms might develop in an (almost) concurrent manner. The test series procedure started by placing the point load at a location expecting to cause flexural failure, which means the load was applied closer to the mid-span. The experiment described flexural failure as the yielding of the longitudinal reinforcement up to a specified strain. Afterward, the unloading of the structure occurred. Then, the point load was reallocated to a position closer to the support, where a second test was performed. Several tests were performed until the transition to shear failure took place. [28] One of the conclusions of the experiment is that for intermediate locations of the point load the Failure Mechanism is not easily identified. In some trials, the failure mechanism for the same load position and reinforcement configuration was different. The latter indicates the possible concurrent nature of flexural and shear failure in some of the specimens in the test.

The three chosen beams are selected since the interpretation of the design capacities, obtained by the GFM with the use of an implicit Limit State Function with NLFEA, is possible due to the existing results presented by Roy in [32]. In his work, the application of a reliability algorithm, better known as the Directional Adaptive Response Surface method (DARS method), to calculate the probability of failure of the three beams provides a possible validation tool. In the case of NLFEA, this is much more efficient than performing a crude Monte Carlo simulation, where millions of simulations would have been necessary.

The simply supported structures are subjected to a point load applied at a distance a from the support. The location of this load, along with the amount of longitudinal reinforcement in relation to the height of the cross-section (excluding the concrete cover in the tension zone), highly influences the development and selection of the critical local failure mechanism (CLFM).

Figures 7.1, 7.2 and 7.3 display the supports, geometry and load configuration. The amount and position of the longitudinal reinforcement are also specified. Table 7.1 summarizes the mean values of the relevant material parameters. The mean value of the concrete compressive strength is taken from testing concrete cubes with dimensions 150×150×150 mm3. The cubes were taken during casting of each specimen. Roy calculated the remaining material parameters by applying the suggested formulas in the *fib* Model Code 2010. The formulas are found in Appendix F The mean value of the Modulus of Elasticity (and the Poisson ratio) of concrete should be used for all the NLFEA performed. [23]

Beam case	$f_c[MPa]$	$f_t[MPa]$	$G_F[N/mm]$	$E_c[MPa]$	$f_y[MPa]$	$G_c[N/mm]$
Bending	78.5	5.1474	0.1269	42729	550	31.73
Shear	78.2	5.1328	0.1266	42675	550	31.64
Mixed	77.5	5.0986	0.1258	42247	550	31.45

Table 7.1: Mean values of the material parameters

Case study 2a: Bending beam
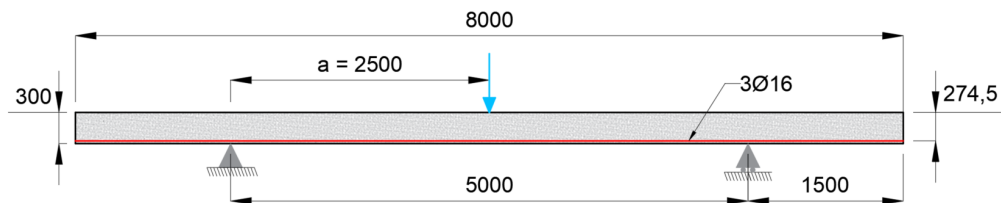
Figure 7.1: Beam failing in flexural bending

Case study 2b: Shear beam
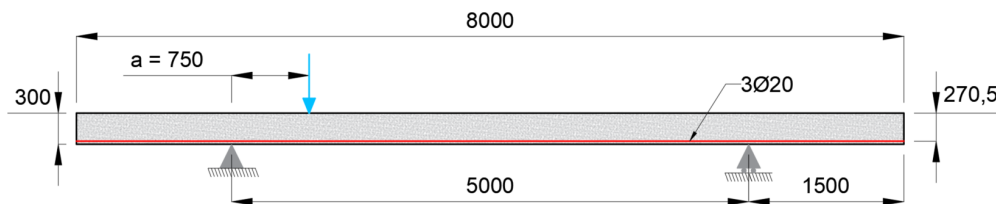
Figure 7.2: Beam failing in shear

Case study 2c: Mixed beam
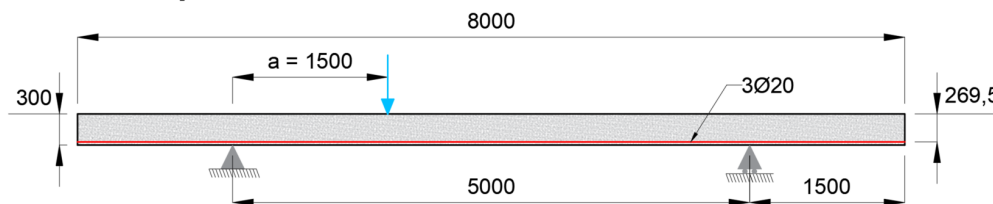
Figure 7.3: Mixed beam

7.3. Solution Strategy

Applying NLFEA is not a straightforward process with only one correct answer. The original structure must be idealized and discretized. During these two steps, several factors related to the model and the decisions performed by the user highly influence the final performance and accuracy of the model. Therefore, the use of existing guidelines decreases the influence and bias introduced by those factors.

The solution strategy applied in the NLFE models of the three RC beams is based on the Dutch Guidelines (DG) for Nonlinear finite element analysis of concrete structures (version 2.2) [23]. The DG applies for reinforced and prestressed concrete structures like bridges and viaducts, in addition to structural elements: beams, girders, slabs, box-girder structures, culverts, and bridge decks. However, its use is restricted only to the analysis of existing structures by the Dutch Ministry of Infrastructure and Water Management. Since the focus of the Guidelines and this thesis is to perform the analysis with certainly required reliability; full models of the structures are required to obtain the ultimate load-bearing capacity for all the pertinent loads.

The process of idealization into the mechanical model includes the assumptions and simplifications related to the selected level of detail; the description of the boundary conditions, the relevant loads and their application, etc. The discretization into the finite element model must include all the factors related to the material models, boundary conditions, and loading conditions.

Modeling a structure must always start with the following steps:

- Definition of the unit system

- Definition of the material and geometrical properties for every part of the structure

- Discretization of the structure along with the application of boundary conditions and loads

This section presents the selected solution strategy. The majority of the decisions have their basis on the ones made by Roy in [32]. The previous is relevant for two main reasons:

1. To have a reference in verifying the accuracy of the models, which allows focusing on the further implementation of the GFM.

2. To allow the comparison of the results obtained by the GFM and the results obtained by the DARS method in [32], looking for validation tools on the applicability of the GFM.

7.3.1. Constitutive models

The constitutive models refer to the strain-stress relationship of the material i.e. the material models. They are simplified representations of the behavior of the material.

Concrete

The Dutch Guidelines advise a total strain-based rotating crack model since it suffers less from spurious stress locking. However, in this thesis, a fixed crack model was selected following [32]. The choice is supported by the results in the work of De Putter [12]; the comparison between several benchmark tests and finite element models concluded that for beams without shear reinforcement (stirrups), a fixed crack model represents a better agreement. The linear-elastic behavior of the material depends on two parameters: Young's Modulus and Poisson ratio. The selected material model for the concrete includes a decrease in the Poisson effect with the developing of cracks, a damaged-based approach.

- Tensile behaviour

An exponential softening diagram (or similar) is selected as advice in [23], resulting in more localized cracks that avoids large areas of diffuse cracking. "Fully open" cracks are assumed to develop after complete softening, and virtually no stresses are transmitted. In the bending beam, case study 2a, the nonlinear softening curve according to Hordijk is implemented. [25]
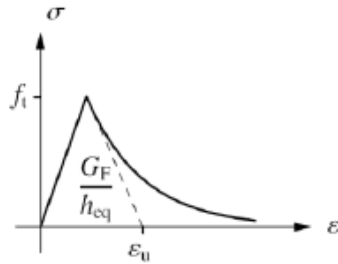
Figure 7.4: Exponential softening curve

Tensile Strength	f_t	MPa
Fracture Energy	G_F	Nmm/mm^2
Crack Bandwidth	h_{cr}	mm

Table 7.2: Parameters - Exponential softening curve

- Shear behaviour

Due to the choice of a fixed crack model, a variable shear retention model in which the shear stiffness reduces after cracking is applied in DIANA FEA by implementing the option: shear retention based on the damage due to cracking. The shear modulus G decreases due to the reduction in the secant tensile stiffness and Poisson's ratio.

- Compressive behaviour

The parabolic stress-strain diagram with a softening branch describes the compressive behavior of the concrete in the selected solution strategy. The maximum compressive stress is limited by a given value f_c. The selection of the constitutive law is especially relevant since the post-peak behavior of concrete is highly complex. The model depends on two parameters: the compressive fracture energy G_c and a crushing bandwidth h_{cr}.
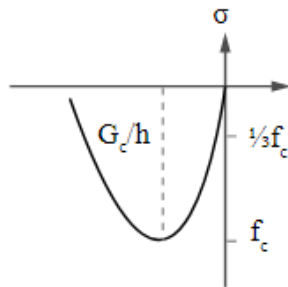
Figure 7.5: Parabolic curve

Compressive Strength	f_c	MPa
Fracture Energy	G_c	Nmm/mm^2
Crack Bandwidth	h_{cr}	mm

Table 7.3: Parameters: Parabolic curve

- Tension-Compression interaction

Tension-compression interaction must be accounted for when the structure is known to be under a state of multi-axial stresses. According to [23] there is a reduction of the concrete compressive strength due to lateral cracking that must be included in modeling the material behavior. The Vecchio and Collins (1986) model [39] is applied for the NLFE models in this section.

- Compression-Compression interaction

Even though this phenomenon could have been ignored in a more conservative approach and it is not as relevant for 2D modeling, a model suggested by Selby and Vecchio [36] is applied as in [32].

- Equivalent length or crack band width - h_{cr}

The equivalent length, or crack bandwidth parameter, should be determined by an automatic procedure, usually available in the finite element program. According to DG, the mentioned procedure should base on

the initial direction of the crack and the element dimensions; however, methods based on the geometrical properties (area or volume) of the selected finite element are also possible. The decision is to implement an automatic procedure in the current models in DIANA FEA, the so-called Rots' element-based method.

Reinforcement

The DG, in [23], advises an elasto-plastic material model with hardening. However, aligning with the decisions by Roy in [32], an elastic-perfectly plastic is preferable for the case. The yielding strength limits the elastic behavior of the reinforcement steel, followed by a post-yielding behavior with no hardening.
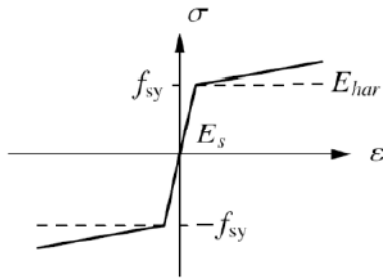
Figure 7.6: Stress-Strain diagram for steel

Yielding Strength	f_{sy}	MPa
Young's Modulus	E_s	MPa

Table 7.4: Parameters: Elastic-Perfectly plastic

Concrete-Reinforcement Interaction

The interaction between concrete and reinforcement is the principal mechanism for stress redistribution in reinforced concrete structures. The tension-stiffening effect is not included in the models as a conservative choice. Moreover, a perfect bond between the reinforcement bars and the surrounding concrete is assumed.
.

7.3.2. Finite Element Discretization

In the process of discretizing the mechanical model the following aspects highly influence the accuracy and quality of the results:

- Finite element model shape

- Shape function degree of the interpolation of the displacement field

- Numerical integration scheme for the internal stresses and strains of the finite elements

Therefore, an appropriate choice regarding each aspect should be based on knowledge of the future developing mechanisms and the structural performance.

Finite elements shape, displacement field interpolation degree, and numerical integration scheme

According to DG, quadrilateral or hexahedral shapes, with quadratic interpolation of the displacement field, should be used in 2D and 3D simulations respectively. These elements are advisable in the guidelines due to their capacity in describing more deformation modes and more complex failure modes. Following the element choice in [32], quadrilateral 8-node iso-parametric plane stress elements are used in the current beam models. Table 7.5 presents all the specifications related to the selected finite element type, the shape function of the displacement field interpolation, and the numerical integration scheme.

Full numerical integration should be used, according to DG: "reduce integration leads to spurious modes when the stiffness of the element becomes small due to extensive cracking" [23]. For quadrilateral 8-noded continuum elements a 3x3 point Gauss numerical integration is selected

Embedded reinforcement elements (perfect bond between the reinforcement bars and the concrete) are used with quadratic interpolation, matching the one selected for the concrete elements where the reinforcement is embedded. Full or reduce numerical integration may be used in this case.

Finite Element Type	8-noded Regular Plane Stress Element	Embedded bar	Structural Line Interfaces
DIANA Type	CQ16M	-	CL12I
DoF	$u_x\, u_y$	Same as mother element	$u_x\, u_y \Delta$
Degree of Interpolation	Quadratic	Same as mother element	Quadratic
Interpolation Scheme	3 x 3 Gauss integration	Same as mother element	3-point Newton-Cotes integration
Structural component	Concrete beam Steel plates	Reinforcement bars	Interface Concrete - Steel plates
Element size	25 x 25 mm	25 mm	25 mm

Table 7.5: Description finite element types

The DG established a minimum element size in function of the maximum aggregate size. Nevertheless, the limitation is closely related to practical considerations since computational time potentially increases with the number of elements, becoming a relevant limiting criterion. The maximum element size is restricted for several reasons: to avoid a "snap-back" stress-strain relationship, to accurately capture geometrical variations, stress and damage distributions, and to obtain a sufficiently smooth stress field.

7.3.3. Loads and Boundary Conditions

The DG defines the boundary conditions as the restrain of the displacements at specific points of the structure. A detailed examination of the loading and support points is not of interest to this thesis. Therefore, support and load plates are modeled to avoid high local stress concentrations around the specific regions. Additionally, linear interface elements are placed between the plate and the concrete.

In NLFEA, the loads applied in the structure increase until failure is observed or when a significant reduction in the capacity has occurred

7.3.4. Analysis

Loading Sequence and Incrementation

Usually, a clear loading sequence must be planned and applied in simulations with several load cases following, for instance, Eurocode specifications: dead weight, prestressing, permanent and variable loads. For the current beams, only one load case is applied for Ultimate Limit State Analysis: a concentrated load. In the simulations performed in this section, the concentrated load is replaced by an equivalent displacement i.e. displacement control method. The size of the step of this displacement is specifically selected for each model.

Equilibrium Iteration and convergence criteria

As stated by [23], a Newton-Raphson iterative method with arc-length control should be implemented in achieving equilibrium between internal and external forces. However, in line with [32] a Quasi-Newton (Secant method) method in combination with a Line Search method is employed instead since for the case of the shear and mixed beam it proved to produce higher quality results. The Line Search method helps to increase the convergence rate when strong nonlinearities, as cracking, take place in the structure.

The solution strategy must specify a convergence criteria to stop the iteration process when a satisfactory solution is obtained for an increment. Iterations may also terminate whether a certain maximum number

is specified beforehand or if the iterations lead to divergence. [13] The maximum number of iterations for each load/displacement increment is set to 100. As recommended in DG, the models adopt an energy-norm together with a force-norm. The option allowing the analysis to continue beyond non-convergence in an iteration is selected; not always non-convergence directly means failure.

Convergence Norm	Tolerance
Energy-norm	0.001
Force-norm	0.001

Table 7.6: Convergence norms criteria

7.4. Modelling Uncertainty

Once the solution strategy is selected, a new source of uncertainty must be accounted for in a reliability-based analysis of RC structures. The forthcoming version of the *fib* Model Code 2020 explicitly formulates the need to calculate the modeling uncertainty, which represents the accuracy of the selected solution strategy in predicting the capacity and behavior of the analyzed structure. Cracked reinforced concrete exhibit a high nonlinear behaviour. Therefore, when using Finite element models to compute their structural capacity an inherit modeling uncertainty must included. [18] The latter is obtained by comparing benchmark experimental outcomes with the results predicted by the selected solution strategy in a NLFEA.

Understanding that there is no correlation between the complexity of the analytical model and the accuracy of the resulting prediction is elementary for the choice of the benchmark experiments. Therefore, it is more efficient to select simple models since they can produce predictions that are just as good or bad as the outcome of highly complex models. [10] It is essential to have sufficient data for the comparison. Since the modeling uncertainty itself is influenced by the randomness of the material parameters, to uncouple the modeling uncertainty from the material uncertainty, a representative number of models and/or experiments must be included.[32]

The experimentally obtained global quantity of a structure, representing the global resistance of the system, and the predicted global quantity of the structure by NLFEA are assumed to be related through the modeling uncertainty as follows:

$$\theta = \frac{R_{\text{exp}}}{R_{\text{NLFEA}}} \tag{7.1}$$

There are a few different approaches in the comparison between the benchmark experiments and the predicted results by NLFEA:

- Based on blind prediction competition: for a single selected experiment, several participants compete in predicting the experimental outcome with their own solution strategy. The resulting modeling uncertainty represents the uncertainty in selecting a random solution strategy.

- Based on a uniform solution strategy: in this case, one experimental outcome is selected for several different types of structures which is compared with one predicted NLFEA output using the same solution strategy for each type of structure. The final modeling uncertainty is strongly related to the selected solution strategy.

Usually, the method which quantifies the modeling uncertainty assumes it is a log-normal distributed random variable. [26] Sometimes, the sample size is relatively small or not enough to account for other types of induced uncertainties: lab conditions, spatial variability of material properties, human errors, and lack of knowledge and measurements errors, to mention some. Thus, there is the need to implement statistical inference methods as Bayesian updating. Additional information might be found in [12][32][17], as the formulation of the modelling uncertainty is out of the scope of this thesis.

In [32], a modeling uncertainty based on a uniform solution strategy is obtained. No Bayesian updating is performed since the sample size is considered to be sufficiently large to account for the statistical uncertainty related to the stochastic parameters: mean and standard deviation (μ_θ and σ_θ). They are calculated

assuming that θ follows a Log-normal distribution. The 53 benchmark tests are conveniently selected from the same experimental set-up carried out in the Delft University of Technology between 2015 and 2016 by Yang et. al presented in [28]; the same as three RC beams analyzed in the present work.

The work of De Putter [12] presents an extensive study regarding multiple solution strategies for RC beams and their accuracy. It proposes a modeling uncertainty for a similar solution strategy (F9) as the currently applied one. Furthermore, it presents different stochastic parameters for the modeling uncertainty according to the selected solution strategy and on the ductility of the failure mechanism. The ductility index proposed in [16] in the criteria to determine whether the failure is brittle or ductile. Table 7.7 shows the different values of the stochastic properties of the modeling uncertainty taken from the approach of Roy [32] and De Putter [12].

Modelling uncertainty		
	μ_θ	V_θ
Roy	0.971	0.136
De Putter: Solution Strategy F9	1.053	0.108
De Putter: F9 - Ductile Failure	1.044	0.096
De Putter: F9 - Brittle Failure	1.170	0.175

Table 7.7: Modelling Uncertainty stochastic properties: Mean and Coefficient of Variation

In the next section, three tailored values of the modeling uncertainty are taken for each of the three beams. Defining that bending is a ductile failure mechanism, and shear is a brittle one. For the mixed case, the more general modeling uncertainty is implemented since the nature of the failure is not clear.

7.5. Design Resistance with existing Safety Formats

For the sake of comparison between existing Safety Formats and the GFM, the global design capacity P_d of the three RC beams is obtained following the procedures stated in the PSF method and ECOV by Cervenka method. Several NLFEA with the mean, characteristic, and design values of the input material parameters are performed. The results are shown in table 7.8.

Global Design Resistance R_d [kN]		
	PSF	ECOV
Case 2a: Bending Beam	52.07	48.71
Case 2b: Shear Beam	165.69	117.53
Case 2c: Mixed Beam	93.20	79.03

Table 7.8: Design value of the resistance for case 2a, 2b and 2c according to PSF and ECOV by Cervenka

8

The New GFM in NLFEA: Case 2

The GFM is applied for the calculation of the design capacity of each beam presented in chapter 7. At the first stage, a NLFEA with the mean values of the material parameters is performed for each beam; the results are presented and discussed, mainly focusing on the expected and obtained LFM, their location, hierarchical organization, and basic variables involved. Afterward, the set of the second NLFEA with the chosen basic variables being perturbed is performed. The latter is needed in the calculation of the coefficient of variation and global safety factor of the resistance.

The design resistance is calculated for each beam: in the case of the mixed beam, three scenarios assuming different Local Failure Mechanisms configurations are applied. Comparison of the GFM performance is done by interpreting the obtained results together with the reliability indexes provided by Roy in [32] with the application of the DARS method, in cases where it was possible to use the same solution strategy. In some of the cases, a modified solution strategy is needed. Consequently, the comparison is possible only in terms of the results obtained with the existing safety formats. Finally, observation on the obtained results, discussion, and conclusions are provided.

8.1. Expected Failure Mechanisms

Referencing the obtained failure mechanism in the experimental setup, the expected three types of failures reproduced in the FE models are bending, shear, and a mixed mechanism. Now, the method requires a clear definition of the description of the ultimate limit states (ULS) related to those types of failure.

A ULS, related to bending failure, is defined as the value of the global load-bearing capacity at the point of onset of the yielding of the longitudinal reinforcement. Usually, after the limit state is reached, the structure can withstand ongoing deformations due to the ductile nature of the mechanism. Shear failure at ULS, on the side, is characterized by a sudden loss of capacity leading the structure to fail in a more brittle manner. At that point, the structure becomes unstable and the characteristic secondary crack pattern for this type of failure might be recognized.

In [28], Yang et al. defined the mixed-mode as a failure mode between bending and shear failure. Apparently, for some specimens, failure is initiated by yielding in the tensile reinforcement followed, almost immediately, by the secondary cracks causing sudden failure of the structural system. The mixed behavior causes difficulty in define the limit state reached in this type of mechanism. The previous directly impacts the localization and identification of the Local Critical Failure Mechanism. Moreover, it increases the complexity in selecting the input basic variables to be perturbed in the second NLFEA.

8.2. NLFEA: Mean value of the resistance

For the three beams, a NLFEA with the mean properties of the input material parameters (Table 7.1) is performed. The global load displacement diagram is illustrated in figures 8.1a, 8.2a and 8.3a. Figures 8.1b, 8.2b and 8.3b illustrate the principal strain contour plot at the defined Limit State for each case. The mean

values of the resistance, $R_{m,NLFEA}$ are summarise in table 8.1.

The identification and location of the obtained LFM and CLFM is done by inspection and interpretation of crack patterns, strains and stresses distributions, and load-displacement curves.

Global Mean Resistance R_m [kN]		
	Arc Length Off	Arc Length On
Case 2a: Bending Beam	72.51	-
Case 2b: Shear Beam	-	217.73
Case 2c: Mixed Beam	127.59	140.37

Table 8.1: Mean value of the resistance for case 2a, 2b and 2c

Modified Solution Strategy

At this point, it is relevant to mention a modification in the solution strategy used by Roy in [32]. During the analysis of case 2b, different resistance values were obtained in every trial. Whether any change was introduced or not in the model or any new mesh was being generated. The analyses did not converge to any solution. Therefore, the Arc Length option was selected in DIANA to achieve consistency in the results. The response of the beam presents a snap-back behavior which made the previous solution strategy inadequate and inconsistent for the beam failing in shear.

The mixed beam (case 2c) was analyzed with both solution strategies. The load-displacement diagram is taken at the point of application of the load. Up to certain displacement, both curves follow a similar path. However, they show a difference in the maximum capacity and in the ductility of the final response towards the end of the analysis. The results for the mixed beam, presented hereafter, are obtained with the initial solution strategy, mainly seeking for the inclusion of the reliability index proposed by Roy in [32]. A more detail discussion is now presented separately for each case 2a, 2b and 2c.

Case 2a

The outputs from the analysis of case 2a, the bending case, confirm the initial assumption regarding the CLFM. The principle strain contour plot and the crack-width plot at the onset of the yielding of the reinforcement exemplifies the typical configuration for this type of failure. Mainly, bending cracks appear below the point of application of the load. Furthermore, the load-displacement curve for this case exposes the ability of the structure to withstand large ongoing deformations after reaching the maximum load-bearing capacity. The mechanism owns its ductile behavior to the yielding of the longitudinal reinforcement way before shear stresses become critical.

Case 2b

Case 2b, the shear beam, reproduced the expected principal strain and crack-width configuration: initially, bending cracks appeared under the point of application of the load. Subsequently, after reaching the maximum load, a diagonal crack develops in the region between the support and the loading plate. Other cracks related to a different type of failure are not observed anymore in the structure or at the surroundings of the main crack. A few load-steps before the loss of the structural capacity, the longitudinal reinforcement reaches the yielding strength in the region below the loading plate. The latter can explain the soft slope and ductility afterward.

The yielding of the longitudinal reinforcement, together with a less brittle failure than expected, might introduce the hypothesis of a mixed mechanism. Nonetheless, the computed strain and the crack width plots clearly show the classical patterns for shear failure. The latter will rule the selection of the CLFM in the application of the GFM. The parts of the reinforcement reaching stresses higher than the yielding one are limited, and only occur in very few steps before failure.

Case 2c

A challenge arises when the results obtained in case 2c, mixed case, are studied. First, the computed results with the initial solution strategy are discussed. Giving a first look at the global load-displacement
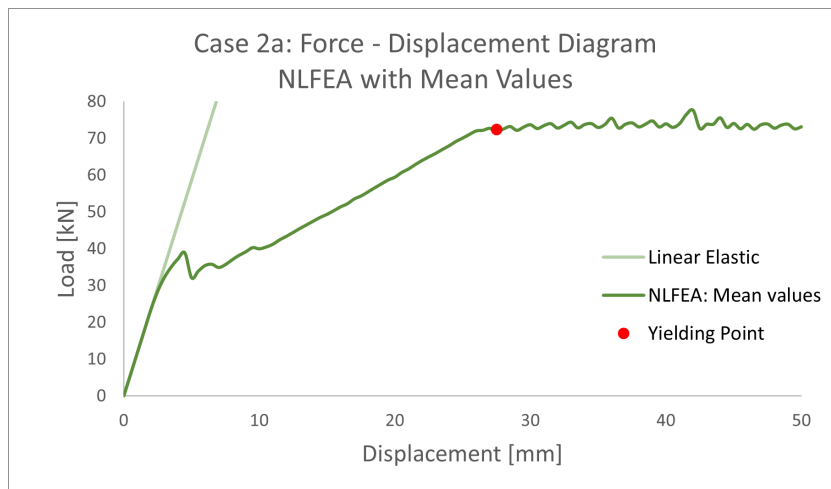
(a) Global Load-Displacement curve
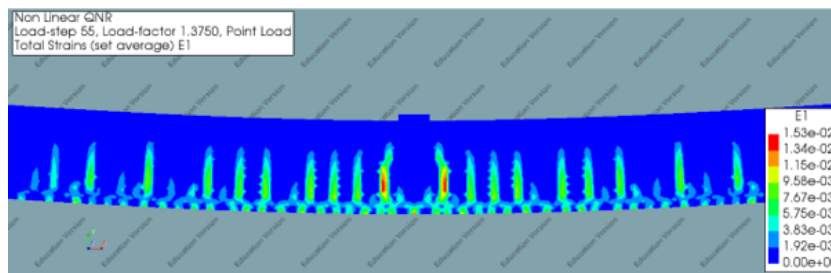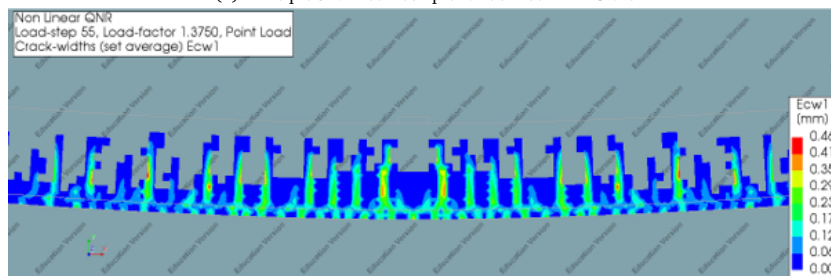
(b) Principle strain contour plot at defined Limit State

(c) Crack width at defined Limit State
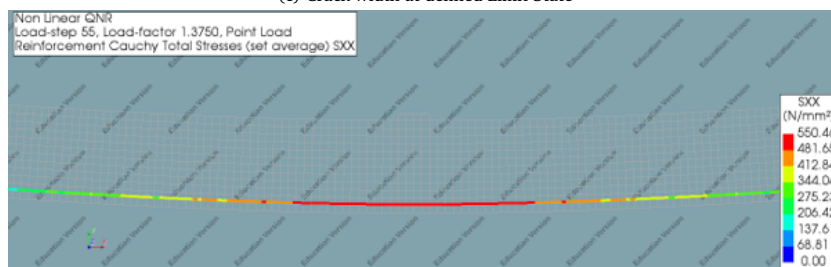
(d) Reinforcement Stresses at defined Limit State

Figure 8.1: Case 2a - NLFEA with mean value of the input critical material parameters
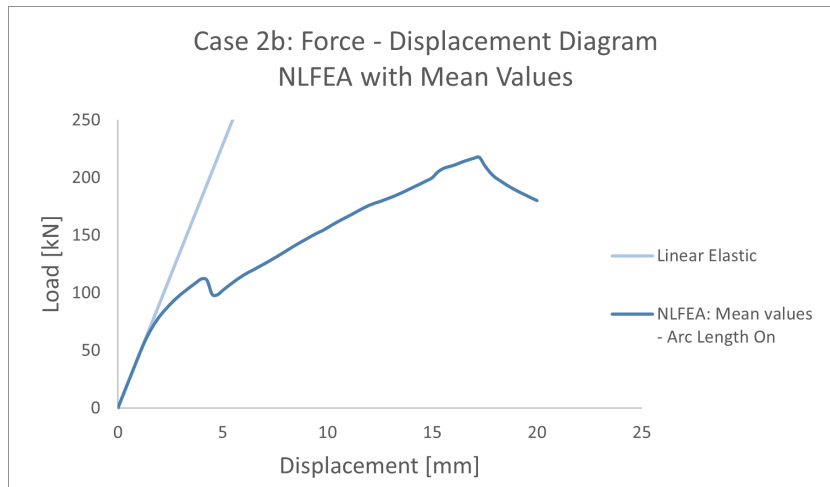
(a) Global Load-Displacement curve
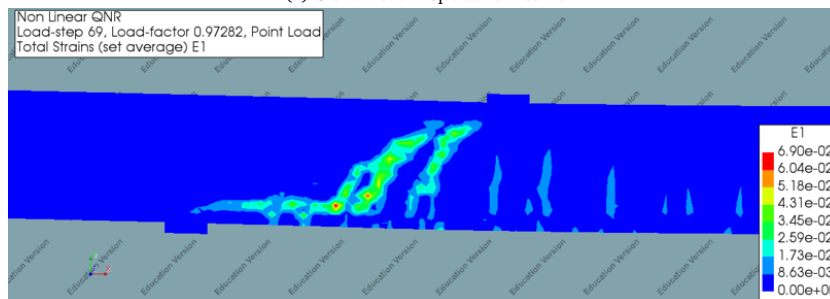
(b) Principle strain contour plot at defined Limit State
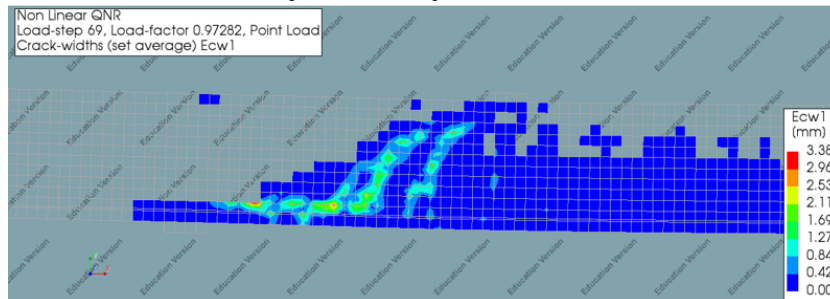
(c) Crack width at defined Limit State
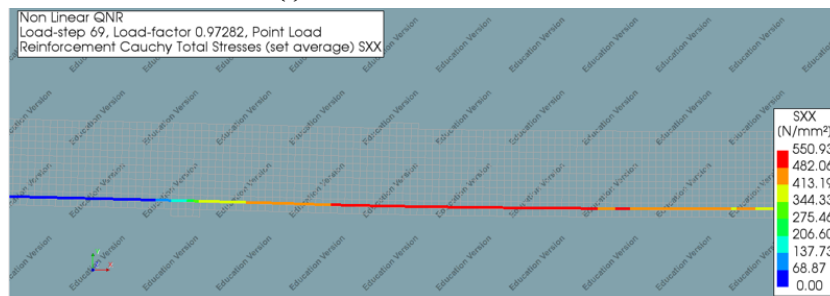
(d) Reinforcement Stresses at defined Limit State

Figure 8.2: Case 2b - NLFEA with mean value of the input critical material parameters
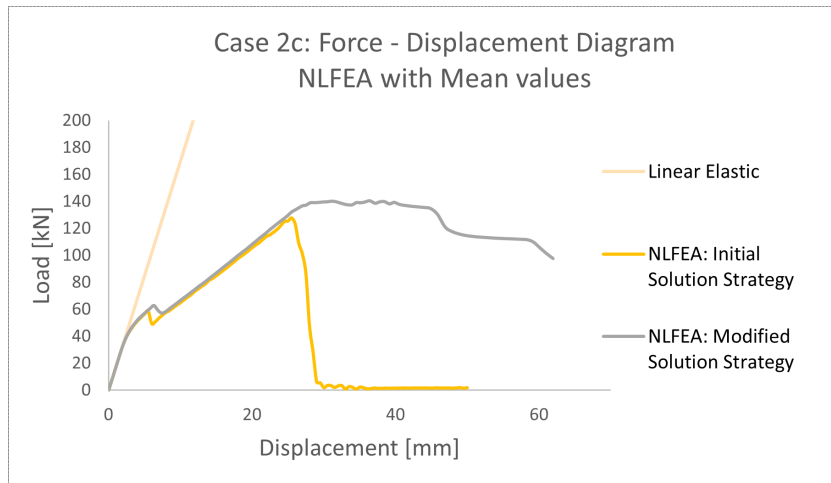
(a) Global Load-Displacement curve
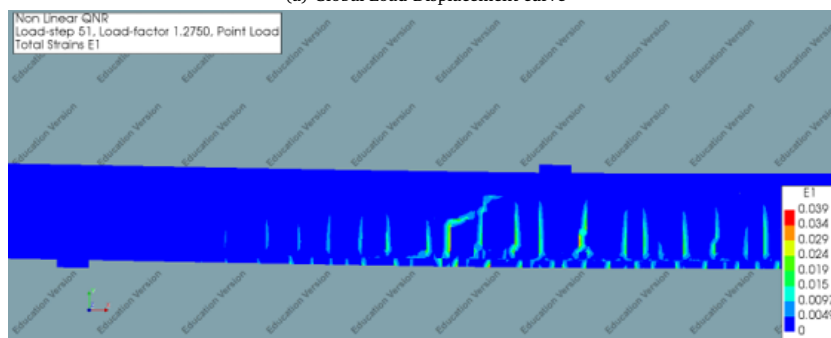
(b) Principle strain contour plot at defined Limit State
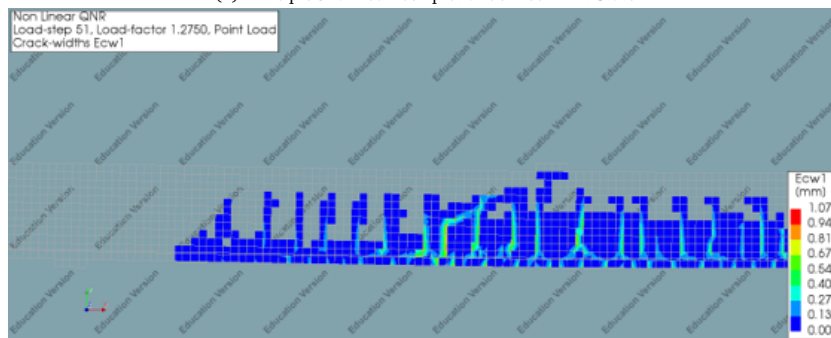
(c) Crack width at defined Limit State
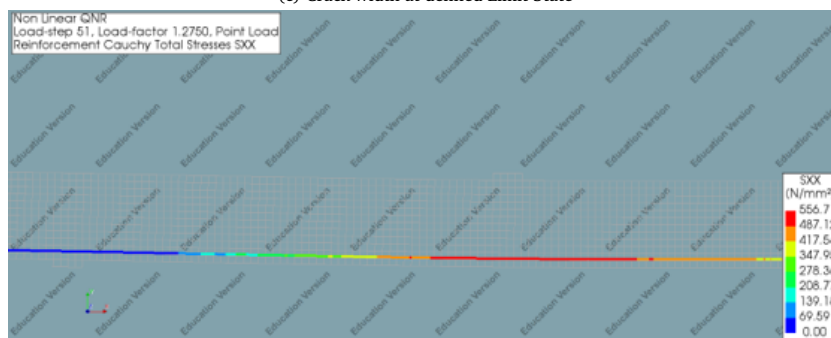
(d) Reinforcement Stresses at defined Limit State

Figure 8.3: Case 2c - NLFEA with mean value of the input critical material parameters

curve, obtained with the Arc length option off, the identification of the CLFM seems straightforward. Shear failure shows due to the abrupt loss in load-bearing capacity and the brittle behavior of the structure following the achievement of the maximum load. Yet, giving a deeper look into the stresses in the different components and locations of the beam proves the presence of the so-called "mixed" behavior: stresses in the longitudinal reinforcement indicated that there was yielding of the reinforcement almost the same time that failure occurred. At the same time, the crack-width pattern and the principal strain contour plots (figures 8.3c and 8.3b) lead into the thought of having a structure with concurrent failure mechanisms. At the point of reaching the maximum capacity, bending cracks are still relevant, and the presence of a secondary shear crack between the closer support and the loading point is remarkable.

Figures 8.3b, 8.2c, and 8.3d display the results computed with the initial solution strategy. The equivalent plots obtained with the modified solution strategy can be found in Appendix G. Figure 8.3a displays two paths. The yellow line is the load-displacement curve for the initial solution strategy: it shows a sudden loss of capacity and brittle behavior. The grey line is the curve computed with the modified solution strategy. Initially, it follows the same behavior. However, it continues beyond the step of the maximum resistance of the analysis run with the initial solution strategy: with the modified solution strategy, the beam shows some ductile behavior before losing its load-bearing capacity. The principal strains and crack-width patterns display a similar mixed pattern for both solution strategies: a combination between flexural cracks and rotated shear cracks near the closest support.

To continue with the established GFM procedure, once the CLFM is identified and hierarchically organized, a second NLFEA with analytical parameters must be performed. In cases 2a and 2b, a single mechanism is identified which simplifies the procedure and reduces the engineering-decision scenarios. Case 2c allows implementing different assumptions to study the impact of the choices regarding the CLFM, the number of concurrent FM, the location of the FM within the structures, and the basic variables to be perturbed.

8.3. Perturbation of the critical input random variables

This section is dedicated exclusively to discuss the chosen critical input parameters to be decreased depending on the CLFM of each beam. A parametric study [18] determined the sensitivity of reinforced concrete beams without shear reinforcement to the stochastic nature of the material parameters. It concluded that the concrete tensile strength and the yielding strength of the reinforcement steel have the highest impact on the structural response. However, in [32], the concrete material parameters included as stochastic basic variables in the Directional Adaptive Response Surface algorithm were:

- Concrete Tensile Strength, f_{ct}
- Concrete fracture energy, G_F
- Concrete Compressive Strength, f_c

For the reinforcement steel:

- Yielding Strength, f_y

Knowing this, three CLFM are described in this document along with the corresponding material variables playing a major role on each mechanism:

1. Bending Failure Mechanism: f_{ct}, G_F, f_c, and f_y
2. Shear Failure Mechanism: f_{ct}, G_F, and f_c
3. Mixed Failure Mechanism: f_{ct}, G_F, f_c, and f_y

Usually, a deterministic (empirical) relation linking the value of concrete compressive strength with the other parameters is used. For instance, the relations presented in the Dutch Guidelines or in the *fib* Model Code. Another approach was followed by Roy [32] when sampling the tensile fracture energy and the

concrete tensile strength. Being both parameters taken as random variables, full correlation was assumed between them. This was maintained once they were transformed to the standard normal world and back by a Nataf's transformation. The transformation of the variables was necessary for the application of the DARS method.

Nevertheless, the focus is now on the proposed GFM. In [29], Monti et al. state that, assuming fully independent failure mechanisms, all the basic variables in the CLFM must be perturbed by assuming them as normally distributed basic variables as equation 8.1 shows. Several values of the parameter c were tested for each of the following cases.

$$x_{\mathrm{var}} = x_{\mathrm{m}} - c\sigma_x \tag{8.1}$$

Case 2a

For this beam configuration, the CLFM is identified as Bending Failure Mechanism. The limit state is reached at the step in which the yielding of the reinforcement occurs first. There are higher loads in the load-displacement diagram but those picks are attributed to the margin error and noise in an NLFEA, which depends on the convergence norm, iteration method, and integration scheme, to mention some.

According to the CLFM, the basic variables to be perturbed are x_{m}: f_{ct}, G_F, f_c, and f_y. The stochastic properties of the parameters and their perturbed values are summarised in table 8.2.

	f_c	f_{ct}	G_F	f_y	E_c	G_c
Mean μ_x	78.5	5.1474	0.1269	550	31.73	42729
Standard Deviation σ_x	9.645	0.8503	0.0309	65	-	-
Distribution	LN	LN	LN	LN	-	-
$V = \sigma_x/\mu_x$	0.1229	0.1652	0.2435	0.1182	-	-
c:						
0.1	77.5355	5.0624	0.1238	543.50	-	-
0.5	73.6775	4.7223	0.1115	514.50	-	-
1.0	68.8550	4.2971	0.0960	485.00	-	-
1.645	62.6340	3.7487	0.0761	443.08	-	-

Table 8.2: Case 2a: Perturbed values of the random variables

In addition to identifying the CLFM and the important basic variables, the GFM requires that the basic variables are perturbed only in the location where the mechanism develops. The approach seems to align with the inhomogeneous spatial variability of the properties in a material with a highly anisotropic nature, like reinforced concrete. Therefore, the previous FE model used with the mean values of the material parameters must be divided into different zones according to the damaged location. The regions are defined by visual inspection of the developed crack pattern. In this case, also the zones of the longitudinal reinforcement that yielded are used as reference. Figure 8.4, shows the division of the model. The perturbed parameters are assigned to zone B.
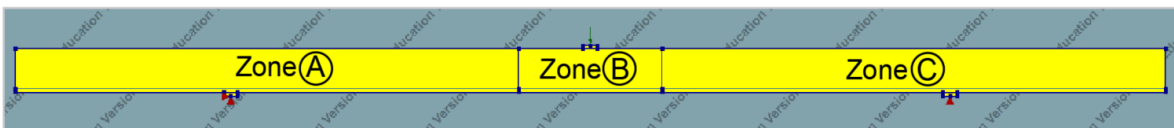
Figure 8.4: Case 2a: Geometry of the NLFEA with localized perturbation of the parameters

Case 2b

The CLFM is identified as Shear Failure Mechanism. The limit state is reached at the maximum load-bearing capacity. According to the identified CLFM, the random variables influencing failure are x_{m}: f_{ct},

G_F, and f_c.In this case, the yielding strength does not have a great influence on the final structural response. The stochastic properties of the parameters and their perturbed values are summarized in table 8.3.

	f_c	f_{ct}	G_F	f_y	E_c	G_c
Mean μ_x	78.2	5.1328	0.1266	550	31.64	42675
Standard Deviation, σ_x	9.645	0.8503	0.0309	-	-	-
Distribution	LN	LN	LN	-	-	-
$V = \sigma_x/\mu_x$	0.1233	0.1657	0.2441	-	-	-
c:						
0.1	77.2355	5.0477	0.1235	-	-	-
0.5	73.3775	4.7076	0.1111	-	-	-
1.0	68.5550	4.2825	0.0957	-	-	-
1.645	62.3340	3.7341	0.0758	-	-	-

Table 8.3: Case 2b: Perturbed values of the random variables

The previous FE model is, once again, divided to be able to indicate a different material in the relevant zone B. This time the region is defined as the beam zone between the left support and the loading plate. The reason is due to the crack pattern observed in 8.2b. Figure 8.4 shows the division in the geometrical model.

Figure 8.5: Case 2b: Geometry of the NLFEA with localized perturbation of the parameters

Case 2c

Section 8.2 already introduced the complex bi-modal behavior towards the failure of the beam in case 2c. Since this work aims to serve as a benchmark procedure and study the consequences of different possible decisions, three different scenarios according to the chosen CLFM are considered in the framework of the GFM. The decreased basic variables are assigned to Zone B in figures 8.6, 8.7, and 8.8.

1. **Bending Failure Mechanism** is assumed to be the CLFM with a R_{var} value chosen at the step where yielding of the longitudinal reinforcement is developed. The model is divided as shown in figure 8.6 and the critical random variables involved are x_m: f_{ct}, G_F, f_c, and f_y. Zone B is placed around location of the main flexural cracks bellow the point of application of the load.
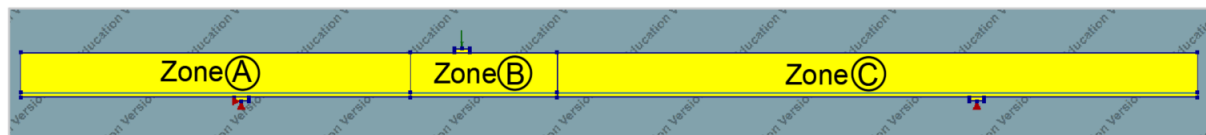
Figure 8.6: Case 2c: Geometry of the NLFEA with localized perturbation of the parameters. CLFM: bending

2. **Shear Failure Mechanism** is assumed to be the CLFM with a R_{var} value chosen at the step where the maximum load-bearing capacity is reached at the global load-displacement curve. The model is divided as shown in figure 8.7 and the critical random variables involved are x_m: f_{ct}, G_F, and f_c. Zone B is placed in the region where the main shear crack is observed, between the loading plate and the closest support plate.

Figure 8.7: Case 2c: Geometry of the NLFEA with localized perturbation of the parameters. CLFM: shear

3. A single **Mixed Failure Mechanism** is assumed to develop. The R_{var} value is selected as the maximum load-bearing capacity of the global load-displacement curve. The model is divided as shown in figure 8.8 and the critical random variables involved are x_m: f_{ct}, G_F, f_c, and f_y. Zone B covers the majority of the main flexural and shear cracks observed at failure of the NLFEA with mean values of the input basic variables.
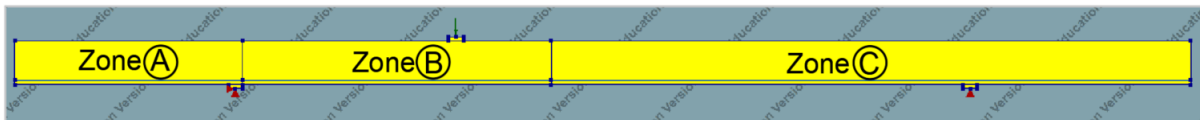
Figure 8.8: Case 2c: Geometry of the NLFEA with localized perturbation of the parameters. CLFM: single mechanism

	f_c	f_{ct}	G_F	f_y	E_c	G_c
Mean μ_x	77.5	5.0986	0.1258	550	31.73	42729
Standard Deviation, σ_x	9.645	0.8503	0.0309	55	-	-
Distribution	LN	LN	LN	LN	-	-
$V = \sigma_x / \mu_x$	0.1245	0.1668	0.2456	0.1	-	-
c:						
0.1	76.5355	5.0136	0.1227	544.5	-	-
0.5	72.6775	4.6735	0.1104	522.5	-	-

Table 8.4: Case 2c: Perturbed values of the random variables

8.3.1. Relation between the Critical input random variable

It is acknowledge that the concrete material properties have indeed a degree of correlation between them. Even though the method accounts for correlation or not between the basic random variables between local failure mechanisms, once the critical failure mechanism is determined the procedure is not clear about how the critical basic random variables interact with each other.

An explanation is presented based on three parameters: f_y, f_t and G_f. Since the yielding strength of the reinforcement f_y is describing one property of this material and f_t refers to the concrete tensile strength, they are usually independent or not correlated. According to the GFM, they both will be perturbed as in equation 8.1 with their respective mean value and standard deviation. Now, f_t and G_f both describe properties related to the same material, even though there are only a few researches in finding their exact correlation, it is evident that they describe physically related characteristics. However, the GFM does not provide any more specific guidance regarding the perturbation of this type of variables. If the same equation 8.1 is used to find the variable value of the resistance R_{var} in the second NLFEA, R_{var} increases instead of decrease (as it is expected due to the decreasing in material parameters). For the specific case of the used constitutive model, the previous phenomena can be explained by observing the tensile-softening curved of the concrete fixed crack model.

By reducing the tensile strength of the concrete and the fracture energy by means of equation 8.1, the tension softening diagram is not escalated in the same proportion. Apparently, the value of G_F is not being reduced enough which increases the ductility of the concrete and therefore a higher value of the resistance is obtained when the perturbation parameter is as small as 0.1. Especially in the case of the beam failing with

the Bending Failure mechanism in case 2a. However, for other values of the perturbation parameter c and for the beams in cases 2b and 2c, the relation to decrease the parameters for the second NLFEA proposed by Monti et al. seems to keep similar ductility in the models.

8.4. GFM: Design Resistance

The expressions, to calculate the design resistance of the three beams by the use of NLFEA in the structural reliability assessment performed by the GFM, were presented in chapter 3, and bring back hereafter. For cases 2a, 2b, and 2c the final expression for the global safety factor is derived. The coefficient of variation expressing the geometrical uncertainty is generalized as $V_G = 0.05$.

$$R_d = \frac{R_m}{\gamma_R} \approx \frac{R_{\text{NLFEA}}(\boldsymbol{x}_m)}{\gamma_R} \tag{8.2}$$

$$V_{R_x} \approx \frac{1}{c} \ln \frac{R_m}{R_{\text{var}}(x_m - c\sigma_x)} \tag{8.3}$$

$$V_R = \sqrt{V_{R_x}^2 + V_G^2 + V_\theta^2} \tag{8.4}$$

In cases 2a and 2b, the variable value of the resistance was obtained with four values of the perturbation parameter c: 0.1, 0.5, 1.0, 1.645. For the three scenarios assumed in case 2c, two perturbation parameters c are tested: 0.1 and 0.5. A unique LFM means that the expression for γ_R is simplified to equation 8.5 with $n_m = n_s = n_p = 1$. Equation 8.6 is employed when two concurrent failure mechanisms in series are present: $n_m = 2$ and $n_s = n_p = 1$. In case 2a, the statistical parameters describing the modeling uncertainty are taken as $\mu_\theta = 1.044$ and $V_\theta = 0.096$, following the values provided by De Putter in [12] for ductile failure mechanisms. Being the failure mechanism of case 2b a brittle one, substantial variability is accounted for with $\mu_\theta = 1.17$ and $V_\theta = 0.108$. More general modeling uncertainty parameters are implemented in case 2c: $\mu_{theta} = 1.053$ and $V_R = 0.108$.

$$\gamma_R = \frac{1}{\mu_\theta} \exp(\alpha_R \beta_{LS} V_R) \tag{8.5}$$

$$\gamma_R = \frac{1}{\mu_\theta} \exp\left(\ln(\sqrt{2})V_R + \alpha_R \beta_L S V_R\right) \tag{8.6}$$

The sensitivity factor for the resistance part is taken as $\alpha_R = 0.8$. The GFM requires the definition of a reliability index, β_{LS}, for the calculation of the Global Safety Factor with equations 8.5 and 8.6. The index is directly related to the attainment of a specific limit state. In this case, the specific β's are taken from the results of the full probabilistic finite element analysis (DARS method) performed by Roy in [32]. The following section 8.5 provides a general explanation of the procedure followed in [32] and how the design resistance might be interpreted by the use of the DARS method results. Table 8.9 indicates the β_{LS} used in the calculation of the design resistance in the three NLFEA cases. The design resistances are summarized in tables 8.5, 8.6, 8.7, and 8.8. The most relevant observations and conclusions about the obtained design resistances are discussed in section 8.6.

Global Design Resistance R_{d} [kN] - Beam Case 2a - $n_{\mathrm{m}} = 1$						
	R_{m} [kN]	R_{var} [kN]	V_{R_x}	V_R	γ_R	R_{d} [kN]
c = 0.1	72.51	73.50	-0.1359	0.1737	1.5775	45.96
c = 0.5		70.25	0.0632	0.1254	1.3729	52.81
c = 1.0		63.60	0.1310	0.1699	1.5605	46.46
c = 1.645		59.34	0.1310	0.1699	1.5296	47.40

Table 8.5: Design value of the resistance for case 2a

Global Design Resistance R_{d} [kN] - Beam Case 2b - $n_{\mathrm{m}} = 1$						
	R_{m} [kN]	R_{var} [kN]	V_{R_x}	V_R	γ_R	R_{d} [kN]
c = 0.1	217.73	214.97	0.1277	0.2223	2.1360	101.94
c = 0.5		213.33	0.0409	0.1865	1.8433	118.12
c = 1.0		198.21	0.0940	0.2048	1.9874	109.55
c = 1.645		201.822	0.0461	0.1878	1.8525	117.53

Table 8.6: Design value of the resistance for case 2b

Global Design Resistance R_{d} [kN] - Beam Case 2c - Arc Length Off						
	R_{m} [kN]	R_{var} [kN]	V_{R_x}	V_R	γ_R	R_{d} [kN]
CLFM: Bending Failure Mechanism - $n_{\mathrm{m}} = 2$						
c = 0.1	127.59	115.03	1.0360	1.0428	34.1256	3.74
c = 0.5		121.05	0.1053	0.1589	1.6390	77.85
CLFM: Shear Failure Mechanism - $n_{\mathrm{m}} = 2$						
c = 0.1	127.59	118.38	0.7493	0.7587	12.86	9.92
c = 0.5		120.04	0.1220	0.1704	1.7052	74.82
CLFM: Mixed Failure Mechanism - $n_{\mathrm{m}} = 1$						
c = 0.1	127.59	117.12	0.8566	0.8648	13.7197	9.30
c = 0.5		127.95	-0.0057	0.1191	1.3720	93.00

Table 8.7: Design value of the resistance for case 2c with the Initial Solution Strategy

Global Design Resistance R_{d} [kN] - Beam Case 2c - Arc Length On						
	R_{m} [kN]	R_{var} [kN]	V_{R_x}	V_R	γ_R	R_{d} [kN]
CLFM: Bending Failure Mechanism - $n_{\mathrm{m}} = 2$						
c = 0.1	140.37	140.23	0.0101	0.1194	1.4313	98.07
c = 0.5		133.53	0.0998	0.1553	1.6191	86.69
CLFM: Shear Failure Mechanism - $n_{\mathrm{m}} = 2$						
c = 0.1	140.37	136.66	0.2675	0.2928	2.5959	54.07
c = 0.5		136.09	0.0619	0.1341	1.5054	93.24
CLFM: Mixed Failure Mechanism - $n_{\mathrm{m}} = 1$						
c = 0.1	140.37	138.11	0.1625	0.2014	1.7687	79.36
c = 0.5		134.50	0.0854	0.1465	1.4928	94.03

Table 8.8: Design value of the resistance for case 2c with the Modified Solution Strategy
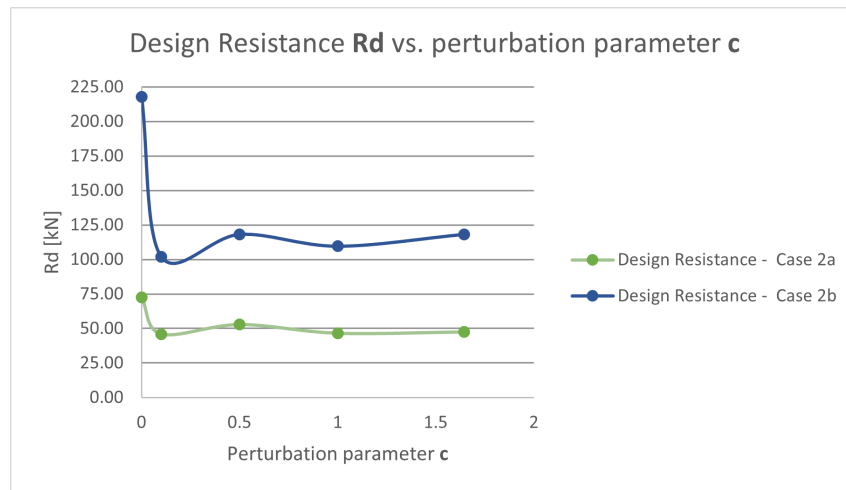
Figure 8.9: Design Resistance as a function of the perturbation parameter c

8.5. Comparison: DARS method

A probabilistic finite element analysis was performed by Roy in his master's thesis project [32] on the same beams presented in cases 2a, 2b, and 2c. A robust method, known as the Directional Adaptative Response surface Sampling (DARS method), was implemented in the reliability evaluation of the three RC beams. The DARS method is one of the Importance sampling methods proposed to reduce the number of simulations needed in a Crude Monte Carlo analysis. This means that Importance Sampling algorithms can control the generation of random samples to concentrate in the region of the response around failure. Furthermore, by implementing Directional simulation, the sampling of the random points is performed along the determined random directions and not all around the stochastic domain. In this way, a line search procedure is used to find the design point intersecting the limit state function.

One of the reasons for the effectiveness of the method is the use of polynomials as response surface functions to explicitly formulate the exact response function, which is given by running NLFEA with a massive number of simulations of the stochastic basic variables. In the DARS method, the response surface is used in unimportant directions far from the failure zone. This decreases the computational burden by decreasing the number of NLFEA that must be performed. In summary, the key advantage of the DARS method, over other full probabilistic methods, is that it only samples in the important region of the limit state function which extremely reduces the number of NLFEA to be performed. [12] [18]

Roy defined a limit state function focusing, once again, on the study of the lower (left) tail of the Resistance, R. The action/effect side was set as an arbitrary deterministic value, $F = 80\,[kN]$. As known, the global quantity expressing the resistance of the beams was taken from the load-displacement curve at the point of application of the load. Failure occurs when $G(\mathbf{X}) < 0$, which translates in $R_{NLFEA}(\mathbf{X}) < F$. $\mathbf{X}$ is a vector with all the selected basic random variables.

$$G(\mathbf{X}) = \frac{R_{NLFEA}(\mathbf{X})}{F} - 1 \tag{8.7}$$

It is relevant to mentioned that in the implementation of the DARS method, all the random basic variables must be transformed to the standard normal world.

The output of the probabilistic analysis is the estimation of the probability of failure, P_f, with the subsequent structural reliability related to the defined limit state function. The reliability index, β, is usually used in measure this quality. The DARS method provides a value for the probability of failure, P_f, therefore the reliability index might be calculated by means of the inverse standard normal cumulative distribution function:

$$\beta = -\Phi^{-1}\left(P_f\right) \tag{8.8}$$

In the DARS method, the probability of failure is calculated for each of the sampling directions. The mean of all those probabilities provides the final probability of failure used in equation 8.8 to compute the reliability index. Clearly, this reliability measure is strongly related to the value of the arbitrary defined effect, F, the limit state function, the solution strategy implemented in the NLFEA and the stochastic parameters and distributions assumed for the basic variables. The values of the reliability index, β, provided by the DARS method of Roy for each model in case 2 are brought up in table 8.9.

Reliability Index β - DARS method		
	β	Basic Variables
Case 2a: Bending Beam	3.59	f_c, f_t, G_F, f_y
Case 2b: Shear Beam	5.15	f_c, f_t, G_F, f_y
Case 2c: Mixed Beam	3.86	f_c, f_t, G_F, f_y

Table 8.9: Reliability Index β - DARS method - Beam Cases 2a, 2b and 2c

According to the Limit state function, equation 8.7, uses $F = 80[kN]$ as an arbitrary deterministic design effect. From the GFM is not possible to know the level of reliability reached with the design resistance, only the imposed target reliability β_{LS} which in this case was taken as the reliability index found by Roy for each beam case. Therefore, the comparison is not as straightforward as in the analytical cases where the reliability of design resistance computed with the GFM was studied by a crude Monte Carlo Simulation.

An alternative approach is suggested as a comparison tool. It follows a simple logic, but it does not provide a strong tool for validating the design resistance calculated by the GFM. Here, the value of $F = 80[kN]$ is going to be assumed as a reference value for the design resistance. If R_d replaces F as in equation 8.9, the following comparison might be possible: for values of R_d smaller than the reference value $F = 80[kN]$ a lower number of failures is expected in the simulation. This means that an smaller probability will be probably found with a higher reliability index. Then, a R_d smaller than 80 [kN] represent a more conservative outcome. Otherwise, if the value of R_d is higher than 80 [kN], the probability of failure would probably decrease. This translates in a less conservative design resistance.

$$G(\mathbf{X}) = \frac{R_{NLFEA}(\mathbf{X})}{R_d} - 1 \tag{8.9}$$

There are several drawbacks in this approach. First, for the case 2a, the reference value $F = 80[kN]$ is higher than the mean value of the resistance. This should have caused an extremely high probability of failure and the reliability index obtained by the DARS method in [32] do not reflect this issue. Second, in case 2b, the modification of the solution strategy in relation to the initial one used by Roy, eliminates the possibility of comparing the results obtained under the exact same conditions. The same problem arises in the results obtained in case 2c with the used of the modified solution strategy.

Only in case 2c, when using the initial solution strategy (Arc Length Off), it is possible to applied the suggested approach. The design values obtained in the situations where the two concurrent failure mechanisms were directly accounted for are smaller than 80 [kN]. The latter means that in this situation the GFM reproduce conservative results when comparing to a full probabilistic simulation.

8.6. Observations and Conclusions

- The design resistance in cases 2a and 2b is not highly sensitive to the value of the perturbation parameter c: this is a relevant finding since the value of the parameter is subjected to the criteria of the analyst. Therefore, even whether an arbitrary selection is performed, it does not cause great variability in the final design capacity. Figure 8.9 illustrates the design resistance, R_d, as a function of c for beam 2a and beam 2b. In both curves, $c = 0.1$ provides the more conservative value of R_d, and $c = 0.5$ the less conservative one: there is a difference of 13.9% and 14.9% between these two boundaries in cases 2a and 2b respectively.

- The selection of the solution strategy highly impacts the equilibrium path towards the final steps of the

nonlinear analysis, especially in the case of the beam with a mixed or bi-modal failure, case 2c. For bending case 2a, the more suitable solution strategy is easily recognized: implementing the modified one the analysis diverges as soon as the first cracks appear and the beam deviates from the linear equilibrium path. On the contrary, by implementing the initial solution strategy, the analysis can run successfully with most of the steps converging before the maximum of 100 iterations. For beam 2b failing in shear, the modified solution strategy proved to compute more stable results as already stated in section 8.2. Both solutions strategies produced a similar equilibrium path. However, several runs of the analysis with the initial solution strategy without any modifications in the model showed a highly variable maximum load-bearing capacity. Even though the equilibrium path was presenting the expected brittle behavior with a sudden loss in the capacity, a different value for the R_{var} was found in each trial, making it impossible to obtain any results in the application of the GFM.

- The modified solution strategy seems to provide less conservative results than the initial solution strategy in the case of the mixed beam. However, the design resistance, R_d, computed with this solution strategy appears less sensitive to the value of the perturbation parameter c. See table 8.8. Implementing the initial solution strategy (table 8.7), a value of c as smaller as 0.1 extremely underestimates the design resistance in the three scenarios regarding the choice of CLFM: Bending Failure Mechanism, Shear Failure Mechanism, and Mixed Failure Mechanism. A value c closer to 0.5 is advisable in this case.

- The design resistance in Case 2c is more sensitive to the value of the perturbation parameter c if the choice of CLFM is the Shear or Mixed Failure Mechanisms. The percentage differences, between the two design values obtained with $c = 0.1$ and $c = 0.5$, are 53.2% and 16.9% respectively. When choosing the CLFM as bending failure, the percentage difference between the two design resistances is 12.3%, once more proving the less variable nature of bending as a failure mechanism.

- For case 2a, the design resistance obtained with the GFM (table 8.5) and the existing safety formats (table 7.8) belong to the same range of values: being the GFM more conservative for most of the values of c. In case 2b, the design value obtained by the ECOV by Cervenka is closer to the range of values obtained by the GFM. The biggest difference is appreciated with the design resistance obtained by the PSF. This is mainly due to the difference in the way to account for the modeling uncertainty: the PSF is accounted for at a material level. Additionally, the highest value of the reliability index implemented for this limit state substantially increases the global safety factor. Therefore, proportionally decreasing the design resistance.

- The values of the design resistance confirmed that ductile failure mechanisms have a more stable nature. The highest overall variability of structures with brittle failure is observed among the obtained results.

- Appendix H, shows that, at least for the structures analyzed in the present document, there is no change in failure mechanisms in the second NLFEA model with the perturbed value of the basic variables. The bending case presents the same ductile behavior, only with a reduction in the maximum load reached. The shear case 2b conserves the brittle behavior towards the end of the analysis for any value of the perturbation parameter c. For case 2c, with the initial solution strategy, all the second NLFEA suddenly fail like in the analysis with mean parameters. With the modified solution strategy, the ductile behavior before failure is maintained in the second NLFEA. However, the duration of the ductile stage is shorter when the Shear Failure mechanism is selected as CLFM.

- In case 2c, when the CLFM is assumed as Bending Failure Mechanism or Shear Failure Mechanisms, the formulation of the Global Safety Factor directly accounts for two concurrent failure mechanisms in series. Only the results obtained with the initial solution strategy and with $c = 0.5$ show a more conservative design resistance than assuming a single failure mechanism. In the case of implementing the Modified solution strategy, the high variability in the results does not give space for final conclusions in this aspect.

9

Final Conclusions and Recommendations

First, the chapter presents some general points of attention and conclusions related with the most relevant findings along the application of the GFM to the case studies. Furthermore, conclusion are drawn by answering the sub-questions and main research question formulated at the begging of this document in chapter 1. Recommendations regarding the future direction of the research and validation of the new GFM as a safety format for NLFEA of RC structures are given.

9.1. General Conclusions

- From section 2.4 it is possible to conclude that existing safety formats for NLFEA do not directly account for several concurrent failure mechanisms in their formulation of the design resistance. The latter is confirmed by the application of existing safety formats in chapters 4 and 7. The analytical case studies showed that the ECOV method proposed by Cervenka conservatively accounts for the randomness of the design resistance in cross-sections where the nature of the Local Failure Mechanisms is either extremely ductile or extremely brittle. Otherwise, for intermediate sections, it has trouble in reaching the desired target reliability in balanced cross-sections where the nature of the Failure mechanisms is in transition.

- The GFM in his derivation does not required any assumption regarding the probability distribution of the Global Resistance quantity, giving space for bi-modal or higher order probability functions. However, the log-normal distribution assumption has yet a strong presence. The method uses the marginal distribution of the Local Failure Mechanisms for the derivation of the expression of the Global Safety Factor and the Coefficient of Variation. The marginal distribution of each Local Failure Mechanisms is assumed to be log-normally distributed.

- The GFM generalizes the probability distribution of all the input random variables: when perturbing the basic variables the method assumes they are all normally distributed. However, due to the statistical parameters usually used for this physical quantities, the difference between a normal and log-normal distribution in the region of interest (around the mean) is not as representative as in the tails. This is a reason to support that the value of the perturbation parameter c should not compute values too far from their mean.

- Even though it is acknowledge that bending failure might be subdivided according to the ductile or brittle nature of the mechanism, in the framework of the newly proposed GFM with analytical expressions more reliable results were reproduced when bending is assumed to be a single mechanism with basic variables being the material parameters related to yielding of the reinforcement and compressive of the concrete. According to this, bending failure is taken as a single failure mechanism in the application of the new Safety Format for NLFEA.

- It is acknowledge that the concrete material properties have indeed a degree of correlation between them. Even though the method accounts for correlation or not between the basic random variables

between local failure mechanisms, once the critical failure mechanism is determined the procedure is not clear enough about how the critical basic random variables interact with each other.

- A clear definition of the Limit state must be done according to the observed behaviour of the structure in the NLFEA with mean values of the parameters.

- For structures with a unique LFM, the coefficient of variation of the resistance related to the material parameters is lower than 20%. This limit is relevant since one of the main simplifications in the derivation of this coefficient in the GFM depends on that condition. For some values of the parameter c in combination with the choice of CLFM, the mixed beam obtains coefficients of variations higher than 20%. The latter leads to extremely high safety factors and unrealistic low design values of the resistance.

- Mixed structures, as the beam study in case 2c, appear to be extremely sensitive to the solution strategy implemented in the NLFEA. The CLFM and its nature (ductile or brittle) can completely change with different solutions implemented, which means that the mixed behavior of the structure must be accounted for even before the application of the formulation of the GFM method. Therefore, the selection of the solution strategy requires prior knowledge of the possible concurrent behavior of mechanisms.

9.2. Answer to Research Question

9.2.1. Sub-question

1. What are the existing safety formats applied to the nonlinear finite element analysis of RC structures, and how do they relate to the new Global Factor Method by Monti et al. (2021)?

   There are several safety formats currently applicable in the framework of NLFEA for reinforced concrete structures. Section EN1992-2 refers specifically to those included in the Eurocode (EN1992-1-1) and in the *fib* Model Code 2020: the PSF, Global Resistance Factor methods, and ECOV methods are the most relevant in literature. Furthermore, the ECOV by Cervenka and by Schlune methods are the most closely related to the GFM. First, the same expression computing the design structural capacity is implemented. The inclusion of the material, geometrical and modeling uncertainty is equivalent as in the method by Schlune. The calculation of a Global Safety Factor, intrinsic to the overall structural behavior, is a common component between the new and existing formats. The new method deviates from the ECOV methods in three key points. First, in the derivation of the formulation of the Global Safety Factor by directly accounting for series and parallel systems of LFM playing different roles in the global failure of the structure. Second, it provides freedom regarding the probability distribution of the global resistance, usually assumed to be a log-normal in the existing formats. Finally, it presents an alternative approach for calculating the Coefficient of Variation of the resistance related to the uncertainty in the material parameters. The characteristic value is meant to be replaced for a value closer to the mean value of the resistance to avoid a change in mechanism and nature between the two non-linear models.

2. While implementing the Global Factor Method, the identification of local failure mechanisms influencing global failure is essential. Sometimes in NLFEA, this is not a straightforward procedure. How does the GFM perform in cases where identification and definition of failure mechanisms and their variables give space for different decision scenarios?

   In the analytical cases, the identification of the LFMs is done with a direct quantitative comparison between the possible resistance values. The fictitious engineer-based scenarios presented within case 1a, for the implementation of the GFM in chapter 5, did not provide conservative values of the design resistances for under-reinforced and balanced cross-sections. When dividing flexural failure into two concurrent failure mechanisms in series, only the yielding strength was chosen as the basic random variable and, subsequently, decreased when the CLFM was defined as Bending Ductile Failure. However, the employed analytical expression is derived from a model where constant interaction between the reinforcement and concrete properties, mainly when calculating the stresses in the reinforcement, does not allow an accurate performance of the GFM.

   With the use of NLFEA, the identification of LFM is more complex. The definition of the Limit State is not as straightforward. Several factors must be accounted for like the nature of the global load-

displacement path or the strain and stress state at different possible critical locations in contrast with the developed crack pattern. Case 2c in chapter 8 gives space for different decision scenarios regarding the definition of the CLFM, its location, and basic variables involved. The GFM does not provide consistent results for the case of a continuum simple structure failing under concurrent mechanisms. In this case, the method is highly sensitive to the solution strategy or to the value of the perturbation parameter c.

3. Global Factor Method by Monti et al. (2021) does not provide a specific value for the perturbation parameter c. How sensible is the resulting design resistance, in the analytical and NLFEA cases, for different values of the perturbation parameter c?

   In the analytical cases involving the study of a reinforced concrete cross-section (cases 1a and 1b), the value of the perturbation parameter c highly influences the reliability of the design resistance in scenarios where a single failure mechanism is adopted. There, small values of the parameter like 0.1 or 0.5 are not advisable. The reliability of the GFM improves when the perturbed value of the resistance is similar to the characteristic value used in the ECOV by Cervenka ($c = 1.645$). The engineer-based scenario 1 (section 5.2.2) does not provide a solid base for conclusions regarding parameter c due to the already mentioned inability of the analytical expression to produce well-grounded results while only perturbing the yielding strength of the reinforcement steel. In analytical case 1c and case 2 analyzed with NLFEA, the value of the perturbation parameter c seems to have a slight influence on the final design resistance. This is especially relevant within the practical application of the NLFEA since the criteria of the analyst applies. Consequently, specific guidelines regarding the value that parameter c must take are not provided. Validation regarding the reliability reached by the GFM in NLFEA is still required.

4. Does the GFM result in a reliable estimation of the global capacity by complying with the set target reliability index in the analytical cases and comparing it with already existing safety formats in the NLFEA cases?

   In analytical cases 1a and 1b, the GFM provides a reliable estimation of the resistance in cases where a single Local Failure Mechanism is assumed. In this case, the reliability reached by the safety format highly depends on the assumptions regarding the identification of LFM and the values taken for the parameter 'c'. From the NLFEA cases, it can be concluded that the design resistance obtained with the GFM and ECOV by Cervenka are within the same range of values for any of the perturbation parameter c. As expected, the mixed behavior of the third simply supported beam provided the biggest range of design values. Therefore, in this case, the performance of the method has a higher variability making a comparison with the existing formats not relevant for conclusions. Consequently, the study shows the importance of continuing the investigation of these types of mixed structures due to their higher sensitiveness to the decisions that must be taken by the analyst when implementing NLFEA in a practical environment.

9.2.2. Main Research Question

How does the new Global Factor Method assess the structural reliability and capacity of a statically loaded reinforced concrete structure failing under concurrent modes?

The GFM implemented to reinforced concrete structures can provide reliable and accurate design value of the resistance part, however, this is subjected to some conditions. For structures with a single LFM, the method works similarly to already existing safety formats. For continuum structures where two concurrent failure mechanisms lead to global failure, the GFM still needs to be revised to provide more accurate guidelines and reduce the space for decisions made by the analyst that highly impact the performance of the method. These decisions are related to identifying and locating the LFM and their basic variables, selecting the solution strategy implemented in the NLFEA, and choosing a suitable modeling uncertainty. At this point, the application of the method demands an experienced analyst and several parametric studies regarding all those decisions, which reduces its efficiency in terms of engineering and computational time

9.3. Recommendations

The GFM has very limited application cases since it is a new proposal in the middle of the highly populated world of Safety Formats. The present thesis intended to give a step forward its validation and possible future implementation in the daily practice of NLFEA. Some future steps and research directions are recommended: more practical and complex analysis should be carried. The most critical aspects influencing the performance of the GFM found along this research must be further studied and redefined.

- To study the influence of choosing different material parameters as random variables or deterministic parameters for several failure mechanisms, especially without being limited by the random variables chosen for the validation in literature.

- A full probabilistic nonlinear finite element analysis, for case study 2, with the implementation of a better-suited solution strategy and including the geometrical and modeling uncertainties.

- An extensive study in how to define the perturbation of material parameters that are highly correlated within the FE model, in which the use of the current assumption of normally independent distributed random variables is not applicable due to inconsistencies in the obtained resistance.

- To continue the application of the GFM in more complex case studies where more than two concurrent mechanisms might occur or where more levels of hierarchy organization might develop.

- A combined study of the influence of noise in the output of a NLFEA and the values of the perturbation parameter c. This might be able to produce standard values of c which will be still in accordance with the derivation of the GFM and will allow for extended use of the method in daily engineering practice.

- Several analysis must be performed in order to identify the degree of influence of the concrete compressive strength for the shear and bending failure mechanisms in a NLFEA. This would determine whether this material parameter might be better introduced in the analysis as a deterministic property, in cases were crushing of the concrete is not as relevant.

Bibliography

[1]   Noman Afzal et al. *Reliability Analysis of Reinforced Concrete using Non-Linear Finite Element Analysis*. Tech. rep. 2016.

[2]   Diego Lorenzo Allaix, Vincenzo Ilario Carbone, and Giuseppe Mancini. "Global safety format for non-linear analysis of reinforced concrete structures". In: *Structural Concrete* 14.1 (2013), pp. 29–42. ISSN: 17517648. DOI: 10.1002/suco.201200017.

[3]   G. Arslan. "Shear strength of reinforced concrete slender beams". In: *Proceedings of the Institution of Civil Engineers: Structures and Buildings*. Vol. 163. 3. ICE Publishing Ltd, 2010, pp. 195–205. DOI: 10.1680/stbu.2010.163.3.195.

[4]   ASCE-ACI Committee 445 on Shear and Torsion. "Recent Approaches to Shear Design of Structural Concrete". In: (2009).

[5]   Klaus-Jürgen Bathe. *ON FINITE ELEMENT METHODS FOR NONLINEAR DYNAMIC RESPONSE*. Tech. rep.

[6]   Fabio Biondini. *Structures 2008: Crossing Borders Use of Simulation in Structural Reliability*. Tech. rep. 2008.

[7]   V. Cervenka, J. Cervenka, and R. Pukl. "Safety assessment in fracture analysis of concrete structures". In: *Proceedings of the 6th International Conference on Fracture Mechanics of Concrete and Concrete Structures*. Vol. 2. 2007, pp. 1043–1049. ISBN: 9780415446167.

[8]   Vladimir Cervenka. "Global Safety Format for Nonlinear Calculation of Reinforced Concrete". In: *Beton- und Stahlbetonbau* 103.S1 (Apr. 2008), pp. 37–42. ISSN: 00059900. DOI: 10.1002/best.200810117.

[9]   Vladimir Cervenka. *Reliability-based non-linear analysis according to fib Model Code 2010*. 2013. DOI: 10.1002/suco.201200022.

[10]   M P Collins, F J Vecchio, and D G Mehlhorn. "An international competition to predict the response of reinforced concrete panels". In: *Canadian Journal of Civil Engineering* 12.3 (1985), pp. 624–644.

[11]   *COM10: Model Codes*. URL: https://www.fib-international.org/commissions/com10-model-codes.html.

[12]   A. De Putter. "Towards a uniform and optimal approach for safe NLFEA of re-inforced concrete beams". PhD thesis. 2020. URL: http://repository.tudelft.nl/..

[13]   DIANA FEA BV. "Diana 10.2 user's manual". In: (2018).

[14]   Hanna Eklund Astrid Skorve Arne Strand, Morten Engen, and KT Jochen Köhler. *Reliability assessments of concrete structures using non-linear finite element analyses*. Tech. rep. 2017.

[15]   *EN 1992-2: Eurocode 2: Design of concrete structures - Part 2: Concrete bridges - Design and detailing rules*. Tech. rep. 1992.

[16]   Morten Engen et al. "A quantification of the modelling uncertainty of non-linear finite element analyses of large concrete structures". In: *Structural Safety* 64 (Jan. 2017), pp. 1–8. ISSN: 01674730. DOI: 10.1016/j.strusafe.2016.08.003.

[17]   Morten Engen et al. "Treatment of modelling uncertainty of NLFEA in fib Model Code 2020".

[18]   Panagiotis Evangeliou. *Probabilistic Nonlinear Finite Element Analysis of Reinforced Concrete Beams without Shear Reinforcement*. Tech. rep. 2016.

[19]   Fédération internationale du béton. "27.10 Evaluation assisted by non-linear finite element analyses". In: 2021.

[20]   Fédération internationale du béton. *Model code 2010 : final draft*. International Federation for Structural Concrete (fib), 2012. ISBN: 9782883941052.

[21] Fédération internationale du béton. *Model code 2010 : final draft.* International Federation for Structural Concrete (fib), 2012. ISBN: 9782883941069.

[22] Davor Grandić, Paulo Šćulac, and Ivana Štimac Grandić. "Shear resistance of reinforced concrete beams in dependence on concrete strength in compressive struts". In: *Tehnicki Vjesnik* 22.4 (Aug. 2015), pp. 925–934. ISSN: 13303651. DOI: 10.17559/TV-20140708125658.

[23] Max A N Hendriks and Marco A Roosen. *Rijkswaterstaat Centre for Infrastructure Page: 2 of 66 Guidelines for Issued: 2 April 2020 Nonlinear Finite Element Analysis of*. Tech. rep.

[24] Antonio A R ; Henriques, Francisco ; Calheiros, and Joaquim A Figueiras. "Safety formats for the design of concrete frames". In: 19 (2002).

[25] D. A. Hordijk. "Local Approach to Fatigue of Concrete". PhD thesis. Delft University of Technology, 1991.

[26] Joint Committee on Structural Safety. "JCSS PROBABILISTIC MODELCODEPART 3 RESISTANCE MODELS". In: (2001).

[27] S N Jonkman et al. *Probabilistic Design: Risk and Reliability Analysis in Civil Engineering Lecture notes CIE4130*. Tech. rep. 2018.

[28] R.T Koekkoek and Y. Yang. *Measurement Report on the Transition between Fexura and Shear Faiure of RC Beams without Shear Reinforcement RELEASE NOTES*. Tech. rep. 2016.

[29] Giorgio Monti et al. "Global Factor Method for Non-Linear Analysis Considering Concurrent Local Failure Mechanisms".

[30] Oladimeji Benedict Olalusi. "Present State of Eurocode 2 Variable Strut Inclination Method for Shear Design and Possible Improvement". In: *Structures* 19 (June 2019), pp. 48–57. ISSN: 23520124. DOI: 10.1016/j.istruc.2018.11.016.

[31] Mário Pimentel, Eugen Brühwiler, and Joaquim Figueiras. "Safety examination of existing concrete structures using the global resistance safety factor concept". In: *Engineering Structures* 70 (July 2014), pp. 130–143. ISSN: 01410296. DOI: 10.1016/j.engstruct.2014.04.005.

[32] Anindya Roy. "Efficient reliability analysis of concrete structures on the basis of non-linear finite element analysis under numerical noise". In: (2019). DOI: 10.4233/uuid:389bbb4d-141d-425f-bc0f-b7e37918720c. URL: https://doi.org/10.4233/uuid:389bbb4d-141d-425f-bc0f-b7e37918720c.

[33] Filipo Sangiorgio. "Brittle Flexural Failures in Reinforced Concrete Frame Structural Systems". In: *ACI STRUCTURAL JOURNAL* (2018).

[34] R. Sarkhosh et al. *Shear Capacity of Concrete Beams without Shear Reinforcement under Sustained Loads*. Tech. rep. 2010.

[35] Hendrik Schlune, Mario Plos, and Kent Gylltoft. "Safety formats for non-linear analysis of concrete structures". In: *Magazine of Concrete Research* 64.7 (July 2012), pp. 563–574. ISSN: 00249831. DOI: 10.1680/macr.11.00046.

[36] R G Selby and F J Vecchio. *A constitutive model for analysis of reinforced concrete solids*. Tech. rep. 1997.

[37] Karel Coenraedt. Terwel. *Structural safety : study into critical factors in the design and construction process.* [s.n.], 2014. ISBN: 9789462591745.

[38] A J Van Eekelen. *Review and Selection of Methods for Structural Reliability Analysis*. Tech. rep. Delft University Press, 1997.

[39] Vecchio FJ and Collins MP. "The modified compression-field theory for reinforced concrete elements subjected to shear." In: *ACI J.* 83.2 (1986), pp. 219–231.

[40] Pavlo Vegera et al. "The improved design method of shear strength of reinforced concrete beams without transverse reinforcement". In: *Selected Scientific Papers - Journal of Civil Engineering* 12.2 (Dec. 2017), pp. 39–45. ISSN: 1338-7278. DOI: 10.1515/sspjce-2017-0017.

[41] J.C. Walraven and C.R. Braam. *CIE4160 Prestressed concrete*. Tech. rep. Technische Universiteit Delft, 2019.

[42]   Dawid F Wisniewski et al. "Probabilistic models for mechanical properties of concrete, reinforcing steel and pre-stressing steel." In: *Structure and Infrastructure Engineering* (2012), pp. 111–123. DOI: 10.1080/15732470903363164.

[43]   Yuguang Yang. "Shear Behaviour of Reinforced Concrete Members without Shear Reinforcement A New Look at an Old Problem". PhD thesis. Delft University of Technology, 2014.

Case 1a: Analytical derivation

Horizontal equilibrium of forces:

$$F_c = F_s \tag{A.1}$$

Equilibrium of moments:

$$M_R = F_s * z \tag{A.2}$$
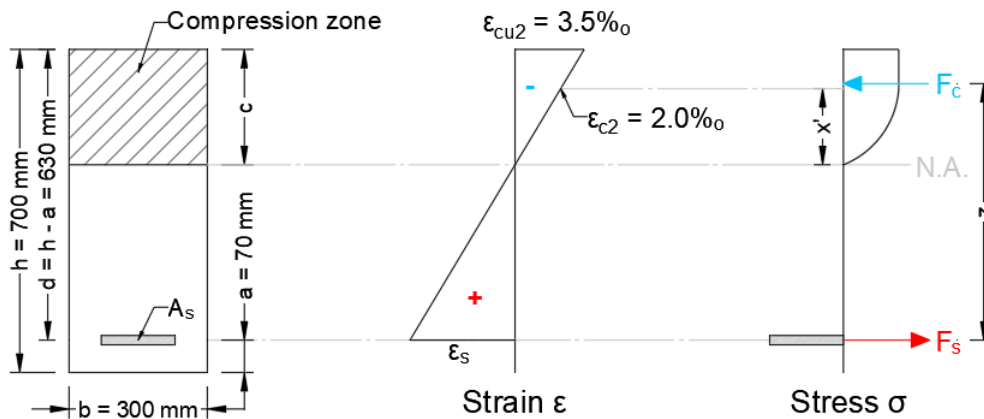
Figure A.1: Stresses, strains and force equilibrium assumed along the cross-section.

$$F_s = A_s \sigma_s \tag{A.3}$$

Resultant for in concrete compressive zone:

$$F_c = F_{c1} + F_{c2} \tag{A.4}$$

F_{c1} is the resultant compressive force caused by the the region along the parabola ($0 \leq x \leq x'$): it is obtained by integrating the stress under the parabola.

$$F_{c1} = b \int_0^{x'} \sigma_c(x) dx \tag{A.5}$$

$$\sigma_c(\varepsilon_c) = f_c \left[1 - \left(1 - \frac{\varepsilon_c}{\varepsilon_{c2}} \right)^2 \right] \tag{A.6}$$

A change in variable must be performed:
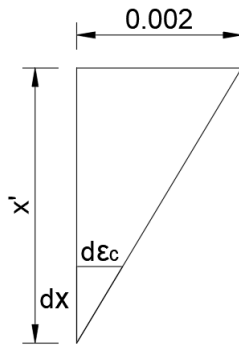
$$\frac{d\varepsilon_c}{dx} = \frac{x'}{0.002} \rightarrow dx = d\varepsilon_c \frac{x'}{0.002}$$

$$x = 0 \rightarrow \varepsilon_c = 0$$

$$x = x' \rightarrow \varepsilon_c = \varepsilon_{c2} = 0.002$$

$$F_{c1} = b \int_0^{0.002} \sigma_c(\varepsilon_c) \frac{x'}{0.002} d\varepsilon_c$$

Then:

$$F_{c1} = b \frac{x'}{0.002} \int_0^{0.002} f_c \left[1 - \left(1 - \frac{\varepsilon_c}{\varepsilon_{c2}}\right)^2\right] d\varepsilon_c \tag{A.7}$$

$$F_{c2} = b(c - x')f_c \tag{A.8}$$

$$F_c = b \frac{x'}{0.002} \int_0^{0.002} f_c \left[1 - \left(1 - \frac{\varepsilon_c}{\varepsilon_{c2}}\right)^2\right] d\varepsilon_c + b(c - x')f_c \tag{A.9}$$

$$F_c = b \frac{x'}{0.002} \frac{1}{750} f_c + b(c - x')f_c \tag{A.10}$$

$$x' = c \frac{\varepsilon_{c2}}{\varepsilon_{cu2}} = \frac{4}{7}c$$

$$F_c = \frac{8}{21} bcf_c + \frac{3}{7} bcf_c = \frac{17}{21} bcf_c \tag{A.11}$$

To determine the point of application, $\bar{x}$, of the concrete compressive resultant force, F_c:

$$\bar{x} = \frac{\int_0^c \sigma(x)x dx}{A} = \frac{\int_0^c \sigma(c)x dx}{\int_0^x \sigma(x) dx} \tag{A.12}$$

$$\bar{x} = \frac{\int_0^{0.002} \sigma(\varepsilon_c)\varepsilon_c \left(\frac{a}{0.002}\right)^2 d\varepsilon_c + \int_a^c f_c x dx}{\int_0^{0.002} \sigma(\varepsilon_c)\frac{a}{0.002} dx + \int_a^c f_c dx} \tag{A.13}$$

$$\bar{x} = \frac{\frac{a^2}{0.002^2} \int_0^{0.002} f_c \left[1 - \left(1 - \frac{\varepsilon_c}{\varepsilon_{c2}}\right)^2\right] \varepsilon_c d\varepsilon_c + \int_a^c f_c x dx}{\frac{a}{0.002} \int_0^{0.002} f_c \left[1 - \left(1 - \frac{\varepsilon_c}{\varepsilon_{c2}}\right)^2\right] dx + \int_a^c f_c dx} \tag{A.14}$$

$$\bar{x} = \frac{a^2 \frac{5}{12} f_c + \frac{33}{98} c^2 f_c}{a \frac{2}{3} f_c + \frac{3}{7} c f_c} \tag{A.15}$$

$$\bar{x} = \frac{\frac{16}{49} c^2 \frac{5}{12} f_c + \frac{33}{98} c^2 f_c}{\frac{4}{7} c \frac{2}{3} f_c + \frac{3}{7} c f_c} \tag{A.16}$$

$$\bar{x} = \frac{\frac{139}{294} c^2 f_c}{\frac{17}{21} c f_c} = \frac{139}{238} c \tag{A.17}$$

Then:

$$a_2 = c - \bar{x} = c - \frac{139}{238}c = \frac{99}{238}c$$

Finally:

$$z = d - a_2 = d - \frac{99}{238}c$$

Replacing F_c, F_s and z in equations A.1 and A.2:

$$\frac{17}{21}bcf_c^* = A_s\sigma_s^* \tag{A.18}$$

$$c = \frac{A_s\sigma_s^*}{\frac{17}{21}bf_c^*} \tag{A.19}$$

$$M_R = A_s\sigma_s^*\left[d - \frac{99}{238}c\right] \tag{A.20}$$

With $\rho = \frac{A_s}{bd}$ and equation A.19 for the height of the compression zone:

$$M_R = bd^2\left[\rho\sigma_s^* - \frac{297}{578}\frac{\rho^2(\sigma_s^*)^2}{f_c^*}\right] \tag{A.21}$$

$$\frac{M_R}{bd^2} = \left[\rho\sigma_s^* - \frac{297}{578}\frac{\rho^2(\sigma_s^*)^2}{f_c^*}\right] \tag{A.22}$$

The stress σ_c in the reinforcement must be determined now. I depends on the value of the actual strain in the reinforcement at the moment when the upper most outer fiber in the concrete reaches its ultimate strain. The theoretical approach for obtaining the value of the strain in the reinforcement, ε_s, is presented hereafter.

$$\sigma_s^* = \begin{cases} f_y^* & \rightarrow \quad if: \ \varepsilon_s \geq \frac{f_y^*}{E_s} \\ E_s\varepsilon_s & \rightarrow \quad if: \ \varepsilon_s < \frac{f_y^*}{E_s} \end{cases}$$

From the strain distribution along the cross section and horizontal equilibrium equation, it is possible to obtain the value of ε_s:

$$\varepsilon_s = \frac{\varepsilon_c}{c}(d - c) \quad \rightarrow \quad \frac{c}{d} = \frac{\varepsilon_c}{\varepsilon_s + \varepsilon_c} \tag{A.23}$$

$$c = \frac{A_s\sigma_s}{\frac{17}{21}bf_c^*} \quad \rightarrow \quad \frac{c}{d} = \frac{\rho E_s\varepsilon_s}{\frac{17}{21}f_c^*} \tag{A.24}$$

$$\frac{\varepsilon_c}{\varepsilon_s + \varepsilon_c} = \frac{\rho E_s\varepsilon_s}{\frac{17}{21}f_c^*} \tag{A.25}$$

Finally, from equation A.25:

$$\varepsilon_s = \frac{-21E_s\rho\varepsilon_c + \sqrt{441E_s^2\rho^2\varepsilon_c^2 + 1428E_s\rho\varepsilon_c f_c^*}}{42E_s\rho} \tag{A.26}$$

Case 1b: Analytical derivation
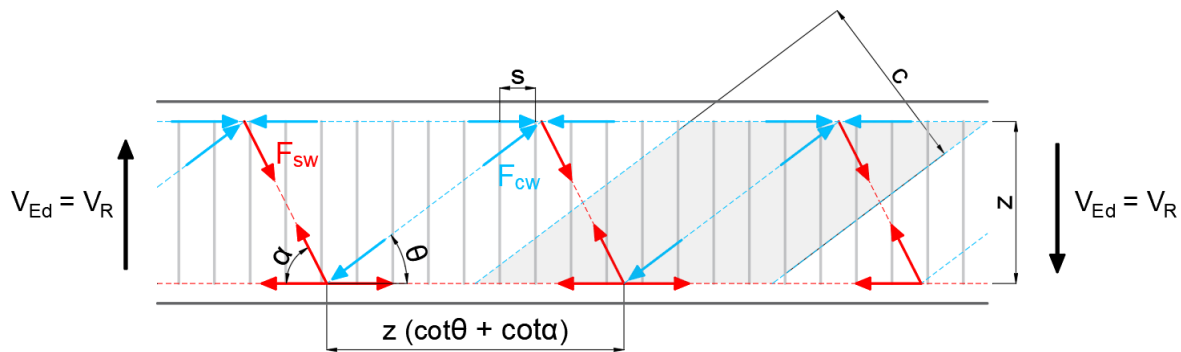
Figure B.1: Forces of the truss model

Shear reinforcement in a member becomes necessary when the design shear force V_{Ed} is higher that the shear resistance of the concrete member alone. A way to describe the load transfer mechanism of members incorporating shear reinforcement is by means of a truss model: with the stirrups represented by the tensile ties and the concrete by the compression struts. [41] Since the amount of reinforcement is the cross-section is already known (assuming is enough to carry the shear solicitation), the area A_{equi} of a tie is given by the stirrups in the beam over a distance $z(\cot \theta + \cot \alpha)$.

$$A_{equi,s} = \frac{A_{sw}}{s} z(\cot \theta + \cot \alpha) \tag{B.1}$$

Where:

- $A_{sw} \rightarrow$ total cross-sectional area per stirrup

- $s \rightarrow$ distance between stirrups

- $\theta \rightarrow$ angle of the compression strut

- $\alpha \rightarrow$ inclination of the tensile ties

Therefor, the tensile force in a tie if $V_{R,s}$ is the vertical force carried by the shear reinforcement:

$$V_{Ed} = V_{R,s}$$

$$F_{sw} = \frac{V_{R,s}}{\sin \alpha} \qquad (B.2)$$

Given the case the stress in the shear reinforcement reaches the yielding point f_{ys}^*, the shear force that can be resisted depending on the shear reinforcement ratio ρ_w is:

$$F_{ws} = \frac{A_{sw}}{s} z (\cot \theta + \cot \alpha) f_{yw}^* \qquad (B.3)$$

$$V_{R,s} = \frac{A_{sw}}{s} z (\cot \theta + \cot \alpha) f_{yw}^* \sin(\alpha) \qquad (B.4)$$

$$V_{R,s} = \rho_w b_w d \cot \theta f_{yw}^* \qquad (B.5)$$

Assuming:

$$\begin{cases} \rho_w = \dfrac{A_{sw}}{b_w s} \\ z = d \\ \alpha = 90° \end{cases}$$

Equation B.5 is a conservative approach for the shear resistance of the transverse reinforcement, due to neglecting several shear resistance mechanisms also present as aggregate interlocking, capacity of the uncracked compression zone, dowel action of the longitudinal reinforcement and the assumption of the forces being transfer only by uni-axial stresses along the truss.

The value of the angle θ related to the inclination of the compressive strut, according to several research and results from shear resistance experiments, should vary according to the amount of reinforcement. During tests (specially for beams with low shear reinforcement) after the initial bending-shear cracks developed, a second crack pattern with a different angle to the beam longitudinal axis is observed. The smaller the reinforcement amount the smaller the angle of the cracks to the beam axis and the more stirrups are crossed increasing the number of bars contributing to the tensile tie resistance. This phenomena can be seen as a rotation of the compressive struts. [41]

Therefore, the following empirical boundaries for θ are established in EN1992-1-1:

$$21.8° \leq \theta \leq 45°$$

Which is equivalent to:

$$2.5 \geq \cot \theta \geq 1.0$$
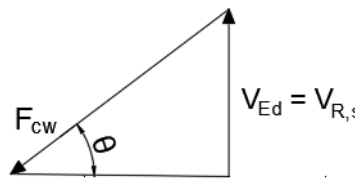
Now, it remains to determine the shear capacity of the compression struts. The equivalent width and the equivalent area of a single strut are:

$$c = z(\cot \theta + \cot \alpha) \sin \theta \qquad (B.6)$$

$$A_{equi,c} = b_w z(\cot \theta + \cot \alpha) \sin \theta \qquad (B.7)$$

The resulting force in the strut from the force equilibrium is:

$$F_{cw} = \frac{V_{R,c}}{\sin\theta} \qquad \text{(B.8)}$$

The normal compressive force in the strut can also be expressed in terms of the stress and the equivalent area:

$$F_{cw} = \sigma_s A_{equi,c} \qquad \text{(B.9)}$$

Then, from equations B.7, B.8 and B.9:

$$\sigma_s b_w z (\cot\theta + \cot\alpha)\sin\theta = \frac{V_{R,c}}{\sin\theta} \qquad \text{(B.10)}$$

If the maximum allowable in the stress in the concrete is known as the concrete compressive strength f_c^*, the shear resistance if the concrete struts is:

$$V_{R,c} = f_c^* b_w z (\cot\theta + \cot\alpha)\sin^2\theta = f_c^* b_w z \frac{\cot\theta + \cot\alpha}{1 + \cot^2\theta} \qquad \text{(B.11)}$$

However, the state of the concrete in the compressive strut must be taken into account:

1. The stirrups induce tensile forces along the concrete, therefor the material can not be loaded up to its uni-axial strength. Thus, a strength reduction factor ν_1 must be included in equation B.11.

Finally, if $\alpha = 90°$ and $z = d$:

$$V_{R,c} = \nu_1 b_w d f_c^* \frac{1}{\cot\theta + \tan\theta} \qquad \text{(B.12)}$$

The final value of the shear resistance V_R, according to EN1992-1-1, is estimated as the minimum value from the comparison between the $V_{R,s}$ and $V_{R,c}$.

C

Python scripts Cases 1a and 1b: Existing Safety Formats and GFM

In chapters 4 and 5.2.2, the existing safety formats (the PSF and ECOV method), and the new GFM were implemented in the reliability analysis of two reinforced concrete cross-sections. The structural analysis was performed by means of analytical expressions. Several values of different varying parameters were investigated under the assumption of Engineer Decision-based Scenarios. Therefore, the development of Python scripts to efficiently implement the safety formats were developed and presented hereafter for each case 1a and 1b. The Python scripts are in the following order:

1. Case 1a: Design value of the Bending Resistance of a Reinforced Concrete Cross-section with the Partial safety Factor, ECOV method by Cervenka and new Global Factor Method

2. Case 1b: Design value of the Bending Resistance of a Reinforced Concrete Cross-section with the Partial safety Factor, ECOV method by Cervenka and new Global Factor Method

Moment Resistance: Rectangular cross-section

Bending cross-section capacity in function of Reinforcement Ratio

```
In [ ]: import numpy as np
        import matplotlib.pyplot as plt
        plt.style.use('seaborn-bright')
```

Moment Capacity Function

```
In [ ]: # Define function for the bending moment capacity analytical expression
        def moment_resist(fc, fy, Rho, eps_s, eps_y, Es):
            if eps_s >= eps_y:
                return ((Rho * fy) - ((297/578) * (((Rho ** 2)*(fy ** 2)) / fc)))
            else:
                return ((Rho * eps_s * Es) - ((297/578) * (((Rho ** 2)*((eps_s * Es) ** 2)) / fc)))

        # Define function for steel strain when concrete reaches a strain of 3.5%o
        def strain(Es, esp_c, rho, fc):
            return((-21 * Es * rho * eps_c + np.sqrt(441 * (Es ** 2) * (rho ** 2) *
                                        (eps_c ** 2) + 1428 * Es * rho * eps_c * fc)) / (42 * Es * rh
        o))
```

Design value of the Resistance Bending Moment with Partial Safety Factors according to Eurocode 2

```
In [ ]: # Partial Safety Factors according to Eurocode 2
        gamma_c = 1.42
        alpha_cc = 1
        gamma_s = 1.06

        #coefficient of variation of the In-situ compressive strength of concrete
        vfc = 0.15

        # Material parameters
        # Concrete
        fcmis = (30 + 8) / 1.15
        fck = fcmis * np.exp(-1.645 * vfc)
        fcd = alpha_cc * (30 / gamma_c)

        eps_c, Es = 0.0035, 200000

        # Reinforcement steel
        fyk = 500
        fym = 534
        fyd = fyk / gamma_s

        # Reinforcement Ratio
        Rho = np.arange(start=0.005, stop=0.051, step=0.001)

        # Reinforcement Strain
        eps_sk = [strain(Es, eps_c, Rho[i], fck) for i in range(0, len(Rho))]

        eps_sd = [strain(Es, eps_c, Rho[i], fcd) for i in range(0, len(Rho))]
```

```
eps_sm = [strain(Es, eps_c, Rho[i], fcmis) for i in range(0, len(Rho))]

eps_sy = [fyk / Es, fyd / Es, fym / Es]

M_Rd = []

# Design value of the Resistance Bending Moment according to Partial Safety Factors
for i in range(0, len(Rho)):
    M = moment_resist(fcd, fyd, Rho[i], eps_sd[i], eps_sy[1], Es)
    M_Rd.append(M)

b, d = 300, 630

M_Rd_PSF_Nm = [((M_Rd[i] * b * (d ** 2)) / (1000 ** 2)) for i in range(0, len(Rho))]

%store M_Rd_PSF_Nm

M_Rm = []

# Mean value of the Resistance Bending Moment
for i in range(0, len(Rho)):
    M = moment_resist(fcmis, fym, Rho[i], eps_sm[i], eps_sy[2], Es)
    M_Rm.append(M)

M_Rk = []

# Characteristic value of the Resistance Bending Moment for the Partial Safety Factors
for i in range(0, len(Rho)):
    M = moment_resist(fck, fyk, Rho[i], eps_sk[i], eps_sy[0], Es)
    M_Rk.append(M)
```

Design value of the Resistance Bending Moment according to ECOV method Cervenka

```
In [ ]:  # Coefficient of variation for concrete and steel: material (f) and model (m) coefficient of variation
         v_f_c = 0.15
         v_m_c = 0
         v_f_y = 0.04
         v_m_y = 0

         # Lumped coefficient of variation for concrete and steel: including material (f) and model (m) coeffici
         ent of variation
         lv_f_c = np.sqrt((v_f_c ** 2 + v_m_c ** 2))
         lv_f_y = np.sqrt((v_f_y ** 2 + v_m_y ** 2))

         # Characteristic values of concrete and steel
         fck_cerv = fcmis * np.exp(-1.645 * lv_f_c)
         fyk_cerv = fym * np.exp(-1.645 * lv_f_y)

         # Reinforcement Strain Cervenka
         eps_sk_cerv = [strain(Es, eps_c, Rho[i], fck_cerv) for i in range(0, len(Rho))]

         eps_sy_cerv = fyk_cerv / Es

         M_Rk_cerv = []

         # Characteristic value of the Resistance Bending Moment for the Ecov Cervenka
         for i in range(0, len(Rho)):
             M = moment_resist(fck_cerv, fyk_cerv,
                               Rho[i], eps_sk_cerv[i], eps_sy_cerv, Es)
             M_Rk_cerv.append(M)
```

113

```
# Coefficients of variation for the geometrical, model and materia uncertainties
V_G = 0
# Modelling uncertainty already included at a material level
V_M = 0
V_F = (1/1.645) * np.log(np.divide(M_Rm, M_Rk_cerv))

# Coefficients of variation of the resistance according to ECOV Cervenka
V_R_cerv = [np.sqrt((V_G ** 2) + (V_M ** 2) + (V_F[i] ** 2))
            for i in range(0, len(Rho))]

# Global factor for the Resistance according to ECOV Cervenka
alpha_R = 0.8
beta_n = 3.8
gamma_R_cerv = [(np.exp(alpha_R * beta_n * V_R_cerv[i]))
                for i in range(0, len(Rho))]

# Design value of the Resistance Bending Moment according to ECOV Cervenka
M_Rd_cerv = np.divide(M_Rm, gamma_R_cerv)

M_Rd_cerv_Nm = [((M_Rm[i] * b * (d ** 2)) / (1000 ** 2)) /
                gamma_R_cerv[i] for i in range(0, len(Rho))]

%store M_Rd_cerv_Nm
```

Comparison between the partial safety factor and global safety factor by Cervenka

```
In [ ]:  # Figure showing the normalized values of Moment Resistance

plt.figure(figsize=(6, 6))
plt.plot(Rho, M_Rm, label='$M_{Rm}$', linewidth = 1)
plt.plot(Rho, M_Rk, label='$M_{Rk}$', linewidth = 1)
plt.plot(Rho, M_Rd, label='$M_{Rd,PSF}$', linewidth = 1)
plt.plot(Rho, M_Rd_cerv, label='$M_{Rd,Cervenka}$', linestyle='--', linewidth = 1.2)
plt.axvline(x=0.02, color='silver', linestyle=':')
plt.axvline(x=0.03, color='silver', linestyle=':')
plt.xlabel("ρ = As/bd", fontsize=16)
plt.ylabel("$M_{R}$/b$d^2$  [MPa]", fontsize=16)
plt.title("Bending moment resistance for $0.005 \leq ρ \leq 0.05$ \n PSF & ECOV Cervenka \n Case 1a", f
ontsize=14)
plt.xlim(0, 0.05)
plt.ylim(0, 16)
plt.legend(fontsize=15)
figname1 = "M_Rd - PSF and ECOV.pdf"
figname2 = "M_Rd - PSF and ECOV.png"
plt.savefig(figname1)
plt.savefig(figname2)

# Figure showing the estimation of the coefficient of variation of the Resistance:
%store -r V_MR

V_R_steel = np.sqrt(0.04 ** 2 + 0 ** 2 + 0 ** 2)
V_R_conc = np.sqrt(0.15 ** 2 + 0 ** 2 + 0 ** 2)

plt.figure(figsize=(6, 6))
plt.plot(Rho, V_MR, label='$V_{R, Monte Carlo}$', linestyle='-',  linewidth = 0.8)
plt.plot(Rho, V_R_cerv, label='$V_{R,Cervenka}$', linestyle='-',  linewidth = 0.8)
plt.xlabel("ρ = As/bd", fontsize=16)
plt.ylabel("$V_{R}$", fontsize=16)
plt.axhline(y=V_R_steel, color='silver', linestyle='--')
plt.axhline(y=V_R_conc, color='silver', linestyle='--')
plt.xlim(0, 0.05)
```

```
plt.xlim(0, 0.05)
plt.ylim(0, 0.20)
plt.legend(fontsize=15)
figname1 = "V_R - ECOV.pdf"
figname2 = "V_R - ECOV.png"
plt.savefig(figname1)
plt.savefig(figname2)

# Graph Global Safety Factor of the Resistance:
gamma_Rd = np.divide(M_Rm, M_Rd)

gamma_Rds = fym / fyd
gamma_Rdc = fcmis / fcd

plt.figure(figsize=(6, 6))
plt.plot(Rho, gamma_Rd, label='$γ_{R,PSF}$',  linewidth = 0.8)
plt.plot(Rho, gamma_R_cerv, label='$γ_{R,Cervenka}$', linestyle='-',  linewidth = 0.8)
plt.axhline(y=gamma_Rdc, color='silver', linestyle='--')
plt.axhline(y=gamma_Rds, color='silver', linestyle='--')
plt.xlabel("\u03C1 = As/bd", fontsize=16)
plt.ylabel('$γ_{R}$', fontsize=16)
plt.title("Global Safety Factor Resistance for $0.005 \leq ρ \leq 0.05$ \n PSF & ECOV Cervenka \n Case
  1a", fontsize=14)
plt.text(0.03, 1.15, '$γ_{Rd,s}=f_{ym}/f_{yd}$', fontsize=14)
plt.text(0.002, 1.6, '$γ_{Rd,c}=f_{cm,is}/f_{cd}$', fontsize=14)
plt.xlim(0, 0.05)
plt.ylim(1, 1.8)
plt.legend(fontsize=15)
figname1 = "gamma_R - PSF and ECOV.pdf"
figname2 = "gamma_R - PSF and ECOV.png"
plt.savefig(figname1)
plt.savefig(figname2)
```

Design value of the Resistance Bending Moment according to New GFM - Version 16.02.2021 (V.1)

Scenario 1: Engineer assumes there are 2 failure modes in the region for intermediate reinforcement ratios, with uncorrelated basic variables.

```
In [ ]:  # Reduction factor c
         c = [0.1, 1, 1.645, 2.5]

         # Standard deviation reinf. steel and concrete
         std_fc = 5.22
         std_fy = 25.2

         # Variation of the basic variables x (materials) of an amount c*σ_x
         fcv_GFM = [fcmis - i * std_fc for i in c]
         fyv_GFM = [fym - i * std_fy for i in c]

         # Reinforcement Strain GFM
         eps_sv_GFM_fcmis = [strain(Es, eps_c, Rho[i], fcmis)
                             for i in range(0, len(Rho))]

         eps_sv_GFM_fcv = [[strain(Es, eps_c, Rho[i], fc)
                           for i in range(0, len(Rho))] for fc in fcv_GFM]

         eps_sy_GFM = [i / Es for i in fyv_GFM]

         # Coefficients of variation for the geometrical and model uncertainties
         V_G, V_M = 0, 0
```

```python
# Assumption: Uncorrelated failure modes

# Variying value of the Resistance Bending Moment for the GFM
M_Rv_GFM1 = []

V_Rx_GFM1 = []

V_R_GFM1 = []

gamma_R_GFM1 = []

# Define ductile bending failure or brittle bending failure
for v in range(0, len(fcv_GFM)):
    M_Rv_GFM1.append([])
    for i in range(0, len(Rho)):
        if eps_sm[i] >= eps_sy[2]:
            M = moment_resist(
                fcmis, fyv_GFM[v], Rho[i], eps_sv_GFM_fcmis[i], eps_sy[2], Es)
            M_Rv_GFM1[v].append(M)
        else:
            M = moment_resist(fcv_GFM[v], fym, Rho[i],
                              eps_sv_GFM_fcv[v][i], eps_sy_GFM[v], Es)
            M_Rv_GFM1[v].append(M)

# Define single failure mode or 2 concurrent failure modes as follows
for v in range(0, len(fcv_GFM)):
    V_Rx_GFM1.append([])
    V_R_GFM1.append([])
    gamma_R_GFM1.append([])
    for i in range(0, len(Rho)):
        if Rho[i] < 0.02:
            CoV = (1/c[v]) * np.log(M_Rm[i] / M_Rv_GFM1[v][i])
            V_Rx_GFM1[v].append(CoV)
            VR = np.sqrt((V_G ** 2) + (V_M ** 2) + (V_Rx_GFM1[v][i] ** 2))
            V_R_GFM1[v].append(VR)
            gammaR = np.exp(alpha_R * beta_n * V_R_GFM1[v][i])
            gamma_R_GFM1[v].append(gammaR)
        elif Rho[i] > 0.03:
            CoV = (1/c[v]) * np.log(M_Rm[i] / M_Rv_GFM1[v][i])
            V_Rx_GFM1[v].append(CoV)
            VR = np.sqrt((V_G ** 2) + (V_M ** 2) + (V_Rx_GFM1[v][i] ** 2))
            V_R_GFM1[v].append(VR)
            gammaR = np.exp(alpha_R * beta_n * V_R_GFM1[v][i])
            gamma_R_GFM1[v].append(gammaR)
        else:
            CoV = (1/c[v]) * np.log(M_Rm[i] / M_Rv_GFM1[v][i])
            V_Rx_GFM1[v].append(CoV)
            VR = np.sqrt((V_G ** 2) + (V_M ** 2) + (V_Rx_GFM1[v][i] ** 2))
            V_R_GFM1[v].append(VR)
            gammaR = np.exp(
                (np.log(np.sqrt(2)) * V_R_GFM1[v][i]) + alpha_R * beta_n * V_R_GFM1[v][i])
            gamma_R_GFM1[v].append(gammaR)

# Design value of the Resistance Bending Moment according to New GFM
M_Rd_GFM1 = [[M_Rm[i] / gamma_R_GFM1[v][i]
             for i in range(0, len(Rho))] for v in range(0, len(fcv_GFM))]

M_Rd_GFM_Nm1 = [[((M_Rm[i] * b * (d ** 2)) / (1000 ** 2)) /
                gamma_R_GFM1[v][i] for i in range(0, len(Rho))] for v in range(0, len(fcv_GFM))]

%store M_Rd_GFM_Nm1
```

116

```
In [ ]:   #Assign the names for the files
          names = [ 1, 10, 1645, 25]

          # Figures showing the normalized values of Moment Resistance for c = [0.1, 1.0, 1.645, 2.5]:

          for i in range(0, len(c)):
              plt.figure(figsize=(6, 6))
              plt.plot(Rho, M_Rm, label='$M_{Rm}$', linewidth=1)
              plt.plot(Rho, M_Rd_cerv,
                       label='$M_{Rd,Cervenka}$', linestyle='--', linewidth=1.2)
              plt.plot(
                  Rho, M_Rv_GFM1[i], label='$M_{R_{var},GFM}$' f' c = {c[i]}', linestyle=':', linewidth=1.8)
              plt.plot(
                  Rho, M_Rd_GFM1[i], label='$M_{Rd,GFM}$' f' c = {c[i]}', linestyle=':', linewidth=1.8)
              plt.plot(Rho, M_Rd, label='$M_{Rd,PSF}$', linewidth=1)
              plt.xlabel("\u03C1 = As/bd", fontsize=21)
              plt.ylabel("$M_{R}$/b$d^2$", fontsize=21)
              plt.xlim(0, 0.05)
              plt.ylim(0, 16)
              plt.axvline(x=0.02, color='silver', linestyle=':')
              plt.axvline(x=0.03, color='silver', linestyle=':')
              plt.legend(fontsize=16)
              plt.xticks(fontsize=15)
              plt.yticks(fontsize=15)
              plt.tight_layout()
              figname1 = "M_Rd_GFM_ES1_c%i.pdf" % names[i]
              figname2 = "M_Rd_GFM_ES1_c%i.png" % names[i]
              plt.savefig(figname1, format = 'pdf')
              plt.savefig(figname2, format = 'png')

          # Figures showing the estimation of the coefficient of variation of the Resistance for c = [0.1, 1.0,
           1.645, 2.5]:

          for i in range(0, len(c)):
              plt.figure(figsize=(6, 6))
              plt.plot(Rho, V_MR, label='$V_{R,Monte Carlo}$', linestyle='-',  linewidth=0.8)
              plt.plot(Rho, V_R_cerv, label='$V_{R,Cervenka}$',
                       linestyle='-',  linewidth=0.8)
              plt.plot(
                  Rho, V_R_GFM1[i], label='$V_{R,GFM}$' f' c = {c[i]}', linestyle=':',  linewidth=1.5)
              plt.xlabel("ρ = As/bd", fontsize=21)
              plt.ylabel("$V_{R}$", fontsize=21)
              plt.axhline(y=V_R_steel, color='silver', linestyle='--')
              plt.axhline(y=V_R_conc, color='silver', linestyle='--')
              plt.xlim(0, 0.05)
              plt.ylim(0, 0.20)
              plt.legend(fontsize=16)
              plt.xticks(fontsize=15)
              plt.yticks(fontsize=15)
              plt.tight_layout()
              figname1 = "V_R_GFM_ES1_c%i.pdf" % names[i]
              figname2 = "V_R_GFM_ES1_c%i.png" % names[i]
              plt.savefig(figname1, format = 'pdf')
              plt.savefig(figname2, format = 'png')

          # Figures Global Safety Factor of the Resistance for c = [0.1, 1.0, 1.645, 2.5]:

          for i in range(0, len(c)):
              plt.figure(figsize=(6, 6))
              plt.plot(Rho, gamma_Rd, label='$γ_{R,PSF}$',  linewidth=0.8)
              plt.plot(Rho, gamma_R_cerv,
                       label='$γ_{R,Cervenka}$', linestyle='-',  linewidth=0.8)
```

117

```python
            label= $γ_{R,Cervenka}$ , linestyle= - ,  linewidth=0.0)
    plt.plot(
        Rho, gamma_R_GFM1[i], label='$γ_{R,GFM}$' f' c = {c[i]}', linestyle=':',  linewidth=1.5)
    plt.axhline(y=gamma_Rdc, color='silver', linestyle='--')
    plt.axhline(y=gamma_Rds, color='silver', linestyle='--')
    plt.xlabel("\u03C1 = As/bd", fontsize=21)
    plt.ylabel('$γ_{R}$', fontsize=21)
    plt.text(0.03, 1.15, '$γ_{Rd,s}=f_{ym}/f_{yd}$', fontsize=18)
    plt.text(0.002, 1.6, '$γ_{Rd,c}=f_{cm,is}/f_{cd}$', fontsize=18)
    plt.xlim(0, 0.05)
    plt.ylim(1, 1.8)
    plt.legend(fontsize=16)
    plt.xticks(fontsize=15)
    plt.yticks(fontsize=15)
    plt.tight_layout()
    figname1 = "gamma_R_GFM_ES1_c%i.pdf" % names[i]
    figname2 = "gamma_R_GFM_ES1_c%i.png" % names[i]
    plt.savefig(figname1, format = 'pdf')
    plt.savefig(figname2, format = 'png')
```

Scenario 2: Engineer assumes there is 1 failure mode called bending without taking into account the difference in the description of failure mechanism.

```python
In [ ]:  # Variying value of the Resistance Bending Moment for the GFM
         M_Rv_GFM1_sf = [[moment_resist(fcv_GFM[v], fyv_GFM[v], Rho[i], eps_sv_GFM_fcv[v]
                                       [i], eps_sy_GFM[v], Es) for i in range(0, len(Rho))] for v in range(0, l
         en(c))]


         V_Rx_GFM1_sf = [[(1/c[v]) * np.log(M_Rm[i] / M_Rv_GFM1_sf[v][i])
                          for i in range(0, len(Rho))] for v in range(0, len(c))]


         V_R_GFM1_sf = [[np.sqrt((V_G ** 2) + (V_M ** 2) + (V_Rx_GFM1_sf[v][i] ** 2))
                        for i in range(0, len(Rho))] for v in range(0, len(c))]


         gamma_R_GFM1_sf = [[np.exp(alpha_R * beta_n * V_R_GFM1_sf[v][i]) for i in range(0, len(Rho))] for v in
         range(0, len(c))]

         # Design value of the Resistance Bending Moment according to New GFM
         M_Rd_GFM1_sf = [[M_Rm[i] / gamma_R_GFM1_sf[v][i]
                         for i in range(0, len(Rho))] for v in range(0, len(fcv_GFM))]

         M_Rd_GFM_Nm1_sf = [[((M_Rm[i] * b * (d ** 2)) / (1000 ** 2)) /
                            gamma_R_GFM1_sf[v][i] for i in range(0, len(Rho))] for v in range(0, len(fcv_GFM))]


         %store M_Rd_GFM_Nm1_sf
```

```python
In [ ]:  #Assign the names for the files
         names = [ 1, 10, 1645, 25]

         # Figures showing the normalized values of Moment Resistance for c = [0.1, 1.0, 1.645, 2.5]:

         for i in range(0, len(c)):
             plt.figure(figsize=(6, 6))
             plt.plot(Rho, M_Rm, label='$M_{Rm}$', linewidth=1)
             plt.plot(Rho, M_Rd_cerv,
                     label='$M_{Rd,Cervenka}$', linestyle='--', linewidth=1.2)
             plt.plot(
                 Rho, M_Rv_GFM1_sf[i], label='$M_{R_{var},GFM}$' f' c = {c[i]}', linestyle=':', linewidth=1.8)
             plt.plot(
```

```python
        Rho, M_Rd_GFM1_sf[i], label='$M_{Rd,GFM}$' f' c = {c[i]}', linestyle=':', linewidth=1.8)
    plt.plot(Rho, M_Rd, label='$M_{Rd,PSF}$', linewidth=1)
    plt.xlabel("\u03C1 = As/bd", fontsize=21)
    plt.ylabel("$M_{R}$/b$d^2$", fontsize=21)
    plt.xlim(0, 0.05)
    plt.ylim(0, 16)
    plt.axvline(x=0.02, color='silver', linestyle=':')
    plt.axvline(x=0.03, color='silver', linestyle=':')
    plt.legend(fontsize=16)
    plt.xticks(fontsize=15)
    plt.yticks(fontsize=15)
    plt.tight_layout()
    figname1 = "M_Rd_GFM_ES3_c%i.pdf" % names[i]
    figname2 = "M_Rd_GFM_ES3_c%i.png" % names[i]
    plt.savefig(figname1, format = 'pdf')
    plt.savefig(figname2, format = 'png')

# Figures showing the estimation of the coefficient of variation of the Resistance for c = [0.1, 1.0,
 1.645, 2.5]:

for i in range(0, len(c)):
    plt.figure(figsize=(6, 6))
    plt.plot(Rho, V_MR, label='$V_{R,Monte Carlo}$', linestyle='-',  linewidth=0.8)
    plt.plot(Rho, V_R_cerv, label='$V_{R,Cervenka}$',
            linestyle='-',  linewidth=0.8)
    plt.plot(
        Rho, V_R_GFM1_sf[i], label='$V_{R,GFM}$' f' c = {c[i]}', linestyle=':',  linewidth=1.5)
    plt.xlabel("ρ = As/bd", fontsize=21)
    plt.ylabel("$V_{R}$", fontsize=21)
    plt.axhline(y=V_R_steel, color='silver', linestyle='--')
    plt.axhline(y=V_R_conc, color='silver', linestyle='--')
    plt.xlim(0, 0.05)
    plt.ylim(0, 0.20)
    plt.legend(fontsize=16)
    plt.xticks(fontsize=15)
    plt.yticks(fontsize=15)
    plt.tight_layout()
    figname1 = "V_R_GFM_ES3_c%i.pdf" % names[i]
    figname2 = "V_R_GFM_ES3_c%i.png" % names[i]
    plt.savefig(figname1, format = 'pdf')
    plt.savefig(figname2, format = 'png')

# Figures Global Safety Factor of the Resistance for c = [0.1, 1.0, 1.645, 2.5]:

for i in range(0, len(c)):
    plt.figure(figsize=(6, 6))
    plt.plot(Rho, gamma_Rd, label='$γ_{R,PSF}$',  linewidth=0.8)
    plt.plot(Rho, gamma_R_cerv,
            label='$γ_{R,Cervenka}$', linestyle='-',  linewidth=0.8)
    plt.plot(
        Rho, gamma_R_GFM1_sf[i], label='$γ_{R,GFM}$' f' c = {c[i]}', linestyle=':',  linewidth=1.5)
    plt.axhline(y=gamma_Rdc, color='silver', linestyle='--')
    plt.axhline(y=gamma_Rds, color='silver', linestyle='--')
    plt.xlabel("\u03C1 = As/bd", fontsize=21)
    plt.ylabel('$γ_{R}$', fontsize=21)
    plt.text(0.03, 1.15, '$γ_{Rd,s}=f_{ym}/f_{yd}$', fontsize=18)
    plt.text(0.002, 1.6, '$γ_{Rd,c}=f_{cm,is}/f_{cd}$', fontsize=18)
    plt.xlim(0, 0.05)
    plt.ylim(1, 1.8)
    plt.legend(fontsize=16)
    plt.xticks(fontsize=15)
    plt.yticks(fontsize=15)
    plt.tight_layout()
```

```
        figname1 = "gamma_R_GFM_ES3_c%i.pdf" % names[i]
        figname2 = "gamma_R_GFM_ES3_c%i.png" % names[i]
        plt.savefig(figname1, format = 'pdf')
        plt.savefig(figname2, format = 'png')
```

Design value of the Resistance Bending Moment according to simplify GFM - Version 21.05.2021 (V.2)

In [ ]:
```python
# The characteristics value obtained for ECOV cervenka is also taken in here

# Coefficient of variation of the resistance related to the material uncertainty
V_Rx_GFM2 = (1/1.645) * np.log(np.divide(M_Rm, M_Rk_cerv))

# Coefficients of variation for the geometrical and model uncertainties
V_G = 0
V_M = 0

# Coefficients of variation of the resistance according to ECOV Cervenka
V_R_GFM2 = [np.sqrt((V_G ** 2) + (V_M ** 2) + (V_Rx_GFM2[i] ** 2))
           for i in range(0, len(Rho))]

# Global safety factor of the resistance gamma_R according to the GFM
gamma_R_GFM2 = []

# Define single failure mode or 2 concurrent failure modes as follows:
# It is assumed the engineer has the knowledge that in the region between Rho=[0.02, 0.03],
# 2 different failure modes might be obtain.
for i in range(0, len(Rho)):
    if Rho[i] < 0.02 or Rho[i] > 0.03:
        gammaR = np.exp(alpha_R * beta_n * V_R_GFM2[i])
        gamma_R_GFM2.append(gammaR)
    else:
        gammaR = np.exp(
            (np.log(np.sqrt(2)) * V_R_GFM2[i]) + alpha_R * beta_n * V_R_GFM2[i])
        gamma_R_GFM2.append(gammaR)

# Design value of the Resistance Bending Moment according to New GFM
M_Rd_GFM2 = np.divide(M_Rm, gamma_R_GFM2)

M_Rd_GFM_Nm2 = [((M_Rm[i] * b * (d ** 2)) / (1000 ** 2)) /
                gamma_R_GFM2[i] for i in range(0, len(Rho))]

%store M_Rd_GFM_Nm2

# Figure showing the normalized values of Moment Resistance

plt.figure(figsize=(6, 6))
plt.plot(Rho, M_Rm, label='$M_{Rm}$', linewidth=1)
plt.plot(Rho, M_Rd_cerv, label='$M_{Rd,Cervenka}$', linestyle='--', linewidth=1.2)
plt.plot(Rho, M_Rk_cerv, label='$M_{Rk,GFM}$',  linewidth=1)
plt.plot(Rho, M_Rd_GFM2, label='$M_{Rd,simpl.GFM}$', linestyle=':', linewidth=1.8)
plt.plot(Rho, M_Rd, label='$M_{Rd,PSF}$', linewidth=1)
plt.xlabel("\u03C1 = As/bd", fontsize=21)
plt.ylabel("$M_{R}$/b$d^2$", fontsize=21)
plt.xlim(0, 0.05)
plt.ylim(0, 16)
plt.axvline(x=0.02, color='silver', linestyle=':')
plt.axvline(x=0.03, color='silver', linestyle=':')
plt.legend(fontsize=16)
plt.xticks(fontsize=15)
```

```python
plt.yticks(fontsize=15)
plt.tight_layout()
figname1 = "M_Rd_GFM_ESS.pdf"
figname2 = "M_Rd_GFM_ESS.png"
plt.savefig(figname1)
plt.savefig(figname2)


# Figure showing the estimation of the coefficient of variation of the Resistance:

plt.figure(figsize=(6, 6))
plt.plot(Rho, V_MR, label='$V_{R,Monte Carlo}$ ', linestyle='-',  linewidth=0.8)
plt.plot(Rho, V_R_cerv, label='$V_{R,Cervenka}$ ',
         linestyle='-',  linewidth=0.8)
plt.plot(Rho, V_R_GFM2, label='$V_{R},simpl.GFM$ ', linestyle=':',  linewidth=1.5)
plt.xlabel("ρ = As/bd", fontsize=21)
plt.ylabel("$V_{R}$", fontsize=21)
plt.axhline(y=V_R_steel, color='silver', linestyle='--')
plt.axhline(y=V_R_conc, color='silver', linestyle='--')
plt.xlim(0, 0.05)
plt.ylim(0, 0.20)
plt.legend(fontsize=16)
plt.xticks(fontsize=15)
plt.yticks(fontsize=15)
plt.tight_layout()
figname1 = "V_R_GFM_ESS.pdf"
figname2 = "V_R_GFM_ESS.png"
plt.savefig(figname1)
plt.savefig(figname2)


# Graph Global Safety Factor of the Resistance:

plt.figure(figsize=(6, 6))
plt.plot(Rho, gamma_Rd, label='$γ_{R,PSF}$',  linewidth=0.8)
plt.plot(Rho, gamma_R_cerv, label='$γ_{R,Cervenka}$', linestyle='-',  linewidth=0.8)
plt.plot(Rho, gamma_R_GFM2, label='$γ_{R,simpl.GFM}$', linestyle=':',  linewidth=1.5)
plt.axhline(y=gamma_Rdc, color='silver', linestyle='--')
plt.axhline(y=gamma_Rds, color='silver', linestyle='--')
plt.xlabel("\u03C1 = As/bd", fontsize=21)
plt.ylabel('$γ_{R}$', fontsize=21)
plt.text(0.03, 1.15, '$γ_{Rd,s}=f_{ym}/f_{yd}$', fontsize=18)
plt.text(0.002, 1.6, '$γ_{Rd,c}=f_{cm,is}/f_{cd}$', fontsize=18)
plt.xlim(0, 0.05)
plt.ylim(1, 1.8)
plt.legend(fontsize=16)
plt.xticks(fontsize=15)
plt.yticks(fontsize=15)
plt.tight_layout()
figname1 = "gamma_R_GFM_ESS.pdf"
figname2 = "gamma_R_GFM_ESS.png"
plt.savefig(figname1)
plt.savefig(figname2)
```

Shear Resistance: Rectangular cross-section

Shear cross-section capacity in function of Reinforcement Ratio

```python
import numpy as np
import matplotlib.pyplot as plt
import math
plt.style.use('seaborn-bright')
```

```python
# Define function for the Shear resistance:
def shear_resist(Rho, theta, fy, v1, fc, theta_max):
    Vs = Rho * (1 / math.tan(theta)) * fy
    Vc = v1 * fc * ( 1 / (math.tan(theta) + (1 / math.tan(theta))))
    theta_var = theta
    while Vs > Vc and theta_var <= theta_max:
        theta_var = theta_var + 0.0001
        Vs = Rho * (1 / math.tan(theta_var)) * fy
        Vc = v1 * fc * ( 1 / (math.tan(theta_var) + (1 / math.tan(theta_var))))
    return min(Vs, Vc)
```

```python
# Partial Safety Factors

gamma_c = 1.42
alpha_cc = 1
gamma_s = 1.06

# Material parameters: design values for PSF
fcmis = (30+8)/1.15
fck = fcmis * np.exp(-1.65 * 0.15)
fcd = alpha_cc * (30/gamma_c)

fyk = 500
fym = 534
fyd = fyk/gamma_s

# v1: strength reduction factor for concrete cracked in shear

if fyd > 0.8 * fyk:
    v1 = 0.6 * (1 - fck/250)
else:
    if fck <= 60:
        v1 = 0.6
    else:
        v1 = max(0.9 - fck/200, 0.5)

# θ: angle of the concrete compressive struts
theta = math.radians(21.8)
theta_max = math.radians(45)

# Shear Reinforcement Ratio
Rho_s = np.arange(start=0.001, stop=0.02, step=0.0005)

V_Rk = []
V_Rd = []
V_Rm = []

# Characteristic value of the Shear Resistance for the Partial Safety Factors
```

```
for i in Rho_s:
    VR = shear_resist(i, theta, fyk, v1, fck, theta_max)
    V_Rk.append(VR)

# Mean value of the Shear Resistance for the Partial Safety Factors
for i in Rho_s:
    VR = shear_resist(i, theta, fym, v1, fcmis, theta_max)
    V_Rm.append(VR)

# Design value of the Shear Resistance for the Partial Safety Factors
for i in Rho_s:
    VR = shear_resist(i, theta, fyd, v1, fcd, theta_max)
    V_Rd.append(VR)
```

Design value of the Shear Resistance according to ECOV method Cervenka

```
In [ ]:  # Coefficient of variation for concrete and steel: material (f) and model (m) coefficient of variation
         v_f_c = 0.15
         v_m_c = 0
         v_f_y = 0.04
         v_m_y = 0

         # Lumped coefficient of variation for concrete and steel: including material (f) and model (m) coeffici
         ent of variation
         lv_f_c = np.sqrt((v_f_c ** 2 + v_m_c ** 2))
         lv_f_y = np.sqrt((v_f_y ** 2 + v_m_y ** 2))

         # Characteristic values of concrete and steel
         fck_cerv = fcmis * np.exp(-1.645 * lv_f_c)
         fyk_cerv = fym * np.exp(-1.645 * lv_f_y)

         if fyd > 0.8 * fyk_cerv:
             v1_cerv = 0.6 * (1 - fck_cerv/250)
         else:
             if fck_cerv <= 60:
                 v1_cerv = 0.6
             else:
                 v1_cerv = max(0.9 - fck_cerv/200, 0.5)

         V_Rk_cerv = []
         V_Rd_cerv = []


         # Characteristic value of the Shear Resistance for the Ecov Cervenka
         for i in Rho_s:
             VR = shear_resist(i, theta, fyk_cerv, v1_cerv, fck_cerv, theta_max)
             V_Rk_cerv.append(VR)

         # Coefficients of variation for the geometrical, model and materia uncertainties
         V_G = 0
         V_M = 0
         V_F = (1/1.645) * np.log(np.divide(V_Rm,V_Rk_cerv))

         # Coefficients of variation of the resistance according to ECOV Cervenka
         V_R_cerv = [np.sqrt((V_G ** 2) + (V_M ** 2) + (V_F[i] **2)) for i in range(0, len(Rho_s))]

         # Global factor for the Resistance according to ECOV Cervenka
         alpha_R = 0.8
         beta_n = 3.8
         gamma_Rv_cerv = [(np.exp((alpha_R * beta_n * V_R_cerv[i]))) for i in range(0, len(Rho_s))]
```

```
# Design value of the Resistance Bending Moment according to ECOV Cervenka
V_Rd_cerv = np.divide(V_Rm, gamma_Rv_cerv)

b = 300
d = 630

V_Rd_cerv_N = [((V_Rm[i] * b * d) / 1000) / gamma_Rv_cerv[i] for i in range(0, len(Rho_s))]

%store V_Rd_cerv_N
```

Comparison between the partial safety factor and global safety factor by Cervenka

```
In [ ]:   # Figure showing the normalized values of Shear Resistance

          plt.figure(figsize=(6, 6))
          plt.plot(Rho_s, V_Rm, label='$V_{Rm}$', linewidth = 1)
          plt.plot(Rho_s, V_Rk, label='$V_{Rk}$', linewidth = 1)
          plt.plot(Rho_s, V_Rd, label='$V_{Rd,PSF}$', linewidth = 1)
          plt.plot(Rho_s, V_Rd_cerv, label='$V_{Rd,Cervenka}$', linestyle='--', linewidth = 1.2)
          plt.axvline(x=0.02, color='silver', linestyle=':')
          plt.axvline(x=0.03, color='silver', linestyle=':')
          plt.xlabel("$ρ_w$ = $A_{sw}/b_{w}s$", fontsize=16)
          plt.ylabel("$V_{R}$/b$d$", fontsize=16)
          plt.title("Shear resistance for $0.001 \leq ρ \leq 0.02$ \n PSF & ECOV Cervenka \n Case 1b", fontsize=1
          4)
          plt.xlim(0, 0.02)
          plt.ylim(0, 10)
          plt.legend(fontsize=15)
          figname1 = "V_Rd - PSF and ECOV.pdf"
          figname2 = "V_Rd - PSF and ECOV.png"
          plt.savefig(figname1)
          plt.savefig(figname2)

          # Figure showing the estimation of the coefficient of variation of the Resistance:
          %store -r V_VR

          V_R_steel = np.sqrt(0.04 ** 2 + 0 ** 2 + 0** 2)
          V_R_conc = np.sqrt(0.15 ** 2 + 0 ** 2 + 0 ** 2)

          plt.figure(figsize=(6, 6))
          plt.plot(Rho_s, V_VR, label='$V_{R,Monte Carlo}$', linestyle='-',  linewidth = 0.8)
          plt.plot(Rho_s, V_R_cerv, label='$V_{R, Cervenka}$ ', linestyle='-',  linewidth = 0.8)
          plt.xlabel("ρ = As/bd", fontsize=16)
          plt.ylabel("$V_{R,CoV}$", fontsize=16)
          plt.axhline(y=V_R_steel, color='silver', linestyle='--')
          plt.axhline(y=V_R_conc, color='silver', linestyle='--')
          plt.title("Coefficient of variation resistance for $0.001 \leq ρ \leq 0.02$ \n PSF & ECOV Cervenka \n C
          ase 1b", fontsize=14)
          plt.xlim(0, 0.02)
          plt.ylim(0, 0.2)
          plt.legend(fontsize=15)
          figname1 = "V_R - ECOV 1b.pdf"
          figname2 = "V_R - ECOV 1b.png"
          plt.savefig(figname1)
          plt.savefig(figname2)

          # Graph Global Safety Factor of the Resistance:
          gamma_Rd = np.divide(V_Rm,V_Rd)

          gamma_Rds = fym / fyd
```

```
gamma_Rdc = fcmis / fcd

plt.figure(figsize=(6, 6))
plt.plot(Rho_s, gamma_Rd, label='$γ_{R,PSF}$',  linewidth = 0.8)
plt.plot(Rho_s, gamma_Rv_cerv, label='$γ_{R,Cervenka}$', linestyle='-',  linewidth = 0.8)
plt.axhline(y=gamma_Rdc, color='silver', linestyle='--')
plt.axhline(y=gamma_Rds, color='silver', linestyle='--')
plt.xlabel("$ρ_w$ = $A_{sw}/b_{w}s$", fontsize=16)
plt.ylabel("$γ_{R}$", fontsize=16)
plt.title("Global Safety Factor Resistance for $0.001 \leq ρ \leq 0.02$ \n PSF & ECOV Cervenka \n Case
 1b", fontsize=14)
plt.text(0.0125, 1.25, '$γ_{Rd,s}=f_{ym}/f_{yd}$', fontsize=14)
plt.text(0.002, 1.68, '$γ_{Rd,c}=f_{cm,is}/f_{cd}$', fontsize=14)
plt.xlim(0, 0.02)
plt.ylim(1, 1.8)
plt.legend(fontsize=15)
figname1 = "gamma_R - PSF and ECOV 1b.pdf"
figname2 = "gamma_R - PSF and ECOV 1b.png"
plt.savefig(figname1)
plt.savefig(figname2)
```

Design value of the Shear Resistance according to New GFM

```
In [ ]:  # Reduction factor c
         c = [0.1, 1,  1.645, 2.5]

         # Standard deviation reinf. steel and concrete
         std_fc = 5.22
         std_fy = 25.2

         # Variation of the basic variables x (materials) of an amount c*σ_x
         fcv_GFM = [fcmis - i * std_fc for i in c]
         fyv_GFM = [fym - i * std_fy for i in c]


         v1_GFM =[]

         for i in range(0, len(c)):
             if fyd > 0.8 * fyv_GFM[i]:
                 v1 = 0.6 * (1 - fck_cerv/250)
                 v1_GFM.append(v1)
             else:
                 if fck_cerv <= 60:
                     v1_GFM[i] = 0.6
                     v1_GFM.append(v1)
                 else:
                     v1_GFM[i] = max(0.9 - fck_cerv/200, 0.5)
                     v1_GFM.append(v1)

         # Coefficients of variation for the geometrical and model uncertainties
         V_VG = 0
         V_VM = 0

         # Variying value of the Shear Resistance for the GFM
         V_Rc_GFM = []

         V_Rd_GFM = []

         V_VRx_GFM = []

         V_VR_GFM = []
```

```
V_gammaR_GFM = []

# Rc value of the Shear Resistance for the GFM
for v in range(0, len(c)):
    V_Rc_GFM.append([])
    for i in range(0, len(Rho_s)):
        VR = shear_resist(Rho_s[i], theta, fyv_GFM[v], v1_GFM[v], fcv_GFM[v], theta_max)
        V_Rc_GFM[v].append(VR)

# Coefficients of variation for the material uncertainties
for v in range(0, len(c)):
    V_VRx_GFM.append([])
    V_VR_GFM.append([])
    V_gammaR_GFM.append([])
    for i in range(0, len(Rho_s)):
        V_Rx = (1/c[v]) * np.log(V_Rm[i]/ V_Rc_GFM[v][i])
        V_VRx_GFM[v].append(V_Rx)
        V_VR = np.sqrt((V_VG ** 2) + (V_VM ** 2) + (V_VRx_GFM[v][i] **2))
        V_VR_GFM[v].append(V_VR)
        gamma = np.exp((alpha_R * beta_n * V_VR_GFM[v][i]))
        V_gammaR_GFM[v].append(gamma)

# Design value of the Resistance Bending Moment according to ECOV Cervenka
V_Rd_GFM = [[V_Rm[i] / V_gammaR_GFM[v][i] for i in range(0, len(Rho_s))] for v in range(0, len(c))]

b = 300
d = 630

V_Rd_GFM_N = [[((V_Rm[i] * b * d) / 1000) / V_gammaR_GFM[v][i] for i in range(0, len(Rho_s))] for v in
range(0, len(c))]

%store V_Rd_GFM_N
```

```
In [ ]:  # Figure showing the normalized values of Shear Resistance for correct formulation of v1

%store -r mean_VR_Nm

mean_VR = [mean_VR_Nm[i] * 1000 / (b * d) for i in range(0, len(Rho_s))]

#Assign the names for the files
names = [ 1, 10, 1645, 25]


for i in range(0, len(c)):
    plt.figure(figsize=(6, 6))
    plt.plot(Rho_s, V_Rm, label='$V_{Rm}$', linewidth=1)
    plt.plot(Rho_s, V_Rd_cerv, label='$V_{Rd,Cervenka}$', linestyle='--', linewidth=1.2)
    plt.plot(Rho_s, V_Rc_GFM[i], label='$V_{Rvar,GFM}$' f' c = {c[i]}', linestyle=':', linewidth=1.8)
    plt.plot(Rho_s, V_Rd_GFM[i], label='$V_{Rd,GFM}$' f' c = {c[i]}', linestyle=':', linewidth=1.8)
    plt.plot(Rho_s, V_Rd, label='$V_{Rd,PSF}$', linewidth=1)
    plt.xlabel("$\rho_w$ = $A_{sw}/b_{w}s$", fontsize=14)
    plt.ylabel("$V_{R}$/b$d$", fontsize=14)
    plt.xlim(0, 0.02)
    plt.ylim(0, 10)
    plt.yticks(ticks=range(0,11,1), fontsize=15)
    plt.xticks(ticks=(0, 0.005, 0.01, 0.015, 0.02), fontsize=16)
    plt.legend(fontsize=16)
    plt.tight_layout()
    figname1 = "V_Rd_GFM_c%i.pdf" % names[i]
    figname2 = "V_Rd_GFM_c%i.png" % names[i]
    plt.savefig(figname1, format = 'pdf')
```

```
                plt.savefig(figname2, format = 'png')
```

```
In [ ]:  # Figure showing the Safety Factor of the Resistance:
         gamma_Rd = np.divide(V_Rm,V_Rd)

         gamma_Rds = fym / fyd
         gamma_Rdc = fcmis / fcd

         for i in range(0, len(c)):
             plt.figure(figsize=(6, 6))
             plt.plot(Rho_s, gamma_Rd, label='$γ_{R,PSF}$',  linewidth=0.8)
             plt.plot(Rho_s, gamma_Rv_cerv, label='$γ_{R,Cervenka}$', linestyle='-',  linewidth=0.8)
             plt.plot(Rho_s, V_gammaR_GFM[i], label='$γ_{R,GFM}$' f' c = {c[i]}', linestyle=':',  linewidth=1.5)
             plt.axhline(y=gamma_Rdc, color='silver', linestyle='--')
             plt.axhline(y=gamma_Rds, color='silver', linestyle='--')
             plt.xlabel("$ρ_w$ = $A_{sw}/b_{w}s$", fontsize=14)
             plt.ylabel('$γ_{R}$', fontsize=16)
             plt.xlim(0, 0.02)
             plt.ylim(1, 1.8)
             plt.legend(fontsize=16)
             plt.yticks(fontsize=15)
             plt.xticks(ticks=(0, 0.005, 0.01, 0.015, 0.02), fontsize=16)
             plt.tight_layout()
             figname1 = "V_gamma_R_GFM_c%i.pdf" % names[i]
             figname2 = "V_gamma_R_GFM_c%i.png" % names[i]
             plt.savefig(figname1, format = 'pdf')
             plt.savefig(figname2, format = 'png')
```

```
In [ ]:  # Figure showing the estimation of the coefficient of variation of the Resistance:
         %store -r V_VR_VG0_01

         V_R_steel = np.sqrt(0.04 ** 2 + 0 ** 2 + 0 ** 2)
         V_R_conc = np.sqrt(0.15 ** 2 + 0 ** 2 + 0 ** 2)

         for i in range(0, len(c)):
             plt.figure(figsize=(6, 6))
             plt.plot(Rho_s, V_VR_VG0_01, label='$V_{R,Monte Carlo}$', linestyle='-',  linewidth=0.8)
             plt.plot(Rho_s, V_R_cerv, label='$V_{R,Cervenka}$', linestyle='-',  linewidth=0.8)
             plt.plot(Rho_s, V_VR_GFM[i], label='$V_{R,GFM}$' f' c = {c[i]}', linestyle=':',  linewidth=1.5)
             plt.xlabel("$ρ_w$ = $A_{sw}/b_{w}s$", fontsize=14)
             plt.ylabel("$V_{R,CoV}$", fontsize=14)
             plt.axhline(y=V_R_steel, color='silver', linestyle='--')
             plt.axhline(y=V_R_conc, color='silver', linestyle='--')
             plt.xlim(0, 0.02)
             plt.ylim(0, 0.2)
             plt.legend(fontsize=16)
             plt.yticks(fontsize=15)
             plt.xticks(ticks=(0, 0.005, 0.01, 0.015, 0.02), fontsize=16)
             plt.tight_layout()
             figname1 = "V_RCoV_GFM_c%i.pdf" % names[i]
             figname2 = "V_RCoV_GFM_c%i.png" % names[i]
             plt.savefig(figname1, format = 'pdf')
             plt.savefig(figname2, format = 'png')
```

D

Python scripts Cases 1a and 1b: Monte Carlo Simulation

Validation of the results obtained by the GFM and existing safety formats required the performance of a full probabilistic method. A crude Monte Carlo simulation was implemented in chapters 4 and 5.2.2. The developed Python scripts are presented hereafter for the case when the perturbation parameter is $c = 0.1$. For the remaining values of the c, small changes are required in the scripts.

1. Case 1a: Crude Monte Carlo Simulation of the resistance, reliability index of the design resistance obtained with the Partial Safety Factor, ECOV by Cervenka and new Global Factor Method with $c = 0.1$

2. Case 1b: Reliability index of the design resistance obtained with the Partial Safety Factor, ECOV by Cervenka and new Global Factor Method with $c = 0.1$

Case 1a: Crude Monte Carlo Simulation (ECOV - PSF)

Moment resistance: rectangular cross-section

In [1]:

```python
import numpy as np
import matplotlib.pyplot as plt
import random
import pandas as pd

import statistics
import seaborn as sns

from numpy.random import seed
from numpy.random import randn
from scipy.stats import norm
from scipy.stats import lognorm
```

In [2]:

```python
# Define function for the bending moment capacity analytical expression
def moment_resist(fc, fy, h, b, a, As, eps_s, eps_y, Es):
    if eps_s >= eps_y:
        return ((As * fy * (h - a)) - ((297/578) * ((As * fy) ** 2 / (b * fc)))) / (100
0 ** 2)
    else:
        return ((As * eps_s * Es * (h - a)) - ((297/578) * ((As * eps_s * Es) ** 2 / (b
* fc)))) / (1000 ** 2)
```

In [3]:

```python
%store -r M_Rd_cerv_Nm
%store -r M_Rd_PSF_Nm
```

```python
# Parameters assumed to be deterministic
eps_c = 0.0035
Es = 200000

# Number of simulations per reinforcement ratio
simulations = 1000000

# Reinforcement ratio
r_r = [round(0.005 + 0.001*i, 3) for i in range(0, int((0.05-0.005)/0.001)+1)]

#Creation of the needed lists
M_R = []
pf_cerv = []
pf_PSF = []
mean_MR = []
std_MR = []
V_MR = []
fm = []

for r in range(len(r_r)):
    # Pseudo random lognormally distributed parameters
    seed()
    mu_log_fc = 33
    sd_log_fc = 5.22

    mu_norm_fc = np.log((mu_log_fc ** 2) /
                    np.sqrt(mu_log_fc ** 2 + sd_log_fc ** 2))
    sd_norm_fc = np.sqrt(np.log(1 + sd_log_fc ** 2 / mu_log_fc ** 2))

    fc = np.random.lognormal(mu_norm_fc, sd_norm_fc, simulations)

    mu_log_fy = 534
    sd_log_fy = 25.2

    mu_norm_fy = np.log((mu_log_fy ** 2) /
                    np.sqrt(mu_log_fy ** 2 + sd_log_fy ** 2))
    sd_norm_fy = np.sqrt(np.log(1 + sd_log_fy ** 2 / mu_log_fy ** 2))

    fy = np.random.lognormal(mu_norm_fy, sd_norm_fy, simulations)

    # Pseudo random normally distributed parameters
    h = 700
    b = 300
    a = 70
    As = r_r[r] * b * (h - a) + 0.02 * (r_r[r] * b * (h - a))

    M_R.append([])
    fm.append([])

    failure_cerv = 0
    failure_PSF = 0

    for i in range(simulations):
        # Calculating the reinforcement ratio
        Rho = As / (b * (h-a))
        # Calculating the strain in the reinforcement steel
        eps_s = (-21 * Es * Rho * eps_c + np.sqrt(441 * (Es ** 2) * (Rho ** 2)
                            * (eps_c ** 2) + 1428 * Es * Rho * ep
```

131

```
    s_c * fc[i])) / (42 * Es * Rho)

        # Calculating the yielding strain in the reinforcement steel
        eps_y = fy[i] / Es

        # Bending moment capacity
        M_R[r].append(moment_resist(fc[i], fy[i], h,
                                     b, a, As, eps_s, eps_y, Es))

        if eps_s >= eps_y:
            fm[r].append('Ductile')
        else:
            fm[r].append('Brittle')

        # Limit state function Cervenka
        G_X_cerv = M_R[r][i] - (M_Rd_cerv_Nm[r])

        if G_X_cerv <= 0:
            failure_cerv += 1

        # Limit state function PSF
        G_X_PSF = M_R[r][i] - (M_Rd_PSF_Nm[r])

        if G_X_PSF <= 0:
            failure_PSF += 1

    # Mean and standard deviation of the simulation of Moment resistance
    # mean1 = sum(M_R[r])/simulations --> This is what statistics.mean(M_R[r]) does
    mean = statistics.mean(M_R[r])
    mean_MR.append(mean)
    std = statistics.stdev(M_R[r])
    std_MR.append(std)

    #Calculating the probability of failure related to each Safety Format
    pf_cerv.append(failure_cerv / simulations)
    pf_PSF.append(failure_PSF / simulations)

V_MR = np.divide(std_MR, mean_MR)
%store V_MR
```

Stored 'V_MR' (ndarray)

Reliability index β

```python
plt.style.use('seaborn-bright')

# Reliability index β for Ecov by Cervenka
beta_cerv = [(-1 * norm.ppf(i) / 0.8) for i in pf_cerv]

# Reliability index β for PSF
beta_PSF = [(-1 * norm.ppf(i) / 0.8) for i in pf_PSF]

# Plot reliability index β for the different safety formats
plt.figure(figsize=(6, 6))
plt.plot(r_r,beta_cerv, label='$β_{SF, Cervenka}$', linestyle='-')
plt.plot(r_r,beta_PSF, label='$β_{SF, PSF}$', linestyle='--')
plt.xlabel("\u03C1 = As/bd", fontsize=16)
plt.ylabel("$β_{SF}$", fontsize=12)
plt.axhline(y=3.8, color='silver', linestyle='--', label='Target $β = 3.8$')
plt.xlim(0, 0.05)
plt.ylim(0, 6.0)
plt.axvline(x=0.02, color='silver', linestyle=':')
plt.axvline(x=0.03, color='silver', linestyle=':')
plt.legend(fontsize=16)
plt.xticks(fontsize=15)
plt.yticks(fontsize=15)
plt.title("Reliability index related to each estimation of the design reistance \n by e
ach safety format for $0.005 \leq ρ \leq 0.05$ \n Case 1a", fontsize=14)
plt.tight_layout()
figname1 = "MC - PSF and ECOV.pdf"
figname2 = "MC - PSF and ECOV.png"
plt.savefig(figname1)
plt.savefig(figname2)
```


Reliability index related to each estimation of the design reistance
by each safety format for $0.005 \leq \rho \leq 0.05$
Case 1a
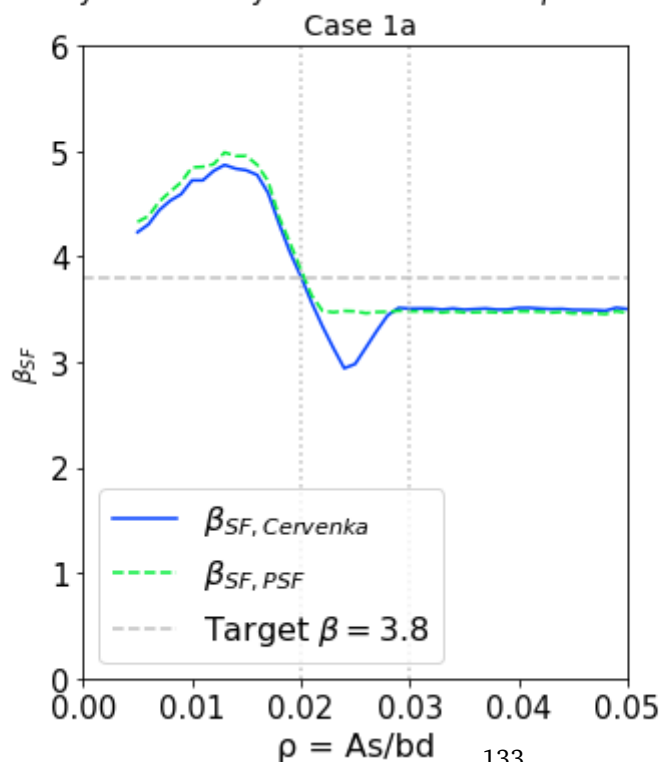
Case 1a: Crude Monte Carlo Simulation - GFM - c = 0.1

Moment resistance: rectangular cross-section

In [1]:

```python
import numpy as np
import matplotlib.pyplot as plt
import random
import pandas as pd

import statistics
import seaborn as sns

from numpy.random import seed
from numpy.random import randn
from scipy.stats import norm
from scipy.stats import lognorm
```

In [2]:

```python
# Define function for the bending moment capacity analytical expression
def moment_resist(fc, fy, h, b, a, As, eps_s, eps_y, Es):
    if eps_s >= eps_y:
        return ((As * fy * (h - a)) - ((297/578) * ((As * fy) ** 2 / (b * fc)))) / (100
0 ** 2)
    else:
        return ((As * eps_s * Es * (h - a)) - ((297/578) * ((As * eps_s * Es) ** 2 / (b
* fc)))) / (1000 ** 2)
```

In [3]:

```python
%store -r M_Rd_cerv_Nm
%store -r M_Rd_GFM_Nm2
%store -r M_Rd_GFM_Nm1
%store -r M_Rd_GFM_Nm1_sf
```

```python
# Parameters assumed to be deterministic
eps_c = 0.0035
Es = 200000

# Number of simulations per reinforcement ratio
simulations = 1000000

# Reinforcement ratio
r_r = [round(0.005 + 0.001*i, 3) for i in range(int((0.05-0.005)/0.001)+1)]

M_R = []
pf_cerv = []
pf_GFM2 = []
pf_GFM1 = []
pf_GFM1_sf = []
mean_MR = []
std_MR = []
V_MR = []
fm = []

for r in range(len(r_r)):
    # Pseudo random lognormally distributed parameters
    seed(7)
    mu_log_fc = 33
    sd_log_fc = 5.22

    mu_norm_fc = np.log((mu_log_fc ** 2) /
                        np.sqrt(mu_log_fc ** 2 + sd_log_fc ** 2))
    sd_norm_fc = np.sqrt(np.log(1 + sd_log_fc ** 2 / mu_log_fc ** 2))

    fc = np.random.lognormal(mu_norm_fc, sd_norm_fc, simulations)

    mu_log_fy = 534
    sd_log_fy = 25.2

    mu_norm_fy = np.log((mu_log_fy ** 2) /
                        np.sqrt(mu_log_fy ** 2 + sd_log_fy ** 2))
    sd_norm_fy = np.sqrt(np.log(1 + sd_log_fy ** 2 / mu_log_fy ** 2))

    fy = np.random.lognormal(mu_norm_fy, sd_norm_fy, simulations)

    # Pseudo random normally distributed parameters
    seed(1)
    h = 700 #+ randn(simulations) * 10
    b = 300 #+ randn(simulations) * 5
    a = 70 #+ randn(simulations) * 10
    As = r_r[r] * b * (h - a) + 0.02 * (r_r[r] * b * (h - a))

    M_R.append([])
    fm.append([])

    failure_cerv = 0
    failure_GFM2 = 0
    failure_GFM1 = 0
    failure_GFM1_sf = 0

    for i in range(simulations):
        # Calculating the reinforcement ratio
        Rho = As / (b * (h-a))
```

```
        # Calculating the strain in the reinforcement steel
        eps_s = (-21 * Es * Rho * eps_c + np.sqrt(441 * (Es ** 2) * (Rho ** 2)
                                         * (eps_c ** 2) + 1428 * Es * Rho * ep
s_c * fc[i])) / (42 * Es * Rho)

        # Calculating the yielding strain in the reinforcement steel
        eps_y = fy[i] / Es

        # Bending moment capacity
        M_R[r].append(moment_resist(fc[i], fy[i], h,
                                    b, a, As, eps_s, eps_y, Es))

        if eps_s >= eps_y:
            fm[r].append(1)
        else:
            fm[r].append(2)

        # Limit state function Cervenka
        G_X_cerv = M_R[r][i] - (M_Rd_cerv_Nm[r])
        G_X_GFM2 = M_R[r][i] - (M_Rd_GFM_Nm2[r])
        G_X_GFM1 = M_R[r][i] - (M_Rd_GFM_Nm1[0][r])
        G_X_GFM1_sf = M_R[r][i] - (M_Rd_GFM_Nm1_sf[0][r])

        if G_X_cerv <= 0:
            failure_cerv += 1

        if G_X_GFM2 <= 0:
            failure_GFM2 += 1

        if G_X_GFM1 <= 0:
            failure_GFM1 += 1

        if G_X_GFM1_sf <= 0:
            failure_GFM1_sf += 1

    # Mean and standard deviation of the simulation of Moment resistance
    # mean1 = sum(M_R[r])/simulations --> This is what statistics.mean(M_R[r]) does
    mean = statistics.mean(M_R[r])
    mean_MR.append(mean)
    std = statistics.stdev(M_R[r])
    std_MR.append(std)

    pf_cerv.append(failure_cerv / simulations)
    pf_GFM2.append(failure_GFM2 / simulations)
    pf_GFM1.append(failure_GFM1 / simulations)
    pf_GFM1_sf.append(failure_GFM1_sf / simulations)

V_MR = np.divide(std_MR, mean_MR)
%store V_MR
```

Stored 'V_MR' (ndarray)

Reliability index β

```python
plt.style.use('seaborn-bright')

# Reduction factor c
c = [0.1, 1, 1.645, 2.5]
n = 0

# Reliability index ß for Ecov by Cervenka
beta_cerv = [(-1 * norm.ppf(i) / 0.8) for i in pf_cerv]

# Reliability index ß for GFM  Version 21.05.2021 (V.2)
beta_GFM2 = [(-1 * norm.ppf(i) / 0.8) for i in pf_GFM2]

# Reliability index ß for GFM Version 16.02.2021 (V.1): Escenario 1
beta_GFM1 = [(-1 * norm.ppf(i) / 0.8) for i in pf_GFM1]

# Reliability index ß for GFM Version 16.02.2021 (V.1) single failure: Escenario 3
beta_GFM1_sf = [(-1 * norm.ppf(i) / 0.8) for i in pf_GFM1_sf]

# Plot reliability index ß for the different safety formats
# Engineer Scenario 1, c=0.1 - 2 LFM in series
plt.figure(figsize=(6, 6))
plt.plot(r_r,beta_cerv, label='$β_{SF,Cervenka}$', linestyle='-')
plt.plot(r_r,beta_GFM1, label='$β_{SF,GFM}$' f' c = {c[n]}', linestyle='--')
plt.xlabel("\u03C1 = As/bd", fontsize=18)
plt.ylabel("$β_{SF}$", fontsize=18)
plt.axhline(y=3.8, color='silver', linestyle='--')
plt.xlim(0, 0.05)
plt.ylim(0, 6.0)
plt.axvline(x=0.02, color='silver', linestyle=':')
plt.axvline(x=0.03, color='silver', linestyle=':')
plt.legend(fontsize=16)
plt.xticks(fontsize=15)
plt.yticks(fontsize=15)
plt.tight_layout()
figname = "MC_ES1_c01.png"
plt.savefig(figname)

# Engineer Scenario 2, c=0.1 - single LFM
plt.figure(figsize=(6, 6))
plt.plot(r_r,beta_cerv, label='$β_{SF,Cervenka}$', linestyle='-')
plt.plot(r_r,beta_GFM1_sf, label='$β_{SF,GFM}$' f' c = {c[n]}', linestyle='--')
plt.xlabel("\u03C1 = As/bd", fontsize=18)
plt.ylabel("$β_{SF}$", fontsize=18)
plt.axhline(y=3.8, color='silver', linestyle='--')
plt.xlim(0, 0.05)
plt.ylim(0, 6.0)
plt.axvline(x=0.02, color='silver', linestyle=':')
plt.axvline(x=0.03, color='silver', linestyle=':')
plt.legend(fontsize=16)
plt.xticks(fontsize=15)
plt.yticks(fontsize=15)
plt.tight_layout()
figname = "MC_ES2_c01.png"
plt.savefig(figname)

# Simplified GFM - 2 LFM in series
plt.figure(figsize=(6, 6))
plt.plot(r_r,beta_cerv, label='$β_{SF,Cervenka}$', linestyle='-')
plt.plot(r_r,beta_GFM2, label='$β_{SF,GFM}$ Simplified', linestyle='--')
```

```
plt.xlabel("\u03C1 = As/bd", fontsize=18)
plt.ylabel("$β_{SF}$", fontsize=18)
plt.axhline(y=3.8, color='silver', linestyle='--')
plt.xlim(0, 0.05)
plt.ylim(0, 6.0)
plt.axvline(x=0.02, color='silver', linestyle=':')
plt.axvline(x=0.03, color='silver', linestyle=':')
plt.legend(fontsize=16)
plt.xticks(fontsize=15)
plt.yticks(fontsize=15)
plt.tight_layout()
figname = "MC_ESS.png"
plt.savefig(figname)
```

139
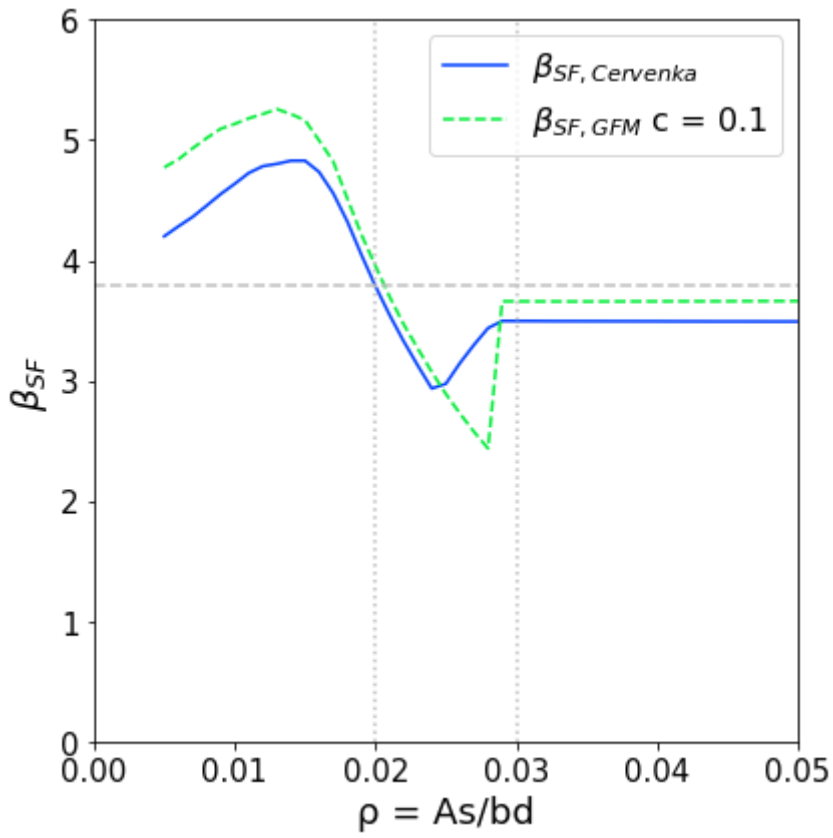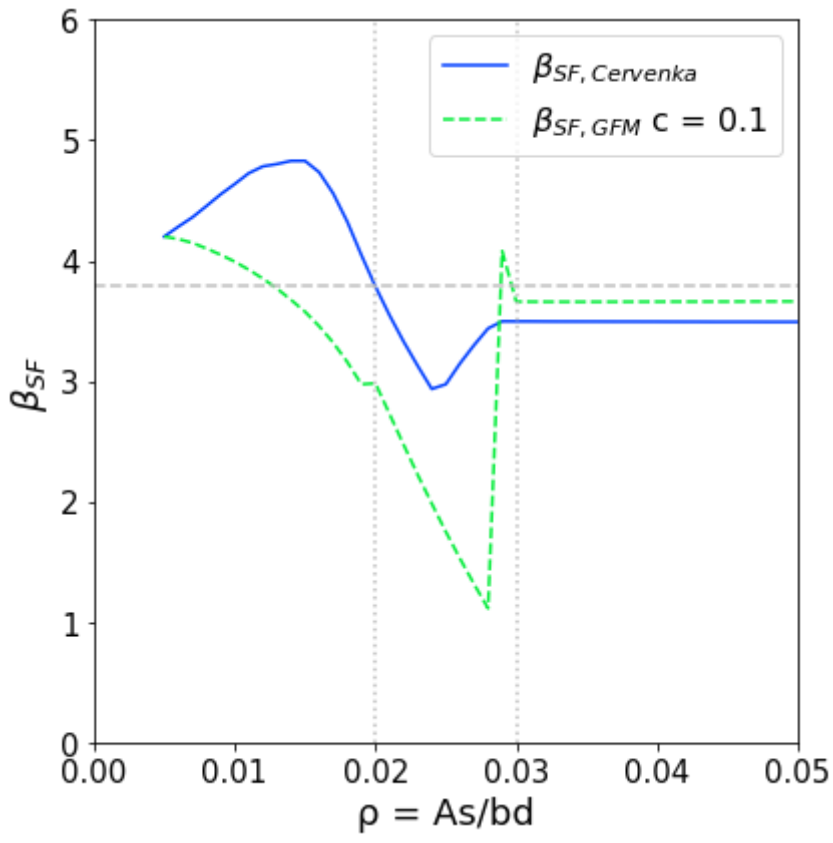
Case 1b: Crude Monte Carlo Simulation GFM - c = 0.1

Shear resistance: rectangular cross-section

In [1]:

```python
import numpy as np
import matplotlib.pyplot as plt
import random
import math
import pandas as pd

import statistics
import seaborn as sns

from numpy.random import seed
from numpy.random import randn
from scipy.stats import norm
from scipy.stats import lognorm
```

In [2]:

```python
# Define function for the Shear resistance analytical expression:
def shear_resist(Asw_s, theta, fy, v1, fc, theta_max, h, b, a):
    Vs = Asw_s * (1 / math.tan(theta)) * fy * (h - a) / 1000
    Vc = v1 * fc * ( 1 / (math.tan(theta) + (1 / math.tan(theta)))) * b * (h - a) / 100
0

    if Vs < Vc:
        fmec = 1
    theta_var = theta
    while Vs > Vc and theta_var <= theta_max:
        theta_var = theta_var + 0.001
        Vs = Asw_s * (1 / math.tan(theta_var)) * fy * (h - a) / 1000
        Vc = v1 * fc * ( 1 / (math.tan(theta_var) + (1 / math.tan(theta_var)))) * b * (
h - a) / 1000
        if Vs < Vc:
            fmec = 2
        else:
            fmec = 3
    VR = min(Vs, Vc)
    return VR, fmec
```

In [3]:

```python
%store -r V_Rd_cerv_N
%store -r V_Rd_GFM_N
```

```python
# Parameters assumed to be deterministic

# ϑ: angle of the concrete compressive struts
theta = math.radians(21.8)
theta_max = math.radians(45)

# Number of simulations per reinforcement ratio
simulations = 1000000

# Shear Reinforcement Ratio
sr_r = np.arange(start=0.001, stop=0.02, step=0.0005)

V_R = []
pf = []
mean_VR_Nm = []
std_VR = []
V_VR = []
fm = []

for r in range(len(sr_r)):
    # Pseudo random lognormally distributed parameters
    seed(7)
    mu_log_fc = 33
    sd_log_fc = 5.22

    mu_norm_fc = np.log((mu_log_fc ** 2) /
                        np.sqrt(mu_log_fc ** 2 + sd_log_fc ** 2))
    sd_norm_fc = np.sqrt(np.log(1 + sd_log_fc ** 2 / mu_log_fc ** 2))

    fc = np.random.lognormal(mu_norm_fc, sd_norm_fc, simulations)

    mu_log_fy = 534
    sd_log_fy = 25.2

    mu_norm_fy = np.log((mu_log_fy ** 2) /
                        np.sqrt(mu_log_fy ** 2 + sd_log_fy ** 2))
    sd_norm_fy = np.sqrt(np.log(1 + sd_log_fy ** 2 / mu_log_fy ** 2))

    fy = np.random.lognormal(mu_norm_fy, sd_norm_fy, simulations)

    # Pseudo random normally distributed parameters
    seed(1)
    h = 700
    b = 300
    a = 70
    Asw_s = sr_r[r] * b

    # v1: strength reduction factor for concrete cracked in shear
    v1 = 0.6 * (1 - fc/250)

    V_R.append([])
    fm.append([])

    failure = 0

    for i in range(simulations):
        # Bending moment capacity
        VR, fmec = shear_resist(Asw_s, theta, fy[i], v1[i], fc[i], theta_max, h, b, a)
        V_R[r].append(VR)
```

141

```python
        fm[r].append(fmec)

        # Limit state function Cervenka
        G_X = V_R[r][i] - V_Rd_GFM_N[0][r]

        if G_X <= 0:
            failure += 1


    # Mean and standard deviation of the simulation of Shear resistance
    # mean1 = sum(V_R[r])/simulations --> This is what statistics.mean(V_R[r]) does
    mean = statistics.mean(V_R[r])
    mean_VR_Nm.append(mean)
    std = statistics.stdev(V_R[r])
    std_VR.append(std)

    pf.append(failure / simulations)

V_VR_VG0_01 = np.divide(std_VR, mean_VR_Nm)

%store V_VR_VG0_01
```

```
0
1
2
3
4
5
6
7
8
9
10
11
12
13
14
15
16
17
18
19
20
21
22
23
24
25
26
27
28
29
30
31
32
33
34
35
36
37
Stored 'V_VR_VG0_01' (ndarray)
```

Reliability index β

E

Python scripts Case 1c: GFM and Monte Carlo Simulation

In chapter 6, the new GFM was used in the reliability analysis of a simply supported reinforced concrete beam subjected to a quasi-static point load. The structural analysis was performed through analytical expressions. The design value of the resistance was computed for various positions of the load and the GFM was implemented with 5 different values of the perturbation parameter c. Therefore, the Python scripts to efficiently implement the safety format and its posterior validation with a Monte Carlo simulation are presented in this Appendix.

145

Case Study 1c: Design Resistance by analytical solution

Mixed simply supported beam: Clustered bending and shear failure modes

In [1]:

```python
import numpy as np
import matplotlib.pyplot as plt
import pandas as pd
from sympy import symbols, Eq, solve

plt.style.use('seaborn-bright')
```

Defined Functions

In [2]:

```python
# Define function for the bending moment capacity analytical expression
def moment_resist(fc, fy, Rho, eps_s, eps_y, Es):
    if eps_s >= eps_y:
        return ((Rho * fy) - ((297/578) * (((Rho ** 2)*(fy ** 2)) / fc)))
    else:
        return ((Rho * eps_s * Es) - ((297/578) * (((Rho ** 2)*((eps_s * Es) ** 2)) / fc)))

# Define function for steel strain when concrete reaches a strain of 3.5%o
def strain(Es, esp_c, rho, fc):
    return((-21 * Es * rho * eps_c + np.sqrt(441 * (Es ** 2) * (rho ** 2) *
                                    (eps_c ** 2) + 1428 * Es * rho * eps_c * fc))
/ (42 * Es * rho))
```

Geometrical Parameters and material parameters

```
#Length units: mm
#load position (a) --> distance from the support
a = np.arange(start=750, stop=2550, step=50)

#Position of the longitudinal posotion
d = 270

#Rectangular cross-section
b = 300

#Reinforcement Ratios
N_bars = [3, 3]
Diameter_bars = [16, 20]
Rho_l = [(N_bars[i] * np.pi * (Diameter_bars[i] ** 2) / 4) / (b * d) for i in range(0,
len(Diameter_bars))]

eps_c, Es = 0.0035, 200000

# Cantilever and midspan length of the beam along wiht total lenght
L1 = 1500
L2 = 5000
L3 = 1500
Lt = L1 + L2 + L3
```

Beam Resistance: analytical expression

- Bending resistance: mean values

```
# Mean values of the material basic values
 # Concrete
fcm = 78.5
fcmis = fcm / 1.15

 # Reinforcement steel
fym = 550

# Reinforcement Strain
eps_sm = [strain(Es, eps_c, Rho_l[i], fcm) for i in range(0, len(Rho_l))]

eps_sym = fym / Es

M_Rm = []

# Mean value of the Resistance Bending Moment in [kN.m]
for i in range(0, len(Rho_l)):
    M_Rm.append([])
    M = moment_resist(fcm, fym, Rho_l[i], eps_sm[i], eps_sym, Es)
    M = M * b * (d ** 2) / 1000000
    for j in range(0, len(a)):
        M_Rm[i].append(M)
```

Cross section Shear Resistance: analytical expression

```python
# Size parameter
k = min(2, 1 + np.sqrt(200 / d))

C_Rm = 0.18

# Mean value of the Resistance Shear in [kN]

V_Rm = []

for i in range(0, len(Rho_l)):
    V_Rm.append([])
    V = C_Rm * k * (100 * Rho_l[i] * fcm) ** (1/3)* b * d / 1000
    for j in range(0, len(a)):
        V_Rm[i].append(V)
```

Finding the CLFM: min max min (μ_Pu) rule

```python
CLFM = []
Pu_m = []
PD = []

for i in range(0, len(Rho_l)):
    CLFM.append([])
    Pu_m.append([])
    PD.append([])
    for j in range(0, len(a)):
        P_Mmax = M_Rm[i][j] / ((a[j]/1000) * ((L2 - a[j]) / L2))
        P_Vmax = V_Rm[i][j] / ((L2 -a[j]) / L2)
        if P_Vmax < P_Mmax:
            Pu_m[i].append(P_Vmax)
            CLFM[i].append('Shear')
            M = P_Vmax * ((a[j]/1000) * ((L2 - a[j]) / L2))
            differ = (abs(M_Rm[i][j] - M) / ((M_Rm[i][j] + M)/2)) * 100
            PD[i].append(differ)
        else:
            Pu_m[i].append(P_Mmax)
            CLFM[i].append('Bending')
            V = P_Mmax * ((L2 - a[j]) / L2)
            differ = (abs(V_Rm[i][j] - V) / ((V_Rm[i][j] + V)/2)) * 100
            PD[i].append(differ)

%store Pu_m
```

Stored 'Pu_m' (list)

```python
from IPython.display import display, HTML

df_Rho1 = pd.DataFrame(list(zip(a, CLFM[0], Pu_m[0], PD[0], M_Rm[0], V_Rm[0])))
df_Rho1.columns = ['a', 'CLFM', 'Pu_m [kN]', '% Difference', 'M_Rm [kNm]', 'V_Rm [kN]']

df_Rho2 = pd.DataFrame(list(zip(a, CLFM[1], Pu_m[1], PD[1], M_Rm[1], V_Rm[1])))
df_Rho2.columns = ['a', 'CLFM', 'Pu_m [kN]', '% Difference', 'M_Rm [kNm]', 'V_Rm [kN]']

display(HTML(df_Rho1.to_html()))
display(HTML(df_Rho2.to_html()))
```

	a	CLFM	Pu_m [kN]	% Difference	M_Rm [kNm]	V_Rm [kN]
0	750	Shear	123.865842	9.880102	87.171685	105.285965
1	800	Shear	125.340435	3.433962	87.171685	105.285965
2	850	Bending	123.560149	2.628012	87.171685	105.285965
3	900	Bending	118.118815	8.339167	87.171685	105.285965
4	950	Bending	113.283542	13.729101	87.171685	105.285965
5	1000	Bending	108.964607	18.824172	87.171685	105.285965
6	1050	Bending	105.089434	23.647934	87.171685	105.285965
7	1100	Bending	101.598701	28.221495	87.171685	105.285965
8	1150	Bending	98.443462	32.563828	87.171685	105.285965
9	1200	Bending	95.582988	36.692037	87.171685	105.285965
10	1250	Bending	92.983131	40.621579	87.171685	105.285965
11	1300	Bending	90.615058	44.366458	87.171685	105.285965
12	1350	Bending	88.454272	47.939392	87.171685	105.285965
13	1400	Bending	86.479847	51.351957	87.171685	105.285965
14	1450	Bending	84.673808	54.614714	87.171685	105.285965
15	1500	Bending	83.020653	57.737315	87.171685	105.285965
16	1550	Bending	81.506952	60.728602	87.171685	105.285965
17	1600	Bending	80.121034	63.596686	87.171685	105.285965
18	1650	Bending	78.852723	66.349026	87.171685	105.285965
19	1700	Bending	77.693124	68.992490	87.171685	105.285965
20	1750	Bending	76.634449	71.533412	87.171685	105.285965
21	1800	Bending	75.669866	73.977647	87.171685	105.285965
22	1850	Bending	74.793381	76.330608	87.171685	105.285965
23	1900	Bending	73.999733	78.597316	87.171685	105.285965
24	1950	Bending	73.284309	80.782428	87.171685	105.285965
25	2000	Bending	72.643071	82.890271	87.171685	105.285965
26	2050	Bending	72.072497	84.924873	87.171685	105.285965
27	2100	Bending	71.569528	86.889986	87.171685	105.285965
28	2150	Bending	71.131526	88.789111	87.171685	105.285965
29	2200	Bending	70.756238	90.625516	87.171685	105.285965
30	2250	Bending	70.441766	92.402257	87.171685	105.285965
31	2300	Bending	70.186542	94.122196	87.171685	105.285965
32	2350	Bending	69.989310	95.788015	87.171685	105.285965
33	2400	Bending	69.849107	97.402227	87.171685	105.285965
34	2450	Bending	69.765254	98.967195	87.171685	105.285965
35	2500	Bending	69.737348	100.485138	87.171685	105.285965

	a	CLFM	Pu_m [kN]	% Difference	M_Rm [kNm]	V_Rm [kN]
0	750	Shear	143.733577	37.625373	134.095149	122.17354
1	800	Shear	145.444691	31.364097	134.095149	122.17354
2	850	Shear	147.197037	25.424310	134.095149	122.17354
3	900	Shear	148.992122	19.781873	134.095149	122.17354
4	950	Shear	150.831531	14.415002	134.095149	122.17354
5	1000	Shear	152.716926	9.303992	134.095149	122.17354
6	1050	Shear	154.650051	4.430970	134.095149	122.17354
7	1100	Bending	156.288053	0.220306	134.095149	122.17354
8	1150	Bending	151.434387	4.664636	134.095149	122.17354
9	1200	Bending	147.034155	8.915531	134.095149	122.17354
10	1250	Bending	143.034826	12.985350	134.095149	122.17354
11	1300	Bending	139.392047	16.885423	134.095149	122.17354
12	1350	Bending	136.068137	20.626151	134.095149	122.17354
13	1400	Bending	133.030902	24.217105	134.095149	122.17354
14	1450	Bending	130.252695	27.667103	134.095149	122.17354
15	1500	Bending	127.709666	30.984286	134.095149	122.17354
16	1550	Bending	125.381159	34.176177	134.095149	122.17354
17	1600	Bending	123.249218	37.249744	134.095149	122.17354
18	1650	Bending	121.298190	40.211447	134.095149	122.17354
19	1700	Bending	119.514393	43.067283	134.095149	122.17354
20	1750	Bending	117.885846	45.822829	134.095149	122.17354
21	1800	Bending	116.402039	48.483277	134.095149	122.17354
22	1850	Bending	115.053753	51.053466	134.095149	122.17354
23	1900	Bending	113.832894	53.537913	134.095149	122.17354
24	1950	Bending	112.732366	55.940838	134.095149	122.17354
25	2000	Bending	111.745958	58.266188	134.095149	122.17354
26	2050	Bending	110.868251	60.517662	134.095149	122.17354
27	2100	Bending	110.094540	62.698723	134.095149	122.17354
28	2150	Bending	109.420766	64.812625	134.095149	122.17354
29	2200	Bending	108.843465	66.862422	134.095149	122.17354
30	2250	Bending	108.359717	68.850987	134.095149	122.17354
31	2300	Bending	107.967109	70.781023	134.095149	122.17354
32	2350	Bending	107.663709	72.655077	134.095149	122.17354
33	2400	Bending	107.448036	74.475549	134.095149	122.17354
34	2450	Bending	107.319047	76.244706	134.095149	122.17354
35	2500	Bending	107.276119	77.964686	134.095149	122.17354

- Desing bending resistance: GFM

In [8]:

```python
# Values of the perturbation parameter c:
c = [0.1, 0.5, 1.0, 1.645, 2.5]

# Resistance part: sensisivity factor and reliability index
alpha_R = 0.8
beta_R = 3.8

# Mean and coefficient of variation of the modelling uncertainty
mu_theta = 1
V_theta = 0

# Standard deviation reinf. steel and concrete
std_fc = 9.645
std_fy = 65

# Variation of the basic variables x (materials) of an amount c*o_x
fcc = [fcm - z * std_fc for z in c]
fyc = [fym - z * std_fy for z in c]

# Var value of the Resistance Bending Moment in [kN.m]:

# Reinforcement Strain

eps_sc = []

for z in range(0, len(c)):
    eps_sc.append([])
    for i in range(0, len(Rho_l)):
        epssc = strain(Es, eps_c, Rho_l[i], fcc[z])
        eps_sc[z].append(epssc)

eps_syc = [fyc[z] / Es for z in range(0, len(c))]

M_Rvar = []

for z in range(0, len(c)):
    M_Rvar.append([])
    for i in range(0, len(Rho_l)):
        M_Rvar[z].append([])
        for j in range(0, len(a)):
            if CLFM[i][j] == 'Shear':
                M = moment_resist(fcm, fym, Rho_l[i], eps_sm[i], eps_sym, Es)
                M = M * b * (d ** 2) / 1000000
                M_Rvar[z][i].append(M)
            elif CLFM[i][j] == 'Bending':
                M = moment_resist(fcc[z], fyc[z], Rho_l[i], eps_sc[z][i], eps_syc[z], Es)
                M = M * b * (d ** 2) / 1000000
                M_Rvar[z][i].append(M)

# Var value of the Resistance Shear in [kN]:
V_Rvar = []

for z in range(0, len(c)):
    V_Rvar.append([])
    for i in range(0, len(Rho_l)):
        V_Rvar[z].append([])
        for j in range(0, len(a)):
            if CLFM[i][j] == 'Shear':
```

153

```python
                V = C_Rm * k * (100 * Rho_l[i] * fcc[z]) ** (1/3)* b * d / 1000
                V_Rvar[z][i].append(V)
            elif CLFM[i][j] == 'Bending':
                V = C_Rm * k * (100 * Rho_l[i] * fcm) ** (1/3)* b * d / 1000
                V_Rvar[z][i].append(V)

#Calculate Pu_var:
CLFM_var = []
Pu_var = []

for z in range(0, len(c)):
    CLFM_var.append([])
    Pu_var.append([])
    for i in range(0, len(Rho_l)):
        CLFM_var[z].append([])
        Pu_var[z].append([])
        for j in range(0, len(a)):
            P_Mmax = M_Rvar[z][i][j] / ((a[j]/1000) * ((L2 - a[j]) / L2))
            P_Vmax = V_Rvar[z][i][j] / ((L2 -a[j]) / L2)
            if P_Vmax < P_Mmax:
                Pu_var[z][i].append(P_Vmax)
                CLFM_var[z][i].append('Shear')
            else:
                Pu_var[z][i].append(P_Mmax)
                CLFM_var[z][i].append('Bending')

V_Rx_GFM = []
gamma_R_GFM = []
Pu_d_GFM = []

for z in range(0, len(c)):
    V_Rx_GFM.append([])
    gamma_R_GFM.append([])
    Pu_d_GFM.append([])
    for i in range(0, len(Rho_l)):
        V_Rx_GFM[z].append([])
        gamma_R_GFM[z].append([])
        Pu_d_GFM[z].append([])
        for j in range(0, len(a)):
            VRx = (1 / c[z]) * np.log(Pu_m[i][j] / Pu_var[z][i][j])
            V_Rx_GFM[z][i].append(VRx)
            if PD[i][j] <= 10:
                gamma = (1 / mu_theta) * np.exp( (np.log(np.sqrt(2)) * V_Rx_GFM[z][i][j
]) + (alpha_R * beta_R * V_Rx_GFM[z][i][j]) )
            else:
                gamma = (1 / mu_theta) * np.exp(alpha_R * beta_R * V_Rx_GFM[z][i][j])
            gamma_R_GFM[z][i].append(gamma)
            Pud = Pu_m[i][j] / gamma_R_GFM[z][i][j]
            Pu_d_GFM[z][i].append(Pud)

Pu_d_rho1_c01 = Pu_d_GFM[0][0]
Pu_d_rho2_c01 = Pu_d_GFM[0][1]

%store Pu_d_rho1_c01
%store Pu_d_rho2_c01

Pu_d_rho1_c25 = Pu_d_GFM[4][0]
Pu_d_rho2_c25 = Pu_d_GFM[4][1]                    154

%store Pu_d_rho1_c25
%store Pu_d_rho2_c25
```

```
# print(Pu_d_GFM)

df_Rho1 = pd.DataFrame(list(zip(a, CLFM[0], CLFM_var[0][0], Pu_m[0], Pu_var[0][0], V_Rx
_GFM[0][0], gamma_R_GFM[0][0], Pu_d_GFM[0][0])))
df_Rho1.columns = ['a', 'CLFM', 'CLFM_var', 'Pu_m [kN]', 'Pu_var [kN]', 'V_Rx_GFM', 'ga
mma_R_GFM', 'Pu_d_GFM [kN]']

df_Rho2 = pd.DataFrame(list(zip(a, CLFM[1], CLFM_var[0][1], Pu_m[1], Pu_var[0][1], V_Rx
_GFM[0][1], gamma_R_GFM[0][1], Pu_d_GFM[0][1])))
df_Rho2.columns = ['a', 'CLFM', 'CLFM_var', 'Pu_m [kN]', 'Pu_var [kN]', 'V_Rx_GFM', 'ga
mma_R_GFM', 'Pu_d_GFM [kN]']

display(HTML(df_Rho1.to_html()))
display(HTML(df_Rho2.to_html()))


# df_Rho1 = pd.DataFrame(list(zip(a, CLFM[0], CLFM_var[0][0], Pu_m[0], Pu_var[0][0], V_
Rx_GFM[0][0], gamma_R_GFM[0][0], Pu_d_GFM[0][0], M_Rm[0], M_Rvar[0][0], V_Rm[0], V_Rvar
[0][0])))
# df_Rho1.columns = ['a', 'CLFM', 'CLFM_var', 'Pu_m [kN]', 'Pu_var [kN]', 'V_Rx_GFM',
 'gamma_R_GFM', 'Pu_d_GFM [kN]', 'M_Rm [kNm]', 'M_Rvar [kNm]', 'V_Rm [kNm]', 'V_Rvar [k
Nm]']

# df_Rho2 = pd.DataFrame(list(zip(a, CLFM[1], CLFM_var[0][1], Pu_m[1], Pu_var[0][1], V_
Rx_GFM[0][1], gamma_R_GFM[0][1], Pu_d_GFM[0][1], M_Rm[1], M_Rvar[0][1], V_Rm[1], V_Rvar
[0][1])))
# df_Rho2.columns = ['a', 'CLFM', 'CLFM_var', 'Pu_m [kN]', 'Pu_var [kN]', 'V_Rx_GFM',
 'gamma_R_GFM', 'Pu_d_GFM [kN]', 'M_Rm [kNm]', 'M_Rvar [kNm]', 'V_Rm [kNm]', 'V_Rvar [k
Nm]']
```

.

F

Formulation of the Mean Value of the Material Parameters

The values of the concrete material parameters for the NLFEA in chapter 8 are the same as calculated by Roy in [32]. There, concrete tensile strength, fracture tensile energy, Young's modulus, compressive fracture energy, and Poisson's ratio are were obtained with the formulation proposed by the *fib* Model Code 2010 [20] They are all based on the experimentally obtained value of the concrete compressive strength. This Appendix presents the formulas for the remaining parameters.

$$f_{ck} = f_{cm} - \Delta f \tag{F.1}$$

With $f_{cm} = f_{c,cube}$

Mean value of the concrete tensile strength:

$$f_{ctm} = f_{ctk0.m} \frac{f_{ck}}{f_{ck0}}^{(2/3)} \tag{F.2}$$

With $f_{ctk0.m} = 1.40\,\text{MPa}$ and $f_{ck0} = 10\,\text{MPa}$.

Mean value of the concrete tensile fracture energy:

$$G_{Fm} = G_{F0} \cdot \frac{f_{cm}}{f_{cm0}}^{0.7} \tag{F.3}$$

With $G_{F0} = 0.030\,\text{Nmm/mm}^2$ for an aggregate size of $d_{aggr} = 16$ mm.

Mean value of the Young's modulus:

$$E_{cm} = E_{c0} \cdot \frac{f_{cm}}{f_{cm0}}^{(1/3)} \tag{F.4}$$

With $E_{c0} = 2.2 \cdot 10^4 \text{MPa}$ and $f_{cm0} = 10\text{Mpa}$

Finally, the mean value of the concrete compressive energy:

$$G_{cm} = 250 \cdot G_{Fm} \tag{F.5}$$

G

NLFEA results for case 2c with the Modified Solution Strategy

NLFEA of beam case 2c with mean value of the input critical material parameters and implementing the modified solution strategy:
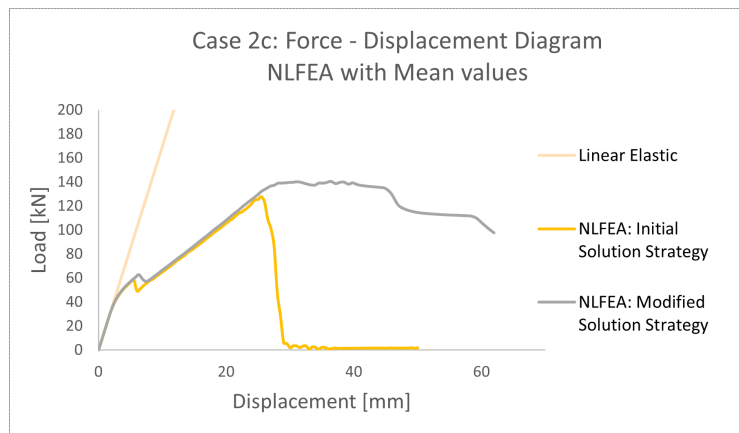
Figure G.1: Global Load-Displacement curve
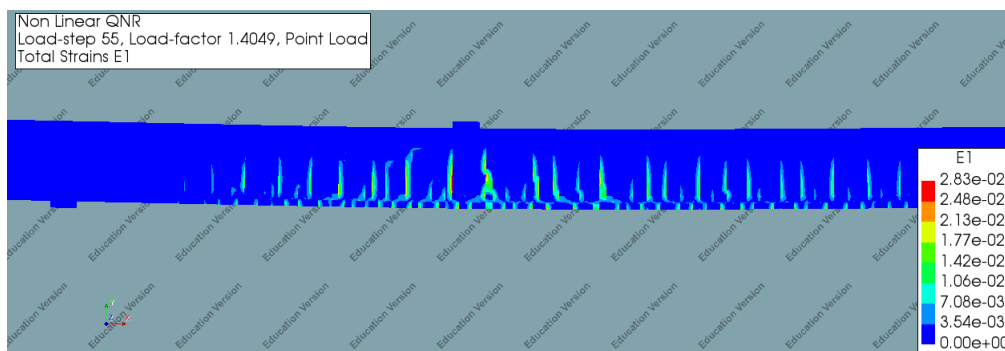
Figure G.2: Principle strain contour plot at Yielding of the Reinforcement
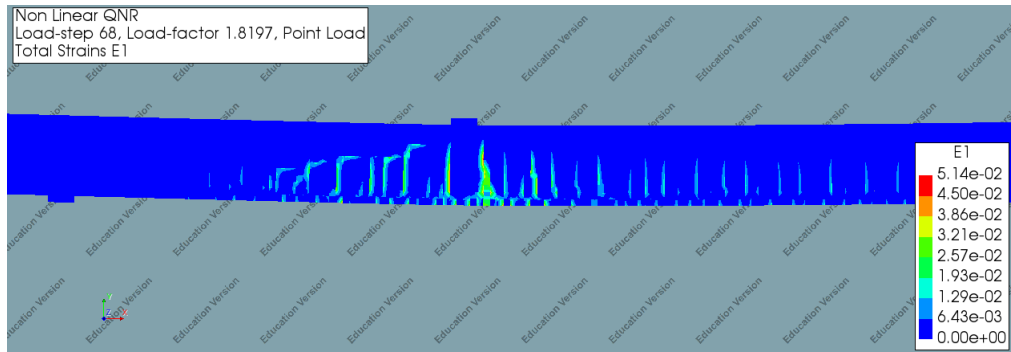
Figure G.3: Principle strain contour plot at Point of Maximum Load
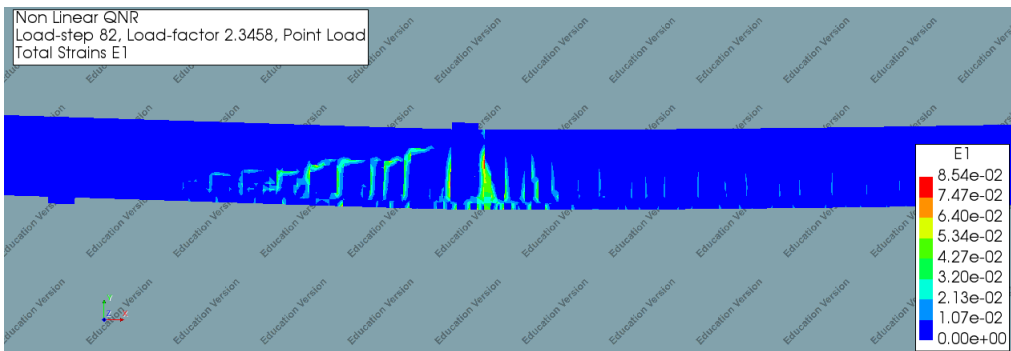
Figure G.4: Principle strain contour plot at loss of capacity
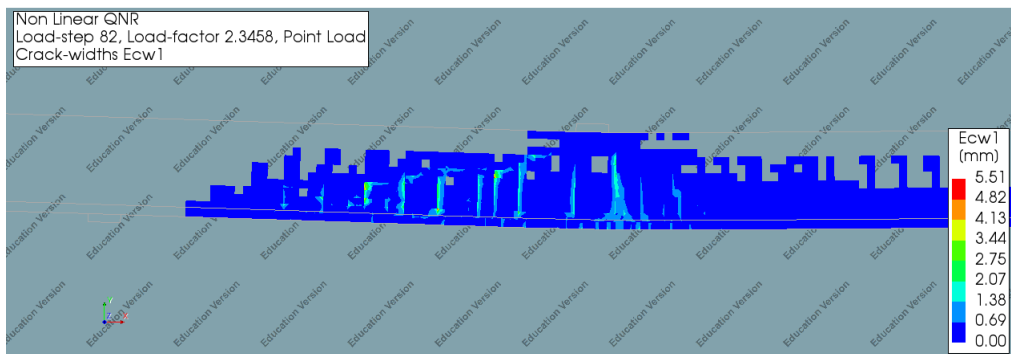
Figure G.5: Crack width at defined loss of capacity

Figure G.6: Reinforcement Stresses at Yielding Step

H

NLFEA results with perturbed values of the input basic variables

Case 2a: Beam subjected to Bending Failure

- c = 0.1
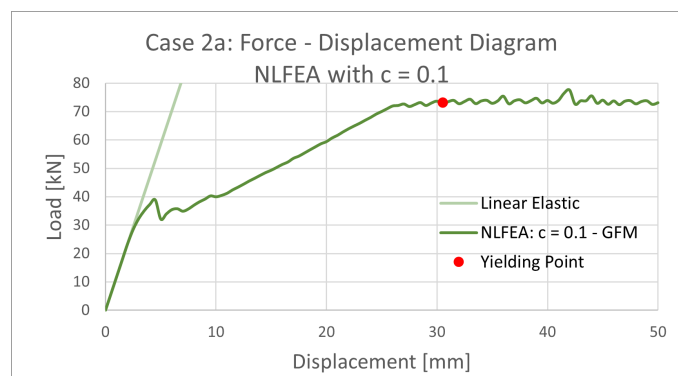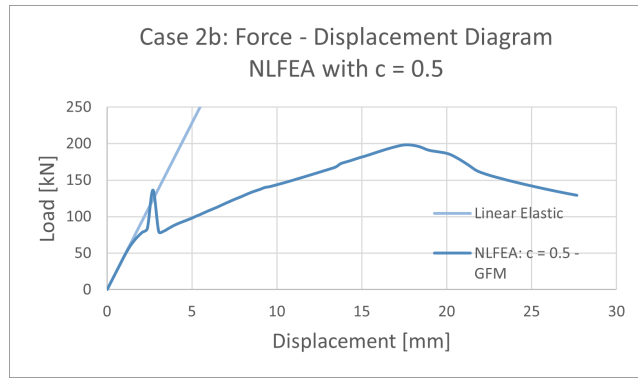

Figure H.1: Global Load-Displacement curve
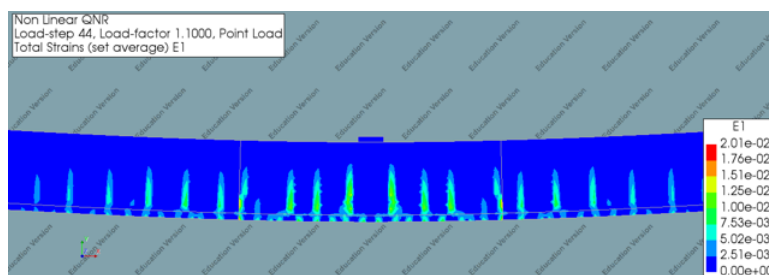
Figure H.2: Principle strain contour plot at yielding point
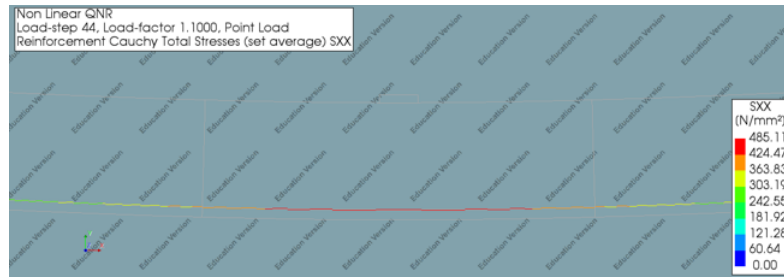
Figure H.3: Reinforcement Stresses at yielding point

- c = 0.5
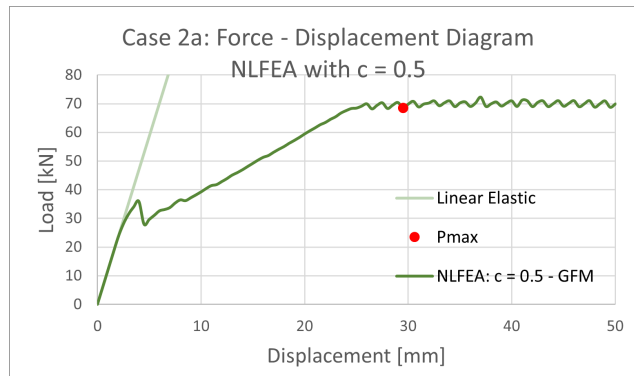
Figure H.4: Global Load-Displacement curve
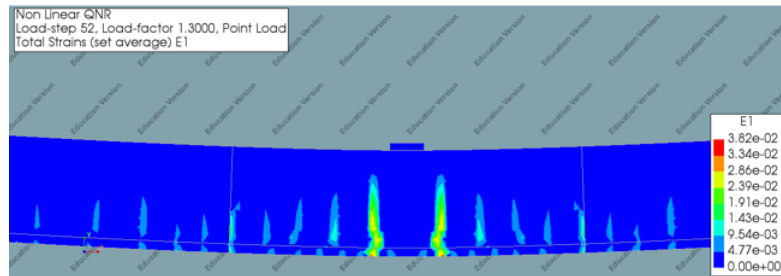
Figure H.5: Principle strain contour plot at yielding point
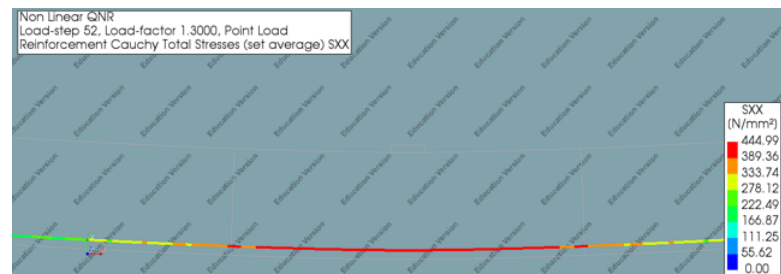
Figure H.6: Reinforcement Stresses at yielding point

- c = 1.0
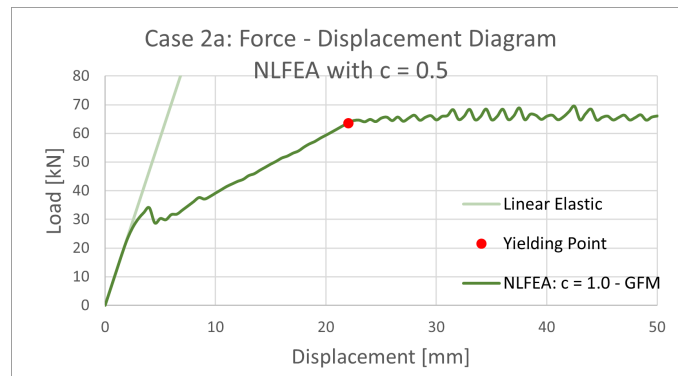
Figure H.7: Global Load-Displacement curve
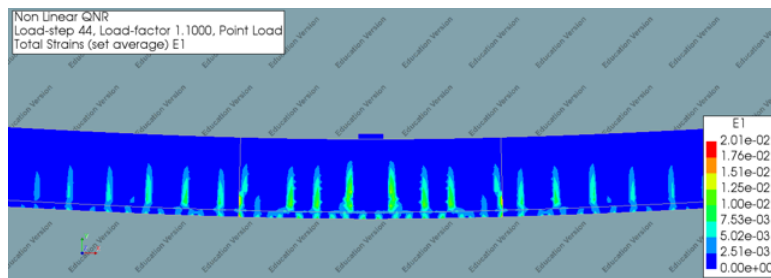
Figure H.8: Principle strain contour plot at yielding point
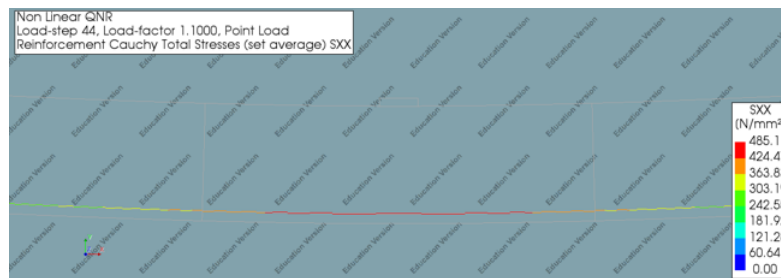
Figure H.9: Reinforcement Stresses at yielding point

- c = 1.0
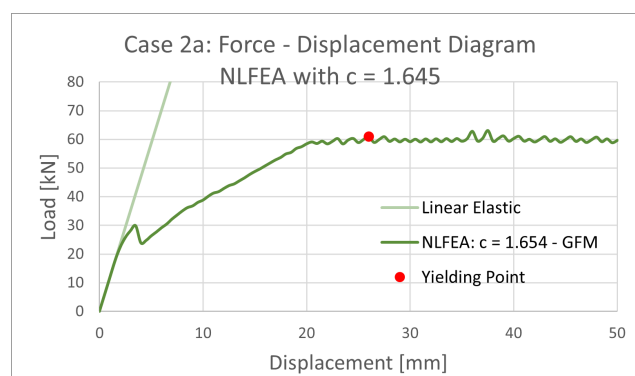
Figure H.10: Global Load-Displacement curve
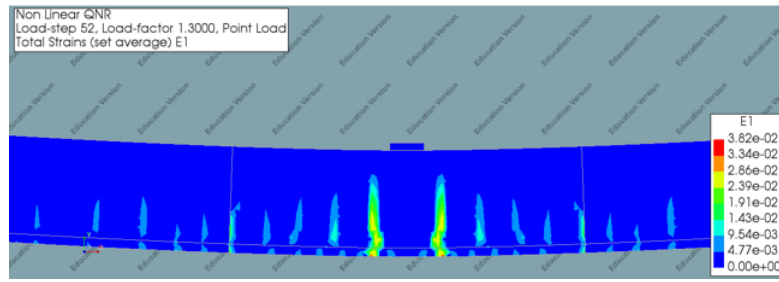
Figure H.11: Principle strain contour plot at yielding point
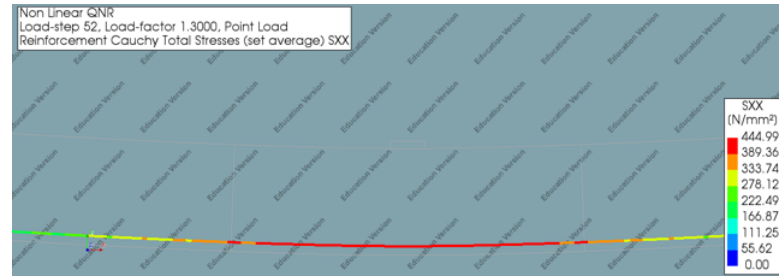
Figure H.12: Reinforcement Stresses at yielding point

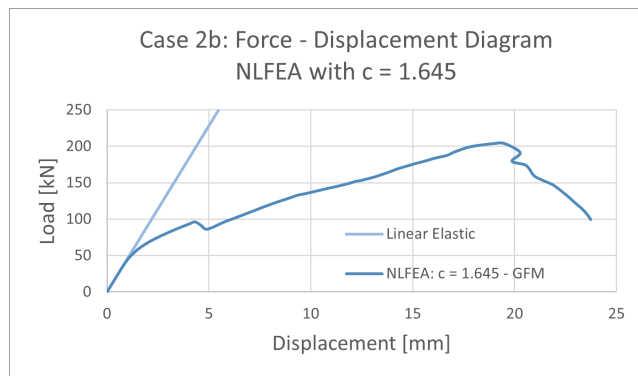**Case 2b: Beam subjected to Shear Failure**

- c = 0.1
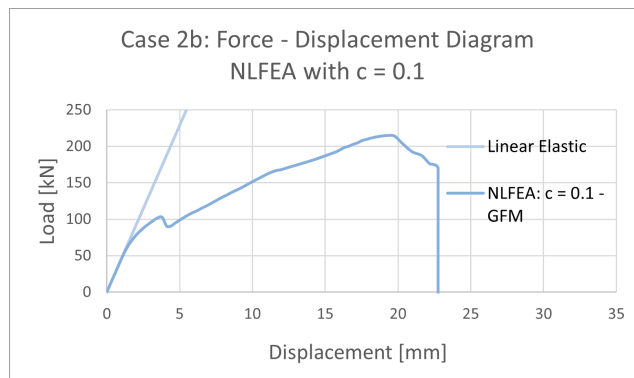
Figure H.13: Global Load-Displacement curve
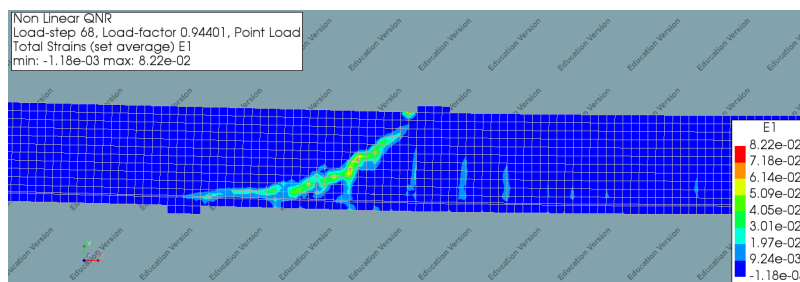
Figure H.14: Principle strain contour plot at maximum Load
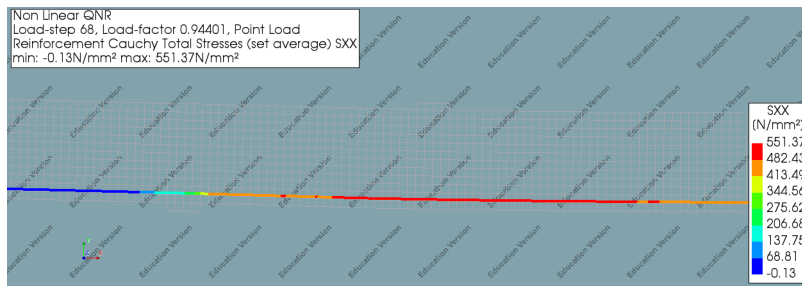
Figure H.15: Reinforcement Stresses at maximum Load
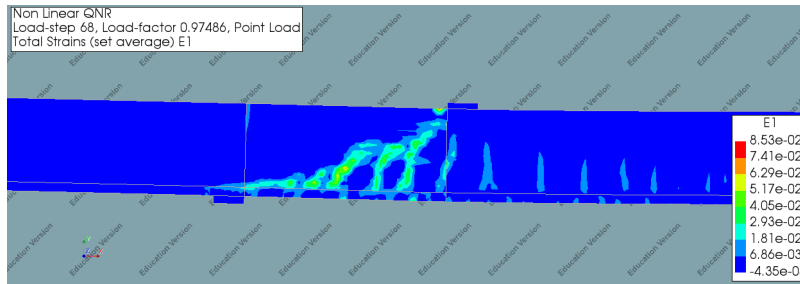
- c = 0.5
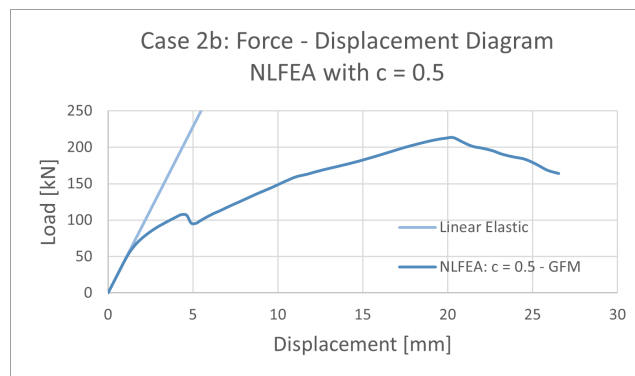
Figure H.16: Global Load-Displacement curve
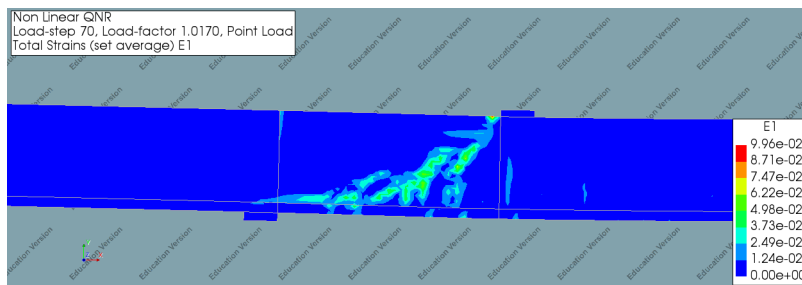
Figure H.17: Principle strain contour plot at maximum Load
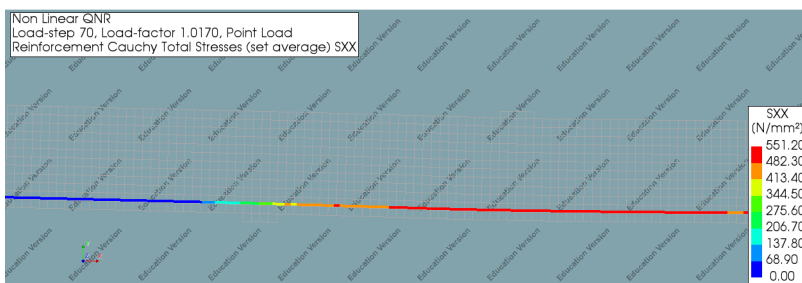
Figure H.18: Reinforcement Stresses at maximum Load

- c = 1.0

Figure H.19: Global Load-Displacement curve
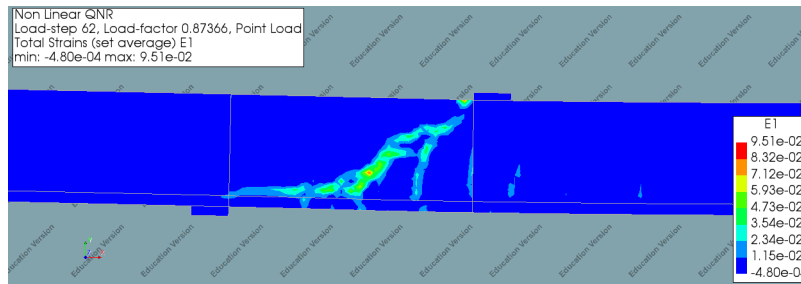
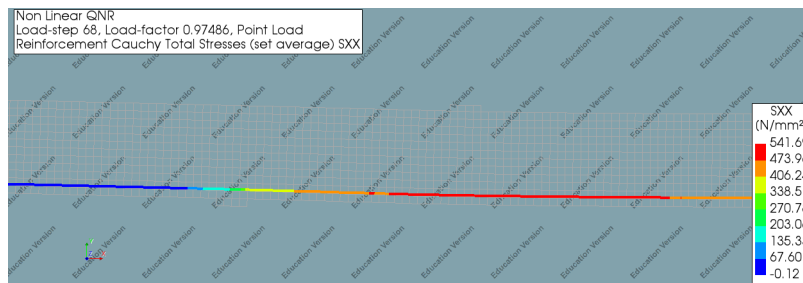
Figure H.20: Principle strain contour plot at maximum Load
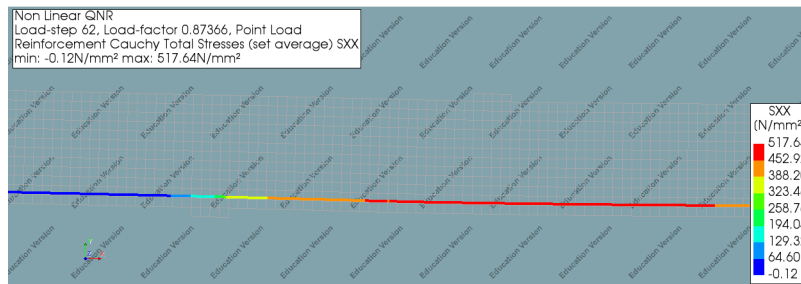
Figure H.21: Reinforcement Stresses at maximum Load

- $c = 1.645$

Figure H.22: Global Load-Displacement curve

Figure H.23: Principle strain contour plot at maximum Load

Figure H.24: Reinforcement Stresses at maximum Load
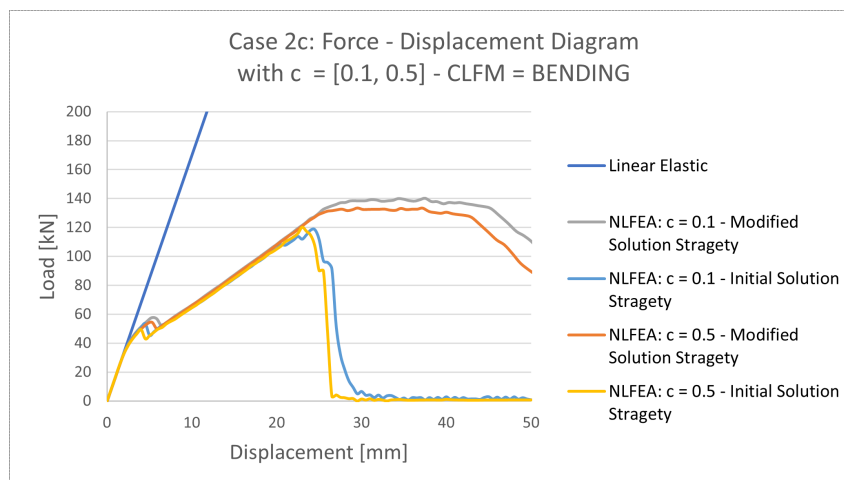
Case 2c: Beam subjected to Mixed Failure
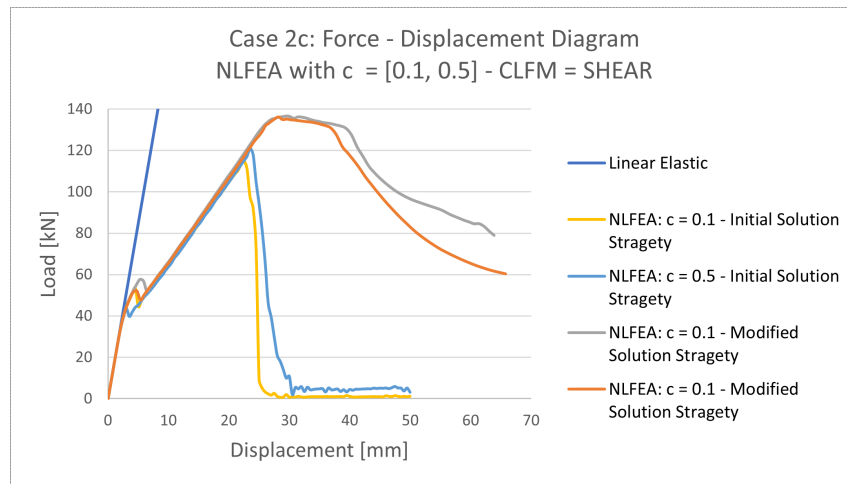

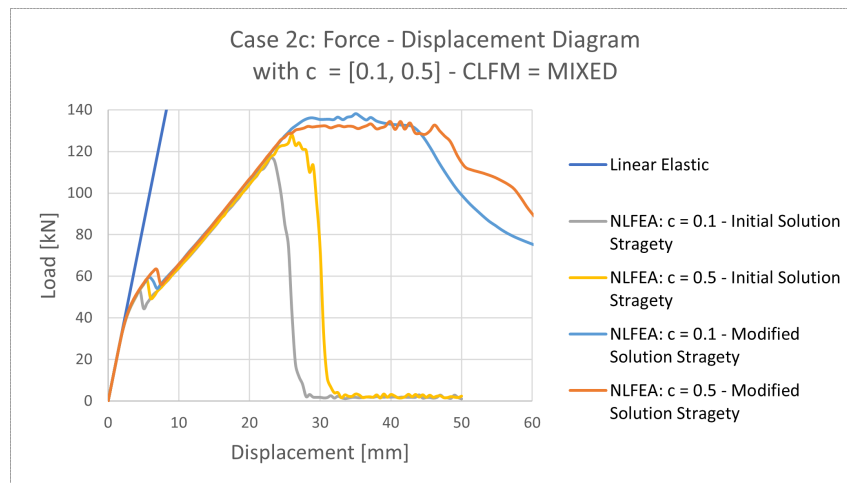Figure H.25: Global Load-Displacement curve

Figure H.26: Global Load-Displacement curve

Figure H.27: Global Load-Displacement curve